Technical Analysis and Recommended Practice for the Double-Drawbar Dolly Using Self-Steering Axles

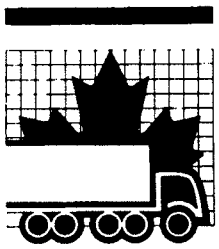

Technical Report

RTAC REPORT DOCUMENTATION FORM

Projet No.	Report No.	Report Date	IRRD No.
1376			

Project Manager

Ralph Campbell

Title and Subtitle

Technical Analysis and Recommended Practice for the Double-Drawbar Dolly Using Self-Steering AnalysisAxles

Author(s)	Corporate Affiliation(s)
J.H.F. Woodrooffe P.A. LeBlanc M. El-Gindy	National Research Council of Canada

Sponsoring/Funding Agency and Address	Performing Agency Name and Address
Roads and Transportation Association of Canada National Research Council	Vehicle Dynamics Laboratory Division of Mechanical Engineering National Research Council, Canada

Abstract

This study examines the double drawbar dolly (C-dolly) and its use in articulated vehicle combinations.

The objective of the study is to recommend a set of technical regulations governing certain performance and design factors relating to the dolly and its key components. The study contains a literature review of previous field test reports and computer simulation exercises. It also makes reference to the performance record of C-dollies currently in use. A detailed theoretical analysis of the mechanics of self-steering axles and their effect on vehicle handing is presented. This theoretical analysis is complemented by a practical analysis which is based on past experience, the effects of design change, and the records of satisfactory and non-satisfacory performance. Finally, the study presents a set of recommended regulations and outlines a test procedure to prove compliance with the standards.

Keywords

(IRRD)

Articulated vehicle
Design (overall design)
Vehicle handling

(Non-IRRD)

D-Train
Double-drawbar dolly
Stelf-steering axle

No. of Pages	No. of Figures	Language	Price
+68			

Supplementary Information

FICHE DE RAPPORT DE L'ARTC

Projet n°	Rapport n°	Date du rapport	IRRD n°
1376			

Gestionnaire du projet

Ralph Campbell

Titre et sous-titre

Technical Analysis and Recommended Practice for the Double-Drawbar Dolly Using Self-Steering Analysis Axles

Auteur(s)	Affilliation(s)
J.H.F. Woodrooffee P.A. LeBlanc M. El-Gindy	National Research Council of Canada

Nom et adresse de l'organisme parrain	Nom et adresse de l'organisme éxécutant
Roads and Transportation Association of Canada National Research Council	Vehicle Dynamics Laboratory Division of Mechnical Engineering National Research Council, Canada

Résume

Le présenté étude traite de l'avaint-train à double timon (avant-train de type C) et de son utilisation dans les ensembles de véhicules articulés.

L'objectif de l'étude est de faire des recommandations dans le but d'établir une réglementation technique touchant certains facteurs de rendement et de conception de l'avaint-train et de ses composantes principales. L'étude contient une analyse de la documentation existante sur les essais sur le terrain et les exercices de simulation par ordinateur déjà effectués, et renvoie aussi aux rapports de rendement des avant-trains en usafge actuellement. De plus, elle contient une analyse théorique déaillée de la mécanique des essieux auto-directeurs et de leurs effets sur la manoeuvrabilité des véhicules. Cette analyse théorique est accompagnée d'une analyse pratique basée sur les expériences passéews, sur les effets causés par les changements apportés à la conception et sur les rapports de rendement. Enfin, l'étude suggère une réglementation de même qu'une procédure d'essai servant à s'assurer que les normes sont respectées.

Mots-clés

(IRRD)

Vehicle articulé
Dimensionement
Stabilité du vehicule

Nombre de pages	Nombre de figures	Langue	Prix
+68			

Renseignements supplementaires

PROJECT ADVISORY COMMITTEE

Project Chairman: Paul Askie,
Ontario Ministry of Transportation

Members: John Billing
Ontario Ministry of Transportation

Norm Burns
Saskatchewan Highways and Transportation

Jean Couture
Ministère des Transports du Québec

Douglas R.S. Jacques
Transport Canada

Doug Kee
Advance Engineered Products Ltd.

Project Manager: Ralph Campbell
Roads & Transportation Association of Canada

Project Consultant: John Woodrooffe
National Research Council of Canada

ABSTRACT

This study examines the double drawbar dolly (C-dolly) and its use in articulated vehicle combinations.

The objective of the study is to recommend a set of technical regulations governing certain performance and design factors relating to the dolly and its key components. The study contains a literature review of previous field test reports and computer simulation exercises. It also makes reference to the performance record of C-dollies currently in use. A detailed theoretical analysis of the mechanics of self-steering axles and their effect on vehicle handling is presented. This theoretical analysis is complemented by a practical analysis which is based on past experience, the effects of design change, and the records of satisfactory and non-satisfactory performance. Finally, the study presents a set of recommended regulations and outlines a test procedure to prove compliance with the standards.

RÉSUMÉ

La présente étude traite de l'avant-train à double timon (avant-train de type C) et de son utilisation dans les ensembles de véhicules articulés.

L'objectif de l'étude est de faire des recommandations dans le but d'établir une réglementation technique touchant certains facteurs de rendement et de conception de l'avant-train et de ses composantes principales. L'étude contient une analyse de la documentation existante sur les essais sur le terrain et les exercices de simulation par ordinateur déjà effectués, et renvoie aussi aux rapports de rendement des avant-trains en usage actuellement. De plus, elle contient une analyse théorique détaillée de la mécanique des essieux auto-directeurs et de leurs effets sur la manoeuvrabilité des véhicules. Cette analyse théorique est accompagnée d'une analyse pratique basée sur les expériences passées, sur les effets causés par les changements apportés à la conception et sur les rapports de rendement. Enfin, l'étude suggère une réglementation de même qu'une procédure d'essai servant à s'assurer que les normes sont respectées.

EXECUTIVE SUMMARY

The commercial vehicle combination known as the C-train has emerged as an attractive alternative to the A-train. Past research and field experience show that the development of appropriate performance standards for the C-train would maximize the benefits of this configuration. The C-dolly, also referred to as the double drawbar dolly, is the principal distinguishing component of the C-train. It consists of a rigid frame that is attached to the lead trailer in a manner that eliminates an articulation joint.

The C-train has one articulation joint per additional trailer, while the A-train has two. The reduction in one articulation joint per unit has a positive effect on vehicle performance as can be quantified by the rearward amplification performance measure. The double drawbar of the C-dolly also provides roll coupling between trailers, another desirable feature.

The self-steering axle used by the C-dolly is the focus of most of the remaining concern regarding the C-train and its performance. The self-steering axle concept, as it originated in Europe during the mid 1950's, was for use in conjunction with standard axles on a load sharing axle group. Now for its use in the C-train, there are unique demands on the self-steering axle and these have been the key factors driving the research study at hand.

The study examines the C-train and the C-dolly and its component parts with a view to identifying what performance regulations would be appropriate for encouraging a balanced development of the C-train within the context of interprovincial transportation.

The study draws on previous research concerned with the comparative performance of vehicle combinations with and without the C-dolly. It contains a detailed analysis of the self-steering axle, the C-dolly, and the vehicle system and is supported by field experience.

The technical findings are placed in the context of a set of proposed C-dolly regulatory recommendations. It also contains a recommended compliance test procedure.

The proposed regulatory principles put forward by the study cover the following items:

(a) lateral and longitudinal minimum force versus steer angle performance for the self-steering axle;
(b) centering force controls for the self-steering axle;
(c) locking systems for self-steering axles;
(d) hitch requirements for the C-dolly, including minimum load ratings, maximum allowable slack or free play, and specifications on the location of the hitches;
(e) minimum frame torsional stiffness requirements for the C-dolly, and minimum torsional limit prior to permanent deformation;
(f) tire requirements for the C-dolly;
(g) drawbar length limit for the C-dolly;
(h) dimensional limitations for the C-train;
(i) gross combination weight limit for the C-train; and
(j) mandatory inspection considerations.

SOMMAIRE

Le véhicule commercial connu sous le nom de train double de type C s'avère une formule intéressante de remplacement du train double de type A. Les recherches et les expériences sur le terrain montrent que la mise au point de normes de rendement appropriées pour le train double de type C, maximiserait les avantages de ce modèle. L'avant-train de type C, appelé aussi avant-train à double timon, est la composante qui distingue le train double de type C des autres trains routiers. Il s'agit d'un cadre rigide que l'on fixe à la remorque principale de manière à éliminer une articulation.

Le train double de type C n'a qu'une articulation par remorque additionnelle, comparativement au train double de type A qui en a deux. L'élimination d'une articulation a un effet positif sur le rendement du véhicule, qui peut être évalué quantitativement par la mesure de l'amplification des forces à l'arrière. Une autre caractéristique intéressante de l'avant-train à double timon est qu'il fournit de la stabilité en torsion entre les remorques.

La performance de l'essieu auto-directeur de l'avant-train de type C est ce qui suscite le plus d'inquiétude. Le concept de base des essieux auto-directeurs, mis au point en Europe dans le milieu des années 1950, s'agissait d'un dispositif utilisé conjointement avec des essieux standards pour former un groupe d'essieux de partage des charges. Les exigences spécifiques de son utilisation dans le train double de type C sont à la base de la présente étude.

L'étude examine le train double de type C ainsi que l'avant-train de type C et ses composantes dans le but d'identifier les règles de rendement qui encourageraient l'exploitation économique et sécuritaire du train double de type C dans les transports interprovinciaux.

L'étude s'est inspirée de recherches antérieures sur la comparaison du rendement des ensembles de véhicules avec et sans avant-train de type C. Elle contient une étude détaillée de l'essieu auto-directeur, de l'avant-train de type C et de l'ensemble de véhicules, et est appuyée par des expériences sur le terrain.

Les découvertes techniques sont recueillies dans le but de faire des recommandations pour établir une réglementation sur l'avant-train de type C. Le rapport propose aussi une méthode d'essai de conformité.

Les principes de réglementation avancés dans l'étude touchent les points suivants:

(a) la force latérale et longitudinale minimale contre l'angle de braquage de l'essieu auto-directeur;
(b) le système de centrage de l'essieu auto-directeur;
(c) les systèmes de verrouillage des essieux auto-directeurs;
(d) les exigences des attaches de l'avant-train de type C, y compris les taux de charge minimales, le mou ou le jeu maximal permis, et les prescriptions sur l'emplacement des attaches;
(e) la rigidité en torsion minimale du cadre de l'avant-train de type C et la limite de torsion minimale avant la déformation permanente;
(f) les exigences en matière de pneus pour l'essieu directeur de l'avant-train de type C;
(g) la longeur maximale du timon de l'avant-train de type C;
(h) les dimensions maximales du train double de type C;
(i) le poids brut maximal de train double de type C; et
(j) considerations relatives aux inspections obligatoires.

CONTENTS

CONTENTS (Cont'd)

LIST OF APPENDICES

CONTENTS (Cont'd)

LIST OF FIGURES

CONTENTS (Cont'd)

LIST OF FIGURES (Cont'd)

NOMENCLATURE

(i) General Nomenclature:

Symbols		Units
a_b	Brake-steer force	g's
a_{bo}	Brake-steer force corresponding to δ_o	g's
a_{bomin}	Minimum level of brake-steer force that a self-steering axle must be capable of generating	g's
a_c	Self-steering axle cornering force	g's
a_{co}	Self-steering axle centering force	g's
a_{comin}	Minimum level of cornering force that a self-steering axle must be capable of generating	g's
B_r	Braking ratio	-
$C_{\alpha i}$	Cornering stiffness of the tire(s) on the i^{th} wheel	kN/deg
C_{si}	Longitudinal stiffness of the tire(s) on the i^{th} wheel	kN/slip
C_s	Single tire longitudinal stiffness	kN/slip
D	Dual tire spacing	m
F_b	Brake-steer force	kN
F_{bo}	Brake-steer force corresponding to δ_o	kN
F_c	Self-steering axle cornering force	kN
F_{co}	Self-steering axle centering force	kN
F_{xi}	Tire longitudinal force of i^{th} wheel	kN

NOMENCLATURE (Cont'd)

Symbol		Units
ΔF_x	$F_{x1} - F_{x2}$	kN
F_y	$F_{y1} + F_{y2}$	kN
F_{yi}	Tire lateral force of i^{th} wheel	kN
g	Acceleration due to gravity	m/s^2
i	Index identifying the axle left or right side wheel	-
k	Self-steering axle cornering stiffness	kN/deg
k_1	Self-steering axle cornering stiffness for $\delta \leq \delta_o$ (idealized self-steering axle having linear spring rates)	kN/deg
k_2	Self-steering axle cornering stiffness for $\delta > \delta_o$ (idealized self-steering axle having linear spring rates)	kN/deg
M_r	Self-steering axle reaction to external moments	kN·m
m_s	Mass of self-steering axle components that exibit movement relative to the vehicle frame	kg
M_{dt}	Dual tire moment generated by a single dual tire	kN·m
R	Steady-state turn radius	m
s_i	Longitudinal slip of the tire(s) on the i^{th} wheel	-
s_{1max}	Longitudinal slip corresponding to the maximum braking force of wheel 1 operating with a defective braking system	-
s_{2max}	Longitudinal slip corresponding to the maximum braking force possible for the tire (or dual tire) of wheel 2	-
t	Corrected caster trail dimension	m
t/w	Moment arm ratio	-
t_m	Mechanical caster trail dimension	m
t_p	Pneumatic trail dimension	m
t_s	Distance between the centre of gravity of m_s and the pivot point about which self-steering axle components rotate	m
V	Steady-state forward speed	m/s
W	Vertical load on single wheel	kN
W_r	Rated axle load of self-steering axle	kN
w	Kingpin offset dimension	m
α	Approximation of the average tire slip angle of both wheels of a self-steering axle	deg
α_i	Slip angle of tire(s) on i^{th} wheel	deg
δ	Self-steering axle steer angle	deg
δ_o	Self-steering axle steer angle corresponding to the axle's centering force, F_{co}	deg
δ_{omax}	Maximum self-steering axle steer angle within which a cornering force equal to a_{comin} must be reached	deg
δ_{xo}	Maximum steer angle assumed by the self-steering axle when subjected to a standard unbalanced braking force	deg

NOMENCLATURE (Cont'd)

Symbol		Units
δ_{xomax}	Maximum allowable steer angle assumed by a self-steering axle when subjected to a standard unbalanced braking force	deg
μ_o	Coefficient of road adhesion for V ≈ 0	-
ϵ_r	Adhesion reduction coefficient	s/m

(ii) Nomenclature Used in Relation With the Steady-state Handling Equations:

Symbol		Units
a_i	Distance between the centre of mass of the vehicle unit, and either the centre of the front steering axle (in the case of the towing vehicle) or the location of the fifth wheel kingpin (in the case of a semitrailer);	m
A_{si}	Static articulation angle coefficient corresponding to Γ_i	deg
A_{di}	Dynamic articulation angle coefficient corresponding to Γ_i	deg
b_i	$L_i - a_i$	m
$C_{\alpha ij}$	Total tire cornering stiffness for the j^{th} axle on the i^{th} vehicle unit	kN/deg
C_{sij}	Single tire longitudinal stiffness for the j^{th} axle on the i^{th} vehicle unit	kN/slip
D_{ij}	Dual tire spacing	m
e_{ij}	Distance between the centre of the trailer axle group and the belly axle	m
F_{cij}	Self-steering axle cornering force	kN
F_{coij}	Self-steering axle centering force	kN
F_{ij}	Total lateral force generated by axle	kN
g	Acceleration due to gravity	m/s^2
H_i	Perpendicular distance seperating the centre of rotation from the vehicle frame	m
i	Index identifying the vehicle unit	-
j	Index identifying the axle on the i^{th} vehicle unit	-
k_{ij}	Self-steering axle cornering stiffness	kN/deg
k_{1ij}	Axle cornering stiffness for idealized self-steering axle when $F_{cij} \leq F_{coij}$	kN/deg
k_{2ij}	Axle cornering stiffness for idealized self-steering axle when $F_{cij} > F_{coij}$	kN/deg
K_d	Dynamic understeer coefficient	deg
K_s	Static understeer coefficient	deg

NOMENCLATURE (Cont'd)

Symbol		Units
L_e	Vehicle effective wheelbase	m
L_i	Vehicle wheelbase	m
m_i	Mass of vehicle unit	kg
m_{sij}	Mass of self-steering axle components that exibit movement relative to the vehicle frame	kg
M_{ij}	Dual tire moment generated by a pair of dual tires (i.e. axle total dual tire moment)	kN·m
n	Number of vehicle units	-
n_{1i}	Number of belly axles	-
n_{2i}	Number of trailer (drive) axles	-
n_{3i}	Number of dolly axles	-
q_i	Distance between the centre of the trailer (drive) axle group and the centre of the C-dolly axle group	m
R, R_i	Steady-state turn radius	m
s_i	Distance seperating the centre of the trailer (drive) axle group from the intersection of the line defining distance H_i and the vehicle frame	m
t_{ij}	Corrected caster trail dimension	m
T_{di}	Dynamic trajectory angle coefficient	deg
T_{si}	Static trajectory angle coefficient	deg
V	Steady-state forward speed	m/s
x_i	Distance between the centre of the fifth wheel and the centre of the axle group over which the fifth wheel is mounted	m
α_{ij}	Average tire slip angle of the j^{th} axle of the i^{th} vehicle unit	deg
β_i	Vehicle unit side splip angle	deg
Γ_i	Articulation angle between i^{th} and i^{th}+1 vehicle unit	deg
δ	Front axle steering angle	deg
δ_{ij}	Self-steering axle steer angle	deg
Δ_{ti}	Interaxle spacing of the trailer axle group	m
Δ_{di}	Interaxle spacing of the C-dolly axle group	m
θ_{ij}	Trajectory angle = $\delta_{ij} + \alpha_{ij}$	deg
θ_{ti}	Trajectory angle at the centre of the trailer (drive) axle group	deg

(iii) Nomenclature Used in Appendix A For Deriving the Dual Tire Moment Expression:

Symbol		Units
C_s, C_{sij}	Single tire longitudinal stiffness	kN/slip
D, D_{ij}	Dual wheel spacing	m

NOMENCLATURE (Cont'd)

Symbol		Units
F_x	Tire longitudinal force	kN
F_{xi}, F_{xo}	Longitudinal force of the inner and outer tire of a dual wheel, respectively	kN
M_{dt}	Dual tire moment generated by a single dual tire	kN·m
M_{ij}	Dual tire moment generated by a pair of dual tires (i.e. axle total dual tire moment)	kN·m
r	Yaw rate of the dual wheel	rad/s
R_e	Effective tire radius	m
u	Speed of dual wheel tangent to path	m/s
u_a	Actual longitudinal tire speed	m/s
u_r	Apparent longitudinal tire speed	m/s
u_i, u_o	Apparent longitudinal speed of the inner and outer tire of a dual wheel, respectively	m/s
s	Tire longitudinal slip	-
s_i, s_o	Tire longitudinal slip of the inner and outer tire of a dual wheel, respectively	-
Ω	Tire spin velocity	rad/s

1.0 INTRODUCTION

The double drawbar dolly (C-dolly) is an innovative device used for coupling two trailers together in a manner that may be beneficial to vehicle stability performance. It takes the form of an extension of the lead trailer's frame, on which the trailing trailer is coupled through a fifth wheel. The dolly is supported by a self-steering axle, that is required to reduce high stress levels in the equipment owing to tire scuffing forces associated with sharp radius turns. The C-dolly represents an improvement over the common A-dolly in several respects as it eliminates one articulation point, couples the two trailers in roll, and improves low speed off-tracking.

Previous studies (Woodroffe and Billing 1983, Ervin and Guy 1986, Billing 1986, Winkler et al. 1986) have shown that a vehicle combination, when coupled together by a C-dolly (forming a C-train), exhibits improved yaw and roll performance characteristics in comparison to the common A-train [Figure 1]. (These studies also caution that the self-steering axle and the C-dolly hitches require specific characteristics in order to be beneficial to improved vehicle handling.) The Canadian Vehicle Weights and Dimensions Study (Ervin and Guy 1986, Billing 1986) examined the C-train, recognized its potential, and also identified the need for further research. At about the same time it became apparent to the Canadian regulatory community that a research effort was required to determine whether the C-train should be formally sanctioned to operate, and, if so, under what constraints.

The study at hand, funded jointly by Council on Highway and Transportation Research and Development (CHTRD) of the Roads and Transportation Association of Canada (RTAC), and the National Research Council of Canada (NRC), has been undertaken to examine the dolly and its components as well as the vehicle combination with which it is used, so that the necessary design and performance criteria can be developed to ensure safe application of this device.

The primary "deliverable" of the study is a set of recommended regulatory principles governing the C-dolly.

2.0 DESCRIPTION OF THE C-DOLLY AND ITS COMPONENTS

2.1 General Description of the C-Dolly

The first C-dolly was developed in Canada by Auto Steering Trailers Ltd. about 1980. The dolly consisted of a rigid structural steel frame, a fifth wheel for attachment to the following trailer, and a self-steering axle assembly suspended by a leaf spring suspension. Attachment to the lead trailer was achieved with two steel eyes fixed to the arms of the dolly on 760 mm centres and two corresponding pintle hooks with vertical latches attached to the rear apron of the lead trailer.

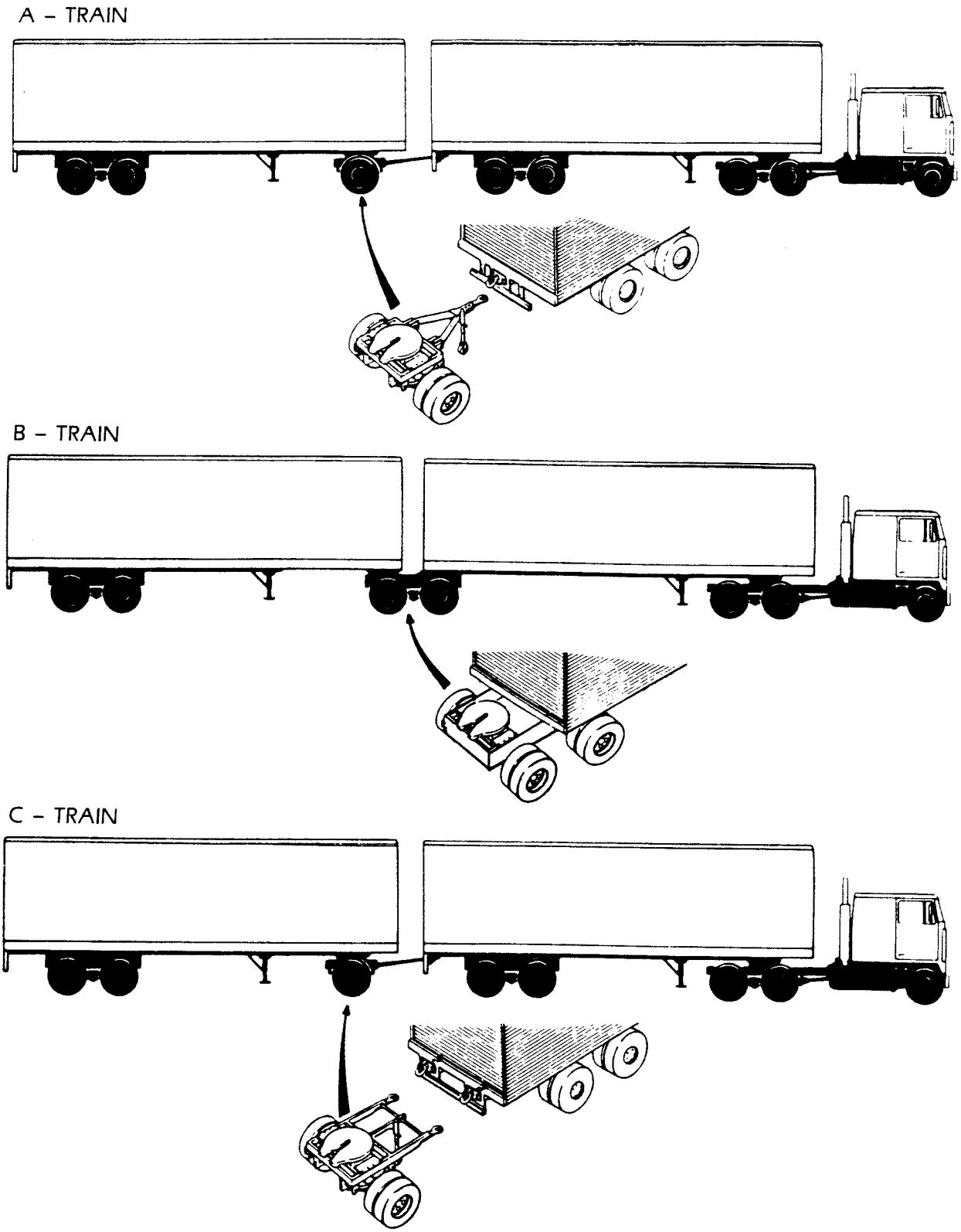

Figure 1. Three Vehicle Combinations Currently in Use in Canada

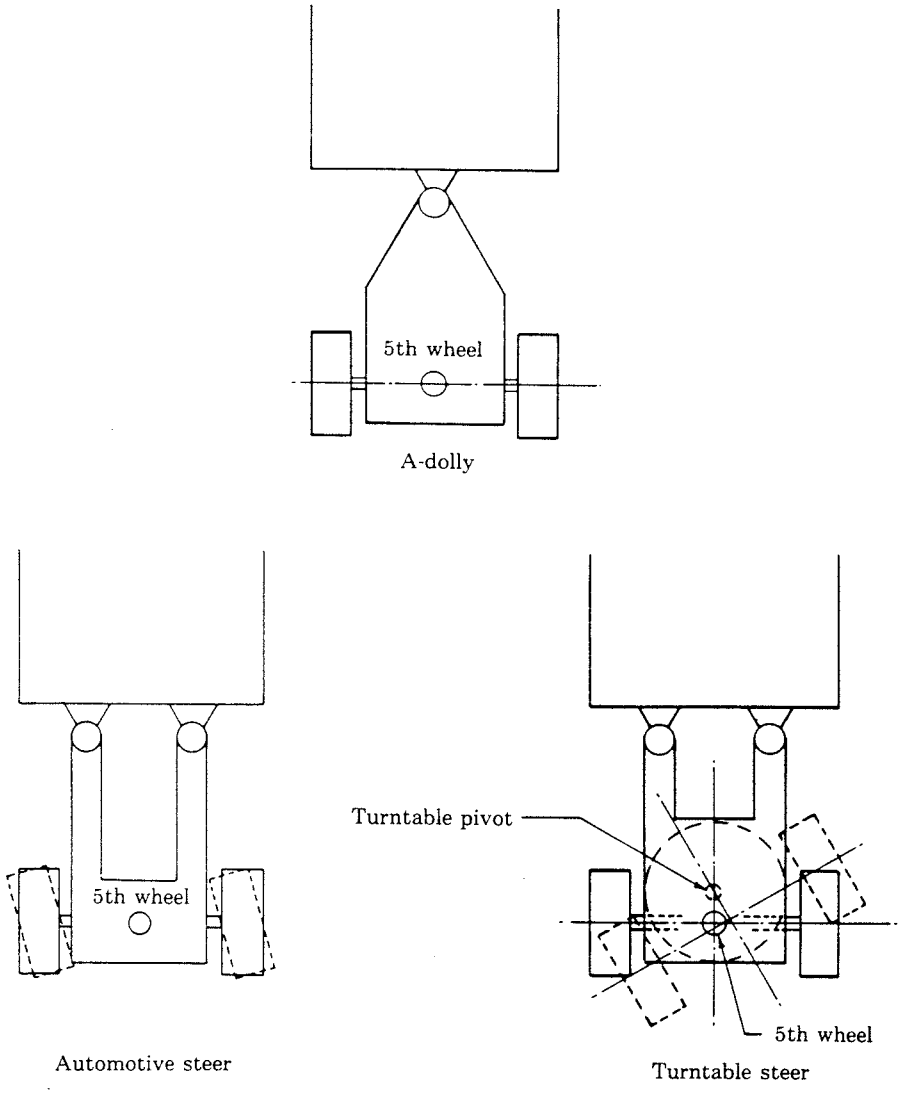

Figure 2. Schematic of A-Dolly and Different C-Dolly Types

Currently there are many manufacturers of C-dollies, each with some unique design feature. All models use one of two main types of self-steering axle assemblies, shown in Figure 2.

THE TURNTABLE SELF-STEERING AXLE ASSEMBLY consists of a large diameter roller bearing or turntable, which allows for relative rotation (parallel to the ground plane) between the main frame of the dolly and the suspension sub frame. The axle is set aft of the centre of rotation of the turntable, thereby providing caster kinematics essential to self-steering operation.

THE AUTOMOTIVE SELF-STEERING AXLE, shown in more detail in Figure 3, uses vertical kingpins and a tie rod assembly similar to that of a heavy truck front end.

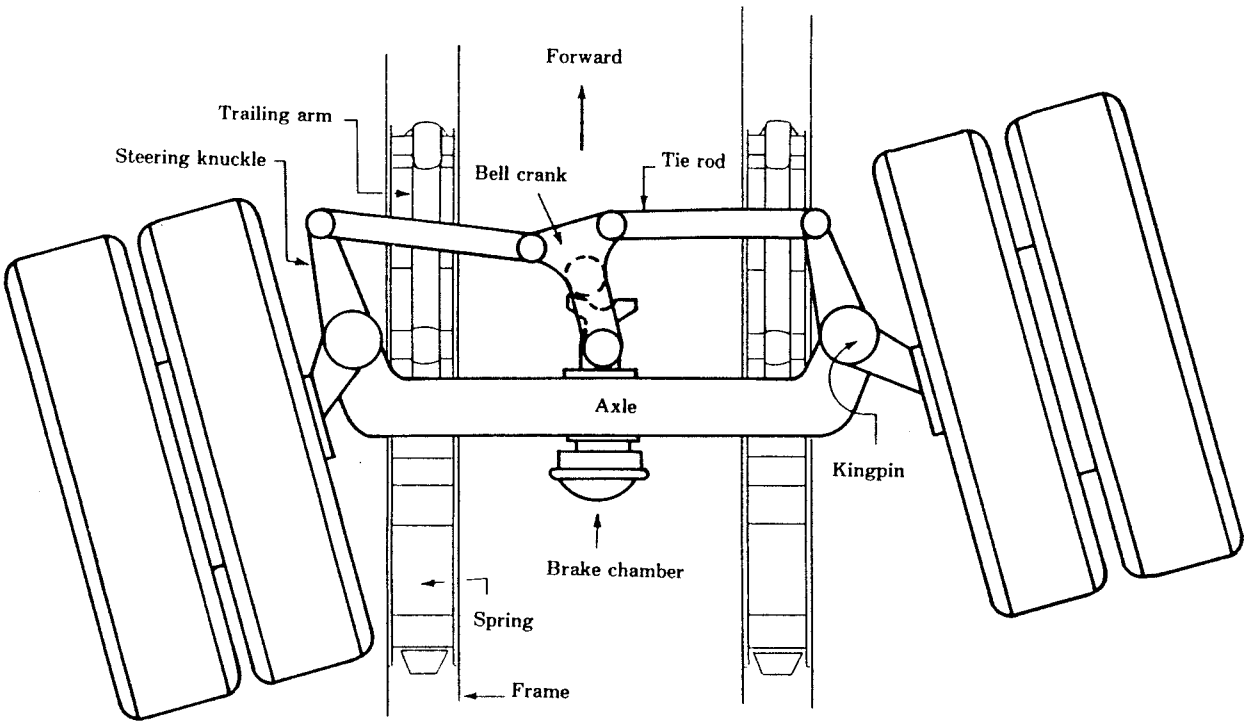

Figure 3. Main Components of the BPW Self-Steering Axle Tested in 1983 (Woodrooffe 1983)

Both the turntable and automotive steer systems utilize a centre-seeking or zero-steer biased forcing system. The centering force system is probably the most varied component among dolly and axle manufacturers. All axles have a locking mechanism to fix the axle in the zero steer position; this is desirable when the vehicle experiences adverse road conditions or when the vehicle travels in reverse.

2.2 Self-steering Axles

Self-steering axles were first developed in the northern Italian city of Verona. They were designed to be used as the second axle of a tandem axle suspension of straight trucks to improve off-tracking and reduce tire scuffing in tight turns. Scuffing was detrimental to both the vehicle and the paving-stone roadways. Used in a tandem axle system, the load equalization of the two axles was biased in favour of the fixed lead axle which carried at least 60 percent of the tandem axle group load.

Since the suspension design ensured that the fixed axle always carried most of the load of the axle group, it was assured that this fixed axle could provide the cornering force requirement of the vehicle. The self-steering axle was not designed to produce primary cornering forces for the vehicle during high speed turns.

The self-centering device, or centering force mechanism, found on most self-steering axles is used to offset the effects of unbalanced braking between the wheels of the axle. It also serves as a mechanism for helping return the steering axle to the zero steer position. Without this centering device, the internal friction within the self-steering axle could freeze the axle in a steered position until the slip angles of the tires on the self-steering axle were large enough to overcome these friction forces. Reliance on this kind of return process is undesirable because of the stiction phenomenon associated with sliding or Coulomb friction and because the side force characteristics of tires are analogous to that of a spring. That is, once sufficient side force has been generated to overcome the friction in the system, there is a rapid change in the steer angle of the self-steer axle, resulting in a lateral force impulse, or jerk, which is transmitted to the vehicle. This has detrimental effects on stability.

The C-train places demands on the self-steering axle that are not found in any other of its known applications. The C-dolly effectively de-couples the two trailers vertically (that is, there is little or no vertical load transfer between the leading and following trailers), but the C-dolly is rigidly coupled laterally so that lateral cornering forces can be transferred from the following trailer to the leading trailer. If the self-steering axle is castering entirely freely, thereby providing no cornering forces, half of the lateral force required by the following trailer during cornering is effectively transferred through the dolly to the lead trailer and so to its tires.

Under certain conditions this extra force on the lead trailer's tires can result in excessive high speed out-board off-tracking and possible yaw divergence of the trailers. One such condition that could lead to this occurrence is when the lead trailer has a light load and the following trailer is full. Since there is no vertical load transfer between the trailers, the tires of the lightly-loaded lead trailer would be incapable of generating much cornering force, yet the fully-loaded following trailer would have high cornering force requirements which the lead trailer's tires would be called upon to provide. This is an untenable situation, but it can be overcome with the use of a centering force system.

In general, self-steering axles are also vulnerable to unequal longitudinal forces imposed through the wheels, which can result from such conditions as frozen or poorly adjusted brakes, failure of the brakes on a single side, or variations in the road surface friction from one side of

the axle compared to the other at a time of heavy brake applications. A very high level of longitudinal force unbalance between the left and right tires of a self-steering axle can also be experienced when one side is on the paved surface of the road and the other is on soft material, such as a very soft shoulder or slushy, high-density snow. If unbalanced longitudinal forces are sufficiently great, they will cause an axle steer angle relative to the vehicle velocity vector, which will produce lateral forces that can, in some cases, suddenly and unexpectedly change the direction in which the trailers of a C-trail are travelling.

Because of these vulnerabilities, the side and longitudinal force requirements that self-steering axles on a C-dolly must meet are significantly higher than those associated with self-steering axles in the traditional straight truck application. This in turn places significant demands on the centering force system. The analysis section of this report will help to provide the necessary technical information required to arrive at reasonable centering force values.

Manufacturers of self-steering axles offer a wide range of axle load capacities and axle track dimensions. Axle capacities range between 6 and 15 tonnes. Track widths depend on the requirements of the customer; however, both a 2.4 and 2.6 metre outer-dimension track width are common. For the automotive-steer type axle, the caster dimension is approximately 150 mm and the lateral moment arm from the kingpin to the centre of the dual tire contact area, referred to as kingpin offset dimension, varies between 370 mm to 430 mm, depending on manufacturer. All automotive self-steering axles examined for this study use kingpins with virtually no inclination. Some manufacturers set about 1° of camber in the axle to allow for slight bending of the axle under rated load. This ensures that both tires of a dual pair will be normal to the road surface when fully loaded.

The alignment of the axle and the toe-in adjustment is achieved with a threaded sleeve coupler or with an eccentric bushing and locknut assembly. All manufacturers recommend toe-in settings varying from 0.05 to 0.15 degrees measured with respect to the rotational plane of the wheel and the centre line axis of the vehicle.

Maximum steer angles of the axles vary among models and manufacturers, ranging from about 14° to 24° off of centre. Along with the centering force system, automotive-type self-steering axles are often fitted with shock absorbers to damp out steer impulses and to retard the dynamic steer response of the system.

Spring centres on automotive-type axles are generally very narrow because of interference allowances required by the tires of the steer axle as they steer. For a steering axle fitted with dual tires on a 2.6 metre track, typical spring centre dimensions range from 0.69 to 0.75 metres. If wide single tires are used, the spring centres can be increased to

about 1.0 metres.

The turntable-type steer axle has much larger spring centres because the tires do not steer relative to the suspension. The tires, suspension, and sub frame all rotate with respect to the main frame; therefore, spring centres can be as wide as 1.1 metres.

2.3 Locking Mechanism

Self-steering axles require locking mechanisms to immobilize the steering action of the axle at the on-centre position when the vehicle moves in reverse. Without it, the axle will instantly steer to its limit of travel. Consequently, the high forces generated by the tires can result in mechanical failure of the entire steering system. The lock is commonly a pin type of device that engages a hole in a steel plate attached to the tie rod assembly. The turntable-type dolly has a similar device that pins the main dolly frame and the sub frame together. The locking devices can be controlled from the tractor cab if fitted with the appropriate hardware.

For a short time there was on the Canadian market a turntable dolly with a unique locking feature whereby a pin was inserted into one of a series of locking holes when the dolly brakes were applied. The locking holes were arranged in a circular fashion that allowed for locking of the steer axle at steer angles other than zero. Because of the pin's design, it would occasionally jam in the locking hole while the axle was in a steered position despite the vehicle having realigned itself. The problems associated with such a failure are obvious and the product was removed from the market. However, the concept may still have merit. Since the steer axle is sensitive to imbalanced, longitudinal wheel forces, for example of the type experienced during heavy brake applications on split friction surfaces, it may be beneficial to have a locking device immobilize the axle when high brake forces are required. If the locking device took the form of a disc brake for example, which could not jam in the locked position, it could be activated when very high brake applications were required, thereby preventing unwanted brake steer. Further investigation of this concept is warranted.

On inspecting different units in the field, the authors found some locking pin assemblies to be of better quality and strength than others. As these devices mature, more uniformity in strength and quality can be expected.

2.4 Tires

Virtually all C-dollies in Canada operate with dual tires ranging in size from 10:00 x 20 inches to 11:00 x 24.5 inches. Tire considerations for self-steering axles are no less important than for the front-steering axle of heavy trucks. That dual tires are used is significant; dual tires produce high aligning moments not seen in single tires. These

aligning moments must be considered when analyzing the self-steering axle, as they tend to counteract the preferred caster action of the axle by working to keep the wheel running tangent to the curve. Similarly, if there is an effective rolling radius differential between the dual pair, such as could occur in rutted road conditions, there is an additional moment, the spin moment, tending to counteract the preferred alignment of the axle. Moreover, if the tires of a dual pair were of different radii, tread type, inflation pressure, or construction (e.g. radial versus bias ply), the relative rolling resistance between the tires would also produce an undesirable spin moment and so it is important that dual tires on a self-steering axle be matched as closely as possible by type, size, state of wear, and inflation pressure. Note that the tires of a self-steering axle need not be of the same construction type as the rest of the vehicle because the self-steering axle is, in effect, partially decoupled from the vehicle. Therefore, there is no technical reason related to vehicle control requiring that uniformity of tire type between the vehicle and the self-steering axle be regulated.

The use of re-caps in the trucking industry has at times prompted heated debate about safety and damage resulting from tread failures at high speeds. In the case of self-steering axles, re-cap tires have potentially more severe consequences upon failure than in other locations. Should a tire failure occur on the inside tire of a dual pair, the kingpin offset dimension would be increased by more than 40 percent, and then for even a normal, balanced brake application (where both brakes produced the same retarding force) the moment induced on the steering system by the longitudinal braking forces would be seriously out of balance. Under moderate to heavy brake applications the axle could steer out of control.

When mounting tires on the C-dolly, care is needed to ensure minimal run-out or wobbling of the wheels as this results in inbalanced tire forces being imposed on the centering force system of the axle. A run-out variation need exceed only one-eight inch to constitute an improperly mounted rim according to the Erie Wheel Catalogue.

2.5 Hitches

Since the C-dolly couples the fore and aft trailers in roll, it transfers high torsionally induced vertical forces through the hitch points. Conventional truck configurations (i.e., non C-dolly) seldom experience such high vertical forces, especially in the upwards direction, and so truck hitches are generally incapable of handling them. This represents a major deficiency in C-dolly applications and needs to be addressed through regulation. The common hitches currently used with the C-dolly are pintle type hitches equipped with a latch mechanism which prevents the drawbar eye from escaping vertically from the hitch. The hitch was not developed specifically for C-dolly use, but does offer positive upward restraint, and to date this has been deemed acceptable in the

absence of something better. Discussions with carriers and operators that use C-dollies revealed concern over the adequacy of the hitches. The authors believe the C-dolly hitches require further development.

Research and testing of the C-dolly has reinforced the view that hitches require special attention. The critical points for hitch performance can be summarized as follows:

1. The hitch and the eye are subjected to high vertical loads in both directions. Forces of nearly 70 kN (15000 lb) have been reported by Woodrooffe and Billing (1983).

2. The hitch and the eye are also subjected to very high drawbar tensile and compressive loads because of yaw-induced moments. During violent manoeuvers of the vehicle, longitudinal hitch forces associated with yaw moment as high as just over 130 kN (30000 lb) can be expected at the hitch, based on findings by Woodrooffe and Billing (1983).

3. Hitch slack, particularly in the longitudinal direction, must be minimized as it permits of yaw freedom of the dolly which is undesirable. The hitches currently in use restrict slack by means of a pneumatic plunger that forces the eye of the drawbar against the pintle hook. The force generated by the plunger is approximately 13 kN (3000 lb), which represents an improvement over a free slack system but is insufficient to overcome the longitudinal hitch forces associated with the yaw moment of the dolly resulting from steer axle forces.

4. The hitch must be operable in severe climatic conditions, must have some fail-safe mechanism to prevent unwanted disengagement, and it must be reliable over the long term, at least equal to the life expectancy of the trailer to which it is attached.

5. The trailer backing plate to which the hitch is attached must provide at least the same minimal force requirements as the hitch.

During the course of this study's investigation into hitch requirements and the availability of hitch hardware for C-dolly applications, it became apparent that Canada is lagging behind most other nations with respect to the development and implementation of sound hitch regulations.

ISO standards 1102 and 3584 have been developed for truck and trailer hitches and mounting requirements. In the opinion of the authors, the hardware that meets these standards is a considerable improvement over hardware now being used in Canada. Some of these hitches have ratings sufficiently high to be suitable for C-dolly applications. Further investigation, including physical tests with these hitches, would be necessary to ensure there would be no unforeseen operational problem associated with their use.

3.0 REVIEW OF RESEARCH AND FIELD EXPERIENCE

3.1 Previous Research

In 1983, as part of its Research Series, RTAC published a study entitled Characteristics of Truck Combinations with the Double Drawbar Dolly (Woodrooffe and Billing 1983). The study examined the relative performance of the A-train, B-train, and C-train through the use of computer modelling techniques and controlled full-scale testing. Its conclusions are extracted as follows:

> This study has found the double drawbar dolly (C-dolly)* to be preferred over the single drawbar dolly (A-dolly) as a method of coupling multiple trailers. The following are specific conclusions regarding the C-dolly use and design:
>
> 1. The C-train with a C-dolly having a self-steering axle of appropriate design combines the flexibility of the A-train with the enhanced stability characteristics of the B-train.
>
> 2. For most vehicle configurations, the free-steering C-train at low speed offtracks less than the A-train; however, the non-steering C-train offtracks more than the A-train.
>
> 3. In a vehicle configuration where the C-dolly has appropriate steering system stiffness, rearward amplification of lateral acceleration is reduced relative to the A-dolly, because the C-dolly requires one less articulation point per connected trailer. This comparative benefit becomes more apparent with an increased number of trailers in a combination.
>
> 4. Dolly jackknife is eliminated due to the yaw constraint provided by the double drawbar hitch.
>
> 5. The C-dolly should exhibit high levels of steering stiffness and, to a lesser degree, damping, at any steer angle associated with vehicle dynamic behaviour, so as to generate the tire side forces required during high speed manoeuvres. Low levels of stiffness that approach free castering result in vehicle stability which is poorer than the A-train.

---

* In previous literature, the double drawbar dolly was abbreviated by B-dolly. Since convention now abbreviates the double drawbar dolly by C-dolly, the authors have taken the liberty of making appropriate changes to all quotations cited here.

6. The steering system of the C-dolly should perform reliably and consistently. Under no circumstances should the unit be capable of seizing or locking off centre.

7. The C-dolly is sensitive to high levels of unbalanced longitudinal wheel loading. In the absence of a speed sensitive locking device, where the potential for high level of the unbalanced loading exists, such as on soft dirt roads or centre bare iced highways, and when vehicle speeds are high, consideration should be given to locking or immobilizing the steer action of the axle at the centre position.

8. When unlocked, the automotive steer dolly is considered to be superior to the turntable steer dolly because of its reduced sensitivity to unequal longitudinal wheel load. However, when both units are locked they are considered equal.

9. The C-train can maneuver in reverse provided the dolly steering is locked. As with any multiple unit vehicle, there is a driver familiarization period required for efficient operation.

10. Both the B- and C-train provide the driver with a feel for impending loss of control, which is considered an advantage. With the A-train, the driver has little feel for lateral, yaw or roll motion of the dolly or rear trailer.

11. It has been shown that high longitudinal and vertical loads, in both directions, occur between the dolly and its hitch even during normal driving manoeuvers. While the longitudinal loads can be handled with most current equipment, some hitches may not provide sufficient vertical restraint because of an apparent low vertical force capability of their latch mechanisms. The tow eyes used with the C-dolly must also be capable of withstanding these loads.

12. The dolly frame structure should be capable of withstanding high torsional and lozenging loads. It follows that routine inspection and maintenance of the device should extend from the attachment points and structural members to the running gear.

13. The C-dolly should display clear, concise stiffness setting instructions and the steer axle lockup procedure should be clearly marked for the operator.

> Future C-dolly designs should be scrutinized carefully to avoid placing an unsuitable product on the market. The major criteria of design suitability are hitching strength and effective steering stiffness during high-speed operation. With these two criteria satisfied, the C-dolly presents a very appealing alternative to the A-dolly in terms of dynamic performance, combining the improved safety of the B-train with the coupling convenience and fleet versatility of a conventional A-train.

Reports prepared for the Vehicle Weights and Dimension Study (Ervin and Guy 1986, Billing 1986) also examined the C-train in the context of vehicle behaviour. Volume 1 (Ervin and Guy 1986) had the following conclusions concerning the C-dolly and the C-train:

> The C-train combination, with a steerable-axle, dual-drawbar dolly installed in place of the conventional A-train dolly, offers great improvements in dynamic response characteristics over the A-train, particularly in the range of 8.2 m (27 ft) trailer lengths. Nevertheless, the rankings of such vehicles would be substantially improved, especially in terms of steady-state and transient high-speed offtracking, if dolly-steering schemes were both improved and closely regulated. At the current juncture, the total lack of regulatory control over dolly-steering behaviour (except in certain provinces granting special permits), together with the potential for performance degradation due to dolly properties, gives the C-train a somewhat unresolved status.
>
> The C-train triple combination, particularly in the eight-axle version, holds promise for the future. In reviewing the technical findings the committee did not recommend the triple (based on stability analysis). Firstly, the triple with 8.2 m (27 ft) trailers is a particularly productive combination for the transport of low density freight. Secondly, the C-train implimentation resolves most of the severe deficiencies in performance exhibited by the A-train triple. Nevertheless, in its current implementation, the C-train triple does exhibit a disturbingly high level of transient high-speed off-tracking. Resolution of this remaining shortcoming, perhaps together with regulation of the steerable dolly to assure its performance qualities, would render the C-train triple highly attractive (simply considering productivity and dynamic performance).
>
> The dynamic performance of C-train doubles and triples degrades whenever the distance from the axle ahead of a dolly to the dolly axle, itself, is increased. This sensitivity applies to increases in both the overhang dimension (from trailer axle(s) to pintle hitches) and the length of the dolly drawbar (from

> pintle hitches to dolly axle(s)). It is particularly problematic to place the axle(s) on the lead trailer in a more forward position, such as with slider-bogie equipment. Such dimensional variations were shown to produce a divergent oscillation in the case of one C-train doubles combination having 8.2 m (27 ft) trailers. It is clear, however, that sensitivity to small changes in the location of hitches and axles declines with increasing trailer length.
>
> Dolly devices which effect a roll-coupling between successive trailers of a vehicle combination will provide great benefit for dynamic roll stability in a rapid path change maneuver as long as the coupling elements are sufficiently stiff in transmitting roll moments.

Volume 6 of the Vehicle Weights and Dimension Study report series (Billing 1986) stated the following conclusions:

> Three series of tests have been conducted on a C-train double trailer combination on behalf of the CCMTA/RTAC Vehicle Weights and Dimensions Study.
>
> The first series investigated the effect of hitch slack on vehicle stability. Tests were conducted with slack from 0 to 50 mm (2 in), at speeds up to 72 km/h. There was no significant reduction in the stability of the vehicle. The C-dolly used was of the automotive steer type. A turntable steer type, which has much less internal friction, may have produced a different result. If a higher speed could have been attained in the test area, instability possibly could have occurred at some slack. Presence of slack tends to be destabilizing, and hence, minimal slack associated with coupling and wear is considered tolerable. The finding of this test does not imply that any slack is either desirable or acceptable. Slack is potentially hazardous, particularly for low-stability combinations such as a triple using turntable-steer C-dollies or a double with a rearward-biased load on the rear trailer. No slack pintle hooks or any other coupling that ensures no slack should be used.

A comprehensive study (Winkler et al. 1986) identified 18 sub-groups of dollies based on the two dolly families known as "modified A-dollies and C-dollies." The dollies were studied in the context of the traditional vehicle stability criteria of rearward amplification of lateral acceleration, rollover threshold, off-tracking, and yaw damping factors. The UMTRI "Yaw/Roll," "Phase IV," "Static Roll," and "simplified off-tracking" models were used as the principal tools of analysis supported by a vehicle test program.

The study devoted a great deal of effort to the C-dolly and clearly demonstrated its superiority over the A-dolly. It was a valuable source of technical data for this current project, particularly regarding the mechanical forces measured at the hitches during demanding maneuvers. The following excerpts from the study are particularly relevant:

> The steerable C-dollies are susceptible to a unique performance problem related to braking. The C-dolly axles steer in response to torque about the steering pivot, which results from tire forces acting at some distance from the pivot. Normally, the force of interest is tire side force acting at the caster length, and generally the steering moments produced by left- and right-side tire forces will be additive. But steering moment may also be generated by braking forces acting at the kingpin offset dimension. Normally, left- and right-side torques deriving from braking forces tend to cancel, but if brake force is unbalanced side-to-side, a net steering torque will result. A brake force imbalance of 20 percent is not uncommon on heavy-duty vehicles due to brake property variations, and much greater imbalances may result from differences in tire/road friction side to side differences in tire/road friction. Given a certain level of brake imbalance, the sensitivity of the system response will depend, in large part, on the kingpin offset dimension. Accordingly, dollies employing the turntable steering mechanism are far more sensitive to unbalanced brake forces, since its kingpin offset dimension is equal to half of the track width of the axle. [Page 31.]
>
> ...With very low steering resistance, the C-dolly shows a wide range of response, depending on loading. In the empty/full condition, rearward amplification is very low. These levels of rearward amplification of less than unity indicate that the second trailer is "under-responding" and not following the path of the tractor. Without the cornering power of the dolly tires, the lightly loaded tires of the first trailer are insufficient to guide both the rear of the first trailer and the front of the second trailer. [Page 84.]
>
> As noted previously, it was to be expected that the level of steering resistance and the tongue length would have considerable influence on yaw damping performance of C-dollies. To demonstrate this influence, pulse-steer runs were conducted using the self-steering C-dolly with very low steering resistance and with long-drawbar C-dollies....The long drawbar was applied to the self-steering C-dolly with both full and low levels of steering resistance....The damping ratios calculated for these vehicles appear in Table 5....[Page 98.]

Table 5. The Influence of Dolly Drawbar Length and Steering Properties on the Damping Ratio of Test Vehicle Equipped with the C-Dollies

Dolly Type	Load Condition	Steering Property	Drawbar length (in)	Damping Ratio
Self-steering C-dolly	F/F	Full resistance	80	0.68
		Full resistance	160	0.65
		Low resistance	80	0.11
		Low resistance	160	-0.10*
	F/E	Low resistance	80	0.51
	E/F	Low resistance	80	-0.16*
	E/E	Low resistance	80	0.16

* Negative damping indicates an unstable system

[For C-dollies,] the yaw coupling moment is substantial (as, after all, it must be, to so substantially alter the yaw response of these vehicles) and results in a couple composed of large, longitudinal forces at either the C-dolly pintles or the "steering-stabilizer" hinge joint; the roll coupling moment exceeds 600,000 in-lb (67,300 N-m) for both C-dollies, producing another couple at the pintles composed of large vertical forces [Table 6]. This third result, however, is highly dependent on the torsional stiffness of the two trailers and of the dolly about their respective longitudinal, elastic axes. While the simulation treats these bodies as rigid in this regard, they of course are not. The choice of 30,000 in-lb (3,390 N-m/deg) of roll coupling compliance at the pintle is, essentially, an educated guess at attempting to "lump" the influence of these three compliances. Since in the simulation process, many of the approximations made are of the type in which (slightly) compliant bodies are assumed to be rigid, we can expect that the simulation programs may be predicting excessive roll coupling moments (and overly effective roll coupling.) [Page 108.]

STRUCTURAL LOADS. Loading patterns at the connection joint between the leading semitrailer and the dolly are of interest in designing dollies with adequate structural strength . . .

Two tests were used, viz. (1) curb climbing, and (2) severe steer. In the curb-climbing test, the vehicle traverses an 8 in (.20 m) raised "curb" at low speed . . . . The 8 in (.20 m) height was chosen as a maximum realistic height for this test, since that number is given as the upper range of "barrier curb" heights in A Policy on Geometric Design of

Highways and Streets, AASHTO, 1984. [Page 175.]

The results pertaining to the C-dolly are as shown in the tables below, which are extracts of information in Tables 6 and 17 from Winkler et al. (1986).

Table 6. Maximum Absolute Drawbar Hitch Loads in Emergency Lane Change Maneuvers at the Rollover Threshold

Dolly Type	Lane Change Freq. (rad/s)	Resultant Forces & Moments at Drawbar Centre F_y (lb)	M_x (in-lb)	M_z (in-lb)	Components Forces & Moments F_{hx} (lb)	F_{hy} (lb)	F_{hz} (lb)
Self-steering dolly, full-steering resistance	2	8,660	672,400	659,800	22,000	8,660	22,413
	3	5,894	312,600	473,200	15,800	5,894	10,400

Table 7. Maximum Loadings

Maneuver	F_y (lb)	M_z (in-lbs)	M_x (in-lbs)
Sine steer	6,256	563,564	219,438
Severe steer	6,409	641,418	-
Curb climbing	-	-	206,706

MOBILITY. Some applications of C-dollies in real service have generated mobility problems. Specifically, in fuel tanker service in Michigan, operators have experienced loss of driving traction at the tractor during tight maneuvering on uneven surfaces. Consider a scenario in which a fuel delivery unit is exiting a service station in which the apron on the service station slopes sharply downward (or upward) toward the public road. The vehicle must descend (ascend) the ramp and make a sharp exit turn onto the road. The difficulty occurs during the later stages of the turn, when the tractor semi-trailer unit has straightened out but (a) the second trailer remains sharply articulated with respect to the semi-trailer, and (b) the rear of the second trailer remains elevated. In this situation, the severely pitched second trailer may apply a large roll moment to the C-dolly through the fifth wheel. The

C-dolly pintle coupling passes this moment through to the semi-trailer and finally to the tractor. In some cases, the conditions were found to be severe enough to lighten one side of the tractor drive axles sufficiently to cause wheel-slip and loss of mobility.

To examine this problem, static experiments were conducted with the test vehicle equipped with the self-steering C-dolly. (The special hinge joint at the left side pintle, which was discussed earlier in this chapter, was made rigid for this test.) The test vehicle was parked with weigh-scales under each of the four tractor wheels, and with the second trailer articulated at 90 degrees with respect to the dolly (and first trailer). The first trailer was fully loaded, but half of the load was removed from the rear of the second trailer. The rear of the second trailer was then elevated to produce a severe pitch angle, and the change in vertical load at the tractor wheels was observed.

The results of this experiment clearly indicate that Western doubles using typical van trailers should not experience mobility problems similar to those observed in fuel tanker service. Unlike tank trailers, the van trailer was found to be sufficiently flexible in torsion along its length that the side-to-side load transfer at the tractor drive axle was low. In the most extreme test condition, the rear of the second trailer was elevated 44 inches (1.1 metres) producing a 9.2 degree pitch angle. At this extreme condition, the wheel loads at the tractor rear axle were found to be 6860 lb (3112 kg) at the left wheel and 9720 lb (4409 kg) at the right wheel, i.e., a 41 to 59 percent side-to-side distribution. Throughout the experiment, load transfer was found to be proportional to pitch angle. [Pages 179 and 182.]

3.2 Field Experience

The most concentrated use of the C-dolly is found in the province of Saskatchewan. The Transportation Agency of Saskatchewan has gained a great deal of experience and knowledge about C-train operations through experimental and analytical studies of C-trains in connection with its special permit program. This agency was consulted, along with some key trucking operations, regarding operational problems with the C-dolly. From these sources emerged the following findings:

1. There is a general lack of confidence in the pintle type hitches currently used to connect the dolly to the lead trailer. There has been at least one case of a hitch eye disengaging from the pintle hook during normal use. Concerns have also been expressed about the long-term performance of hitches resulting from wear and fatigue.

2. C-dollies with centering force mechanisms that produce low cornering forces to the self-steering axle, appear highly susceptible to road irregularities and unbalanced braking. These conditions are liable to cause the axle to steer uncontrollably.

3. C-dollies that produce high cornering forces have performed very well; however, high cornering forces generate high stresses in a C-dolly's frame and high longitudinal forces at the hitch points.

4. The unlocked self-steering axles of the C-dolly perform poorly on very soft ground, particularly on the extreme edges of roadways or on very poor gravel or dirt roads. Several vehicle roll-over accidents have been traced to this problem, and it appears to be equally as serious at low speed as high. This is of particular concern.

5. The steer axle locking pins of some axles have been found to stick or jam, or in some cases to have been underdesigned for long service duty.

6. Axle beams and/or kingpins in some automotive steer axles are prone to wear or fatigue cracking after lengthy service. It was suggested to authors that the that axle beams, kingpins, and other critical components should be inspected annually or after 500000 km, whichever comes first. It appears to be imperative that lubrication and maintenance inspection similar to that regularly performed on truck front ends be applied to the self-steering axles used in C-dollies.

Field experience with C-dollies has provided a documented case (Woodrooffe 1984) of a unit that became dynamically unstable in a classic yaw divergent manner that eventually overpowered the tractor, resulting in a jackknife. The dolly was unusual in that it had two self-steering axles; it also had a very long drawbar and the lead trailer was equipped with a tridem axle group. The distance from the dolly's fifth wheel to the centre of the lead trailer tridem was large compared to the lead trailer's wheelbase, all of which resulted in high side force demands at the tractor drive axles that in turn caused the tractor to jackknife. Excessive vehicle speed and hitch slack were cited as the two main generators of the initial instability.

4.0 ANALYSIS

4.1 General Approach

Previous research has not only demonstrated the benefits of the C-train but raised concern about the specification of the C-dolly and the C-train. The analysis and test methods used to date have focussed on the larger issues of vehicle behaviour, particularly in comparative terms. Complex computer modelling methods have taken the study of the C-dolly as far as is currently practical.

The task remaining required a more detailed examination of the C-train, (in particular the C-dolly), using basic engineering techniques, followed by a rationalization of the knowledge pool on this subject.

This study provides the foundation for a set of operational and regulatory recommendations addressing the C-train and C-dolly.

4.2 Theoretical Analysis

Self-steering mechanisms used in C-train applications must meet two fundamental performance criteria, with the first relating to the axle's cornering performance. A self-steering axle must be capable of generating a nominal level of cornering force, and this level of cornering force must be attained within a specific angular displacement of the axle relative to the vehicle frame. The second criterion is related to the axle's brake-steer performance: the self-steering axle must be capable of resisting a nominal level of differential longitudinal force without steering uncontrollably.

The following analysis illustrates the predominant operational characteristics of self-steering axles and formulates the two performance criteria stipulated above. The criteria are first developed for linear self-steering systems and are subsequently expanded to include general nonlinear systems.

We complete the section with the derivation of the steady-state handling equations for vehicle combinations equipped with self-steering axles.

4.2.1. Steady-state Analysis of Self-steering Axles

Free body diagrams of the turntable self-steering axle assembly and the automotive self-steering axle are illustrated in Figures 4 and 5. Although very different in terms of hardware, the two mechanisms are governed by equivalent steady-state moment balance equations.

Let M_r represent the moment resisting any angular displacement of the tires about their pivot point. In the case of the turntable system, the pivot point is the centre of the roller bearing, represented by point O in Figure 4, while for the automotive self-steering axle, the pivot point consists of the wheel kingpins. Moment balance about the pivot requires that

$$M_r = (F_{y1} + F_{y2})t + (F_{x1} - F_{x2})w - 2M_{dt} - m_s t_s \cos\alpha \cdot V^2/R \qquad (1)$$

where F_{yi}* is the tire lateral force, F_{xi} is the tire longitudinal force, and M_{dt} is the dual tire moment. The dimension w is the kingpin offset dimension, while t is the corrected caster trail dimension and is equal

* Index i refers to the wheel identification numbers 1 and 2.

to the sum of the pneumatic trail, t_p, and the mechanical caster trail, t_m. The mass taken for inertial purposes, m_s, comprises the sum of the inertial masses of all self-steering axle components, which exhibit movement relative to the vehicle frame when the axle is subjected to an angular displacement. The inertial mass is subjected to a lateral acceleration whose magnitude is obtained from the square of the vehicle's velocity, V, and its turn radius, R. The moment arm on which the inertial force acts is represented by the product $t_s \cos\alpha$, where t_s defines the locationof the centre of gravity of the inertial mass relative to its pivot point, and angle α is found to be approximately equal to the average tire slip angle (positive in the counterclockwise direction).

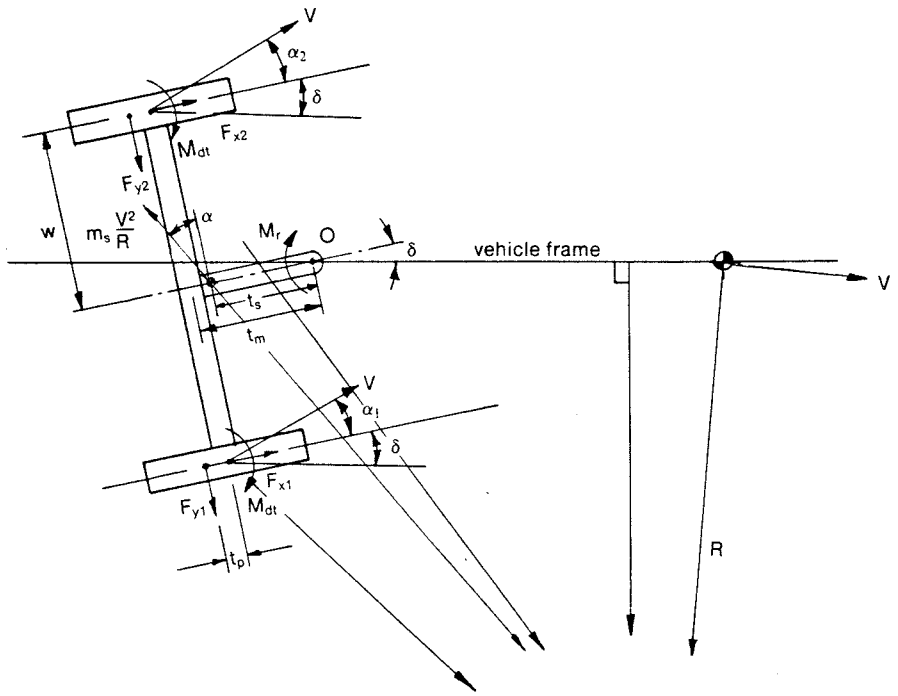

Figure 4. Turntable-type Self-steering Axle

Despite the presence of longitudinal forces, Equation 1 represents the axle's steady-state (i.e., constant speed) moment balance equation. The self-steering axle is assumed to be mounted on a vehicle generating sufficient drive to maintain constant speed.

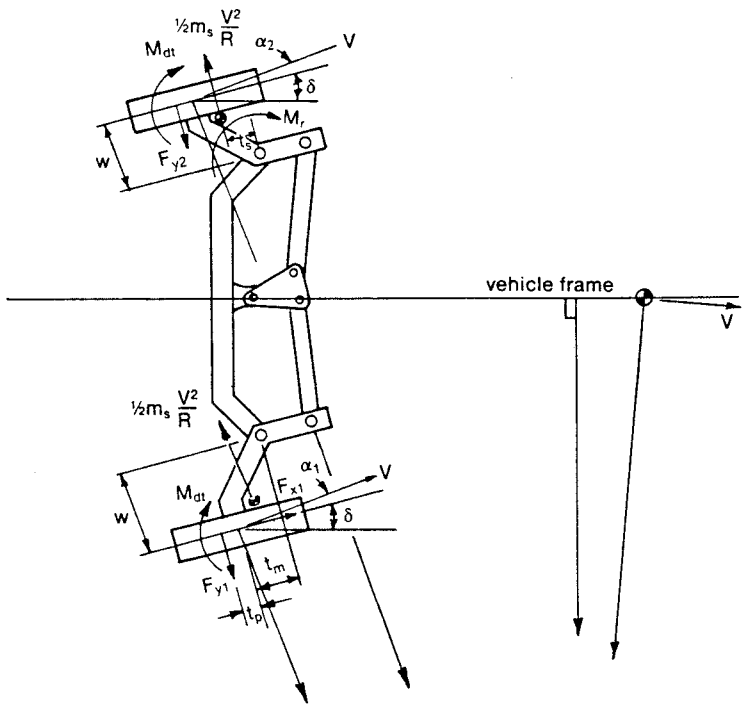

Figure 5. Automotive-type Self-steering Axle

4.2.2 Self-steering Axle Cornering Characteristics

The performance of a self-steering axle can be more readily analysed if Equation 1 is rewritten in terms of lateral forces. Dividing each term in Equation 1 by the corrected caster trail, t, gives

$$F_c = F_{y1} + F_{y2} + (F_{x1} - F_{x2})w/t + C_s D^2/Rt - m_s V^2/R \qquad (2)$$

where the ratio $t_s \cos\alpha/t$ is approximated to unity and the dual tire moments are expressed as the single tire longitudinal stiffness, C_s, the square of the dual wheel spacing, D, and the turn radius, R [Appendix A]. F_c ($= M_r/t$) is the apparent lateral force resisting angular displacement and acting at a distance, t, from the pivot. F_c will be referred to as the self-steering axle cornering force. In the absence of longitudinal forces and for cases where dual tire moments and self-steering axle inertial forces are negligible, the axle cornering force, F_c, is equal in magnitude and opposite in direction to the tire lateral forces $F_{y1} + F_{y2}$.

Equation 2 implicitly indicates that the presence of dual tire moments reduces the self-steering axle's ability to resist angular displacement caused by tire lateral forces, whereas the presence of inertial forces of the self-steering axle enhances its ability to resist angular displacement caused by tire lateral forces.

The self-steering axle cornering stiffness, k, is defined as the rate of change of the axle cornering force with respect to change in self-steering angle, δ. In mathematical terms, we write:

$$k = \partial F_c / \partial \delta \tag{3}$$

The axle cornering characteristics (i.e., the relationship between the axle cornering force and the self-steering angle) for a self-steering system having linear spring rates is shown in Figure 6. The relationship $F_c = k_1 \delta$ holds for $0 \leq \delta \leq \delta_o$, where δ_o is the steer angle corresponding to the inflection point on the curve. Beyond $\delta = \delta_o$ the self-steering axle cornering stiffness is substantially reduced, and the axle steers with relative ease. The cornering stiffness in this region is represented by k_2. The value of the axle cornering force F_{co} shown in Figure 6 is called the self-steering axle centering force, and the steer angle corresponding to this value is represented by δ_o. The axle cornering characteristics shown in Fig. 6 may be expressed as follows:

$$F_c = k_2\delta - F_{co}(1 + k_2/k_1) \qquad \text{for } F_c < -F_{co} \tag{4-a}$$

$$F_c = k_1\delta \qquad \text{for } -F_{co} \leq F_c \leq F_{co} \tag{4-b}$$

$$F_c = k_2\delta + F_{co}(1 - k_2/k_1) \qquad \text{for } F_c > F_{co} \tag{4-c}$$

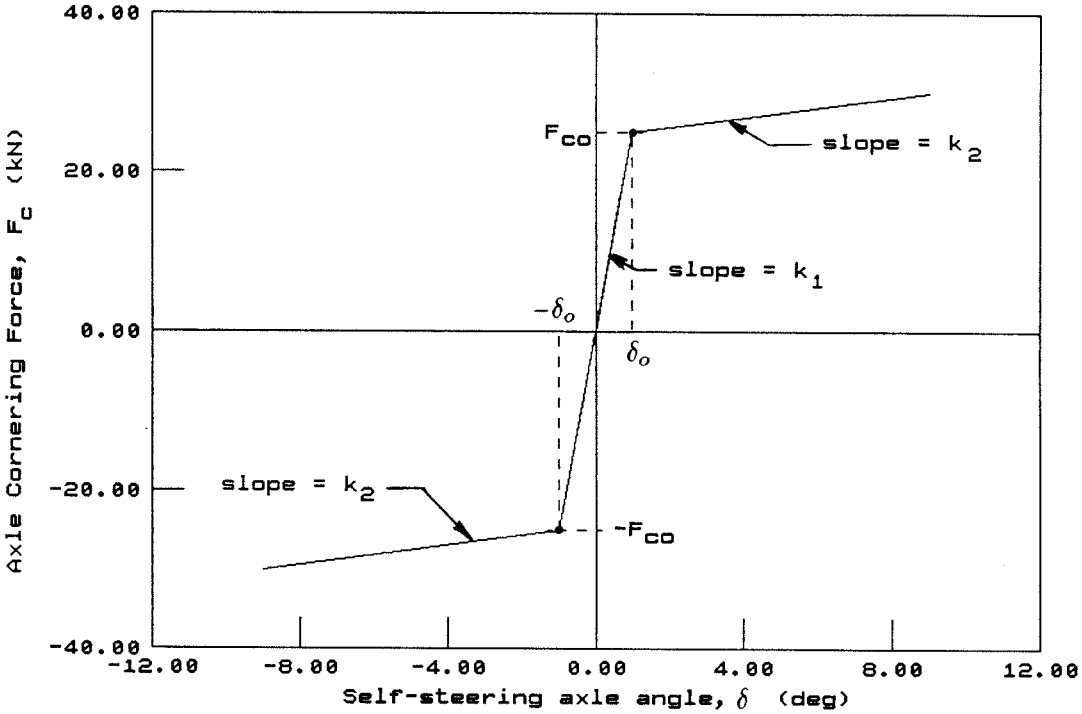

Figure 6. Cornering Characteristics for a Self-steering Axle with Linear Spring Rates

4.2.3 Cornering Performance

Self-steering axles can significantly alter the handling characteristics of vehicle systems. The ideal magnitude for each of parameters F_{co} and δ_o depends greatly on the specific application for which the self-steering axle is used.

Self-steering axle cornering forces are frequently expressed in units of g, where g represents the acceleration due to gravity. To transform the cornering force from units of force to units of g, F_c is divided by the effective mass carried by the self-steering axle, W_r/g, where W_r is the rated axle load. Hence, we write:

$$a_c = F_c \div W_r/g$$

Although a_c is expressed in units of g, it is referred to as the axle's cornering force. For example, a self-steering axle may be described as generating a cornering force of 0.25 g. Similarly, the self-steering axle's centering force can also be expressed in units of g:

$$a_{co} = F_{co} \div W_r/g$$

As shown in Table 5, a self-steering axle with very soft cornering stiffness can render the vehicle dynamically unstable in yaw. Hence, to satisfy high-speed handling characteristics, a self-steering axle must have a sufficiently high level of cornering stiffness extending over a sufficiently broad range of cornering force. Both of these requirements are taken into account by establishing the two following conditions:

$$a_{co} \geq a_{comin} \tag{5}$$

$$a_{co}/\delta_o \geq a_{comin}/\delta_{omax} \tag{6}$$

where, for a given application, a_{comin} is the minimum allowable centering force of the self-steering axle and δ_{omax} is the maximum steering angle within which a cornering force of magnitude equal to a_{comin} must be reached.

4.2.4 Brake-steer Performance

Improperly designed self-steering axles can be induced to steer uncontrollably by even small unbalanced longitudinal forces. It is therefore necessary to develop a means for evaluating the brake-steer performance of self-steering axles. Consequently, the authors have developed a Brake-steer Performance Criterion.

This Criterion is proposed as the test by which self-steering axles are to be judged. It takes into account several variables, setting minimum acceptable values for each one. Because of the need to avoid selecting

these minima in an arbitrary way, and because of the inherent value in linking research results to real-world conditions, the concept of a "baseline axle" is adopted in this report; any axle being tested for certification would have to perform at least as well as the baseline axle in terms of brake-steer. The axle selected as the baseline is representive of a group of self-steering axles already in service in Canada with a proven performance record. Details of its parameters are outlined in Section 4.3.2.

In the meantime, we shall elaborate on the Brake-steer Performance Criterion in a conceptual way. The Criterion has two parts. The first, which we call the "Brake-Steer Diagram Requirement" (BSDR), is based on the self-steering axle's ability to resist angular displacement when equipped with a pair of reference dual tires and subjected to a standard differential braking force. The BSDR takes into account the presence of tire lateral forces. The second part, which we call the "Brake-Steer Characteristics Requirement" (BSCR), on the other hand considers only the axle's ability to resist unbalanced longitudinal forces. It is used to cover situations where tire lateral forces are negligible compared to the unbalanced longitudinal forces, such as would occur, for example, when the self-steering axle is travelling straight ahead with one wheel on wet pavement and the other on a soft shoulder. It will be shown in Section 4.3 that, depending on the magnitude of a self-steering axle's cornering force, either the BSDR or the BSCR can prevail as the governing requirement.

Brake-steer Diagram Requirement (BSDR)

Consider a multi-axle vehicle equipped with a self-steering axle. Let the self-steering axle be subjected to the unbalanced braking force $\Delta F_x = F_{x1} - F_{x2}$, where ΔF_x is positive and thus seeks to steer the self-steering axle in the positive angular direction as defined in Figures 4 and 5. All other wheels on the vehicle are either free-rolling or driving. The driving force is sufficient to maintain the vehicle travelling at constant speed, and the steering input is such that the vehicle travels along a straight line. Given these conditions, the side force balance equation, Equation 2, reduces to

$$\Delta F_x = (F_c - F_y) \cdot t/w \qquad (7)$$

where

$$F_y = F_{y1} + F_{y2}.$$

In addition, we consider the case in which the magnitude of the side slip angle (of the vehicle unit on which the self-steering axle is mounted) remains negligible when compared with the dual tire slip angles, α_i, and the self-steering angle, δ. This implies that $\alpha_i = -\delta$, a condition that prevails when the total cornering stiffness of the vehicle unit in question is large in comparison to the effective cornering stiffness of the self-steering axle.

The magnitude of the tire lateral force is highly dependent on the magnitude of the tire braking force. As shown in Appendix B, the relationship between the two forces is found to be accurately represented by the following set of equations (Wong 1978, Dugoff et al. 1969), where the longitudinal force is given by

$$F_{xi} = \frac{C_{si} s_i}{1-s_i} f(\sigma) \tag{8}$$

the lateral force is given by

$$F_{yi} = \frac{C_{\alpha i} \tan\alpha_i}{1-s_i} f(\sigma) \tag{9}$$

and function $f(\sigma)$ takes the form

$$f(\sigma) = \sigma(2-\sigma) \qquad \text{for } \sigma < 1$$

$$= 1 \qquad \text{for } \sigma > 1$$

with

$$\sigma = \frac{\mu_o W[1-\epsilon_r V(s_i^2 + \tan^2\alpha_i)^{0.5}](1-s_i)}{2(C_{si}^2 s_i^2 + C_{\alpha i}^2 \tan^2\alpha_i)^{0.5}}$$

In these equations,

s_i = longitudinal slip of the tires on the i^{th} wheel;
α_i = slip angle of the tires on the i^{th} wheel;
C_{si} = longitudinal stiffness of the tires on the i^{th} wheel;
$C_{\alpha i}$ = cornering stiffness of the tires on the i^{th} wheel;
V = tire speed;
μ_o = coefficient of road adhesion for $V \approx 0$;
ϵ_r = adhesion reduction coefficient;
W = vertical load on the dual tire; and
i = index corresponding to wheels 1 and 2 [Figures 4 and 5].

As shown in Section 4.2.2, a self-steering axle with linear spring elements is governed, for values of $F_c \geq 0$, by the following function:

$$F_c = k_1 \delta \qquad \text{for } 0 \leq F_c \leq F_{co} \tag{10-a}$$

$$F_c = k_2 \delta + F_{co}(1 - k_2/k_1) \qquad \text{for } F_c > F_{co} \tag{10-b}$$

The self-steering axle's ability to resist angular displacement that

results from unbalanced braking forces can be examined by constructing a family of curves displaying the relationship between ΔF_x and F_c - F_y for constant self-steering axle angles δ [Figure 7]. The longitudinal and lateral forces shown in Figure 7 have been transformed into units of g by dividing each variable by the effective mass supported by the axle, W_r/g. As noted before, W_r is the axle's rated load. The tire parameters used to generate Figure 7 are found in Appendix B.

Constant self-steering angle curves are constructed by holding α_1 and α_2 constant at $-\delta$ and varying the longitudinal slip s_1 and s_2. To simulate unbalanced braking forces, we simultaneously vary s_1 and s_2 from 0 to s_{1max}, at which point s_1 is kept constant while s_2 is increased to s_{2max}. The magnitude of s_{2max} corresponds to the maximum braking force that can be generated by the reference dual tire mounted on wheel 2. The magnitude of s_{1max} corresponds to a braking force (of lower magnitude) that would result from a malfunction in braking mechanism of wheel 1. The axle cornering force F_c is evaluated using Equations 10 for a constant self-steering angle δ, and forces $F_y = F_{y1} + F_{y2}$ and $\Delta F_x = F_{x1} - F_{x2}$ are evaluated by appropriately substituting s_1, s_2, $\alpha_1 = -\delta$ and $\alpha_2 = -\delta$ into Equations 8 and 9.

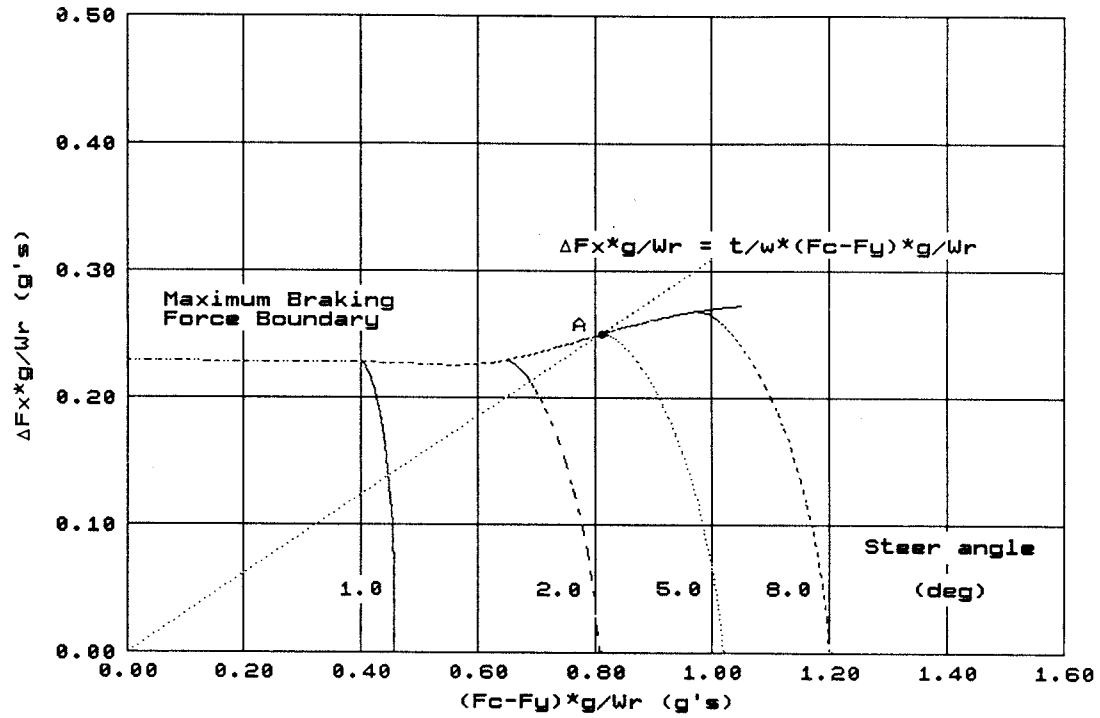

Figure 7. Typical Brake-steer Diagram

By dividing each term in Equation 7 by W_r/g, and superimposing the resulting equation over the constant self-steering angle curves of Figure 7, it is possible to determine the angle assumed by a self-steering axle

for a given unbalanced braking force. By joining the end points for each constant self-steering angle curve, we obtain a boundary referred to as the maximum braking force boundary [Figure 7]. The intersection of the maximum braking force boundary and the straight line expressed by Equation 7 [point A on the diagram] defines the maximum self-steering angle, δ_{xo}, that the axle will assume when subjected to the unbalanced braking forces described above.

The physical meaning of the braking scenario described above is brought into perspective by introducing a new parameter referred to as the braking ratio, B_r. We define the braking ratio as being the ratio of the maximum braking force of wheel 1 to the maximum braking force of wheel 2 for tires travelling at 90 kph with a slip angle of 0°, that is,

$$B_r = \frac{F_{x1}(s_{1max},\ \alpha_1 = 0°,\ V = 90\ kph)}{F_{x2}(s_{2max},\ \alpha_2 = 0°,\ V = 90\ kph)}$$

Therefore the Brake-steer Diagram Requirement can be stated as follows: when equipped with a pair of reference dual tires, and subjected to unbalanced braking forces defined by the braking ratio B_r, to be acceptable a self-steering axle must satisfy the condition

$$\delta_{xo} \leq \delta_{xomax} \qquad (11)$$

where δ_{xomax} is the maximum steering angle assumed by a selected baseline self-steering axle that has been subjected to identical braking conditions. The value of B_r is somewhat arbitrary but should be representive of a severe unbalanced braking force. The value of δ_{xomax}, on the other hand, depends on the steering characteristics of the baseline self-steering axle.

Equation 11 inherently establishes a constraint on the magnitude of the moment arm ratio, t/w. This point is illustrated with the following hypothetical example.

Let the baseline self-steering axle be defined as the rather idealized axle shown in Figure 6. It will have the following values:

$$a_{co} = 0.30\ g$$

$$k_1 = 0.30\ g/deg$$

$$k_2 = 0.01\ g/deg$$

$$t/w = 0.350$$

As shown in Figure 8 [Point A], this axle will steer to a maximum angle of 5.0° when subjected to unbalanced braking forces defined by $B_r = 0.38$. If an axle being evaluated is to pass the Brake-steer Diagram Requirement, it must perform as well as or better than our baseline axle, that is, it must satisfy the condition

$$\delta_{xo} \leq \delta_{xomax} = 5.0°$$

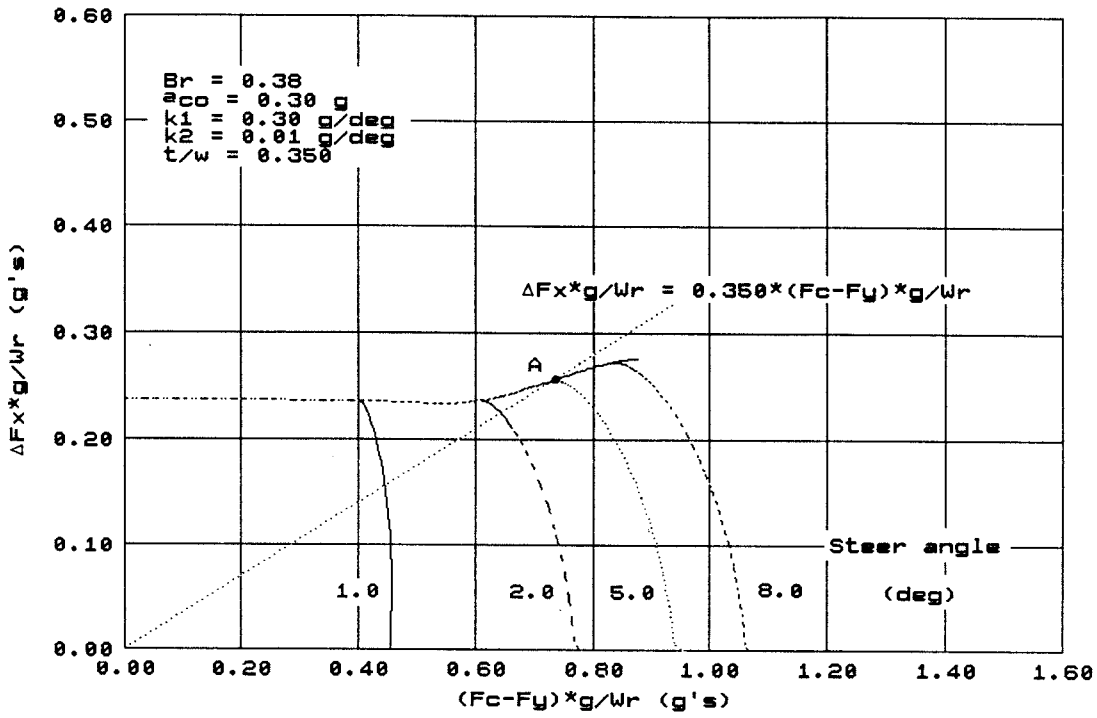

Figure 8. Brake-steer Diagram for a Hypothetical Baseline Self-steering Axle

Let the axle being evaluated have cornering characteristics as follows:

$$a_{co} = 0.25 \text{ g}$$

$$k_1 = 0.25 \text{ g/deg}$$

$$k_2 = 0.01 \text{ g/deg}$$

As shown in Figure 9, this axle will pass the Brake-steer Diagram Requirement, $\delta_{xo} \leq \delta_{xomax} = 5.0°$, only if the moment arm ratio is greater than or equal to 0.375. Hence, in this example the acceptable range for the moment arm ratio is constrained by Equation 11 to values greater than or equal to 0.375.

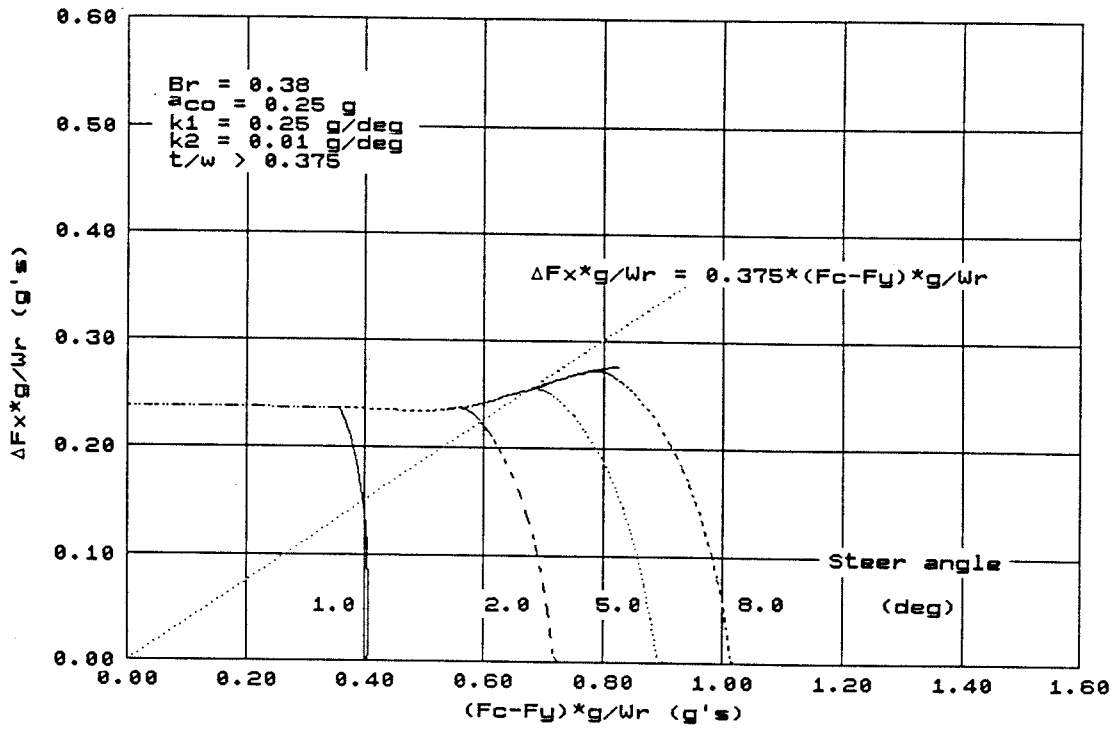

Figure 9. Brake-steer Diagram for Arbitrary Self-steering Axle

Brake-steer Characteristics Requirements (BSCR):

Dividing the moment balance equation [Equation 1] by the kingpin offset dimension, w, leads to:

$$F_b = (F_{y1} + F_{y2})t/w + F_{x1} - F_{x2} + C_s D^2/Rw - m_s t_s \cos\alpha \cdot V^2/Rw \qquad (12)$$

where F_b (= M_r/w) represents an apparent longitudinal force that resists angular displacement and acts at a distance w from the pivot. F_b is referred to as the self-steering axle brake-steer force.

The brake-steer characteristics for a self-steering axle with linear spring rates are shown in Figure 10, where the brake-steer force is plotted against the self-steering axle angle, δ. The brake-steer forces $\pm F_{bo}$ and the steer angle $\pm\delta_o$ define the inflection points in the brake-steer curve. We note that the self-steering angle $\pm\delta_o$ corresponds to the values of both $\pm F_{bo}$ and $\pm F_{co}$ (the latter as shown in Figure 6).

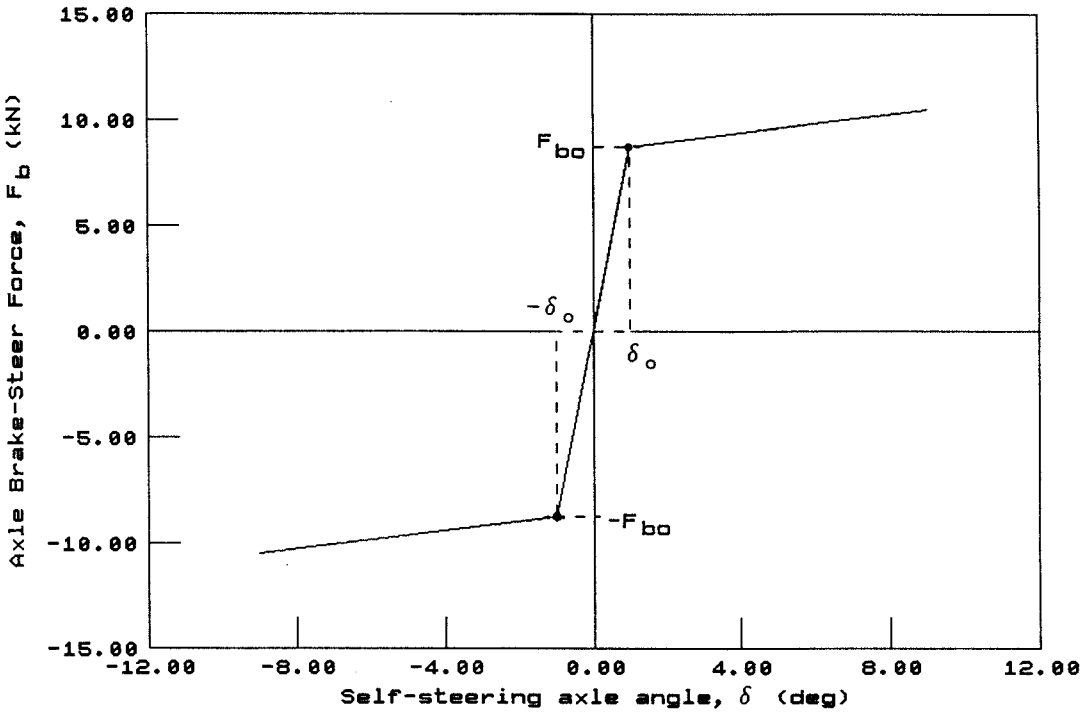

Figure 10. Brake-steer Characteristics

A relationship between the brake-steer force and the cornering force of a self-steering axle can be obtained by dividing Equation 12 through by Equation 2:

$$F_b = F_c \cdot t/w \tag{13}$$

Hence, the brake-steer force can be obtained from the product of the self-steering axle cornering force and the moment arm ratio t/w.

As with self-steering axle cornering forces, brake-steer forces may be expressed in units of g, by dividing F_b by the effective mass supported by the axle at its rated load, W_r/g, that is,

$$a_b = F_b \div W_r/g$$

$$a_{bo} = F_{bo} \div W_r/g$$

and Equation 13 may be written as

$$a_b = a_c \cdot t/w \tag{14}$$

To satisfy the Brake-steer Characteristics Requirement, a self-steering axle must perform as well as or better than the baseline self-steering axle, in terms of its brake-steer characteristics. Sufficient control over the the axle's brake-steer performance can be obtained fairly simply by requiring that the brake-steer characteristic curve lie above the point ($\delta = \delta_{omax}$, $a_b = a_{bomin}$) and below the point ($\delta = -\delta_{omax}$, $a_b = -a_{bomin}$), where a_{bomin} is the baseline axle's brake-steer force for a steer angle of δ_{omax}.

The difference between the Brake-steer Diagram Requirement and the Brake-steer Characteristics Requirement is subtle, yet leads to substantially different results. To illustrate the difference between the two requirements, their governing equations [Equations 7 and 13] are rewritten below:

$$\Delta F_x = (F_c - F_y) \cdot t/w \tag{7}$$

$$F_b = F_c \cdot t/w \tag{13}$$

Consider a self-steering mechanism that is altered so that the cornering force F_c is increased by 15 percent while the the moment arm ratio is decreased by 15 percent. Then, according to Equation 13, the brake-steer characteristic curve is unchanged, whereas according to Equation 7, the axle's ability to resist unbalanced longitudinal forces has been reduced (compromised).

4.2.5 Consideration of Nonlinearity in Self-steering Systems

In general, self-steering axles exhibit substantial levels of Coulomb friction in their angular movements. Also, the variation in cam profiles used among different axles in service has the effect of creating nonlinearity in their spring rates. A more realistic representation of the axle cornering characteristics is shown in Figure 11, characterized by rounder inflection points and directionally-dependent curves that show a hysteresis effect from frictional losses.

A self-steering axle with characteristics represented by Figure 11 must also comply with the cornering constraints established in Section 4.2.3 [Equations 5 and 6]. Since the centering force, a_{co}, is not as clearly delineated in Figure 11 as in Figure 6, the cornering constraints given by Equations 5 and 6 have been combined into the following criterion, termed the self-steering axle Cornering Performance Criterion: this criterion is met when the point ($\delta = \delta_{omax}$, $a_c = a_{comin}$) lies below the loop segment in Figure 6 corresponding to an increase in self-steer angle (i.e., the axle's outward excursion), and when the point ($\delta = -\delta_{omax}$, $a_c = -a_{comin}$) lies above loop segment corresponding to an increase in the self-steering angle in the opposite direction [Figure 11].

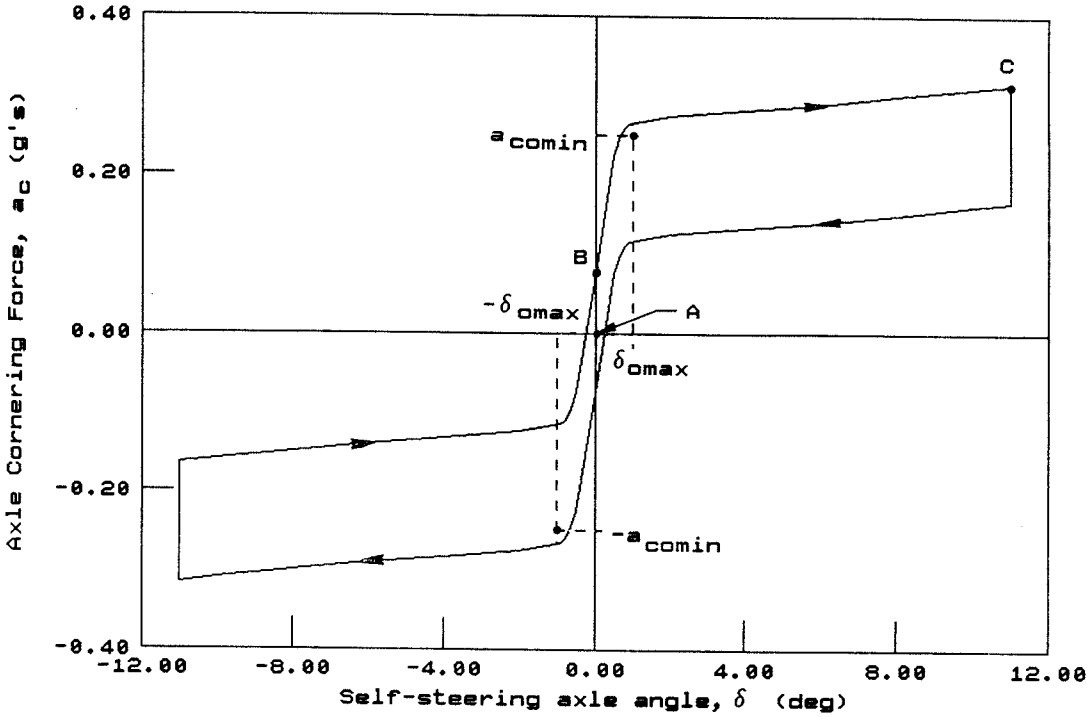

Figure 11. Cornering Characteristics for a Typical Self-steering Axle

A self-steering axle with the characteristics shown in Figure 11 must meet the same BSDR as a system with linear spring rates. When equipped with a pair of reference dual tires and subjected to a standard unbalanced braking force, the self-steering axle must satisfy the condition

$$\delta_{xo} \leq \delta_{xomax}$$

Note that the loop segment used for the BSDR extends from point A to point C, passing through point B on Figure 11.

Turning now to the BSCR, this is satisfied when the point ($\delta = \delta_{omax}$, $a_b = a_{bomin}$) lies below the loop segment corresponding to an increase in the selfsteering angle, and when the point ($\delta = -\delta_{omax}$, $a_b = -a_{bomin}$) lies above the loop segment corresponding to an increase in the self-steering angle in the opposite direction [Figure 12].

4.2.6 Steady-state Analysis of Vehicle Combinations Equipped with Self-steering Axles

The governing steady-state handling equations derived in Appendix C are presented here.

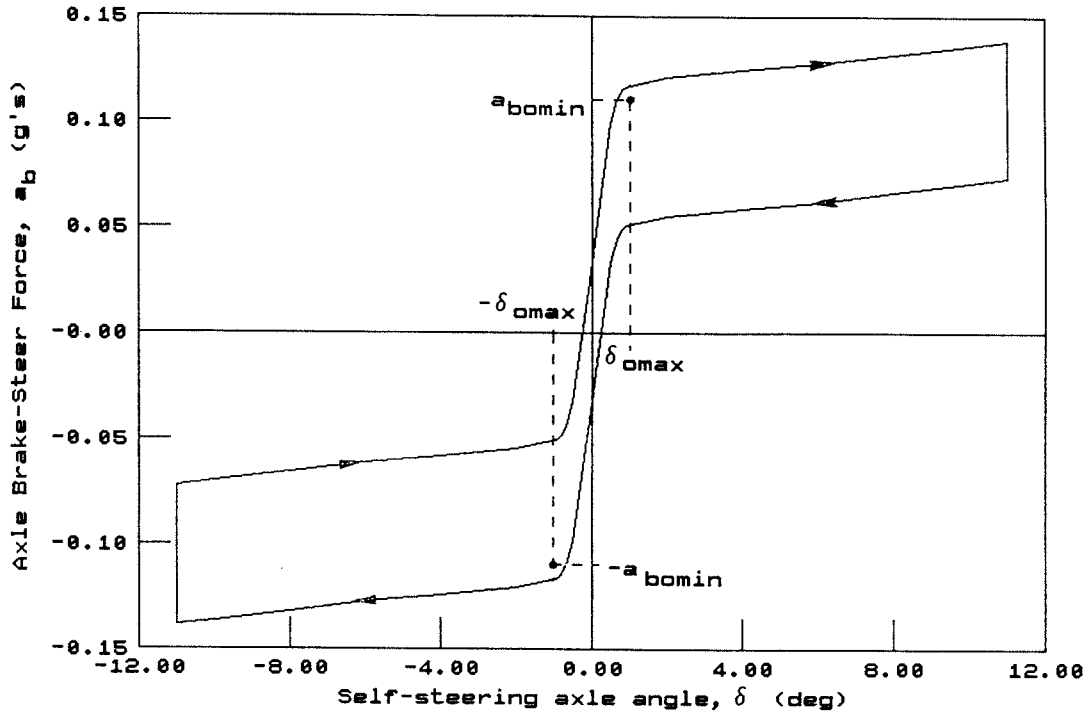

Figure 12. Brake-steer Characteristics for Typical Self-steering Axle

The two predominant effects of a reduction in self-steering axle cornering stiffness and centering force are, premature saturation of tires on axles adjacent to the self-steering axle, and deterioration of the overall handling characteristics of the vehicle combination. Hence, it is important to have analytical expressions relating tire slip angles and vehicle yaw response to self-steering axle cornering properties.

In deriving the linear steady-state handling equations for the C-train, it became apparent to the authors that a general set of equations, encompassing a wide variety of vehicle combinations, could be developed with minimal additional effort. The following discussion is valid for a vehicle towing a variable number of semitrailers. Each individual semitrailer in the vehicle combination is supported at the front by a C-dolly or by the rear end of a B-train type semitrailer. Typical vehicles that lie within the scope of the formulae are straight trucks, tractor-semitrailers, B-trains, C-trains, and truck-fulltrailers with C-dolly.

Owing to the recent growth in popularity of self-steering axle mechanisms and, to a certain extent, the relative ease of solution, it was decided that each axle would be modelled with a self-steering mechanism whose cornering stiffness could be varied all the way from free-caster to

the non-steer condition. The cornering characteristics used to model self-steering axles are described in the following paragraphs.

The lateral force, F_{ij}*, is related to the axle's average tire slip angle, α_{ij}, by the expression

$$F_{ij} = C_{\alpha ij}\alpha_{ij} \tag{15}$$

where $C_{\alpha ij}$ is the axle's total tire cornering stiffness.

The trajectory angle is defined as the angle between the velocity vector at the centre the wheel and the longitudinal orientation of the vehicle frame. From Figures 4 and 5, it can be seen that the average trajectory angle, θ_{ij}, satisfies the equation,

$$\theta_{ij} = \alpha_{ij} + \delta_{ij} \tag{16}$$

Also, in the absence of braking forces, Equations 2 and 4 yield

$$\delta_{ij} = \frac{C_{\alpha ij}}{k_{1ij}} \cdot \alpha_{ij} - \frac{M_{ij}}{t_{ij}k_{1ij}} - \frac{m_{sij}V^2/R}{k_{1ij}} \tag{17-a}$$

for $0 \leq F_{cij} \leq F_{coij}$, and

$$\delta_{ij} = \frac{C_{\alpha ij}}{k_{2ij}} \cdot \alpha_{ij} - \frac{M_{ij}}{t_{ij}k_{2ij}} - \frac{m_{sij}V^2/R}{k_{2ij}} - \frac{F_{coij}(k_{1ij} - k_{2ij})}{k_{1ij}k_{2ij}} \tag{17-b}$$

for $F_{cij} > F_{coij}$.

In both Equations 17-a and 17-b, k_{1ij} and k_{2ij} are the self-steering axle cornering stiffnesses, M_{ij} is the aligning moment for a pair of dual tires, t_{ij} is the corrected caster trail, m_{sij} is the self-steering system inertial mass, and F_{coij} is the axle's centering force.

Although the model developed in Appendix C makes use of Equations 17-a and 17-b as written above, a better understanding of the first order effect of self-steering axles can be obtained by simplifying Equation 17 to

$$\delta_{ij} = \frac{C_{\alpha ij}}{k_{ij}} \alpha_{ij} \tag{18}$$

* Index j corresponds to the j^{th} axle of the i^{th} vehicle unit. When dealing with equations with double subscripts, longitudinal braking forces F_x are not considered. Hence, the subscript y in F_{ij} is dropped.

By manipulating Equations 15, 16 and 18 we obtain

$$F_{ij} = \frac{C_{\alpha ij}\, k_{ij}}{C_{\alpha ij} + k_{ij}}\, \theta_{ij} \tag{19}$$

The above equation reveals that the self-steering axle and tire cornering stiffness combine to form a system that is analytically equivalent to two springs in series. As the self-steering axle cornering stiffness (k_{ij}) increases from zero (i.e., free castering) to infinity (i.e., a fixed axle), the tire's lateral force (F_{ij}) increase from zero to a cornering force magnitude of $C_{\alpha ij}\alpha_{ij}$.

Expressions for trajectory angles, the handling equation, and semitrailer articulation angles are obtained by deriving force and moment balance equations, by establishing the required compatibility equations, and by solving for the unknowns. The results are as follows:

$$\theta_{ti} = T_{si} + \frac{V^2}{Rg} \cdot T_{di} \tag{20}$$

$$\delta = \frac{L_1}{R} + K_s + \frac{V^2}{Rg} \cdot K_d \tag{21}$$

$$\Gamma_i = \frac{L_{i+1} + q_i - x_i}{R} + A_{si} + \frac{V^2}{Rg} \cdot A_{di} \tag{22}$$

where θ_{ti} is the trajectory angle at the centre of the trailer axle group of the i^{th} vehicle unit, δ is the steering angle of the front axle, and Γ_i is the articulation angle between the i^{th} and i^{th}+1 vehicle unit. T_{si} and T_{di} are the static and dynamic trajectory angle coefficients, K_s and K_d are the static and dynamic understeer coefficients, and A_{si} and A_{di} are the static and dynamic articulation angle coefficients. Expressions for these six coefficients, found in Appendix C, are written as the following variables:

m_i = vehicle unit mass;
a_i = distance between the centre of mass of the vehicle unit, and either the centre of the front steering axle (in the case of a towing vehicle) or the location of the fifth wheel kingpin (in the case of a semitrailer);
L_i = vehicle unit wheelbase measured from either the centre of the drive axle group to the front steering axle (in the case of the towing unit) or the centre of the semitrailer axle group to the location of the kingpin (in the case of a semitrailer);

q_i = distance between the centre of the trailer (drive) axle group and the centre of the C-dolly axle group;
x_i = distance between the centre of the fifth wheel and the centre of the axle group over which the fifth wheel is mounted (trailer or drive axle group in the case of B-train type semitrailer or tractor, respectively; or C-dolly axle group in the case of a C-train type semitrailer). Note that positive values indicate the fifth wheel is forward of the centre of the axle group;
Δ_{ti} = interaxle spacing of the trailer axle group;
Δ_{di} = interaxle spacing of the C-dolly axle group;
e_{ij} = distance between the centre of the trailer axle group and the belly axle;
$C_{\alpha ij}$ = total tire cornering stiffness of the axle;
F_{coij} = centering force of the self-steering axle;
k_{1ij} = cornering stiffness of the self-steering axle for $F_{cij} \leq F_{coij}$;
k_{2ij} = cornering stiffness of the self-steering axle for $F_{cij} > F_{coij}$
t_{ij} = corrected caster trail of the self-steering axle;
m_{sij} = inertial mass of the self-steering axle;
C_{sij} = tire longitudinal stiffness;
D_{ij} = dual wheel spacing;
R = turn radius;
n_{1i} = number of belly axles;
n_{2i} = number of trailer axles;
n_{3i} = number of C-dolly axles; and
n = number of vehicle units.

The approach used in solving Equations 20, 21, and 22 is similar to the approach used by Gillespie and Winkler (1977), where the steady-state handling equations were solved for a straight truck with fixed axles. The sum $L_1/R + K_s$ in Equation 19 is equivalent to the term L_e/R introduced by Gillespie and Winkler, where L_e is referred to as the effective wheelbase of the vehicle.

4.2.7 Discussion of Steady-state Simulations

The governing equations presented in 4.2.6 [Equations 20,21,22] form the basis of a computer simulation program written by the authors for the steady-state analysis of vehicle systems. The program provides a means of evaluating and understanding the effect that self-steering axle parameters have on the steady-state handling behaviour of vehicle systems. It calculates the front axle steering angle, the semitrailer articulation angle, and the tire slip angles, all as a function of the independent variables listed in the section immediately preceeding.

The vehicle parameters used for the computer simulations and output

graphs described below are found in Appendix D. The most pertinent graphs are presented and described immediately following.

We first wished to determine the effect of introducing a self-steering axle on the handling response of a straight truck. The computer simulation program was used to generate the handling curve shown in Figure 13a for a straight truck with two fixed drive axles. It gives the relationship between the front axle's steering angle and the vehicle's lateral acceleration for a constant turn radius of 200 m.

The effect of substituting a self-steering axle for the first (non-steering) drive axle is shown in Figure 13b. This was found to decrease the understeer gradient of the vehicle (i.e., the slope of the handling curve). The decrease in understeer is attributed for the most part to the self-steering axle's reduced cornering stiffness (k_1) compared to that of the fixed axle. Not until the level of acceleration exceeds 0.36 g does the axle centering force (F_{co}) introduce any detectable effect.

If a self-steering axle were substituted for the straight truck's second (non-steering) drive axle [Figure 13c], a pronounced decrease in the vehicle's understeer gradient would result, even more than that which resulted from the substitution noted above. When installed as the second drive axle, a self-steering axle suffers high tire slip angles that result in lateral tire forces exceeding the steering mechanism's centering force. Upon reaching this point the vehicle switches rather abruptly from a state of understeer to one of oversteer (i.e., its understeer gradient becomes negative).

The reduction of the vehicle's understeer characteristics is even more pronounced for a straight truck-fulltrailer with C-dolly [Figure 13d]. In this configuration, the vehicle switches from a state of understeer to one of oversteer at relatively low levels of acceleration. In general, as a result of tire nonlinearity (which is not considered in the present computer simulation model), straight trucks with a high center of gravity have the tendency to switch from a state of understeer to a state of oversteer as the level of lateral acceleration increases. Hence, the use of a C-dolly in a truck-fulltrailer unit has the effect of severely magnifying the level of oversteer of the straight truck.

We next wished to examine the C-train. The use of a self-steering axle on the dolly in a C-train application was found not to decrease the understeer gradient; on the contrary, it provides a marginal increase in the understeer gradient. There is a different effect that causes some concern, however, in that the use of a self-steering axle in this configuration increases the lateral force required from the tires of the lead trailer.

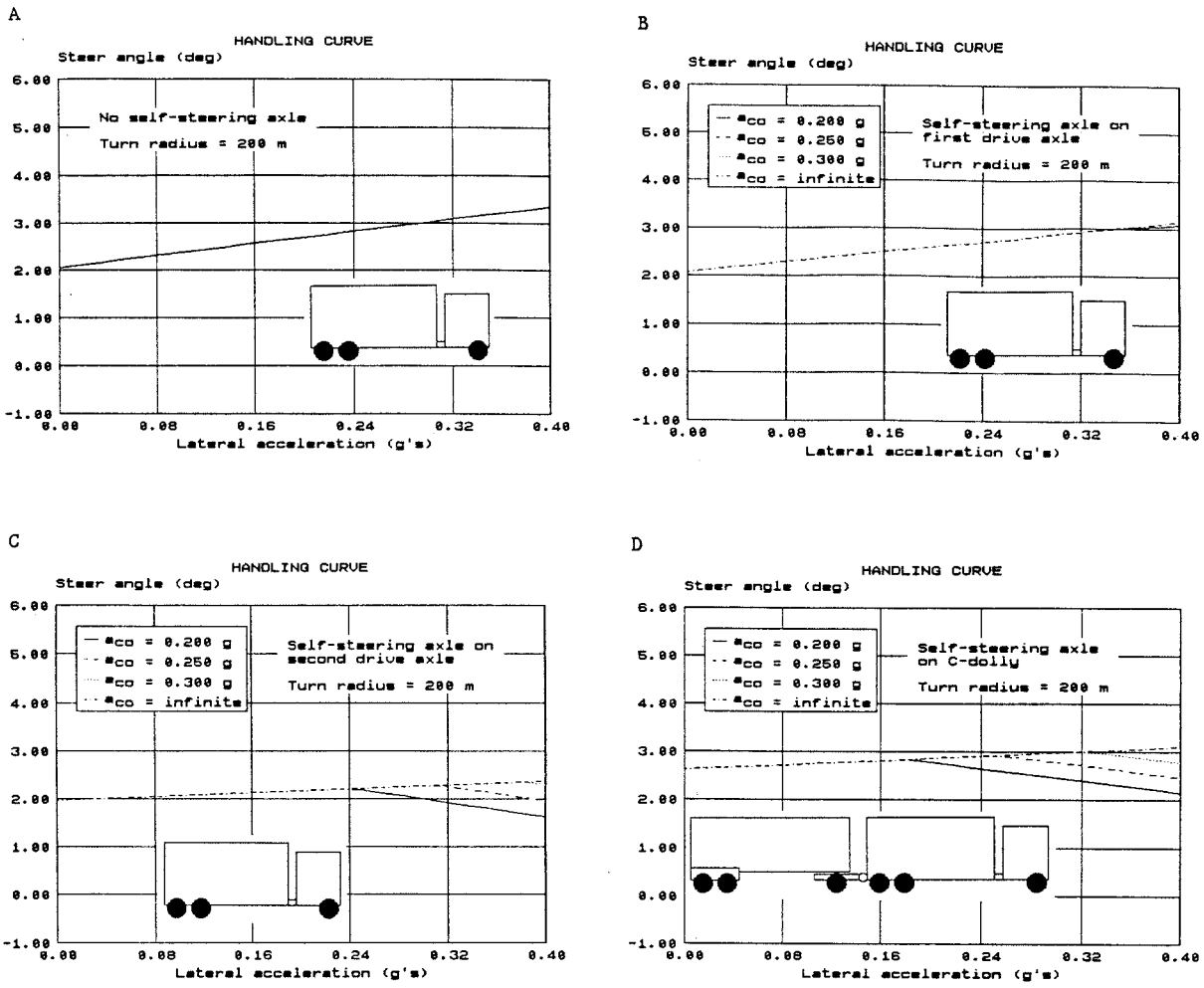

Figure 13. Straight Truck and Truck-fulltrailer With C-dolly With One Self-steering Axle

The handling curve and the tire slip angles for the lead trailer and dolly axles are shown for a C-train equipped with a fixed axle on its C-dolly [Figures 14] and for a C-train with two self-steering axles [Figures 15]. The latter is similar to the vehicle that was involved in the accident reported by Woodrooffe (1984).

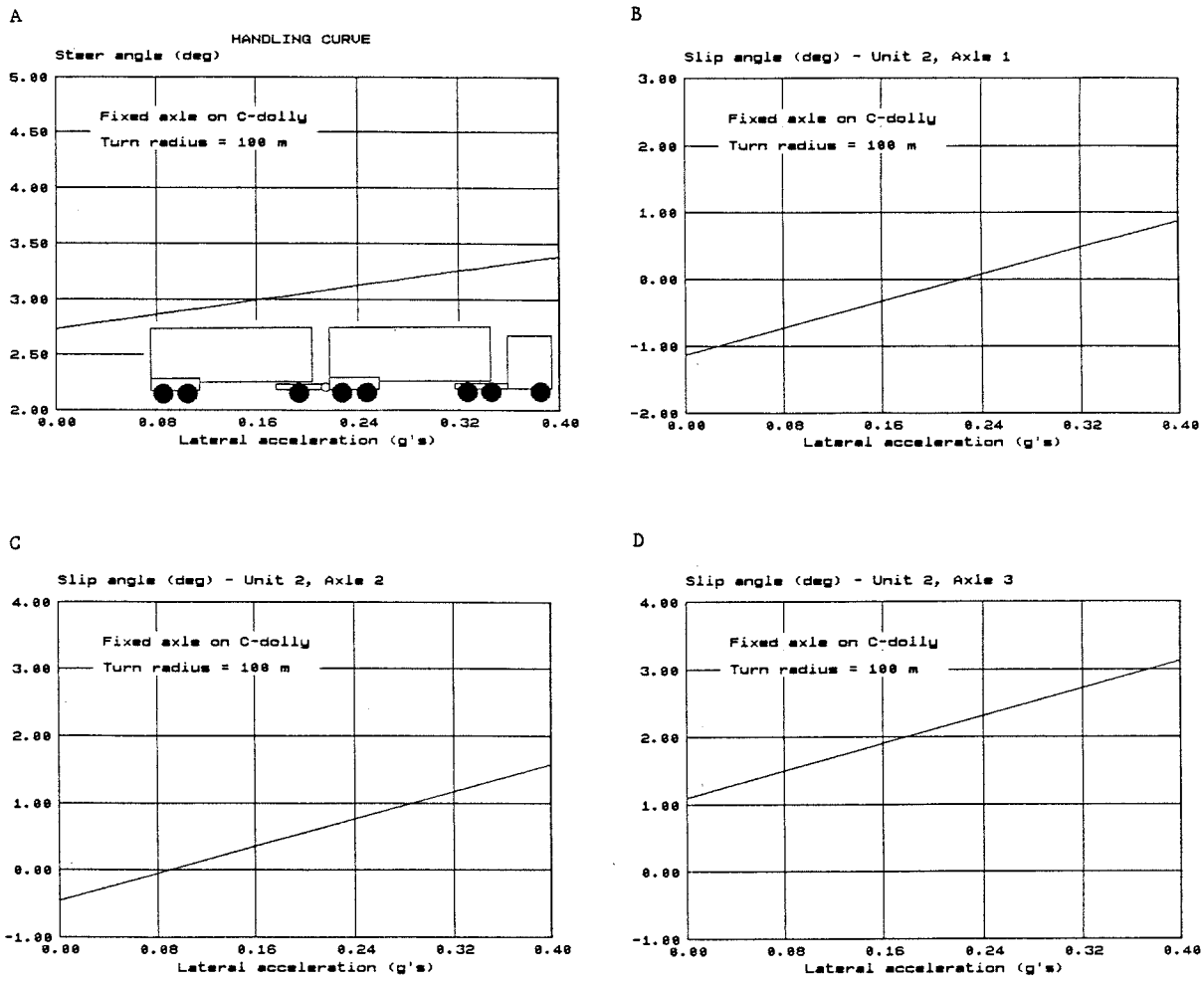

Figure 14. C-train with Fixed C-dolly Axle

In the dual-axle C-train simulation, the load carried by the C-dolly was assumed to be twice the load carried by a C-dolly with a single axle. The results show that the magnitude of the lead trailer tire slip angles are very sensitive to changes in the magnitude of the centering force (F_{co}). Hence, this configuration is inherently susceptible to tire saturation when travelling on a wet surface or when carrying a cargo with a low center of gravity.

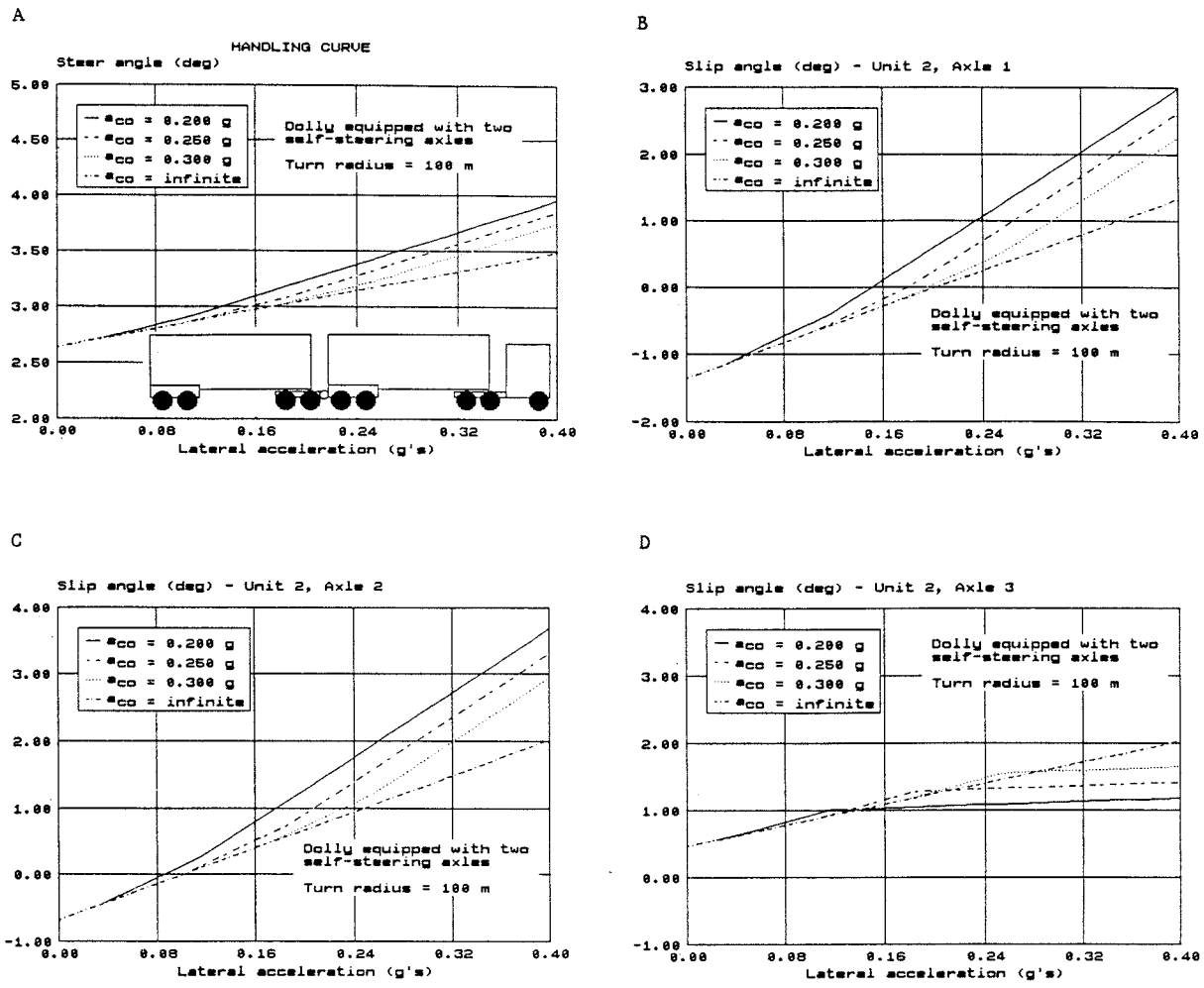

Figure 15. C-train With Two Self-steering Axles

The results for a C-train with one self-steering axle, such as those currently in service in some parts of Canada [Figures 16] show that the influence of varying the self-steering axle centering force has little effect on the vehicle handling characteristics and on the magnitude of the lead trailer tire slip angles. In fact, for a centering force of 0.25 g, the tire slip angles on the lead trailer and C-dolly are, in general, more evenly distributed on this particular C-train than they are on a C-train with a fixed C-dolly axle.

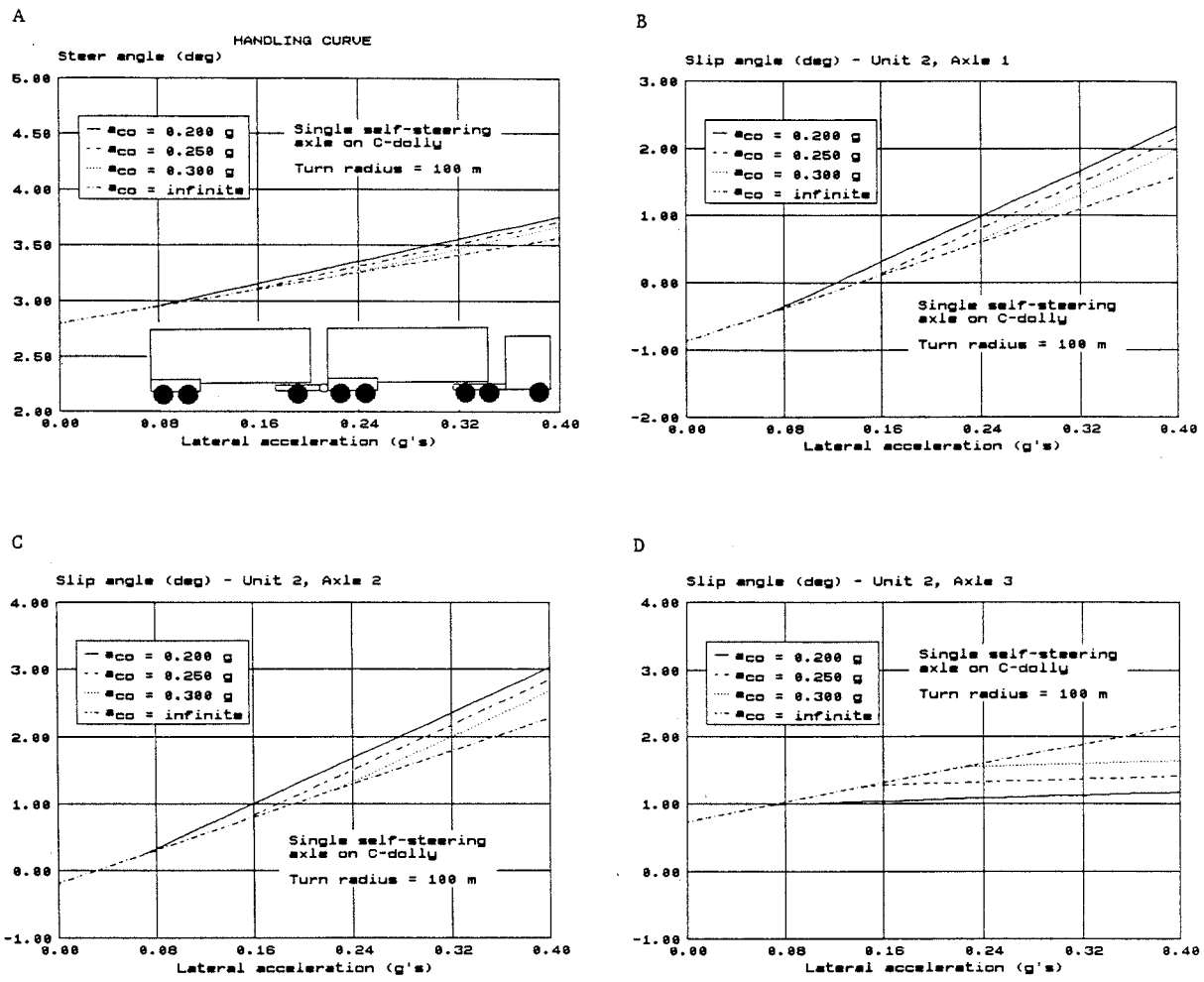

Figure 16. C-train With One Self-steering Axle

Based on these simulations, it is clear that the straight truck-fulltrailer with C-dolly exhibits such high levels of oversteer that the yaw stability of the vehicle can be seriously degraded and therefore the use of this configuration should be strongly discouraged. It is also clear that the C-train with two self-steering axles on its C-dolly exhibits high tire slip angles on the lead trailer's axles, making the vehicle very susceptible to tire saturation and consequent yaw instability. As a result, the use of this configuration should also be strongly discouraged.

These simulations also indicate that the C-train with a fixed axle exhibits high tire slip angles on the C-dolly's axle, making it very sus-

ceptible to tire saturation. Although this does not imply that yaw instability of the vehicle is imminent, it translates into very high loads on the pintle hooks and high stresses within the C-dolly's frame. Premature structural failure could easily result.

Finally, these simulations reveal that the C-train with one self-steering axle does not exhibit the undesirable characteristics found for the other three configurations noted above. Conceptually speaking, this particular configuration avoids deteriorating the vehicle's handling characteristics (in terms of yaw instability caused by tire saturation), while it relieves structural stresses in cornering. Moreover, this configuration makes better use of the available cornering forces from each tire, and also helps to prolong tire life.

4.3 Practical Analysis of Self-steering Axle Centering Force

Self-steering axles used in the C-dolly application must be capable of generating some magnitude of side force and must resist steering action caused by differential brake or rolling resistance loads. An examination of the service record of the C-dolly reveals that the most common performance problem associated with the axle is related to unwanted steer action caused by imbalanced braking and/or rolling resistance forces. There have been at least three accidents attributed to this problem. Therefore, along with requirements pertaining to lateral forces, resistance to unbalanced longitudinal forces must also be among the performance criteria for self-steering axles. If regulatory principles are devised that differentiate between these two forces, the designers of self-steering axles will be provided some valuable creative latitude in the development of self-steering systems specifically geared to the C-dolly application.

4.3.1 Cornering Force Characteristics, and Minimum Requirements

In determining a reasonable minimum level of cornering force to recommend for C-dolly applications in C-trains, the authors have taken into account the cornering force values of C-dollies currently in service in Canada which have displayed a good field record; the steady-state analysis in Section 4.2.7 of this report, which reveals that the C-train is relatively insensitive to small changes in the minimum level of cornering forces (changes in the order of no more than 0.05 g); and views expressed by UMTRI to the Province of Saskatchewan in December 1987. It was also evident that excessively high cornering forces generated by a self-steering axle could overstress and possibly fracture the C-dolly's frame and/or hitch assembly while in service.

During the course of the study, the Province of Saskatchewan introduced a regulation that all C-dolly self-steering axle assemblies be capable of generating a cornering force of at least 0.30 g. The incidence of stability problems, culminating sometimes in loss of vehicle control, was

thereafter effectively reduced to zero. This field experience provided a valuable benchmark for the determination of minimum acceptable performance requirement for self-steering axles.

The primary benefit arising from this requirement came from an improvement in the C-dolly axle's brake-steer performance, to a level which the authors recommend maintaining in all future C-dollies. This is discussed in Section 4.3.2 later in this report. It is the authors' opinion that, provided this minimum brake-steer requirement is retained, a technically-sound minimum level of cornering force for a C-dolly self-steering axle in a C-train configuration would be 0.25 g, or 25 percent of the rated axle load.

As indicated in Section 4.2, it is also important that the minimum level of cornering force be reached within a specified angular displacement. All self-steering axles tested on the C-dolly facility built for this study reached the plateau region of their cornering force curve within a steer angle of 1.0°. Hence, to avoid any deterioration in this important aspect of cornering performance, self-steering axles should be required to reach a cornering force of 0.25 g within a steer angle of 1.0°.

The limits noted above effectively establish values for the variables introduced in Section 4.2.5 as follows:

$$a_{comin} = 0.25 \text{ g}$$

$$\delta_{omax} = 1.0°$$

The Cornering Performance Criterion therefore is met when the self-steering axle cornering characteristics are such that the point (δ = 1.0°, a_c = 0.25 g) lies below the loop segment corresponding to an increase in the self-steering angle (i.e., the axle's outward excursion), and the point (δ = -1.0°, a_c = -0.25 g) lies above the loop segment corresponding to an increase in the self-steering angle in the opposite direction.

The discussion of axle stiffness requirements so far has dealt only with its behaviour when moved outwards from zero steer. The characteristics of the returning force vs. angular displacement must also be specified because in some cases Coulomb friction can be high. A lower spring rate on the axle's return is beneficial to the vehicle because it reduces the total side force generated by the axle group and, therefore, acts to reduce corrective lateral accelerations of the vehicle. This phenomenon was observed during field tests (Woodrooffe and Billing 1983). An excessively low return spring rate (for example, a "negative" spring rate) would also be undesirable because the axle could easily get caught in the steer position. Therefore, when returning, the axle must reach an angular displacement of less than 1.0° by the time the cornering force reaches zero. This is represented by Point A on Figure 17, a diagram

which denotes the cornering forces of an axle with acceptable return characteristics. Further examination of Figure 17 reveals that in general, to meet the return characteristics noted above, while at the same time just barely achieving a 0.25 g cornering force at 1.0° of steer angle on the outward excursion, the magnitude of the Coulomb friction will be less than half of a_{comin}.

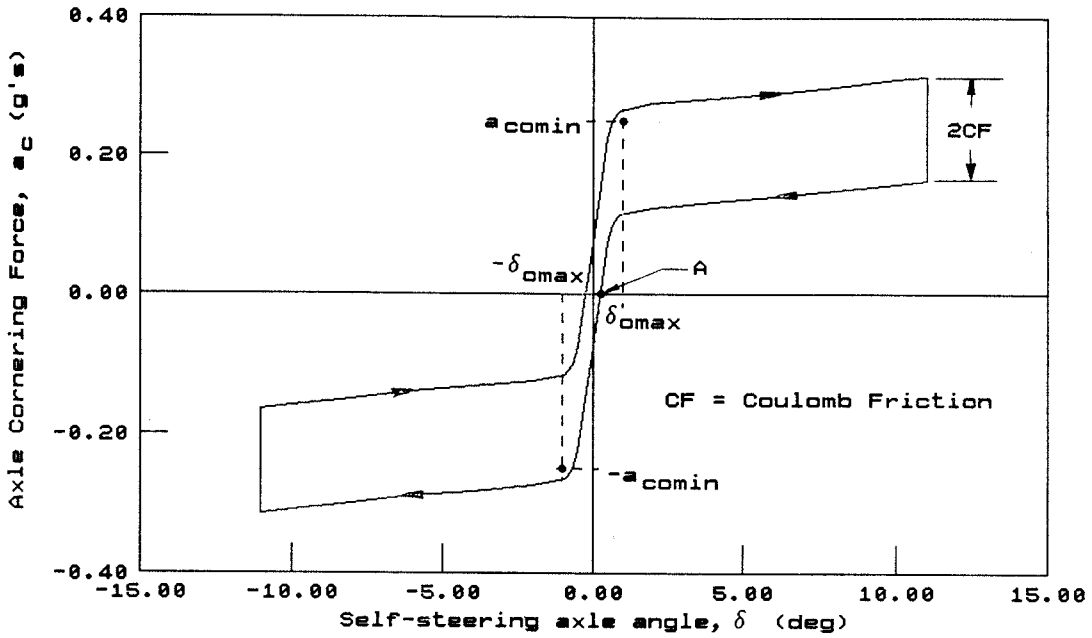

Figure 17. Self-steering Axle with Acceptable Return Characteristics

In contrast to Figure 17, Figure 18 shows the cornering performance of a (hypothetical) self-steering axle with unacceptable return characteristics, owing largely to the presence of excess Coulomb friction.

As mentioned in Section 4.2.2, the side force balance equation [Equation 2] reveals that the presence of dual tire moments deteriorates the self-steering axle's ability to generate side force. However, in practice the magnitude of these moments is small and does not significantly alter the performance of self-steering axles. This is revealed as follows:

The moment M_{dt} generated by a pair of dual tires is given by $C_s D^2/R$ [Appendix A], where C_s is the single tire longitudinal stiffness, D is the dual wheel spacing, and R is the turn radius. For a typical pair of dual tires, we obtain:

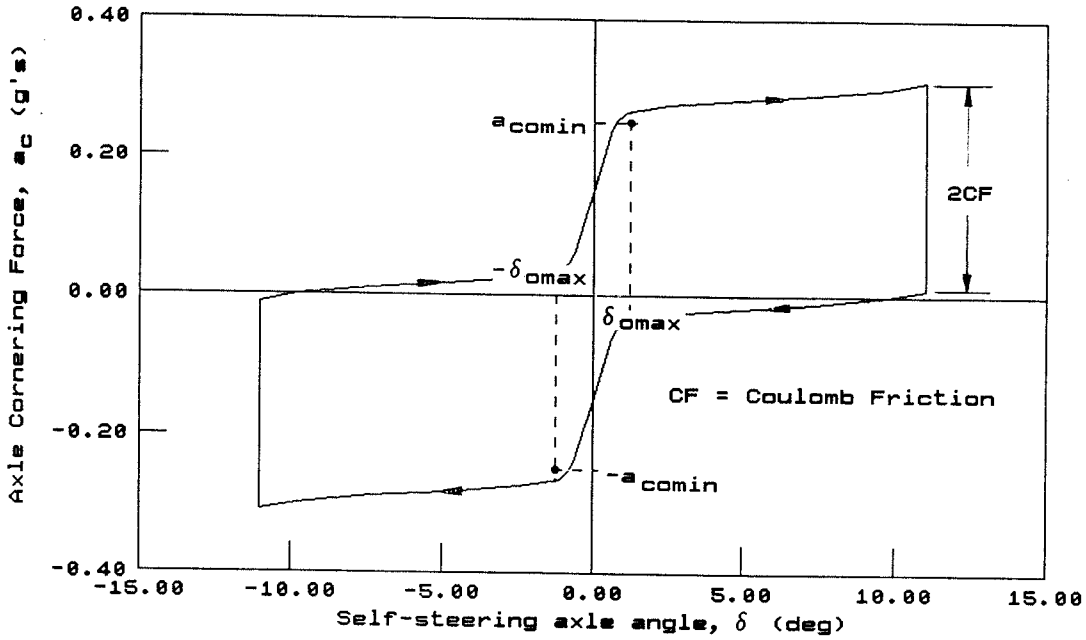

Figure 18. Self-Steering Axle with Unacceptable Return Characteristics

$$C_s = 225 \text{ kN/slip } (50500 \text{ lb/slip})$$

$$D = 0.32 \text{ m } (1.05 \text{ ft})$$

$$R = 30 \text{ m } (98 \text{ ft})$$

$$M_{dt} = 766 \text{ N·m } (567 \text{ ft·lb})$$

This means that for a turn radius of 30 meters, a pair of dual tires will produce a total aligning moment of 766 N·m; on a turntable self-steering axle this is equivalent to a cornering force of 0.02 g, while on an automotive self-steering axle it is equivalent to approximately 0.03 g. If the turn radius were increased to 60 m, the aligning moment would be decreased by factor of two to 383 N·m. For speeds where stability and control are a concern, these moments are so small as to be within the error range to which self-steering axles are tested (i.e., ± 2.5% of the required centering force).

4.3.2 Brake-steer Performance, and Minimum Requirements

As mentioned in Section 4.3.1, field experience in Saskatchewan provides a valuable benchmark for the minimum acceptable performance of self-

steering axles, particularly as regards their brake-steer behaviour. Following the introduction of a minimum cornering force requirement (of 0.30 g), incidents arising from unwanted steer caused by unbalanced longitudinal loads were effectively reduced to zero. In the present study, therefore, the authors adopt the position that the brake-steer performance level of all future axles must meet or exceed that achieved by axles currently fulfilling the Saskatchewan requirements. To provide a basis for comparison, we establish a reference or "baseline" axle chosen from among those certified as acceptable by the Province of Saskatchewan.

As part of this study, a test facility was designed and built by NRC to measure the characteristics of self-steering axles. The apparatus, shown in Figure 19, uses air bearings to eliminate forces in the surface plane between the tires and the road. It also permits the axle to be loaded vertically while a steering moment is applied to the axle. As the axle steers, both the steer angle and steer moment are measured and recorded, thus yielding the steer moment diagram for that particular axle. Using this data in conjunction with the kingpin offset and caster trail dimensions permits full characterization of the axle. The baseline axle was characterized in this way. Its cornering force characteristic curve is shown in Figure 20. Its moment arm ratio (t/w) was measured to be 0.364. (The characteristic curves of several other typical axles, as measured on the test facility, are shown in Appendix E.)

To prevent deterioration of the ability of self-steering axles to resist steer action when subjected to unbalanced longitudinal forces, all new self-steering axles must satisfy the requirements of the Brake-steer Performance Criterion developed in Section 4.2.4.

Figure 20 shows that the baseline axle generates a cornering force of 0.30 g at a self-steering angle of 1.0°. Note also that the moment arm ratio (t/w) measured for the axle is 0.364. Hence, from the expression that relates the cornering force to the brake-steer force, namely,

$$a_b = a_c \cdot t/w \qquad 14$$

we find that the baseline self-steering axle will generate a brake-steer force of 0.11 g (= 0.30 · 0.364) at a steer angle of 1.0°.

The numbers obtained above from the baseline axle are effectively the values for the parameters introduced in Section 4.2.5 as follows:

$$a_{bomin} = 0.11 \text{ g}$$

$$\delta_{omax} = 1.0°$$

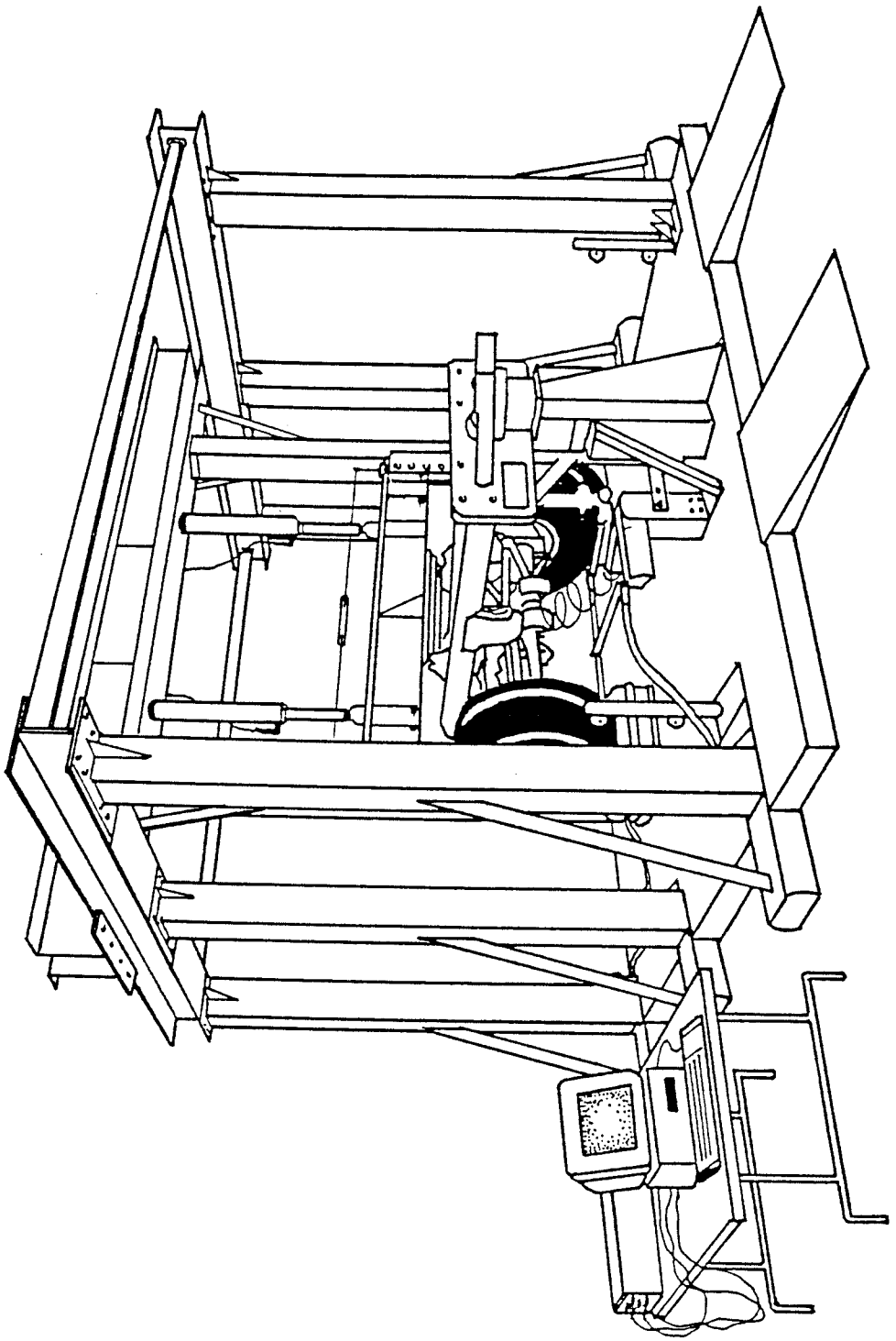

Figure 19. The Self-steering Axle Test Facility Developed for this Study

Hence, the Brake-Steer Characteristics Requirement is met when a self-steering axle's brake-steer characteristics are such that the point (δ = 1.0°, a_b = 0.11 g) lies below the loop segment corresponding to an increase in self-steering angle and the point (δ = -1.0°, a_b = -0.11 g) lies above the loop segment corresponding to an increase in self-steering angle in the opposite direction.

We now select a braking ratio (B_r) of 0.36 to define the braking condition to be used in the Brake-steer Diagram Requirement. This value represents a severe unbalanced braking condition and, as shown in the brake-steer diagram [Point A on Figure 21], the baseline self-steering axle steers to a maximum of 5.0° when subjected to this braking condition, or in other words that:

$$\delta_{xomax} = 5.0°$$

Hence, to satisfy the BSDR a self-steering axle must steer by an amount less than or equal to 5.0° when equipped with a pair of standard dual tires and subjected to an unbalanced braking force in which

$$B_r = 0.36.$$

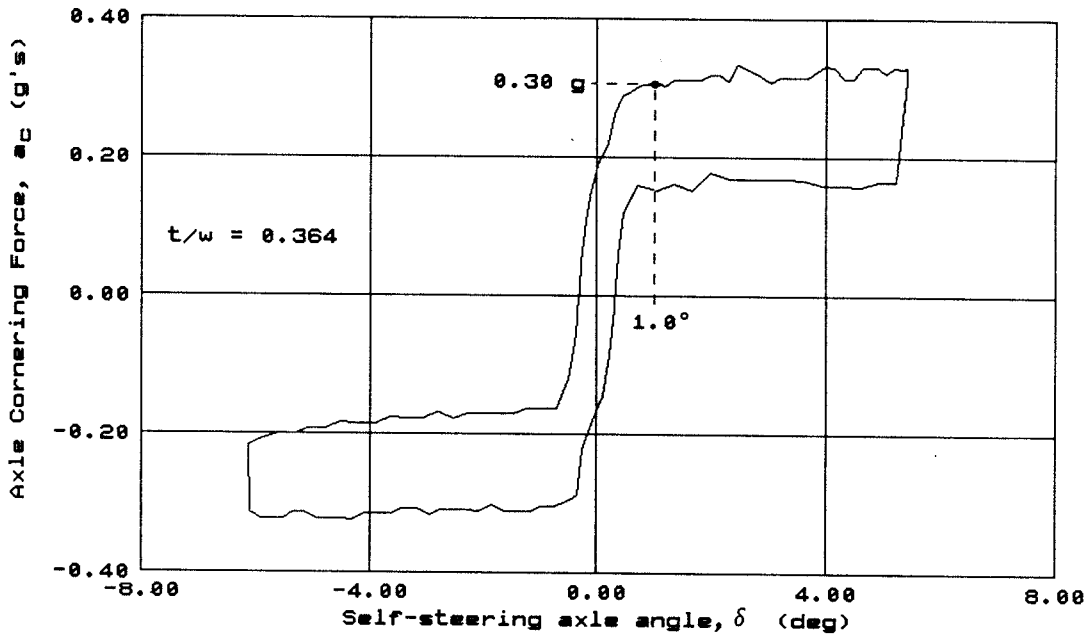

Figure 20. Cornering Force for the Baseline Self-steering Axle.

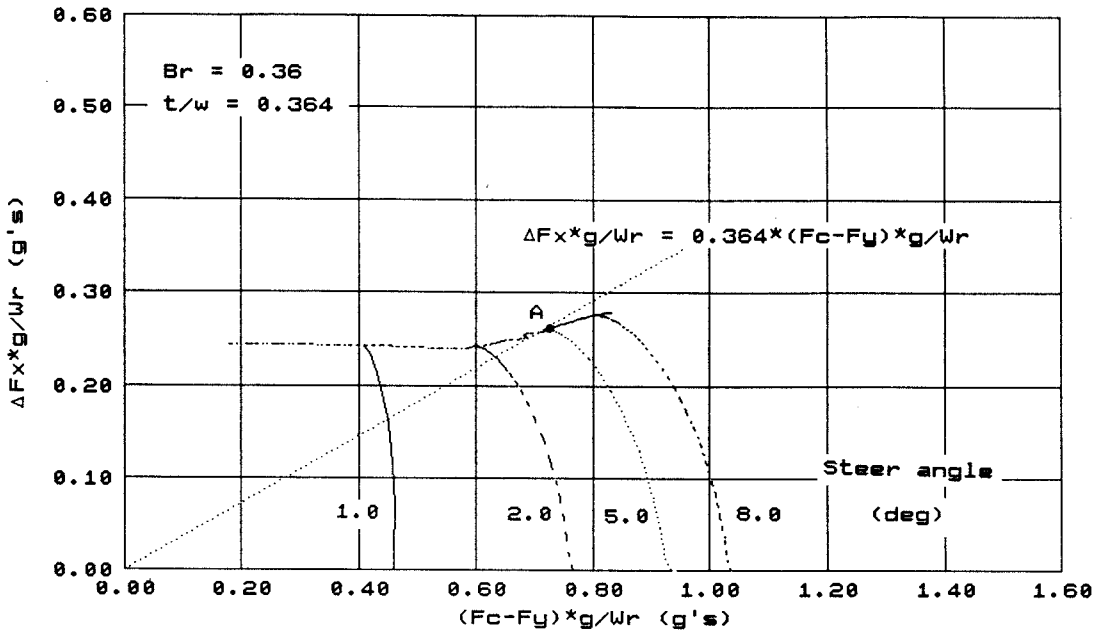

Figure 21. Brake-steer Diagram for the Baseline Self-steering Axle

We now illustrate, with two examples, how either the BSCR or the BSDR can be the governing requirement within the Brake-steer Performance Criterion. First, take a self-steering axle whose cornering forces are less than those of the baseline self-steering axle. Its characteristic curve is shown in Figure 22. It will generate 0.25 g at a steer angle of 1.0°. When equipped with a pair of reference dual tires and subjected to a braking condition defined by B_r = 0.36, the handling diagram [Figure 23] reveals that the moment arm ratio (t/w) for the axle must be greater than or equal to 0.393 in order to satisfy the BSDR. As far as the BSCR is concerned, this axle will generate the necessary minimum brake-steer force of 0.11 g at a steer angle of 1.0° provided that its moment arm ratio (t/w) is greater than or equal to 0.440 (= 0.11/0.25). Consequently, the BSCR places a more stringent demand on the moment arm ratio than does the BSDR, and so the BSCR governs. Hence, the axle must have a moment arm ratio of greater than or equal to 0.440.

Now take a second axle whose cornering forces are greater than those of the baseline self-steering axle. Its characteristic curve is shown in Figure 24. It will generate 0.35 g at a steer angle of 1.0°. To satisfy the BSDR, this axle must have a moment arm ratio of greater than or equal to 0.338, as revealed by its brake-steer diagram [Figure 25]. As regards the BSCR, its minimum brake-steer force requirement will be satisfied if

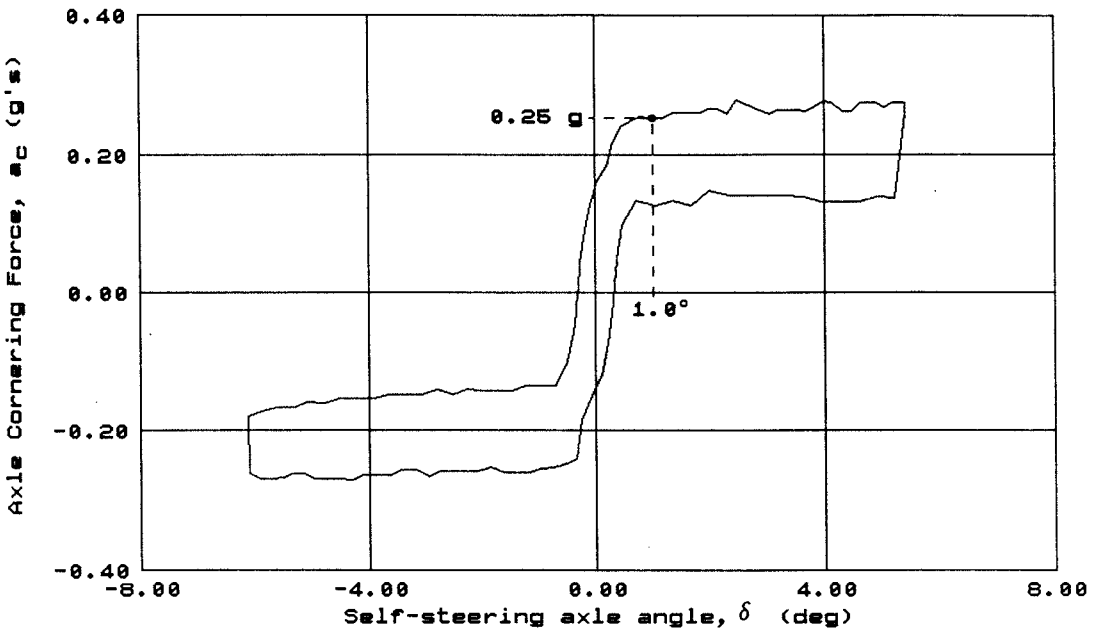

Figure 22. Cornering Characteristics for Self-steering Axle Generating 0.25 g at 1.0°

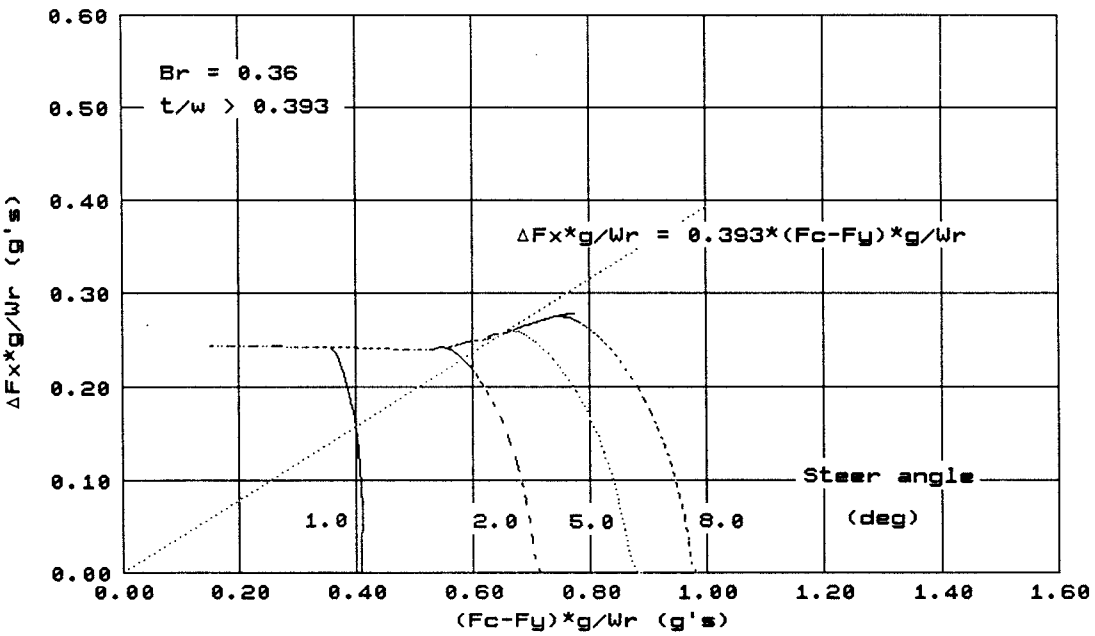

Figure 23. Brake-steer Diagram for Self-steering Axle with Characteristics as Illustrated in Figure 22

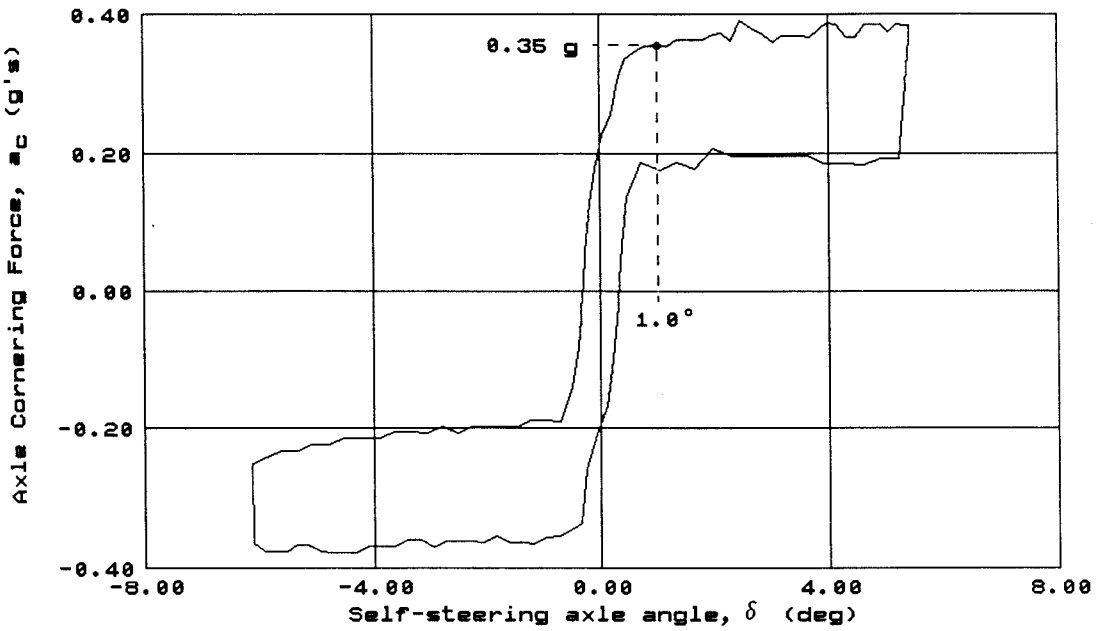

Figure 24. Cornering Characteristics for Self-steering Axle Generating 0.35 g at 1.0°

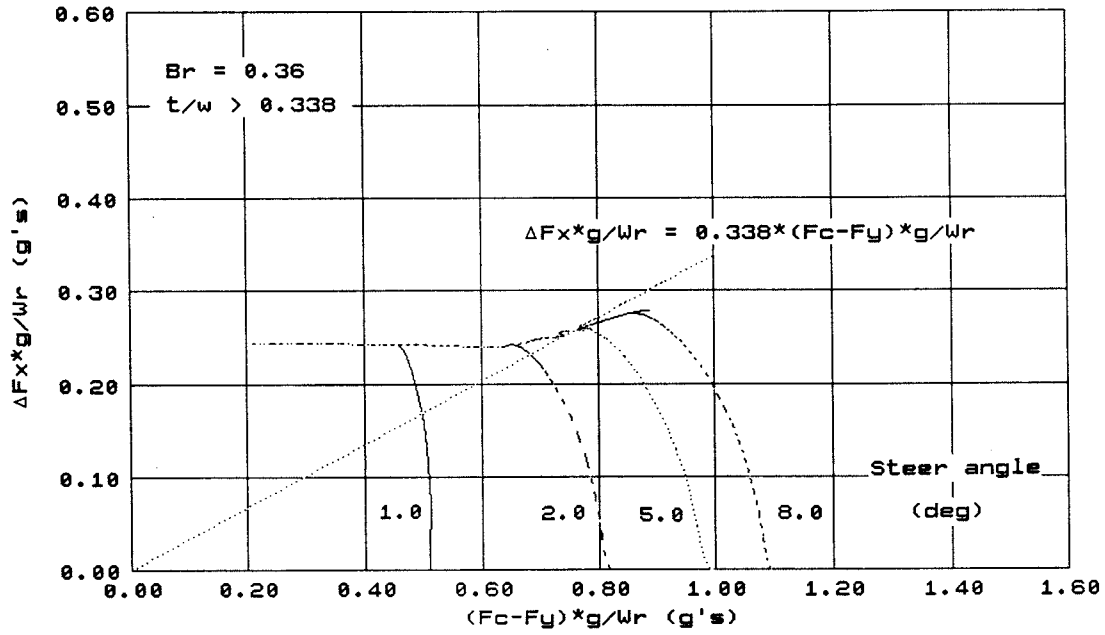

Figure 25. Brake-steer Diagram for Self-steering Axle with Cornering Characteristics as Illustrated in Figure 24

the moment arm ratio is greater than or equal to 0.314. In this example, the BSDR places the more stringent demand on the moment arm ratio, and so it governs. Therefore, the moment arm ratio must be greater than or equal to 0.338.

In general, the brake-steer performance of an axle whose cornering forces are lower than those of the baseline self-steering axle will be governed by the BSCR, whereas the brake-steer performance of an axle whose cornering forces are higher than those of the baseline self-steering axle will be governed by the BSDR.

Given the unlikelihood that a manufacturer will produce a self-steering axle that generates a cornering force greater than that of the baseline axle, (i.e., 0.30 g at 1.0° of steer), the BSDR becomes superfluous and need not be considered further.

At this point, the authors would note that for rounding purposes they would propose setting a_{comin} at 0.10 g.

4.3.3. Hitch Forces

The documentation from previous work has been helpful in establishing the magnitude and direction of maximum expected hitch loads. From Winkler et al. (1986), the maximum loading predicted at the hitches is as follows:

Longitudinal $F_x = \pm 22000$ lb (98 kN);

Vertical $F_z = \pm 22400$ lb (100 kN); and

Lateral $F_y = \pm 8660$ lb (38.5 kN).

These hitch loads represent maximum expected values, i.e., resulting from a worst-case dynamic incident. Some experimental data on hitch loads were reported by Woodrooffe and Billing (1983):

> Under normal conditions, the highest hitch load experienced was as a result of cornering at a 90° intersection type turn. The 34 kN (7600 lb) longitudinal maximum load was essentially equal and opposite in the drawbars of the dolly. This is a result of the moment induced by the side force of the C-dolly tires and the resultant force of the rear trailer focussed at the C-dolly fifth wheel. These forces act over the drawbar length of the dolly, and are balanced by the lateral spread of the C-dolly drawbars. This illustrates the importance of dolly drawbar length and lateral spread.
>
> Two unusual maneuvers produced high loads. Negotiating a 90° turn with the C-dolly axle locked, resulted in an equal and

opposite longitudinal, or lozenging, forces in the drawbars of 56 kN (12500 lb). Climbing an 18 cm (7 inch) high curb with the C-dolly inner wheel resulted in high torsion and longitudinal loads.

The torsion of the dolly frame induced opposed vertical loads in roll moment at the pintle hooks of approximately 37 kN (8300 lb). Extreme maneuvers, such as high speed lane changes that resulted in roll of the trailers, also resulted in high hitch loads, as a function of tractor lateral acceleration. All three components tended to increase approximately linearly, except that as rollover was approached the vertical component started to increase very rapidly. Maximum resultant loads just before rollover were generally in the range 30 - 35 kN (6700 - 7800 lb), but would be much higher (though possibly of academic interest) if rollover had not been prevented by the outriggers.

During one run on a low friction surface when outriggers were not installed, a tractor jackknife occurred which resulted in total loss of control of the vehicle, which slid off the paved test area onto the adjacent grass. When the tractor and lead trailer tires dug into soft ground, the vehicle stopped abruptly which resulted in roll angles for these units of close to 45° and 30° respectively. The roll restraint provided by the C-dolly undoubtedly prevented rollover of the vehicle. The first crossmember of the dolly frame yielded in torsion, and the misalignment of the drawbars was about 2.9°. The measured peak vertical load on the hitch at yield was about 37.7 kN (8500 lb) but the longitudinal load was close to 130 kN (29000 lb). It is possible that failure was due to the combined high vertical and longitudinal loads. In a laboratory test of a spare dolly frame, yield started at a vertical load of about 35.7 kN (8000 lb) and the plastic limit was reached at a load of 66.9 kN (15000 lb). [Pages 29 and 30.]

Considering the two sources and recognizing that safety factors are built into hitch designs, it would be appropriate to expect a rated load capacity of each hitch used by C-dollies as follows:

Longitudinal F_x = 400 kN (90000 lb);

Vertical F_z = 100 kN (22500 lb); and

Lateral F_y = 40 kN (9000 lb).

Note that the 400 kN longitudinal hitch force requirement represents the sum of two forces, that is, (a) 220 kN, which is calculated on the basis of 115 percent of the 26.1 tonne maximum gross trailer weight as recommended by SAE J849b, which we then reduce by 25 percent in recognition that two hitches will bear the load in a C-dolly as opposed

to one hitch in the SAE calculations; and (b) 180 kN associated with the unique mechanics of the C-dolly. The assumptions are that in a tight radius turn where the lead trailer is in pure rotation about a turn centre, 2.3 metres ahead of the dolly axle, the dolly tires are saturated. Having a 9.1 tonne axle load operating on a road surface with a coefficient of friction of 0.8, a force of 180 kN is seen at the hitches based on a drawbar length of 2 m and a hitch spread of of 760 mm.

With any vehicle coupling system, it is beneficial to eliminate hitch slack as it reduces longitudinal action of the vehicle. Because of the geometry of the C-dolly, hitch slack not only produces longitudinal action but also provides unwanted yaw action of the frame. This yaw freedom is, in fact, equivalent to steer freedom at the axle. A dolly with 10 mm of slack in both hitches will exhibit a 1.5° of steer freedom. This steer freedom counteracts the benefits of the centering action of the steering system. Therefore, it is important that slack be removed from the hitches.

The mounting position of hitches would benefit from uniformity. Failure to do so could result in variations from the level position, which would cause inclination of the steering axle's kingpin. The lateral centre-to-centre spacing of hitches currently is 30 inches (762 mm). The mounting height of the hitches, measured from the ground to the centre of the drawbar eye on an unloaded vehicle, is approximately 36 inches (914 mm).

It would seem appropriate to recommend standard hitch mounting dimensions, when expressed in SI units and rounded for convenience, as follows:

Lateral centre-to-centre hitch spacing: 760 mm $\pm$ 2 mm; and

Vertical centre-of-eye mounting height on unloaded vehicle: 900 mm $\pm$ 10 mm.

4.3.4 Roll Coupling/Drawbar Torsion

In general, roll coupling of the trailers in a C-train increases the roll stability of the entire vehicle. This roll (torsional) coupling is provided by the C-dolly frame structure and the lateral positioning of the hitch points. Some torsional flexibility between the trailers is nevertheless important for reducing the forces and stresses within the trailer and dolly frame members during normal maneuvers. Without it, unnecessarily high loads will occur frequently, possibly causing fatigue failure of components. The trucking industry already provides some torsional flexibility by the use of compensating fifth wheels and pitch-pivoting or "limp wrist" drawbar eye assemblies.

The torsional flexibility required between trailers joined by a C-dolly, however, can, and should, be provided through a well-engineered design of

the dolly frame structure itself. Torsional stiffness need not be linear, and if nonlinear, it should be biased toward increasing stiffness as a function of rotational displacement. The frame must also be capable of transmitting a minimum level of torque.

There is a dearth of literature to help establish the choice of an appropriate minimum torsional compliance value for the C-dolly frame. The torsional stiffness of heavy truck frames ranges from 900 N·m/deg to 1800 N·m/deg (8000 and 16000 in-lb/deg), as reported by Fancher et al. (1986), but for purposes of improved steering control, truck frames are known to be inherently weak in torsion. This is because the drive axle group of the tractor provides all the roll stiffness for the front end of the semitrailer. Considering the C-dolly must provide adequate roll coupling between the trailers without excessive torsional compliance, it is clear that the net torsional stiffness of the C-dolly frame must be significantly greater than that of a tractor frame. As mentioned earlier in this section, a significant amount of torsional flexibility, particularly at low relative roll angles, would be helpful in reducing hitch loads during maneuvers in rough freight yards or during curb climbing. These seemingly contradictory requirements can be accommodated by developing a two-stage minimum torsional compliance requirement, which would give the designers of frame structures some freedom for innovation.

There is also a need to specify a minimum value for torsional strength of the dolly frame. Here, again, there is no published recommended minimum value; however, considering the hitch forces experienced during field tests (Woodrooffe and Billing 1983), it appears that the C-dolly frame structure should be capable of withstanding at least 45000 N·m (400000 in·lb) torque without permanent deformation.

The principal benefit of roll coupling is seen during sinusoidal or evasive maneuvers of a loaded vehicle on high friction surfaces. There is a phase shift in the roll action of the two trailers. Under this condition, the coupling of the trailers in roll helps to counterbalance the relative roll of the trailers, allowing the kinetic energy of the roll to be transferred between trailers and equalized, thereby increasing the probability of a successful maneuver. During this maneuver, the maximum relative roll between the trailers should be no more than 15 degrees. Therefore, the maximum torsional limit of the dolly frame should be achieved within 15 degrees. Simple deduction suggests that the minimum torsional stiffness of the dolly frame that must be provided is 45000 N·m ÷ 15 degrees = 3000 N·m/deg (26500 in·lb/deg).

5.0 PROPOSED C-DOLLY REGULATIONS DERIVED FROM THE TECHNICAL FINDINGS

As with most heavy truck components, C-dollies must endure rough service in extreme environmental conditions over a long period of time. In establishing performance criteria and regulatory principles for the

C-dolly, a major consideration is to formulate clear, simple, and straightforward requirements and to constrain only the key parameters so as not to inhibit further innovations. It is also important that any control systems for the C-dolly be simple and foolproof, in recognition of the effects of long term abuse, extended maintenance intervals, and possible neglect. It is not unreasonable to assume that life of a dolly may exceed five million kilometers.

A point summary of relevant findings of this study, pertaining to hardware and performance of the C-dolly and its mechanisms, follows:

5.1 Self-steering Axle Cornering and Brake-steer

Caster steering systems must contribute to the cornering force requirements of the C-train. They must also resist unwanted steer due to imbalanced brake or rolling resistance forces. This leads to a requirement that **the caster steering system must generate a minimum lateral force equal to 25 percent of a specified axle load capacity and a minimum longitudinal force of 10 percent of the same specified axle load capacity.** The lateral force measurement shall include a correction to account for pneumatic trail, which will be taken as a 50 cm addition to the mechanical caster trail dimension. No correction factor is required for the longitudinal force measurement. **The minimum force requirement must be attained within the 1.0 degree of steer on either side of the zero steer position. The angular displacement over which the minimum force requirement must be maintained is 15° relative to the zero steer position. On return of the axle from 15° to the zero steer position, the axle must return on its own to within 1° of centre.** Any test for compliance must be conducted with a vertical load on the axle equal to the 9.1 tonnes which is equivalent to the legal single axle load limit for the C-dolly. The tires of the axle must be supported by frictionless pads, or the equivalent, to eliminate tire friction forces and tire aligning moments during the test.

5.2 Centering Force Control

Most C-dollies have controls that allow an operator to change the magnitude of the self steering centering force. Varying the magnitude of this centering force allows the steering system to function during cornering when the vehicle is empty. The ostensible need to have the axle steer in the empty condition is questionable, as the consequences of no steer action during cornering in an empty vehicle are minor. While there is a slight increase in tractive effort needed from the power unit, as well as scuffing on the trailer and C-dolly and a marginal increase in vehicle offtracking, no significant stresses are imposed on the vehicle when compared with the loaded condition because of the low axle loads in the empty condition.

By comparison, the consequences of a low centering force, whether by choice or accident, on the behaviour of a loaded vehicle can be severe, as revealed by previous research. It is recommended, therefore, that **in the interest of road safety, any control on the C-dolly that allows for variations in the magnitude of the steer centering force should be prohibited.** It is also recommended that **centering force systems operated by compressed air or hydraulic pressure should be equipped with a good-quality pressure gauge readout at the C-dolly showing the amount of pressure at the centering device. Adjacent to the gauge should be a label clearly indicating the minimum design pressure that the C-dolly must have to comply with the centering force requirements.**

5.3 Self-steering Axle Lock

Locking the self-steering axle in the zero steer position is required when reversing the vehicle because caster steering systems are absolutely unstable when travelling in reverse. Most self-steering axles are fitted with electrically- or pneumatically-actuated locking pins. Locking the steer axle at highway speeds has merit because the axle performs like a non-steering axle and does not respond to lateral inputs.

Operators should be encouraged to lock the steering axle at highway speeds, especially when operating under adverse weather conditions, when on gravel or icy roads, or when travelling sections of highway that are very rough or under repair. Since any of these factors can occur during the course of a trip, it would be beneficial if the axle lock system could be activated from the cab. Therefore, it is recommended that **all C-dollies be equipped with a steer-locking system that can be activated by the driver in the cab of the tractor and that C-train tractors be equipped with the necessary switch hardware. The label (noted in Section 5.2) to be affixed adjacent to the air pressure gauge readout at the C-dolly, should include a warning that the axle must be locked when the vehicle is operating on anything other than a hard surfaced dry road.**

For emergency purposes, the C-dolly must also be equipped with a separate manual locking mechanism that allows the steering to be locked independently of the remote locking system.

Automatic locking systems activated by a speed threshold or by keying to a particular gear shift should be viewed favourably. Because these locking systems would leave the axle unlocked at lower speeds -- perhaps 50 km/hr -- they must **not** be used in place of the recommended centering force requirements of the axle. However, if a C-dolly were used in heavy-duty hauls on poor quality roads, it may be appropriate to request that speed-activated locking systems be installed as a condition for issuing a special permit.

5.4 Frame and Hitch Considerations

The two hitches, or an equivalent mechanism and backing plate assembly that attaches the C-dolly to the lead trailer, will require the following minimum ratings:

Longitudinal F_x = ±400 kN (90000 lb) or equivalent moment based on 760 mm moment arm;

Vertical F_z = ±100 kN (22500 lb) or equivalent moment based on 760 mm moment arm; and

Lateral F_y = ±40 kN (9000 lb).

The above calculations have been based on a hitch spacing of 760 mm. A hitch spacing of less than 760 mm will result in higher hitch forces which will render the above hitch ratings invalid.

Where possible and practical, the lateral centre-to-centre mounting position of the hitch should be 760 mm ± 2 mm and the mounting height as measured from the ground to the centre of the drawbar eye on an unloaded vehicle should be 900 mm ± 10 mm. Longitudinal slack or free play between the hitch and the drawbar eye should not exceed 5 mm.

An effective means of control over the mounting height of the hitches is important to vehicle safety when considering vehicle interchangeability. Variation in vertical hitch location from the dolly design height will result in kingpin angulation which will change the effective caster trail dimension of the dolly. Changes in caster trail due to practical variations in hitch height, (± 20 cm) can render the axle unstable or can reduce the side force generated by the axle by approximately 50%.

The means by which the drawbar eye connects to the hitch is a matter which requires further investigation. Very few hitches on the market are suitable for the C-dolly. However, ISO standards 1102 and 3584 specify hitch and mounting details that serve as an example of the type of hitch design and performance specification that would be beneficial to the industry in Canada.

Hitches that do not comply with the ISO standards 1102 and 3584, despite meeting the rated load requirements for C-dolly applications as outlined in this report, may not prove to be suitable in terms of reliability, method of operation, long-term service potential, and safety. **It would be appropriate to strike a committee to develop guidelines for the design, construction, and operation of such hitches and to put in place an approval (certification) process as soon as possible so that manufacturers could respond with suitable equipment.**

With respect to the torsional stiffness and strength of the C-dolly draw-

bar frame structure, **the minimum torsional stiffness provided about the hitch point of the C-dolly should be 3000 N·m/deg (26500 in·lb/deg) of roll and the drawbar and dolly structure should be capable of providing at least 45000 N·m (400000 in·lb) of torque within 15 degrees of torsional displacement without suffering any residual deformation.**

5.5 Tires

Tires fitted to the steering axles of trucks already receive special attention; self-steering axles on the vehicle must be treated in a similar manner, and in addition, there are some unique considerations.

As shown in the analysis part of this report, dual tires impose an aligning moment on the steering axle when curving because, in a curve, the tire of a dual pair on the outer radius of the curve will travel farther than the tire on the inner radius of the curve. Since the dual pair cannot revolve with respect to each other, an aligning or steering moment is generated by the longitudinal slip characteristic of the tire. If the tires are not matched in both diameter and inflation pressure, this aligning moment will tend to counteract the beneficial effect of the steer centering force mechanism. It is, therefore, extremely important that the pair of tires forming a dual tire set be matched in terms of size and state of wear.

Because different manufacturers produce slightly different tread designs and rubber compounds, which affect the longitudinal stiffness of the tires, it is important that self-steering axles be fitted with matched tires. This implies that **the tires of a self-steering axle should be of the same manufacturer, size, tread, style, and tread wear. It is recommended that a rib style tread be used on the self-steering axle and that re-capped tires be prohibited from use on a self-steering axle.**

5.6 Vehicle Configuration

The C-train represents a unique vehicle combination that, if inappropriately configured, can induce dynamic instability (Woodrooffe 1984). Because the C-dolly eliminates yaw articulation at the hitch point, it can be thought of as an extension of the lead trailer frame. The most significant parameter in this respect is the distance from the turn centre of the lead trailer to the steering axle of the C-dolly; the longer this dimension, the larger the aligning forces associated with the lead trailer that must be counteracted by the tires of the tractor. As demonstrated by Ervin and Guy (1986), increased axle spread causes increased tractive effort at the tractor, which is of particular concern during cornering on low friction surfaces. In addition, a large overhang requires the dolly to achieve greater steer angles. By all accounts, therefore, it is beneficial from a vehicle stability point-of-view to minimize the distance between the lead trailer's turn centre and the dolly axle. Minimizing the drawbar length is also beneficial as it

reduces the tensile and compressive forces at the hitches which are a result of lateral forces originating at the tires of the dolly.

The C-dolly also has been used in straight truck fulltrailer applications. Although this configuration does not technically qualify as a C-train, the authors are compelled to note that the use of C-dollies in straight truck applications is cause for most serious concern.

Unlike the case of a tractor semitrailer, the straight truck receives all of its directional force input from the steering axle. (A tractor semitrailer receives its cornering input from both the tractor's steering axle and its drive axles. The steering axle is called on to provide only a relative yaw displacement of the tractor chassis compared to the semitrailer, while the drive axles provide the cornering force input to the trailer.) The fundamental difference between these two vehicle classes is extremely significant. On lower friction surfaces, a straight truck's steering axle can be easily overpowered by lateral forces originating at the trailer and being transferred forward to the steer axle, resulting in complete loss of directional control.

The C-dolly affects the cornering force demand on the steering axle of the truck to such an extent that controllability can easily become grossly impaired. **The use of a C-dolly in a straight-truck and trailer combination therefore should be strictly prohibited.**

In true C-train applications, the distance from the turn centre of the lead trailer bogie to the C-dolly's steering axle must be minimized; the distance from the turn centre of the lead trailer to the lead trailer's kingpin should be maximized. This will reduce tire side force demands at the tractor and thereby help maintain both high-speed and low-speed performance.

With respect to the current dimensional layout for C-train doubles, contained in The Memorandum of Understanding on Interprovincial Vehicle Weights and Dimensions of February 1988, the following recommendations can be made about allowable dimensional limits:

(a) **C-dolly drawbar length should be limited to a maximum of 2.0 m. The current hitch offset of 1.8 m maximum should remain. This requires that the maximum values of tandem axle spread on the lead trailer be reduced from 1.85 to 1.60 m to eliminate dimensional contradiction.** This allows the C-train to comply with the 3 m interaxle spacing requirement that qualifies the C-dolly to carry 9100 kg. It also ensures that the distance from the turn centre of the lead trailer to the C-dolly steering axle can be held to 3.8 m. A 2.0 m drawbar maximum will improve fleet compatibility. If, in place of a drawbar length specification, the single-dimensional limit of 3.8 m from the C-dolly axle to the turn centre of the lead trailer were chosen, there would be potential for dimensional

conflict within the fleet. Exchanging equipment would result in a high level of incompatibility as some unit combinations could have the distance from the turn centre of the lead trailer to the C-dolly steering axle as high as 4.4 m. Provisions should be made to allow the C-dolly with an interaxle spacing dimension of less than 3 m to be treated as the third axle of a tridem. Much can be gained by keeping these axles as tightly spaced as possible.

(b) There is a benefit to vehicle handling if the wheelbase of the lead trailer is equal to or greater than that of the following trailer. **The wheelbase of the following trailer should never be greater than the wheelbase of the leading trailer.** Wheelbase in this context is defined as the distance from the kingpin of a given trailer to the geometric centre of the axle group of that trailer.

(c) Since there is no vertical load transfer from the following trailer to the leading trailer, **it is necessary to ensure that the weight of the following trailer is never greater than that of the lead trailer.** For example, a C-train with an empty lead trailer and a loaded following trailer would be considered dangerous.

(d) When the trailers of a C-train are examined by themselves, there is no apparent disadvantage to increasing the box length of the C-train from 18.5 to 20 metres. However, if an overall vehicle length limit of 23 metres were to apply, this would result in a reduction of the allowable tractor wheelbase. Short wheelbase tractors are known to have poor handling characteristics irrespective of the vehicle combination to which they are connected. Further study is warranted to determine whether design parameter restrictions should apply to shorter wheelbase tractors. If such a study could establish design criteria, addressing such parameters as wheelbase, drive axle spread, and fifth wheel settings, and if these proved compatible with the 20 m box length and the 23 m overall vehicle length rule, then there would be no vehicle dynamic grounds for discouraging the use of 20 m box lengths on C-trains.

(e) The C-train is invariably a more complex vehicle than the B-train. Because of such factors as self-steering axle control, hitch systems, and the lack of load transfer from the following trailer to the lead trailer, the C-train cannot be considered to be equal in performance to the B-train. It is clear, however, that the C-train represents a significant improvement over the A-train. Although there is a good technical rationale to support an increase in the allowable gross vehicle weight of C-trains from the present 53500 kg, there is equally good technical rationale for not allowing the C-train to achieve as high a gross vehicle weight as

that allowed for the B-train (62500 kg). Technically speaking, a maximum gross combination weight of approximately 58000 kg, which is midway between the current A- and B-train values, would seem appropriate. It is also appropriate that the C-dolly axle qualify as a single axle with a maximum load of 9100 kg provided that it complies with the 3.0 m interaxle spacing rule. If the interaxle spacing were less than 3 m, consideration should be given to treating the C-dolly axle as the third axle of a tridem because this tighter axle spread is highly beneficial to the C-train.

(f) There may be situations where C-trains will be configured outside the dimensional limits agreed upon collectively by the provinces. In such cases, it is recommended that proposed vehicle layout satisfy the following design rule: **the ratio of (a) the lead trailer wheelbase to (b) the distance between the geometric centre of the lead trailer's suspension and the C-dolly's self-steering axle, should be greater than or equal to 1.5, noted in equation form as follows:**

$$\frac{\text{WHEELBASE OF LEAD TRAILER}}{\text{DIST. FROM THE LEAD TRAILER SUSPENSION CENTRE TO SELF STRG. AXLE}} \geq 1.5$$

Although somewhat crude, this design rule respects the dimensional preference of the C-train in light of the findings of this study.

(g) **A C-train must not make use of lift axles, or self-steering axles in any other position than on the C-dolly itself.** The presence of a self-steering axle on any element of a C-train, including the tractor, would degrade the net cornering force available to the vehicle. The presence of a non-steering lift axle on any element of a C-train would increase cornering force demands because of high aligning moments, and this too can be critical to C-train performance.

(h) All self-steering axles examined in this report had a non-inclined kingpin or turntable axis design. However, an analysis was conducted on the characteristics of dual-tire self-steering axles with inclined kingpins, and these were found to be undesirable. It is recommended, therefore, that **only axles with vertical kingpins or vertical-axis turntables be used for heavy vehicle self-steering axle applications.**

5.7 Mandatory Inspection

The performance of the C-train depends on the mechanical condition of the C-dolly. Located far from the driver, the C-dolly cannot benefit from constant driver monitoring, as is the case with the front-end steering systems of a heavy truck. During the field evaluation of this study, some dollies were found in service with nonfunctioning centering force

systems. It is difficult to spot this kind of defect with a casual visual inspection and it is not likely that it would be noticed by the driver during a circle check. Because of the unique performance and design requirements imposed on the C-dolly, **an annual inspection program should be established to certify the dolly is in good working order.**

It is also recommended that the C-dolly be treated as a priority device for inclusion into current safety inspection programs, such as the successful Preventative Maintenance Progam of British Columbia. The following items should be among those contained on the inspection check list.

1. Locking System: Check condition of wear or damage to both manual and automatic lock systems. Inspect automatic control system and associated hardware. Confirm that both systems engage and disengage, and that when engaged the steering is in the zero steer position.

2. Centering Force System: Inspect all moving parts of the centering force system for wear, fracture, bending, and ease of operation. Inspect support bracketry for cracks or bending. Inspect and test all centering force actuators and record the air pressure at the actuators of pneumatic systems.

3. Steering System: Inspect the steering system for wear or free play in the main turntable bearing of the turntable C-dolly, or the steer ing linkage and kingpins of the automotive-steer type C-dolly. Inspect all lubrication points to ensure that grease can be injected into the components.

4. Axles: Inspect the axle for bending, cracking, and alignment as per manufacturer's specifications.

5. Wheel Bearings and Tires: Inspect the axle wheel bearings for wear and free play. Inspect wheels and tires for runout and wobble. Inspect the tires to ensure they are made by the same manufacturer, and are of the same size, tread, style, state of wear, and inflation pressure.

6. Hitch and Fifth Wheel: Inspect the C-dolly drawbar hitch system, including the hitch mechanism on the lead trailer. Examine for wear, slack (5 mm or less is acceptable) and condition of the latch and engagement system. Examine the structural integrity of the hitch backing plate and frame attachment on the lead trailer. Examine the frame members of the C-dolly for cracks and signs of strain. Examine the dolly's fifth wheel, the locking jaws, and the attachment points of the fifth wheel to the dolly frame.

7. Brakes: Examine all brake parts, including slack adjuster, brake drums, brake shoes, 'S' cams and bearings, brake chambers, pressure

tank, relay valve, air lines, and glad hands.

6.0 RECOMMENDED COMPLIANCE TEST PROCEDURE

Unlike most prevailing regulations governing truck weight and dimensions in Canada, the regulatory recommendations of this report cannot all be verified for compliance with linear measurements and the recording of weights. A more diverse set of verification measurements is needed.

The following are recommended test procedures for verifying compliance of a particular C-dolly model with the specifications recommended by this study.

6.1 C-dolly Steering System Lateral and Longitudinal Force Requirement

1. The dolly will be tested in a "ready to run" state of assembly, including tires and hitches.

2. The hitch assembly components intended for the lead trailer will be mounted on the test facility.

3. The dolly will be engaged into the hitches on the test facility and supplied with full trailer line pressure through the glad hands.

4. Frictionless bearings will be inserted between the floor and the underside of the tires to eliminate any resisting tire forces between the dolly and the ground plane.

5. Full brake application will be made on the dolly brakes and held throughout the duration of the test to prevent wheel rotation.

6. The dolly will be loaded vertically through the fifth wheel to a value equivalent to the rated load capacity of the dolly. Shims will be placed between the fifth wheel and the loading frame if necessary to eliminate slack in the roll axis. If a slider fifth wheel is used, it will be set so that the fifth wheel trunion centre is located no more than 30 mm forward of the axle's centre line.

7. A measured steer moment will be applied to the steer axle, and the axle steer angle of the steering system will be measured. The movement of the dolly drawbar arm relative to the hitch assembly also will be measured. The force steer characteristics and the hitch slack data must comply with those required in the final specifications. (The necessary correction for pneumatic trail will be made.)

6.2 C-dolly Frame Torsional Compliance

1. The C-dolly will be engaged by a loading frame at the fifth wheel and by the hitch components fixed to the test facility.

2. The test facility will lift the C-dolly so that the tires are free of the ground, and the test facility will be locked in this position for the duration of the test.

3. Wedges will be placed between the fifth wheel plate and the loading frame to eliminate all slack.

4. A measured torsional load will be applied at the hitch point of the C-dolly in accordance with the specifications, and the relative rotational displacement of the C-dolly measured between the fifth wheel vertical plane and the hitch centre vertical plane will be recorded.

6.3 Dimensional Compliance

1. The C-dolly will be measured to ensure the drawbar length complies with the specifications. It will be measured from the central axis of the axle to the vertical plane passing through the hitch centre or drawbar eye centre of the dolly.

2. The lateral spread of the hitches will be measured from the lateral centre point of the hitch or eye to the lateral centre point of the other hitch or eye.

3. The vertical position of the hitch will be measured. With the dolly unloaded, and the drawbar and suspension assembly on level ground, the vertical distance from the ground to the drawbar eye centre or to the hitch centre will be measured.

6.4 Axle Locking Mechanism

1. The C-dolly will be examined to ensure the presence of required locking mechanisms.

2. The locking systems will be exercised to ensure free engagement and disengagement, and proper alignment of the axle system when locked. Judgment will be passed as to the appropriateness of the hardware.

   If the hardware is considered questionable, the manufacturer may be asked to provide supporting documentation to describe the design and service rationale and, where necessary, engineering strength calculations.

7.0 CONCLUSIONS

A close examination of previous research and field experiences, coupled with the analysis and considerations contained in this report, have led to the general conclusion that the C-train vehicle configuration is a desirable component of Canada's road transportation system, given appropriate constraints on its design and use. The nature of the C-train, and, in particular, the C-dolly itself, suggests there is a need to establish regulations to ensure adequate vehicle performance as well as basic uniformity within the fleet. Such regulations would need to cover the following items:

(a) Lateral and longitudinal minimum forces of the self-steering axle versus its steer angle performance;

(b) Centering force controls of the self-steering axle;

(c) Locking systems of the self-steering axle;

(d) Hitch requirements for the C-dolly, including minimum load ratings, maximum allowable lash or free play, and the location of the hitches;

(e) Minimum frame torsional stiffness of the C-dolly, and minimum torsional limit before permanent deformation;

(f) Tire recommendations for the C-dolly;

(g) Drawbar length limit for the C-dolly;

(h) Dimensional considerations for the overall C-train;

(i) Gross combination weight limits for the C-train; and

(j) Mandatory inspection considerations.

8.0 ACKNOWLEDGEMENTS

The authors wish to thank the C-dolly Steering Committee members, Messrs. P. Askie, J.R. Billing, N. Burns, J. Couture, D.R.S. Jacques, and D. Kee, for their valuable input and guidance throughout this project. We are particularly grateful for the assistance of Messrs. Billing, Burns, and Kee in supplying detailed information on countless (and perhaps inconvenient) occasions.

The authors are also indebted to the Ministry of Transportation of Ontario, the Transportation Systems Branch of the Saskatchewan Highway and Transportation Department, Advanced Engineered Products, Independent Trailer Inc., Ingersoll Machine and Tool Co. Ltd, The Integrated Group,

Westank-Willock a Division of Willock Industries Ltd, and Whelan Ltd for their generosity in furnishing C-dollies and related hardware for experiments and measurements needed in the study.

The authors are especially grateful to Mr. R. Campbell of the Roads and Transportation Association of Canada for his skilled and steady management of the project.

We also gratefully acknowledge the support of NRC employees, Mr. H. Blass, Mr. B. Allen and Mr. H. Staudinger, who furnished a high level of technical insight and support throughout the project to help ensure its success and to Mrs. J. Fyffe for her effort in the preparation of this report.

We are indebted to Mr. T.A. Zahacy, a co-op student from the University of Alberta who conducted experiments and analysis during the dolly test phase with dedication and commitment rarely seen.

Finally, we wish to thank our spouses, who, over the course of the study, patienly endured endless references to our involvement with "C-dollies," without raising a single eyebrow.

9.0 LIST OF REFERENCES

1. Woodrooffe, J.H.F. and Billing, J.R. 1983. Characteristics of Truck Combinations with the Double Drawbar Dolly. Roads and Transportation Association of Canada Research Series.

2. Ervin, R.D. and Guy, Y. 1986. The Influence of Weights and Dimensions and Control of Heavy Trucks in Canada - Parts I and II, Vehicle Weights and Dimensions Study (RTAC), Report Volume 1; ISBN: 0-919098-79-7.

3. Billing, J.R. 1986. Hitch Slack and Drawbar Length Effects on C-train Stability and Handling, Vehicle Weights and Dimensions Study (RTAC), Report Volume 6; ISBN: 0-919098-83-5.

4. Winkler, C.B. et al. July 1986. Improving the Dynamic Performance of Multitrailer Vehicles: A Study of Innovative Dollies, Volume 1, UMTRI-86-26/1.

5. Woodrooffe, J.H.F. 1984. Accident Investigation Report, National Research Council of Canada, Division of Mechanical Engineeirng, Report TR-RW-1.

6. Wong, J.Y. 1978. Theory of Ground Vehicles, John Wiley & Sons.

7. Dugoff, H., Fancher, P.S. and Segel, L. August 1969. Tire Performance Characteristics Affecting Vehicle Response to Steering and Braking Control Inputs, Final Report for Contract No. CST-460, Office of Vehicle Systems Research, National Bureau of Standards, Washington, D.C.

8. Gillespie, T.D. and Winkler, C.B. 1977. "On the Directional Response Characteristics of Heavy Vehicles", The Dynamics of Vehicles on Roads and on Trucks, Proceedings of the 5th VSD 2nd IUTAM Symposium, Sept. 19-23, 1977. Vienna, Amsterdam, Swets and Zeitlinger, 1978.

REPORT DOCUMENTATION PAGE/PAGE DE DOCUMENTATION DE RAPPORT

REPORT NO./ N° DU RAPPORT 1a DM-010	REPORT NO./ N° DU RAPPORT 1b	SECURITY CLASSIFICATION/ CLASSIFICATION DE SÉCURITÉ 2 ___ Top Secret/Très secret ___ Secret ___ Confidential/Confidentiel ___ Protected/Protégée _X_ Unclassified/Non classifiée
DISTRIBUTION/DIFFUSION 3 ___ Controlled/Controlée _X_ Unlimited/Illimitée		

DECLASSIFICATION: DATE OR REASON/DÉCLASSEMENT : DATE OU RAISON
4

TITLE, SUBTITLE/TITRE, SOUS-TITRE

5 Technical Analysis and Recommended Practice for the Double-Drawbar Dolly Using Self-Steering Axles

AUTHOR(S)/AUTEUR(S)

6 Woodrooffe, J.H.F.; LeBlanc, P.A.; El-Gindy, M.

SERIES/SÉRIE

7 Division of Mechanical Engineering Report

CORPORATE AUTHOR/PERFORMING ORGANIZATION/
AUTEUR D'ENTREPRISE/AGENCE D'EXÉCUTION

National Research Council of Canada
8 Division of Mechanical Engineering

SPONSORING OR PARTICIPATING AGENCY/AGENCE DE SUBVENTION OU PARTICIPATION
Council on Highway and Transportation Research and Development
9 of the Roads and Transportation Association of Canada

DATE	FILE/DOSSIER	SPECIAL CODE/ CODE SPÉCIALE	PAGES	FIGURES	REFS.
1989/09			68x	25	8
10	11	12	13a	13b	13c

NOTES
14

DESCRIPTORS(KEY WORDS)/MOTS-CLÉS

15 C-dolly; double drawbar dolly; C-train; self-steering axles.

SUMMARY/SOMMAIRE
Evaluates double drawbar dolly; defines and recommends minimum characteristics of self-steering axles, dolly structure, and C-trains.
16 Identifies operational concerns, gives test and inspection procedures.

ADDRESS/ADRESSE
Vehicle Dynamics Laboratory (J. Coleman)
Division of Mechanical Engineering
Montreal Road, Ottawa, Canada
17 K1A 0R6 (613) 998-9638

APPENDIX A

Moment Induced by a Dual Tire

MOMENT INDUCED BY A DUAL TIRE

The derivation that follows is similar to that used by Gillespie and Winkler (1987). It is included here merely to ensure that consistent sign convention is adopted throughout the derivation of the handling equations. Let longitudinal slip be defined as

$$s = \frac{u_a - u_r}{u_a}$$

where u_a is the actual longitudinal speed of the tire and u_r is the apparent longitudinal speed of the tire as defined by the product of the spin velocity, Ω, and the effective tire radius, R_e. The above definition leads to a positive longitudinal slip value when a braking torque is applied.

Let r be the yaw rate of the dual wheel and R be the turn radius of the path followed by the dual wheel (Fig. A1). It is clear that the speeds tangent to the path for the outer tire, u_o, for the centre of the dual wheel, u, and for the inner tire, u_i, are given by:

$$u_o = r\ (R + \tfrac{1}{2}D)$$

$$u = r\ R$$

$$u_i = r\ (R - \tfrac{1}{2}D)$$

where D is the dual wheel spacing. For the outer tire, $u_a = u_o$ and $u_r = u$. Similarly, for the inner tire, $u_a = u_i$ and $u_r = u$. The longitudinal slip for the outer tire, s_o, and the inner tire, s_i, can therefore be expressed as follows:

$$s_o = 1 - R\ /\ (R + \tfrac{1}{2}D) \qquad\qquad s_i = 1 - R\ /\ (R - \tfrac{1}{2}D)$$

Let the tire longitudinal force, F_x, be linearly related to slip, that is, $F_x = -C_s s$, where C_s is the single tire longitudinal stiffness. The outer and inner tire longitudinal forces may be expressed as

$$F_{xo} = -\ C_s s_o \qquad\qquad F_{xi} = -\ C_s s_i$$

The dual wheel moment, M_{dt}, generated by tire longitudinal forces is given by $M_{dt} = \frac{1}{2}D\ (F_{xo} - F_{xi})$ or when expressed in terms of R and D gives,

$$M_{dt} = -\ \tfrac{1}{2}C_s\ \frac{R\ D^2}{R^2 - \frac{1}{4}D^2}$$

For the j^{th} axle of the i^{th} vehicle unit equipped with a pair of dual wheels, the moment generated by tire longitudinal forces, M_{ij}, for cases where R >> D, is given by

$$M_{ij} = - C_{sij} D_{ij}^2 / R$$

Figure A.1 - Moment Generated by Dual Tire

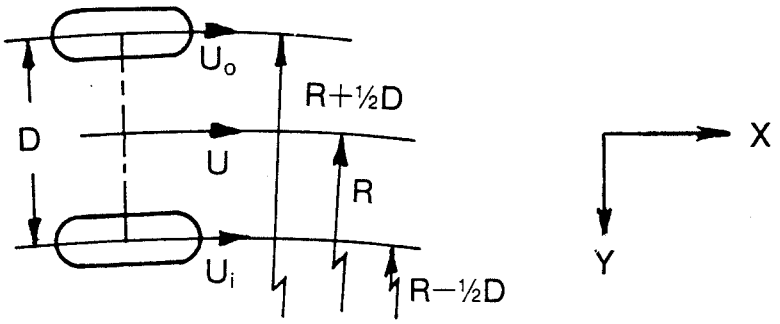

APPENDIX B

Characteristics of Reference Dual Tire Used for the Brake-Steer Diagram

The reference tire used for the brake-steer diagram is a Michelin XZA 11:00R22.50 radial tire. This tire was experimentally tested and the results were reported by Ervin and Guy (1986). The parameters for the reference dual tire, loaded at 44.50 kN, are:

$$C_\alpha = 386.4 \text{ kN/rad}$$

$$C_s = 449.0 \text{ kN/slip}$$

$$\mu_o = 0.90$$

$$W = 44.50 \text{ kN}$$

$$V = 90 \text{ kph}$$

$$\epsilon_r = 0.015 \text{ s/m}$$

The cornering stiffness for a dual wheel loaded at 44.5 kN was obtained by curve-fitting the existing data.

The μ_y vs. α table calculated according to Eq. 9 for a single tire loaded at 26.55 kN, having a cornering stiffness of 214.6 kN/rad, and a speed of 17.9 m/sec leads to the following results

α	μ_y
1.00	0.14
2.00	0.28
4.00	0.54
8.00	0.70
12.00	0.74

The experimental values for identical conditions are

α	μ_y
1.00	0.14
2.00	0.27
4.00	0.47
8.00	0.66
12.00	0.73

The lateral roll-off predicted by Eq. 9 is:

α	0.00	0.04	0.10	0.24	0.25	0.50	1.00
1.00	1.00	1.04	0.79	0.38	0.37	0.18	0.08
2.00	1.00	1.04	0.76	0.38	0.36	0.18	0.08
4.00	1.00	0.95	0.73	0.39	0.37	0.19	0.08
6.00	1.00	0.96	0.79	0.46	0.45	0.23	0.10
8.00	1.00	0.98	0.85	0.54	0.52	0.28	0.12
12.00	1.00	0.99	0.92	0.67	0.66	0.38	0.17

Whereas the experimental values are:

α	0.00	0.04	0.10	0.24	0.25	0.50	1.00
1.00	1.00	1.00	0.83	0.40	0.38	0.17	0.06
2.00	1.00	1.00	0.81	0.39	0.38	0.17	0.06
4.00	1.00	0.97	0.75	0.39	0.38	0.17	0.06
6.00	1.00	0.96	0.79	0.45	0.44	0.21	0.07
8.00	1.00	0.97	0.84	0.52	0.50	0.25	0.09
12.00	1.00	0.97	0.89	0.63	0.62	0.33	0.12

The μ_x vs. α table calculated according to Eq. 8 for an angle tire loaded at 26.87 kN, having a cornering stiffness of 215.9 kN/rad, and a speed of 24.6 m/sec leads to the following results:

α	μ_x
0.04	0.35
0.10	0.66
0.24	0.76
0.25	0.76
0.50	0.72
1.00	0.57

The experimental values for identical conditions are:

α	μ_x
0.04	0.30
0.10	0.67
0.24	0.79
0.25	0.78
0.50	0.70
1.00	0.44

The longitudinal roll-off predicted by Eq. 8 is:

α	0.04	0.10	0.24	0.25	0.50	1.00
1.00	1.00	0.99	1.00	1.00	1.00	1.00
2.00	1.00	0.96	0.99	0.99	1.00	1.00
4.00	0.87	0.87	0.96	0.97	0.99	1.00
6.00	0.71	0.77	0.92	0.93	0.98	0.99
8.00	0.58	0.65	0.87	0.88	0.96	0.99
12.00	0.41	0.49	0.75	0.77	0.91	0.97

Whereas the experimental values are:

α	0.04	0.10	0.24	0.25	0.50	1.00
2.00	1.00	0.96	0.99	0.99	1.00	1.00
4.00	0.93	0.87	0.96	0.97	0.99	1.00
6.00	0.78	0.77	0.92	0.93	0.98	0.99
8.00	0.65	0.67	0.87	0.88	0.96	0.99
12.00	0.47	0.52	0.77	0.78	0.92	0.98

Comparison between theoretical and experimental results show that the set of equations used for the brake-steer criteria represents a highly realistic mathematical model of the tire and thus confirms the appropriateness of Equations 8 and 9.

APPENDIX C

Steady-state Handling Equations of Vehicles Equipped With Self-steering Axles

STEADY-STATE HANDLING EQUATIONS OF VEHICLES EQUIPPED WITH SELF-STEERING AXLES

The objective of the current exercise is to arrive at a set of analytical equations that govern the steady-state handling characteristics of a specific group of vehicle combinations equipped with self-steering axles. The group of vehicles under consideration is described in the following paragraphs.

The general layout of the towing vehicle is shown in Fig. C1. It consists of a vehicle with a front steering axle and a variable number of belly axles, trailer axles, and C-dolly axles. The semitrailers that follow the towing unit are supported at the front by a fifth wheel and are also equipped with a variable number of belly, trailer, and C-dolly axles. The fifth wheel is mounted on either a C-dolly, or on the rear end of a tractor, or on a B-train type semitrailer.

The i^{th} vehicle unit is modelled as having n_{1i} belly axles, n_{2i} trailer axles, and n_{3i} dolly axles where n_{1i}, n_{2i} and n_{3i} are integers and

$$n_{1i} \geq 0 \qquad n_{2i} \geq 1 \qquad n_{3i} \geq 0.$$

If n represents the number of vehicle units in the vehicle combination, then the above equations are valid for i = 1,...,n, with the exception that n_{3n} is always zero since there is no C-dolly following the last unit of the vehicle combination.

We note from Fig. C1 that in terms of steady-state analysis, a C-dolly is considered to be an integral part of the vehicle unit that precedes it. If the i^{th} vehicle unit is not followed by a C-dolly, then for $n_{3i} = 0$, the distance between the centre of the trailer and C-dolly axle groups, q_i, is zero, and the linear dimension x_i is effectively a measure of the distance between the centre of the trailer axle group and the fifth wheel kingpin. The variable x_i assumes a positive value when the fifth wheel is positioned forward of the centre of the axle group over which it is mounted.

The handling equations are derived with parameters n, n_{1i}, n_{2i}, and n_{3i} as variables. Hence, the equations are valid for straight trucks, tractor-semitrailers, B-trains, C-trains, and truck-fulltrailers with C-dolly.

The remaining linear dimesions shown on Fig. C1 are defined as follows:

a_i = distance between the centre of mass of the vehicle unit and either (a) the centre of the front steering axle, in the case of the towing vehicle, or (b) the location of the fifth wheel kingpin, in the case of the semitrailer.

Figure C1

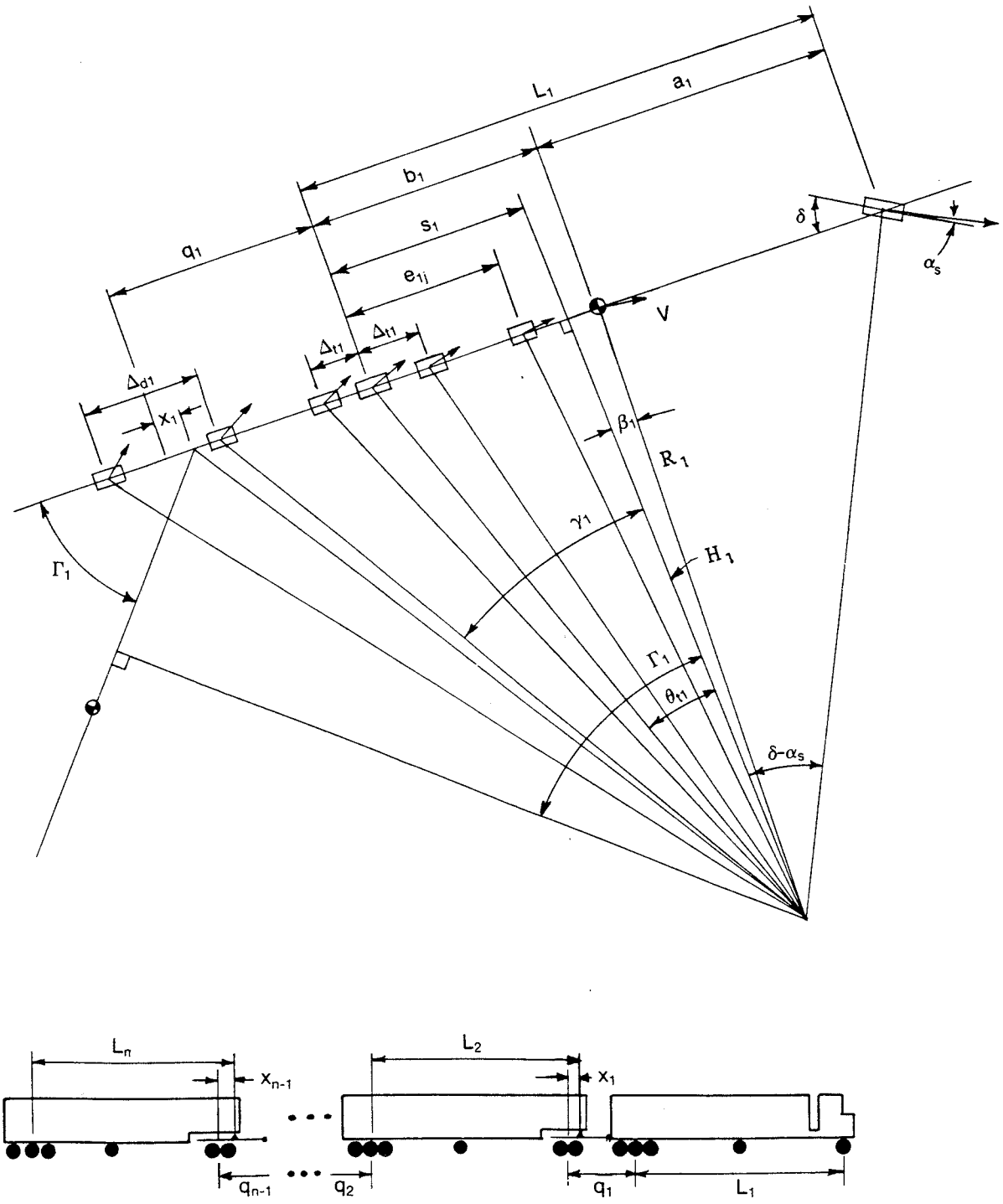
L1
a1
b1
s1
e1j
q1
δ
αs
V
Δd1
Δt1
Δt1
x1
β1
R1
γ1
H1
Γ1
Γ1
θr1
δ-αs
Ln
xn-1
L2
x1
qn-1
q2
q1
L1

b_i = distance between the centre of mass of the vehicle unit and either (a) the centre of the drive axle group, in the case of a towing vehicle, or (b) the centre of the trailer axle group, in the case of a semitrailer.

L_i = sum $a_i + b_i$

Δ_{ti} = trailer axle group interaxle spacing

Δ_{di} = C-dolly axle group interaxle spacing

e_{ij} = distance between centre of trailer axle group and the belly axle

j = index identifying the j^{th} axle of the i^{th} vehicle unit, excluding the steering axle of the towing vehicle

The axle total tire lateral force, F_{ij}, is assumed to be linearly related to the average slip angle, α_{ij}, that is

$$F_{ij} = C_{\alpha ij}\alpha_{ij} \qquad \text{C1}$$

where $C_{\alpha ij}$ is the total tire cornering stiffness of the axle.

As mentioned in the main body of the report, every axle following the front steering axle is modelled as being equipped with a self-steering mechanism whose stiffness may be set from free-caster to non-steer condition. The type of self-steering axle cornering curve considered in the present analysis is described by Equation 4 and is illustrated in Figure 6 (Section 4.2.2). The self-steering axle angle, δ_{ij}, is related to α_{ij} as follows (Equations 2 and 4).

$$\delta_{ij} = \frac{C_{\alpha ij}}{k_{1ij}} \cdot \alpha ij - \frac{M_{ij}}{t_{ij}k_{1ij}} - \frac{m_{sij}V^2/R}{k_{1ij}} \qquad \text{C2-a}$$

for $0 \leq F_{cij} \leq F_{coij}$ and

$$\delta_{ij} = \frac{C_{\alpha ij}}{k_{2ij}} \alpha ij - \frac{M_{ij}}{t_{ij}k_{2ij}} - \frac{m_{sij}V^2/R}{k_{2ij}} - \frac{F_{coij}(k_{1ij} - k_{2ij})}{k_{1ij}k_{2ij}} \qquad \text{C2-b}$$

for $F_{cij} > F_{coij}$ where k_{1ij} and k_{2ij} are the self-steering stiffnesses, $M_{ij}$is the aligning moment for a pair of dual tires, t_{ij} is the corrected caster trail, m_{sij} is the self-steering axle inertial mass and F_{coij} is the centering force.

The angle between the velocity vector at the centre of the wheel and the longitudinal orientation of the vehicle frame is referred to as the wheel trajectory angle. Hence, as it can be seen from Figure C2, the average trajectory angle, θ_{ij}, is defined as the sum of the slip and self-steering angles, that is,

$$\theta_{ij} = \alpha_{ij} + \delta_{ij} \qquad \text{C3}$$

Figure C2

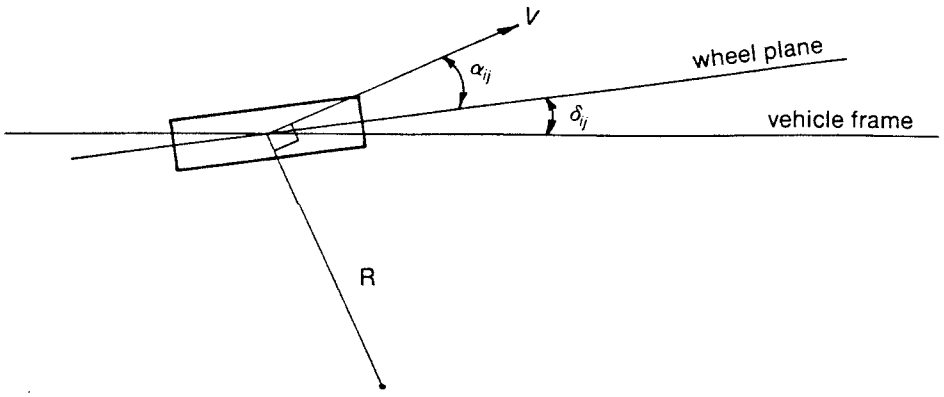

A solution for the handling equations is more readily obtained if F_{ij} is expressed in terms of θ_{ij}. By manipulating terms in Equations C1, C2 and C3, we arrive at the following expression:

$$F_{ij} = CK_{ij}\theta_{ij} + MF_{ij} + cm_{ij}V^2/R \qquad C4$$

where

$$CK_{ij} = C_{\alpha ij}K_{ij}$$

$$MF_{ij} = c_{ij}M_{ij}/t_{ij} + r_{ij}F_{roij}$$

$$cm_{ij} = c_{ij}m_{sij}$$

For $0 \leq F_{cij} \leq F_{coij}$

$$K_{ij} = k_{1ij}/(k_{1ij} + C_{\alpha ij})$$

$$c_{ij} = C_{\alpha ij}/(k_{1ij} + C_{\alpha ij})$$

$$r_{ij} = 0$$

and for $F_{cij} > F_{coij}$

$$K_{ij} = k_{2ij}/(k_{2ij} + C_{\alpha ij})$$

$$c_{ij} = C_{\alpha ij}/(k_{2ij} + C_{\alpha ij})$$

$$r_{ij} = C_{\alpha ij}(k_{1ij} - k_{2ij})/k_{1ij}(k_{2ij} + C_{\alpha ij})$$

The steering axle total tire lateral force, F_s, is also considered to be linearly related to the average slip angle, α_s, that is,

$$F_s = C_{\alpha s}\alpha_s \qquad C5$$

where $C_{\alpha s}$ is the total tire cornering stiffness of the steering axle.

Consideration of equilibrium conditions for individual vehicle units leads to the following linearized side force balance equations:

$$F_s + \sum_{j=1}^{N_{31}} F_{1j} + R_{12} = m_1 V^2/R \qquad \text{C6-1}$$

$$\sum_{j=1}^{N_{32}} F_{2j} - R_{12} + R_{23} = m_2 V^2/R \qquad \text{C6-2}$$

$$\vdots$$

$$\sum_{j=1}^{N_{2n}} F_{nj} - R_{(n-1)n} = m_n V^2/R \qquad \text{C6-n}$$

and linearized moment balance equations:

$$a_1 \cdot F_s - \sum_{j=1}^{N_{11}} (b_1 - e_{1j}) \cdot F_{ij} - \sum_{j=N_{11}+1}^{N_{21}} [b_1 - (n_{t1} - j)\Delta_{t1}] \cdot F_{1j}$$

$$- \sum_{j=N_{21}+1}^{N_{31}} [b_1+q_1-(n_{d1}-j)\Delta_{d1}] \cdot F_{1j} - (b_1+q_1-x_1) \cdot R_{12} + \sum_{j=1}^{N_{31}} M_{1j} = 0 \qquad \text{C7-1}$$

$$-a_2 \cdot R_{12} - \sum_{j=1}^{N_{12}} (b_2 - e_{2j}) \cdot F_{2j} - \sum_{j=N_{12}+1}^{N_{22}} [b_2 - (n_{t2} - j)\Delta_{t2}] \cdot F_{2j}$$

$$- \sum_{j=N_{22}+1}^{N_{32}} [b_2+q_2-(n_{d2}-j)\Delta_{d2}] \cdot F_{2j} - (b_2+q_2-x_2) \cdot R_{23} + \sum_{j=1}^{N_{32}} M_{2j} = 0 \qquad \text{C7-2}$$

$$\vdots$$

$$-a_n \cdot R_{(n-1)n} - \sum_{j=1}^{N_{1n}} (b_n - e_{nj}) F_{nj} - \sum_{j=N_{1n}+1}^{N_{2n}} [b_n - (n_{tn} - j)\Delta_{tn}] F_{nj}$$

$$+ \sum_{j=1}^{N_{2n}} M_{nj} = 0 \qquad \text{C7-n}$$

where

$$N_{1i} = n_{1i} \qquad \text{C8-1}$$

$$N_{2i} = n_{1i} + n_{2i} \qquad \text{C8-2}$$

$$N_{3i} = n_{1i} + n_{2i} + n_{3i} \qquad \text{C8-3}$$

$$n_{ti} = n_{1i} + (n_{2i} + 1) / 2 \qquad \text{C9-1}$$

$$n_{di} = n_{1i} + n_{2i} + (n_{3i} + 1) / 2 \qquad \text{C9-2}$$

$R_{i(i+1)}$ is the fifth wheel reaction between the i^{th} and $i^{th}+1$ vehicle unit and m_i is the vehicle unit mass.

Substituting Equations C4 and C5 into Equations C6 and C7 leads to a set of equations whose number of unknowns is equal to the number of axles (i.e. trajectory angles θ_{ij} and α_s) plus the number of the fifth wheel reactions. In general, the total number of unknowns exceeds the number of equations derived from equilibrium conditions. That is, the problem is statically indeterminate and compatibility equations are required to obtain a solution.

Compatibility equations are obtained from trigonometric relationships that exist between the tire trajectory angles for a given vehicle unit. The solution method that follows is similar to the method used by Gillespie and Winkler (1977) to derive the steady-state handling equation for a straight truck with multiple non-steering axles.

The following trigonometric relationships are readily obtained from Figure C1:

$$s_i - e_{ij} = H_i \tan \theta_{ij}, \qquad j=1, \ldots, N_{1i} \qquad \text{C10-1}$$

$$s_i - (n_{ti}-j)\Delta_{ti} = H_i \tan \theta_{ij}, \qquad j=N_{1i}+1, \ldots, N_{2i} \qquad \text{C10-2}$$

$$s_i + q_1 - (n_{di}-j)\Delta_{di} = H_i \tan \theta_{ij}, \qquad j=N_{2i}+1, \ldots, N_{3i} \qquad \text{C10-3}$$

and

$$s_i = H_i \tan \theta_{ti} \qquad \text{C11-1}$$

$$H_i = R_i \cos \beta_i \qquad \text{C11-2}$$

Angle θ_{ti} is the trajectory angle at the centre of the trailer axle group (or drive axle group in the case of the towing unit).

By linearizing Equations C10 and C11 and substituting s_i by $R_i\theta_{ti}$ we obtain the compatibility equations

$$\theta_{ij} = \theta_{ti} - e_{ij} / R, \qquad j=1, \ldots, N_{1i} \qquad \text{C12-1}$$

$$\theta_{ij} = \theta_{ti} - (n_{ti}-j)\Delta_{ti} / R, \qquad j=N_{1i}+1, \ldots, N_{2i} \qquad \text{C12-2}$$

$$\theta_{ij} = \theta_{ti} + [q_i-(n_{di}-j)\Delta_{di}] / R, \qquad j=N_{2i}+1, \ldots, N_{3i} \qquad \text{C12-3}$$

R_i is approximated by a constant path curvature radius, R, for all vehicle units.

Substituting Equation C12 into Equation C4 and, subsequently, substituting Equations B4 and C5 into Equations C6 and C7 leads to 2n equations with 2n unknowns; the unknowns being θ_{t1} to θ_{tn}, α_s, and fifth wheel reactions R_{12} to $R_{(n-1)n}$.

Systematic substitution of equations C6-n to C6-i into Equations C7-i from i=n to i=1, leads to the following general expression for θ_{ti}

$$\theta_{ti} = T_{si} + \frac{V^2}{Rg} T_{di}$$

where

$$T_{si} = A_i/Q_i, \qquad T_{di} = B_i/Q_i$$

and

$$A_i = \sum_{j=1}^{N_{1i}} (L_i - e_{ij})\left(\frac{e_{ij}}{R} CK_{ij} - MF_{ij}\right) + \sum_{j=N_{1i}+1}^{N_{2i}} \left[L_i - (n_{ti} - j)\Delta_{ti}\right] \left[\frac{\Delta_{ti}}{R} (n_{ti}-j) \cdot CK_{ij} - MF_{ij}\right] - \sum_{j=N_{2i}+1}^{N_{3i}} \left[L_i + q_i - (n_{di} - j)\Delta_{di}\right]\left[\frac{q_i}{R} CK_{ij} - \frac{\Delta_{di}}{R} (n_{di}-j) \cdot CK_{ij} + MF_{ij}\right] + \sum_{j=1}^{N_{3i}} M_{ij} - (L_i + q_i - x_i) \sum_{k=i+1}^{n} \left[T_{sk} \sum_{j=1}^{N_{3k}} CK_{kj} - \sum_{j=1}^{N_{1k}} \frac{e_{kj}}{R} \cdot CK_{kj} - \sum_{j=N_{1k}+1}^{N_{2k}} \frac{\Delta_{tk}}{R} (n_{tk} - j)\, CK_{kj} + \sum_{j=N_{2k}+1}^{N_{3k}} \left[\frac{q_k}{R} - (n_{dk}-j)\, \frac{\Delta_{dk}}{R}\right] CK_{kj} + \sum_{j=1}^{N_{3k}} MF_{kj}\right]$$

$$B_i = a_i m_i g - \sum_{j=1}^{N_{1i}} (L_i - e_{ij}) cm_{ij} g - \sum_{j=N_{1i}+1}^{N_{2i}} [L_i - (n_{ti} - j)\Delta_{ti}] cm_{ij} g$$

$$- \sum_{j=N_{2i}+1}^{N_{3i}} [L_i + q_i - (n_{di} - j)\,\Delta_{di}] cm_{ij} g - (L_i + q_i - x_i) \sum_{k=i+1}^{n} [T_{dk} \cdot$$

$$\sum_{j=1}^{N_{3k}} CK_{ij} + \sum_{j=1}^{N_{3k}} m_{kj} g - m_k g]$$

$$Q_i = L_i \sum_{j=1}^{N_{3i}} CK_{ij} - \sum_{j=1}^{N_{1i}} e_{ij} CK_{ij} - \sum_{j=N_{1i}+1}^{N_{2i}} \Delta_{ti}\,(n_{ti} - j)\,CK_{ij}$$

$$+ \sum_{j=N_{2i}+1}^{N_{3i}} [q_i - (n_{di} - j)\,\Delta_{di}]\,CK_{ij}$$

Coefficients T_{si} and T_{di} are referred to as the static and dynamic trajectory angle coefficients, respectively.

Substituting Equations C6-2 to C6-n into C6-1 and making use of Equation C13-1 leads to the following expression for α_s:

$$\alpha_s = S_s + \frac{V^2}{Rg} \cdot S_d \qquad \text{C14}$$

where

$$S_s = \{ \sum_{i=1}^{n} [-T_{si} \sum_{j=1}^{N_{3i}} CK_{ij} + \sum_{j=1}^{N_{1i}} \frac{e_{ij}}{R} CK_{ij} + \sum_{j=N_{1i}+1}^{N_{2i}} \frac{\Delta_{ti}}{R} (n_{ti} - j)\,CK_{ij}$$

$$- \sum_{j=N_{2i}+1}^{N_{3i}} [\frac{q_i}{R} - (n_{di} - j)\,\frac{\Delta_{di}}{R}]\,CK_{ij} - \sum_{j=1}^{N_{3i}} MF_{ij}\} \div C_{\alpha s}$$

$$S_d = \{ \sum_{i=1}^{n} [m_i g - T_{di} \sum_{j=1}^{N_{3i}} CK_{ij} - \sum_{j=1}^{N_{3i}} cm_{ij} g]\} \div C_{\alpha s}$$

Coefficients S_s and S_d are referred to as the static and dynamic slip angle coefficients for the front steering axle, respectively.

Making use once again of the geometry displayed in Figure C1 we obtain the following expression that relates the average steering angle, δ, of the front axle to θ_{t1} and α_s;

$$\delta = \frac{L_1}{R} + \alpha_s - \theta_{t1} \qquad \text{C15}$$

When written in terms of trajectory angle and slip angle coefficients, the handling equation, Equation C15, takes the form

$$\delta = \frac{L_1}{R} + K_s + \frac{V^2}{Rg} \cdot K_d \qquad \text{C16}$$

where

$$K_s = S_s - T_{s1}$$

$$K_d = S_d - T_{d1}$$

Coefficients K_s and K_d are referred to as the static and dynamic understeer coefficients, respectively.

Another variable of interest is the steady-state articulation angle, Γ_i. $\Gamma_i$represents the articulation angle between the i^{th} and $i^{th}+1$ vehicle unit. From Figure C1 we obtain

$$s_i + q_i - x_i = H_i \tan\gamma_i \qquad \text{C17-1}$$

$$L_{i+1} - s_{i+1} = H_{i+1} \tan(\Gamma_i - \gamma_i) \qquad \text{C17-2}$$

By linearizing Equations C17, substituting s_i by $R\theta_{ti}$ and s_{i+1} by $R\theta_{t(i+1)}$, we obtain, after manipulating terms,

$$\Gamma_i = (L_{i+1} + q_i - x_i)/R + \theta_{ti} - \theta_{t(i+1)}$$

When expressed in terms of trajectory angle coefficients, Γ_i takes the form

$$\Gamma_i = \frac{L_{i+1} + q_i - x_i}{R} + A_{si} + \frac{V^2}{Rg} \cdot A_{di} \qquad \text{C18}$$

where

$$A_{si} = T_{si} - T_{s(i+1)}$$

$$A_{di} = T_{di} - T_{d(i+1)}$$

Coefficients A_{si} and A_{di} are referred to as the static and dynamic articulation angle coefficients, respectively.

APPENDIX D

Computer Simulation Results

Computer simulations were conducted using the steady-state analysis program developped for this study. The results for each computer simulation consists of the constant radius handling curve and tire slip angle curves for every axle of the vehicle. The simulations were conducted for the following configurations and operating conditions:

i) - straight truck
   - two fixed drive axles
   - turn radius of 200 m

ii) - straight truck
    - self-steering mecanism on first drive axle
    - turn radius of 200 m

iii) - straight truck
     - self-steering mecanism on second drive axle
     - turn radius of 200 m

iv) - truck-fulltrailer with C-dolly
    - one self-steering axle on C-dolly
    - turn radius of 200 m

v) - C-train
   - fixed axle on dolly
   - turn radius of 200 m

vi) - C-train
    - fixed axle on dolly
    - turn radius of 100 m

vii) - C-train
     - two self-steering axles on dolly
     - turn radius of 200 m

viii) - C-train
      - two self-steering axles on dolly
      - turn radius of 100 m

ix) - C-train
    - one self-steering axle on C-dolly
    - turn radius of 200 m

x) - C-train
   - one self-steering axle on C-dolly
   - turn radius of 100 m

xi) - C-train
    - single self-steering axle on C-dolly
    - turn radius of 50 m

The computer program input parameters are listed in tabular form with the following column headers:

LOAD = single axle load;
Cα = single tire cornering stiffness normalized with respect to 3700 N/deg;
Dual = presence or absence of dual tires;
e = distance between the centre of the trailer (drive) axle group and the belly axle;
k1 = cornering stiffness of the self-steering axle for Fc ≤ Fco;
t = corrected caster trail dimension of the self-steering axle;
Ms = inertial mass of the self-steering axle;
Fco = centering force of the self-steering axle expressed in g's (equivalent to a_{co} from main text);
k2 = cornering stiffness of the self-steering axle for Fc > Fco;
L = vehicle unit wheelbase measured from either the centre of the drive axle group to the front steering axle (in the case of the towing unit) or from the centre of the semitrailer axle group to the location of the kingpin (in the case of a semitrailer);
q = distance between the centre of the trailer (drive) axle group and the centre of the C-dolly axle group;
x = distance between the centre of the fifth wheel and the centre of the axle group over which the fifth wheel is mounted (trailer or drive axle group in the case of B-train type semitrailer or tractor, respectively; or C-dolly axle group in the case of a C-train type semitrailer). Note that positive values indicate the fifth wheel is forward of the centre of the axle group;
del t = interaxle spacing of the trailer axle group;
del d = interaxle spacing of the C-dolly axle group;
W5 = front axle load in the case of the towing vehicle or fifth wheel load in the case of a semitrailer
DUAL WHEEL = dual wheel spacing
Cαs = cornering stiffness for single tire on the front axle normalized with respect to 3700 kN/deg
RADIUS = turn radius

The y-axis label 'Unit 1, Axle 1' refers to the first axle following the front steering axle of the vehicle combination. The y-axis label used for the tire slip angle of the front steering axle is simply 'Front axle'.

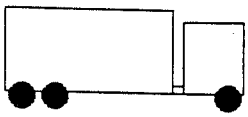

STRAIGHT TRUCK WITH TWO FIXED DRIVE AXLES

Filename: STRAIGHT.I03

UNIT 1 - STRAIGHT TRUCK

	1	2	3	4	5	6	7	8	9
AXLE	LOAD kg	Cα norm.	DUAL -	e m	k1 g/deg	t m	Ms kg	Fco g	k2 g/deg
1 1st DRIVE	8500.	1.000	Y	-	∞	∞	0.0	∞	∞
2 2nd DRIVE	8500.	1.000	Y	-	∞	∞	0.0	∞	∞
	L m	q m	x m	del t m	del d m	W5 kg			
3 UNIT DATA	6.70	0.00	0.00	1.52	0.00	6700.			

GENERAL DATA

1	2	3	4
DUAL WHEEL m	Cαs normalized	RADIUS m	ACCELERATION g
0.33	1.000	200.	0.0

Independent Variable - LATERAL ACCELERATION
- Range: 0.00 to 0.40

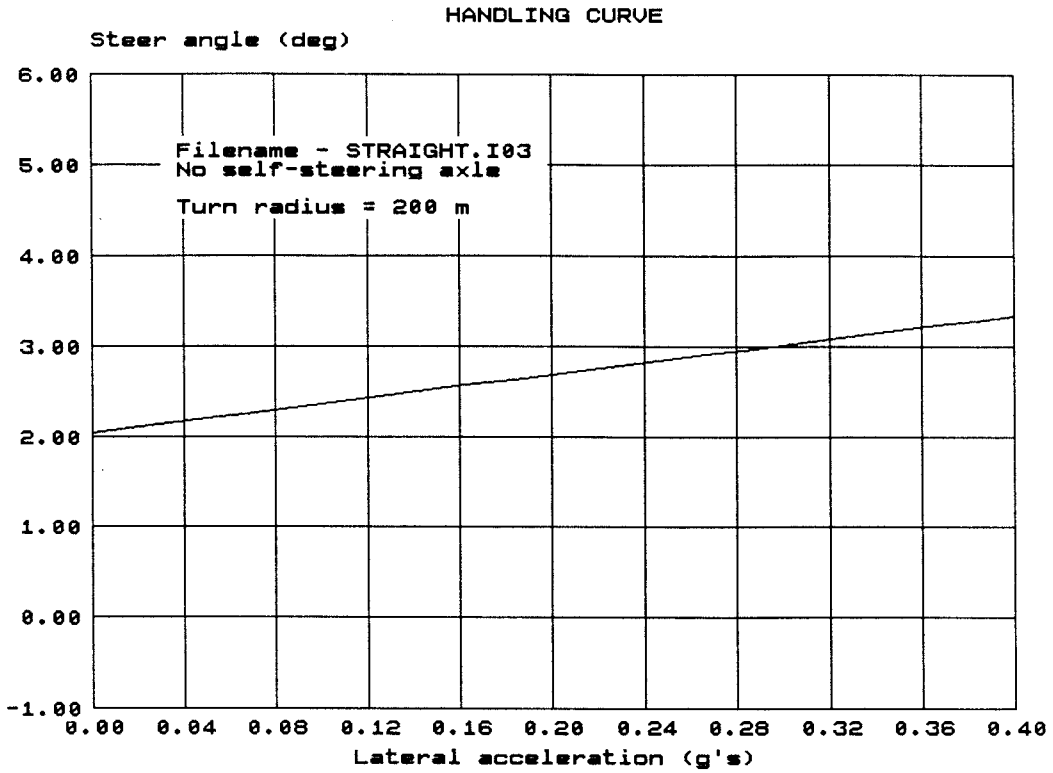
HANDLING CURVE
Steer angle (deg)
6.00
5.00
4.00
3.00
2.00
1.00
0.00
-1.00
Filename - STRAIGHT.I03
No self-steering axle
Turn radius = 200 m
0.00 0.04 0.08 0.12 0.16 0.20 0.24 0.28 0.32 0.36 0.40
Lateral acceleration (g's)

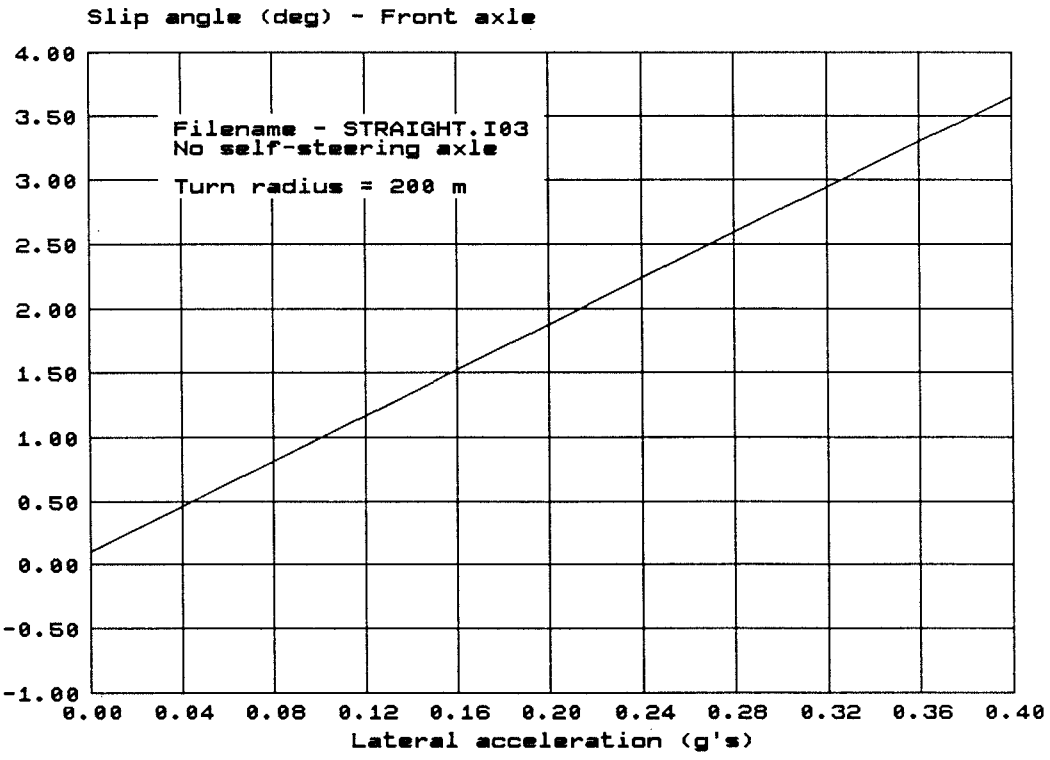
Slip angle (deg) - Front axle
4.00
3.50
3.00
2.50
2.00
1.50
1.00
0.50
0.00
-0.50
-1.00
Filename - STRAIGHT.I03
No self-steering axle
Turn radius = 200 m
0.00 0.04 0.08 0.12 0.16 0.20 0.24 0.28 0.32 0.36 0.40
Lateral acceleration (g's)

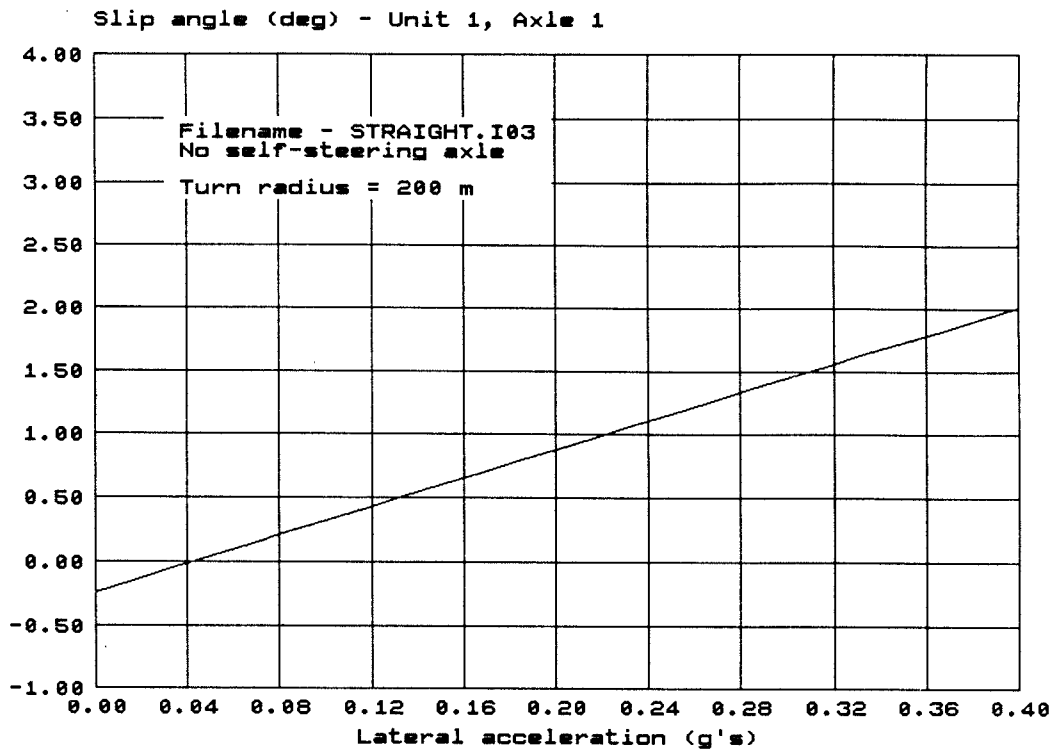
Slip angle (deg) - Unit 1, Axle 1
Filename - STRAIGHT.I03
No self-steering axle
Turn radius = 200 m
4.00
3.50
3.00
2.50
2.00
1.50
1.00
0.50
0.00
-0.50
-1.00
0.00 0.04 0.08 0.12 0.16 0.20 0.24 0.28 0.32 0.36 0.40
Lateral acceleration (g's)

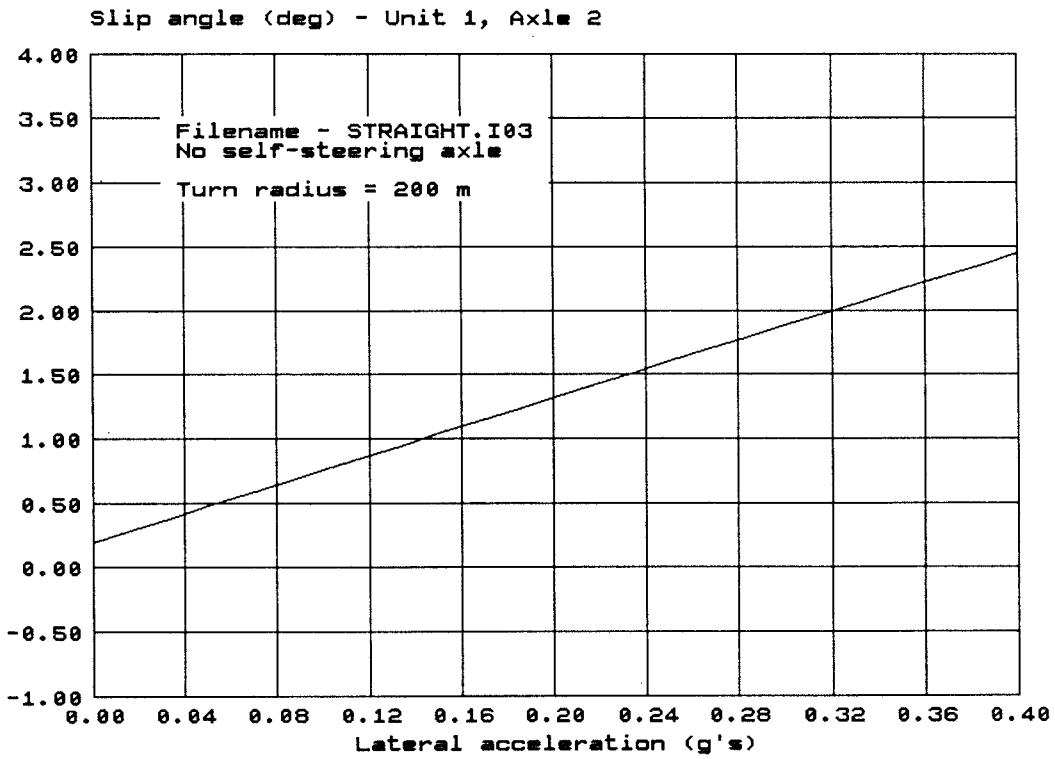
Slip angle (deg) - Unit 1, Axle 2
Filename - STRAIGHT.I03
No self-steering axle
Turn radius = 200 m
4.00
3.50
3.00
2.50
2.00
1.50
1.00
0.50
0.00
-0.50
-1.00
0.00 0.04 0.08 0.12 0.16 0.20 0.24 0.28 0.32 0.36 0.40
Lateral acceleration (g's)

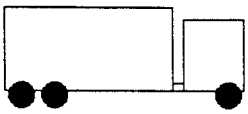

STRAIGHT TRUCK WITH SELF-STEERING AXLE ON FIRST DRIVE AXLE

Filename: STRAIGHT.I04

UNIT 1 - STRAIGHT TRUCK

	1	2	3	4	5	6	7	8	9
AXLE	LOAD kg	Cα norm.	DUAL -	e m	k1 g/deg	t m	Ms kg	Fco g	k2 g/deg
1 1st DRIVE	8500.	1.000	Y	-	0.250	0.360	600.	0.200	0.025
2 2nd DRIVE	8500.	1.000	Y	-	∞	∞	0.0	∞	∞
	L m	q m	x m	del t m	del d m	W5 kg			
3 UNIT DATA	6.70	0.00	0.00	1.52	0.00	6700.			

Arbitrarily Set Values - AXLE CENTRING FORCE (Fco)
- 1st DRIVE AXLE
- Values: 0.20 0.25 0.30 ∞

GENERAL DATA

1	2	3	4
DUAL WHEEL m	Cαs normalized	RADIUS m	ACCELERATION g
0.33	1.000	200.	0.0

Independent Variable - LATERAL ACCELERATION
- Range: 0.00 to 0.40

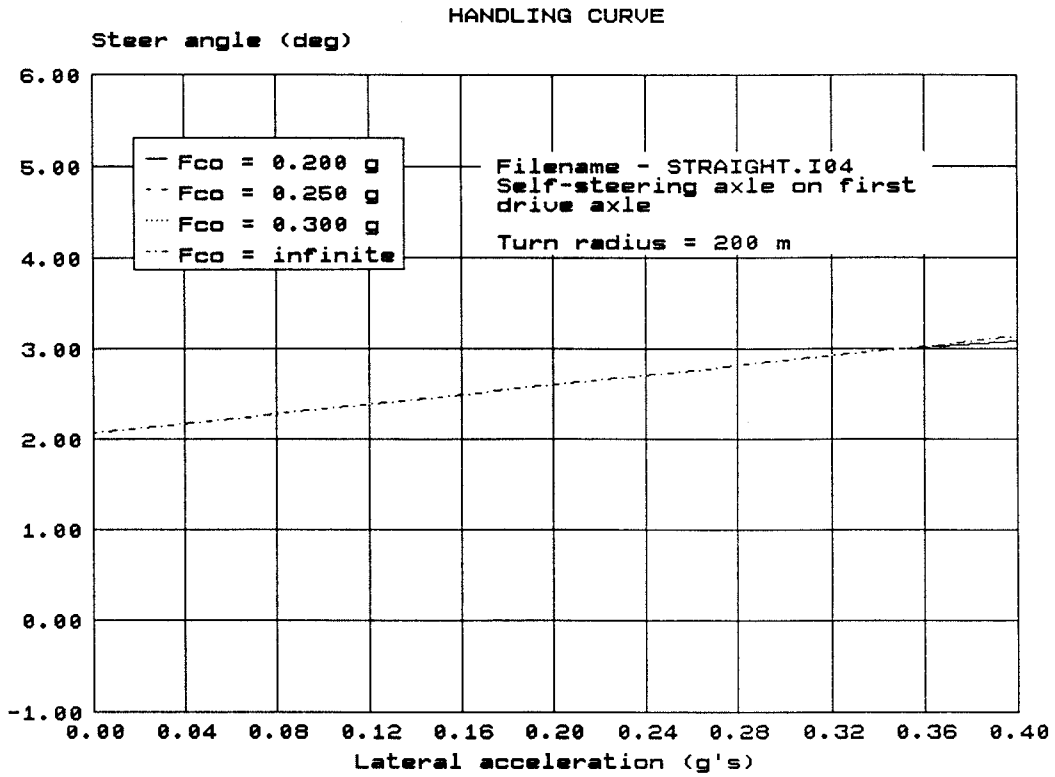
HANDLING CURVE
Steer angle (deg)
6.00
5.00
4.00
3.00
2.00
1.00
0.00
-1.00
Fco = 0.200 g
Fco = 0.250 g
Fco = 0.300 g
Fco = infinite
Filename - STRAIGHT.I04
Self-steering axle on first drive axle
Turn radius = 200 m
0.00 0.04 0.08 0.12 0.16 0.20 0.24 0.28 0.32 0.36 0.40
Lateral acceleration (g's)

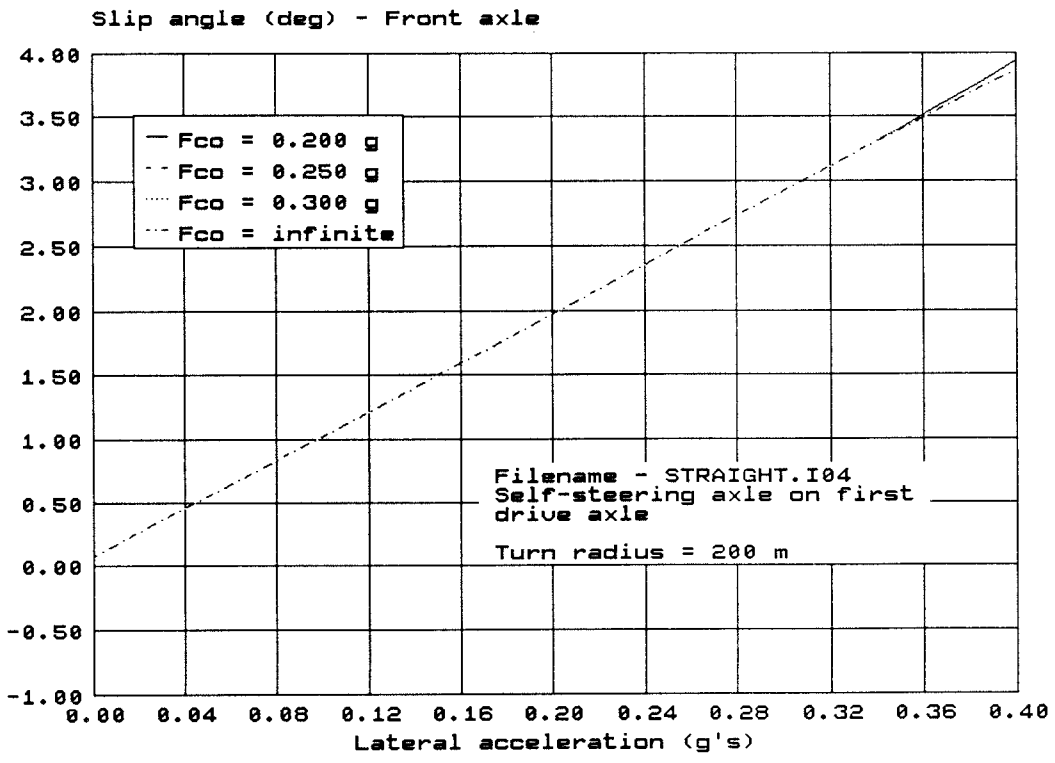
Slip angle (deg) - Front axle
4.00
3.50
3.00
2.50
2.00
1.50
1.00
0.50
0.00
-0.50
-1.00
Fco = 0.200 g
Fco = 0.250 g
Fco = 0.300 g
Fco = infinite
Filename - STRAIGHT.I04
Self-steering axle on first drive axle
Turn radius = 200 m
0.00 0.04 0.08 0.12 0.16 0.20 0.24 0.28 0.32 0.36 0.40
Lateral acceleration (g's)

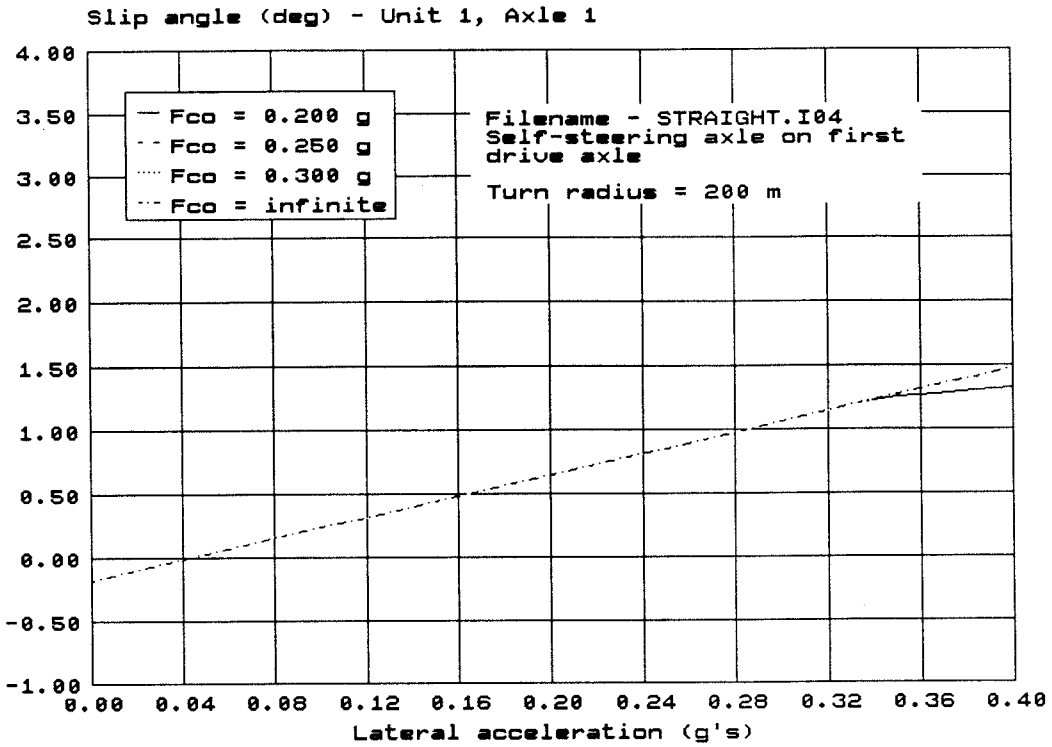
Slip angle (deg) - Unit 1, Axle 1
4.00
3.50
3.00
2.50
2.00
1.50
1.00
0.50
0.00
-0.50
-1.00
Fco = 0.200 g
Fco = 0.250 g
Fco = 0.300 g
Fco = infinite
Filename - STRAIGHT.I04
Self-steering axle on first drive axle
Turn radius = 200 m
0.00 0.04 0.08 0.12 0.16 0.20 0.24 0.28 0.32 0.36 0.40
Lateral acceleration (g's)

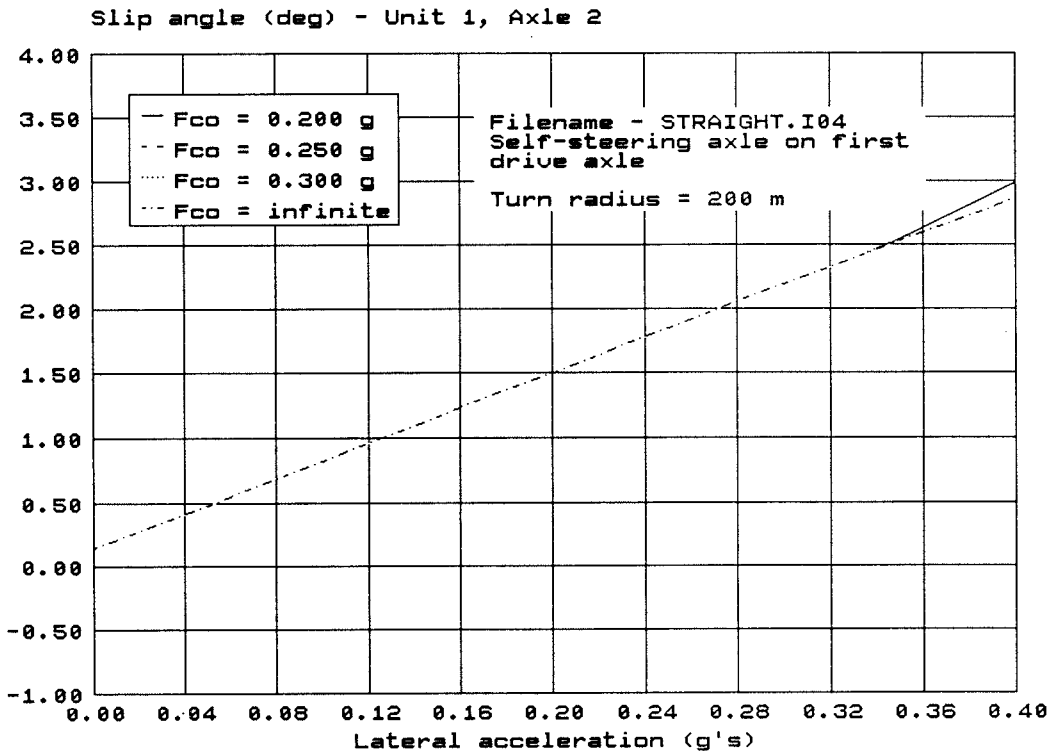
Slip angle (deg) - Unit 1, Axle 2
4.00
3.50
3.00
2.50
2.00
1.50
1.00
0.50
0.00
-0.50
-1.00
Fco = 0.200 g
Fco = 0.250 g
Fco = 0.300 g
Fco = infinite
Filename - STRAIGHT.I04
Self-steering axle on first drive axle
Turn radius = 200 m
0.00 0.04 0.08 0.12 0.16 0.20 0.24 0.28 0.32 0.36 0.40
Lateral acceleration (g's)

STRAIGHT TRUCK WITH SELF-STEERING AXLE ON SECOND DRIVE AXLE

Filename: STRAIGHT.I05

UNIT 1 - STRAIGHT TRUCK

	1	2	3	4	5	6	7	8	9
AXLE	LOAD kg	Cα norm.	DUAL -	e m	k1 g/deg	t m	Ms kg	Fco g	k2 g/deg
1 1st DRIVE	8500.	1.000	Y	-	∞	∞	0.0	∞	∞
2 2nd DRIVE	8500.	1.000	Y	-	0.250	0.360	600.	0.200	0.025
	L m	q m	x m	del t m	del d m	W5 kg			
3 UNIT DATA	6.70	0.00	0.00	1.52	0.00	6700.			

Arbitrarily Set Values - AXLE CENTRING FORCE (Fco)
- 2nd DRIVE AXLE
- Values: 0.20 0.25 0.30 ∞

GENERAL DATA

1	2	3	4
DUAL WHEEL m	Cαs normalized	RADIUS m	ACCELERATION g
0.33	1.000	200.	0.0

Independent Variable - LATERAL ACCELERATION
- Range: 0.00 to 0.40

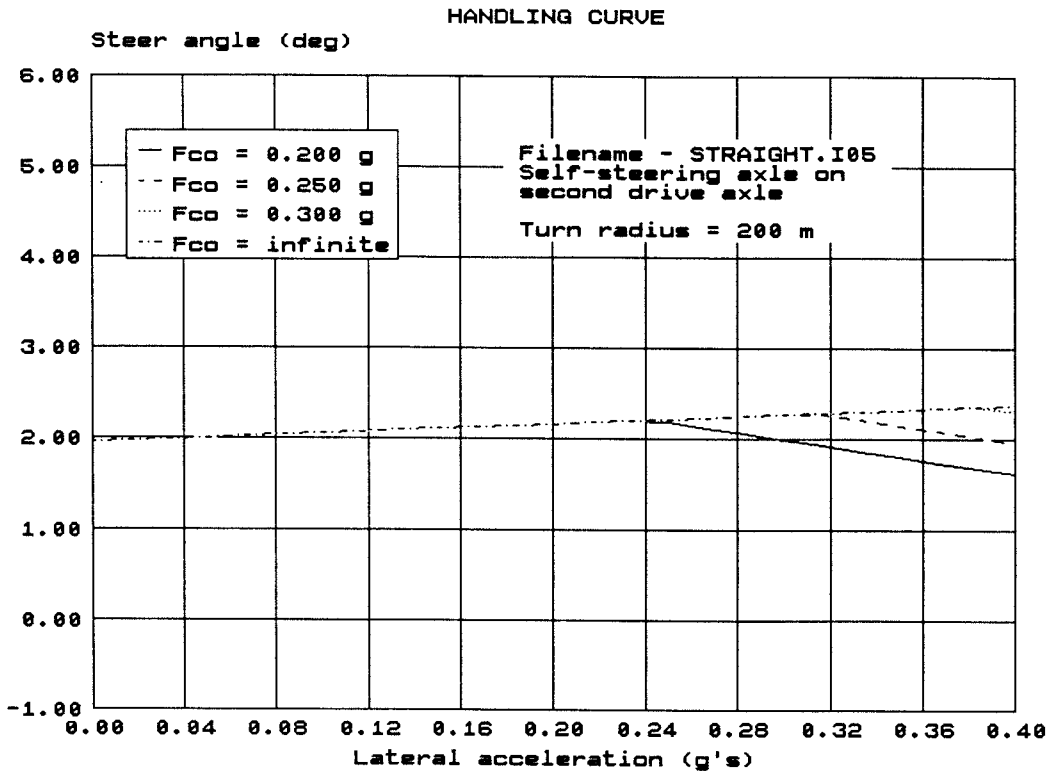
HANDLING CURVE
Steer angle (deg)
6.00
5.00
4.00
3.00
2.00
1.00
0.00
-1.00
Fco = 0.200 g
Fco = 0.250 g
Fco = 0.300 g
Fco = infinite
Filename - STRAIGHT.I05
Self-steering axle on
second drive axle
Turn radius = 200 m
0.00 0.04 0.08 0.12 0.16 0.20 0.24 0.28 0.32 0.36 0.40
Lateral acceleration (g's)

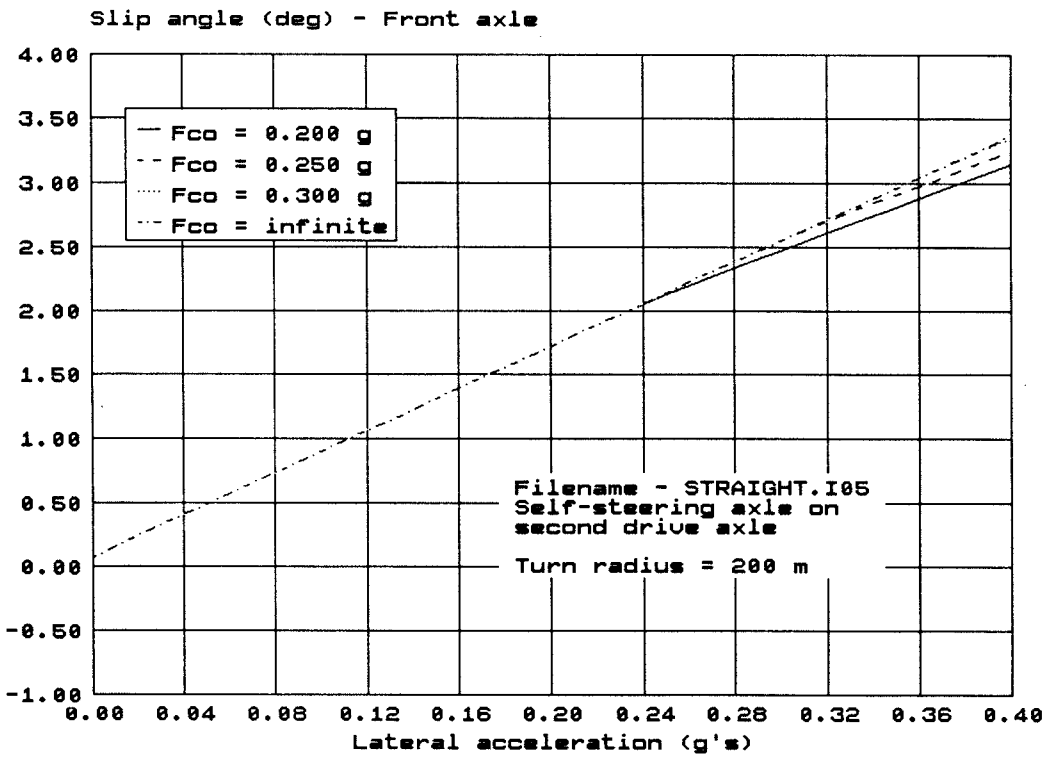
Slip angle (deg) - Front axle
4.00
3.50
3.00
2.50
2.00
1.50
1.00
0.50
0.00
-0.50
-1.00
Fco = 0.200 g
Fco = 0.250 g
Fco = 0.300 g
Fco = infinite
Filename - STRAIGHT.I05
Self-steering axle on
second drive axle
Turn radius = 200 m
0.00 0.04 0.08 0.12 0.16 0.20 0.24 0.28 0.32 0.36 0.40
Lateral acceleration (g's)

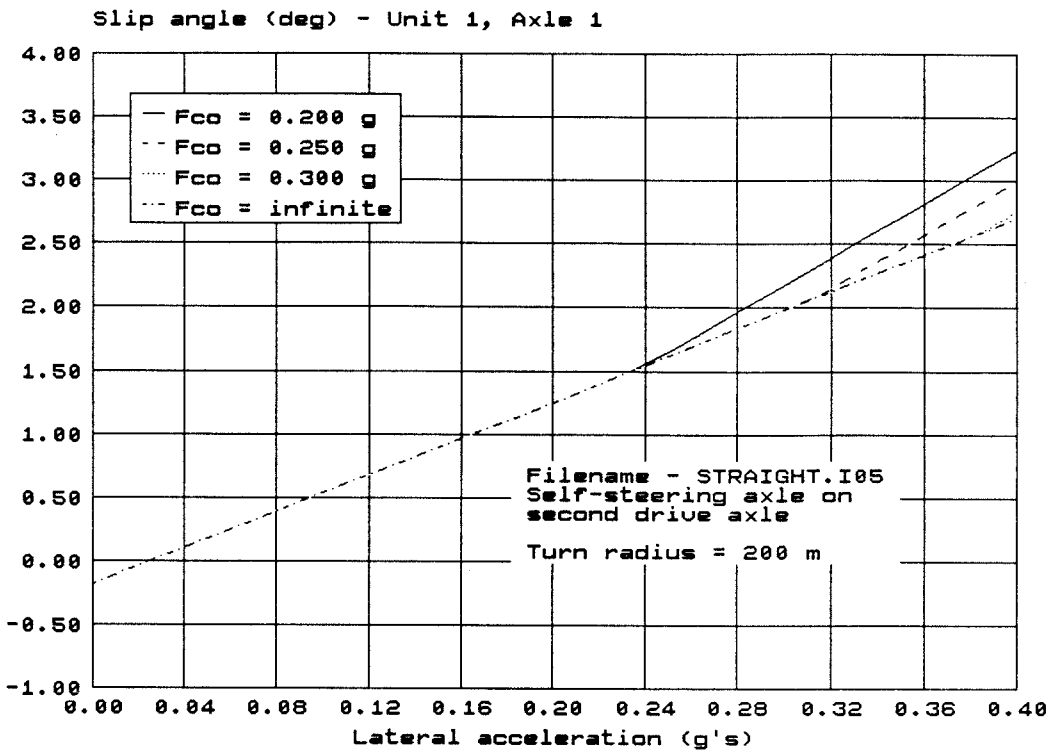
Slip angle (deg) - Unit 1, Axle 1
4.00
3.50
3.00
2.50
2.00
1.50
1.00
0.50
0.00
-0.50
-1.00
Fco = 0.200 g
Fco = 0.250 g
Fco = 0.300 g
Fco = infinite
Filename - STRAIGHT.I05
Self-steering axle on
second drive axle
Turn radius = 200 m
0.00 0.04 0.08 0.12 0.16 0.20 0.24 0.28 0.32 0.36 0.40
Lateral acceleration (g's)

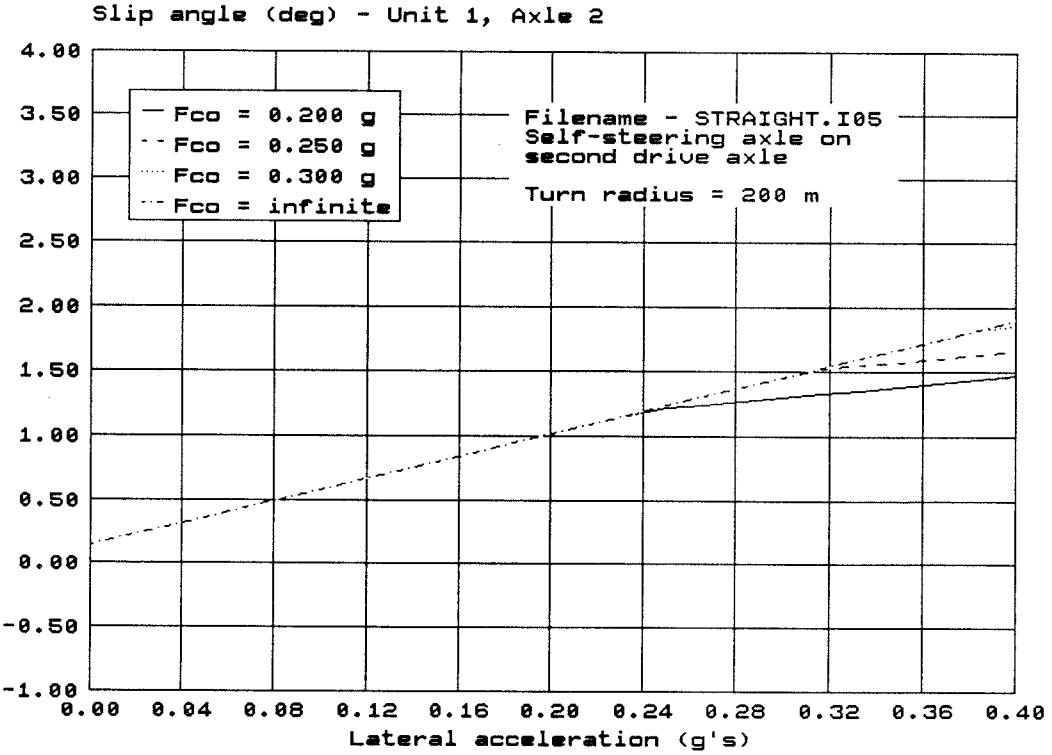
Slip angle (deg) - Unit 1, Axle 2
4.00
3.50
3.00
2.50
2.00
1.50
1.00
0.50
0.00
-0.50
-1.00
Fco = 0.200 g
Fco = 0.250 g
Fco = 0.300 g
Fco = infinite
Filename - STRAIGHT.I05
Self-steering axle on
second drive axle
Turn radius = 200 m
0.00 0.04 0.08 0.12 0.16 0.20 0.24 0.28 0.32 0.36 0.40
Lateral acceleration (g's)

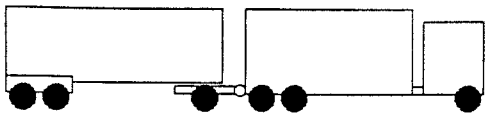

TRUCK FULLTRAILER WITH C-DOLLY

Filename: TRKTRL.I01

UNIT 1 - TOWING UNIT

	1	2	3	4	5	6	7	8	9
AXLE	LOAD kg	Cα norm.	DUAL -	e m	k1 g/deg	t m	Ms kg	Fco g	k2 g/deg
1 1st DRIVE	8500.	1.000	Y	-	∞	∞	0.0	∞	∞
2 2nd DRIVE	8500.	1.000	Y	-	∞	∞	0.0	∞	∞
3 1st DOLLY	7500.	1.000	Y	-	0.250	0.364	600.	0.200	0.025
	L m	q m	x m	del t m	del d m	W5 kg			
4 UNIT DATA	6.70	3.30	0.00	1.52	0.00	6700.			

Arbitrarily Set Values - AXLE CENTRING FORCE (Fco)
- 1st DOLLY AXLE
- Values: 0.20 0.25 0.30 ∞

UNIT 2 - 1st SEMITRAILER

	1	2	3	4	5	6	7	8	9
AXLE	LOAD kg	Cα norm.	DUAL -	e m	k1 g/deg	t m	Ms kg	Fco g	k2 g/deg
1 1st TRAILER	8500.	1.000	Y	-	∞	∞	0.0	∞	∞
2 2nd TRAILER	8500.	1.000	Y	-	∞	∞	0.0	∞	∞
	L m	q m	x m	del t m	del d m	W5 kg			
3 UNIT DATA	5.61	3.80	0.00	1.22	0.00	6800.			

GENERAL DATA

1	2	3	4
DUAL WHEEL m	Cαs normalized	RADIUS m	ACCELERATION g
0.33	1.000	200.	0.0

Independent Variable - LATERAL ACCELERATION
- Range: 0.00 to 0.40

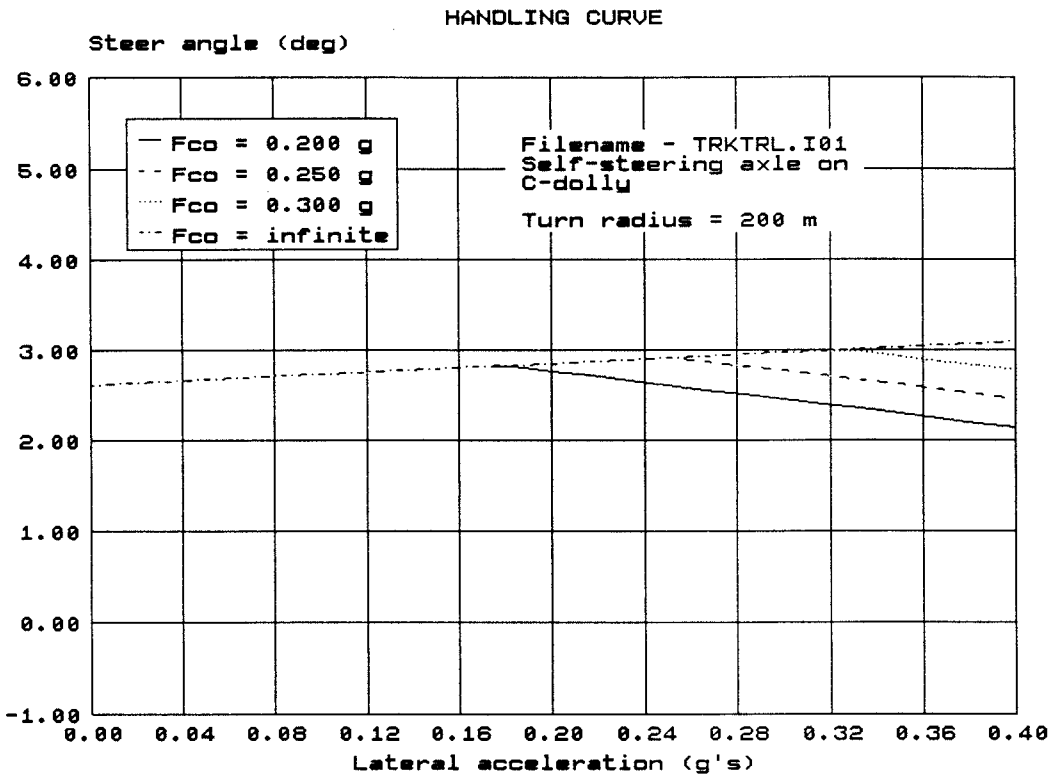
HANDLING CURVE
Steer angle (deg)
6.00
5.00
4.00
3.00
2.00
1.00
0.00
-1.00
Fco = 0.200 g
Fco = 0.250 g
Fco = 0.300 g
Fco = infinite
Filename - TRKTRL.I01
Self-steering axle on
C-dolly
Turn radius = 200 m
0.00 0.04 0.08 0.12 0.16 0.20 0.24 0.28 0.32 0.36 0.40
Lateral acceleration (g's)

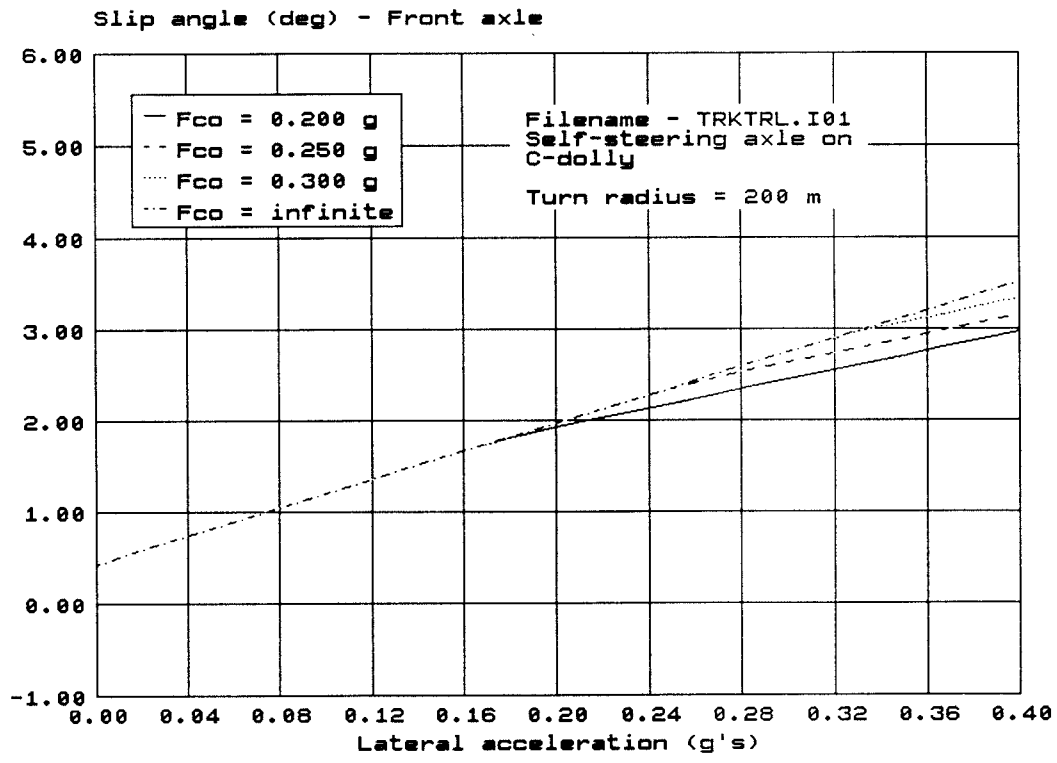
Slip angle (deg) - Front axle
6.00
5.00
4.00
3.00
2.00
1.00
0.00
-1.00
Fco = 0.200 g
Fco = 0.250 g
Fco = 0.300 g
Fco = infinite
Filename - TRKTRL.I01
Self-steering axle on
C-dolly
Turn radius = 200 m
0.00 0.04 0.08 0.12 0.16 0.20 0.24 0.28 0.32 0.36 0.40
Lateral acceleration (g's)

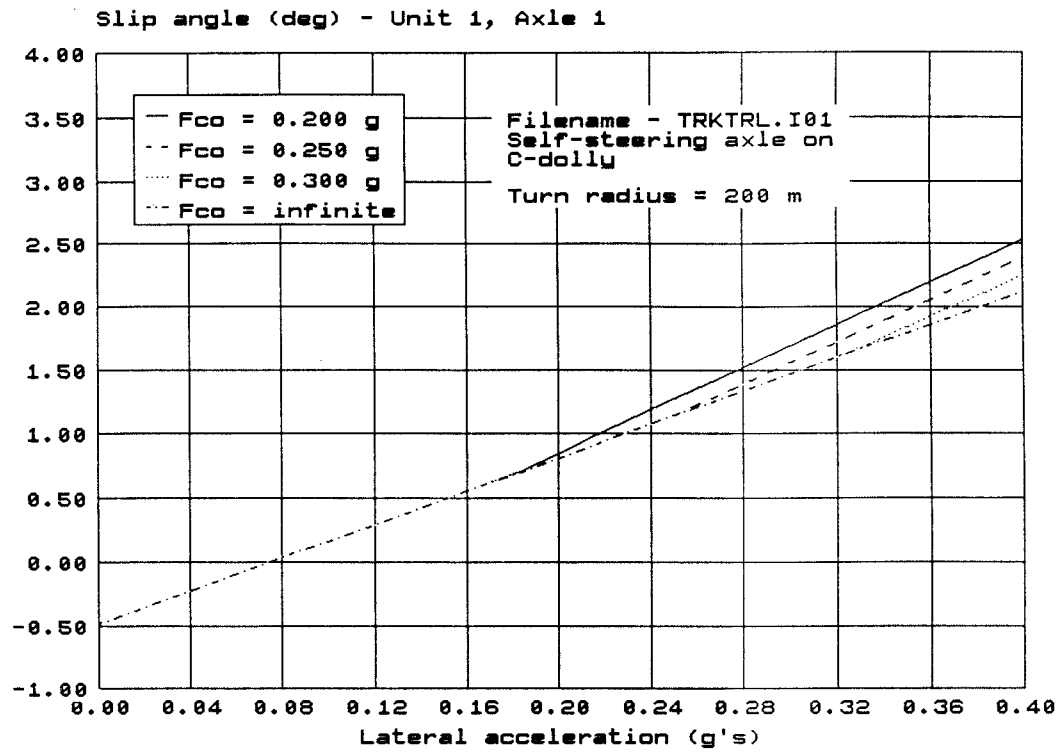
Slip angle (deg) - Unit 1, Axle 1
4.00
3.50
3.00
2.50
2.00
1.50
1.00
0.50
0.00
-0.50
-1.00
Fco = 0.200 g
Fco = 0.250 g
Fco = 0.300 g
Fco = infinite
Filename - TRKTRL.I01
Self-steering axle on
C-dolly
Turn radius = 200 m
0.00 0.04 0.08 0.12 0.16 0.20 0.24 0.28 0.32 0.36 0.40
Lateral acceleration (g's)

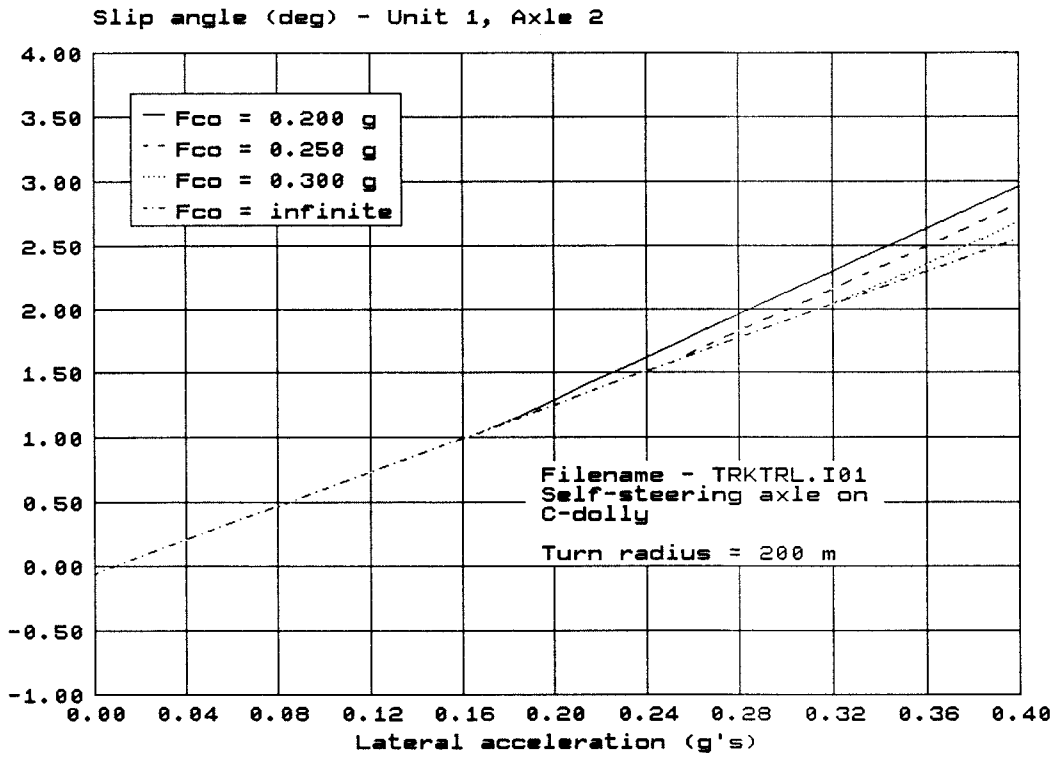
Slip angle (deg) - Unit 1, Axle 2
4.00
3.50
3.00
2.50
2.00
1.50
1.00
0.50
0.00
-0.50
-1.00
Fco = 0.200 g
Fco = 0.250 g
Fco = 0.300 g
Fco = infinite
Filename - TRKTRL.I01
Self-steering axle on
C-dolly
Turn radius = 200 m
0.00 0.04 0.08 0.12 0.16 0.20 0.24 0.28 0.32 0.36 0.40
Lateral acceleration (g's)

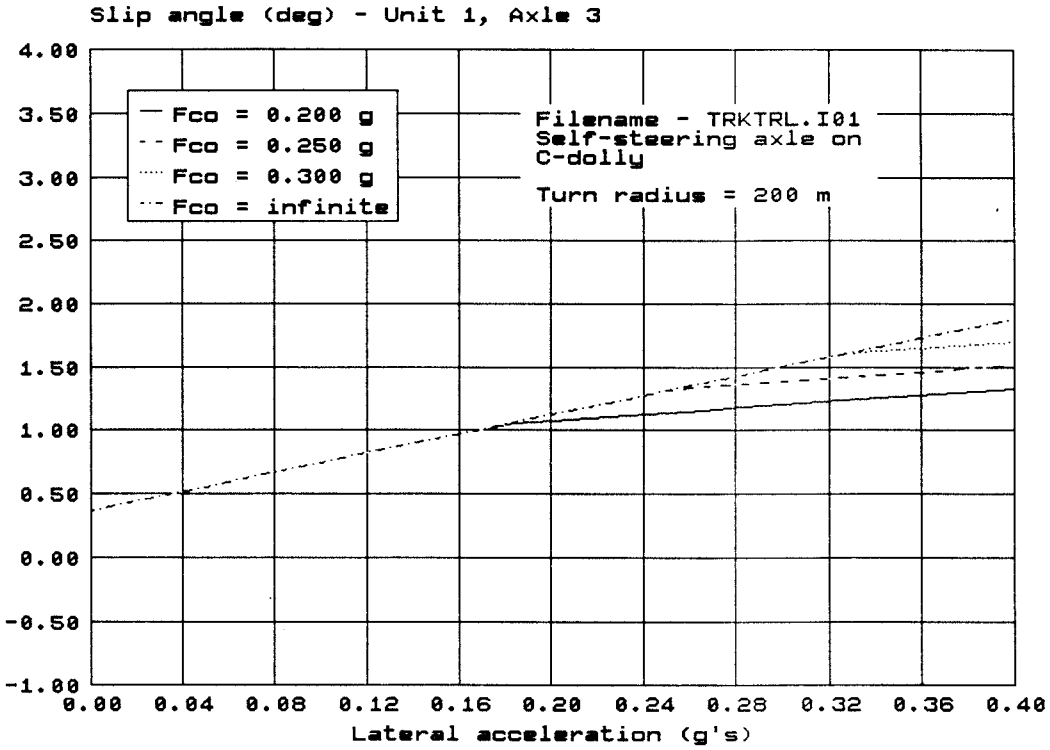
Slip angle (deg) - Unit 1, Axle 3
4.00
3.50
3.00
2.50
2.00
1.50
1.00
0.50
0.00
-0.50
-1.00
Fco = 0.200 g
Fco = 0.250 g
Fco = 0.300 g
Fco = infinite
Filename - TRKTRL.I01
Self-steering axle on
C-dolly
Turn radius = 200 m
0.00 0.04 0.08 0.12 0.16 0.20 0.24 0.28 0.32 0.36 0.40
Lateral acceleration (g's)

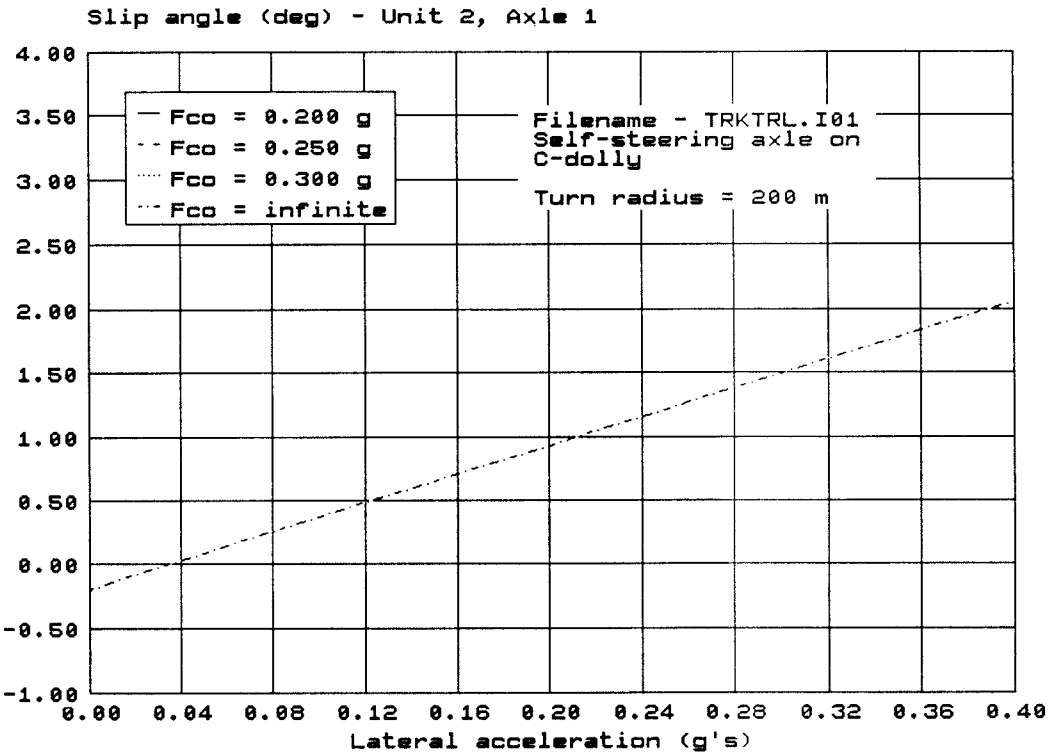
Slip angle (deg) - Unit 2, Axle 1
4.00
3.50
3.00
2.50
2.00
1.50
1.00
0.50
0.00
-0.50
-1.00
Fco = 0.200 g
Fco = 0.250 g
Fco = 0.300 g
Fco = infinite
Filename - TRKTRL.I01
Self-steering axle on
C-dolly
Turn radius = 200 m
0.00 0.04 0.08 0.12 0.16 0.20 0.24 0.28 0.32 0.36 0.40
Lateral acceleration (g's)

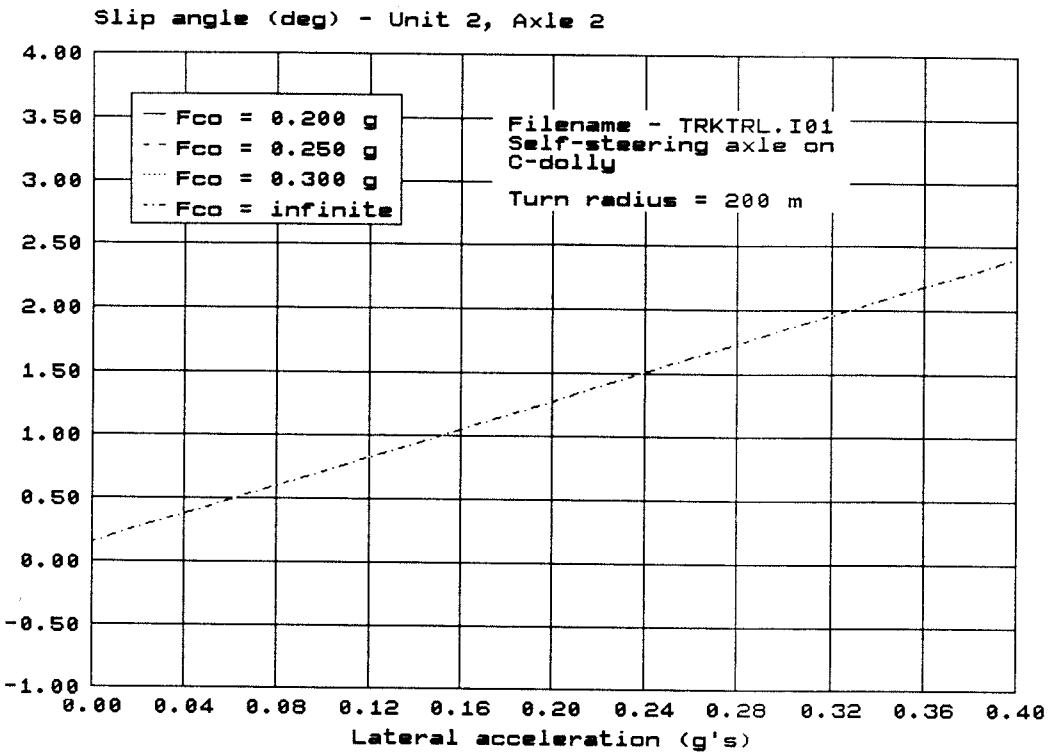
Slip angle (deg) - Unit 2, Axle 2
4.00
3.50
3.00
2.50
2.00
1.50
1.00
0.50
0.00
-0.50
-1.00
Fco = 0.200 g
Fco = 0.250 g
Fco = 0.300 g
Fco = infinite
Filename - TRKTRL.I01
Self-steering axle on C-dolly
Turn radius = 200 m
0.00 0.04 0.08 0.12 0.16 0.20 0.24 0.28 0.32 0.36 0.40
Lateral acceleration (g's)

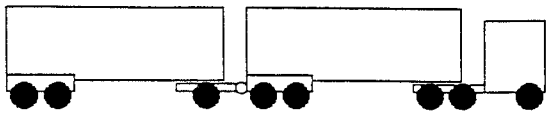

C-TRAIN WITH FIXED AXLE ON C-DOLLY

Filename: C-TRAIN.I09

UNIT 1 - TRACTOR

	1	2	3	4	5	6	7	8	9
AXLE	LOAD kg	Cα norm.	DUAL -	e m	k1 g/deg	t m	Ms kg	Fco g	k2 g/deg
1 1st DRIVE	8500.	1.000	Y	-	∞	∞	0.0	∞	∞
2 2nd DRIVE	8500.	1.000	Y	-	∞	∞	0.0	∞	∞
	L m	q m	x m	del t m	del d m	W5 kg			
3 UNIT DATA	4.40	0.00	0.20	1.60	0.00	5500.			

UNIT 2 - 1st SEMITRAILER

	1	2	3	4	5	6	7	8	9
AXLE	LOAD kg	Cα norm.	DUAL -	e m	k1 g/deg	t m	Ms kg	Fco g	k2 g/deg
1 1st TRAILER	7750.	1.000	Y	-	∞	∞	0.0	∞	∞
2 2nd TRAILER	7750.	1.000	Y	-	∞	∞	0.0	∞	∞
3 1st DOLLY	7500.	1.000	Y	-	∞	∞	0.0	∞	∞
	L m	q m	x m	del t m	del d m	W5 kg			
4 UNIT DATA	6.80	3.30	0.00	1.20	0.00	15000.			

UNIT 3 - 2nd SEMITRAILER

	1	2	3	4	5	6	7	8	9
AXLE	LOAD kg	Cα norm.	DUAL -	e m	k1 g/deg	t m	Ms kg	Fco g	k2 g/deg
1 1st TRAILER	6500.	1.000	Y	-	∞	∞	0.0	∞	∞
2 2nd TRAILER	6500.	1.000	Y	-	∞	∞	0.0	∞	∞
	L m	q m	x m	del t m	del d m	W5 kg			
3 UNIT DATA	5.80	0.00	0.00	1.20	0.00	6000.			

GENERAL DATA

1	2	3	4
DUAL WHEEL m	Cαs normalized	RADIUS m	ACCELERATION g
0.33	1.000	200.	0.0

Independent Variable - LATERAL ACCELERATION
- Range: 0.00 to 0.40

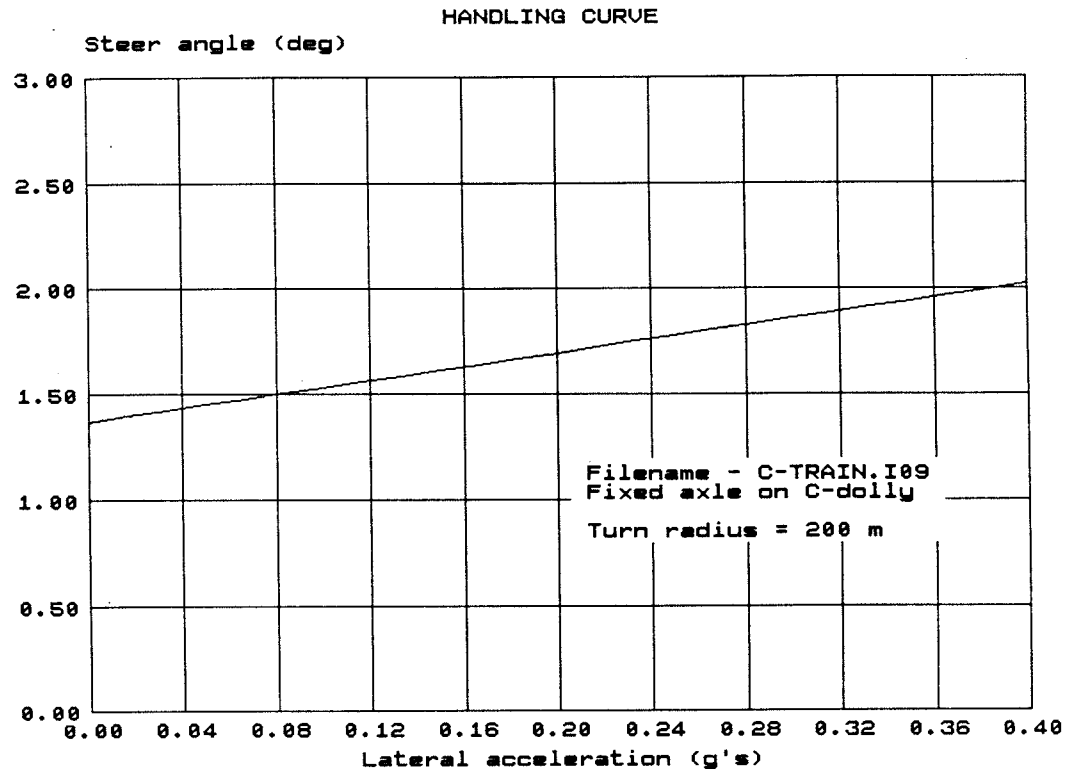
HANDLING CURVE
Steer angle (deg)
3.00
2.50
2.00
1.50
1.00
0.50
0.00
0.00 0.04 0.08 0.12 0.16 0.20 0.24 0.28 0.32 0.36 0.40
Lateral acceleration (g's)
Filename - C-TRAIN.I09
Fixed axle on C-dolly
Turn radius = 200 m

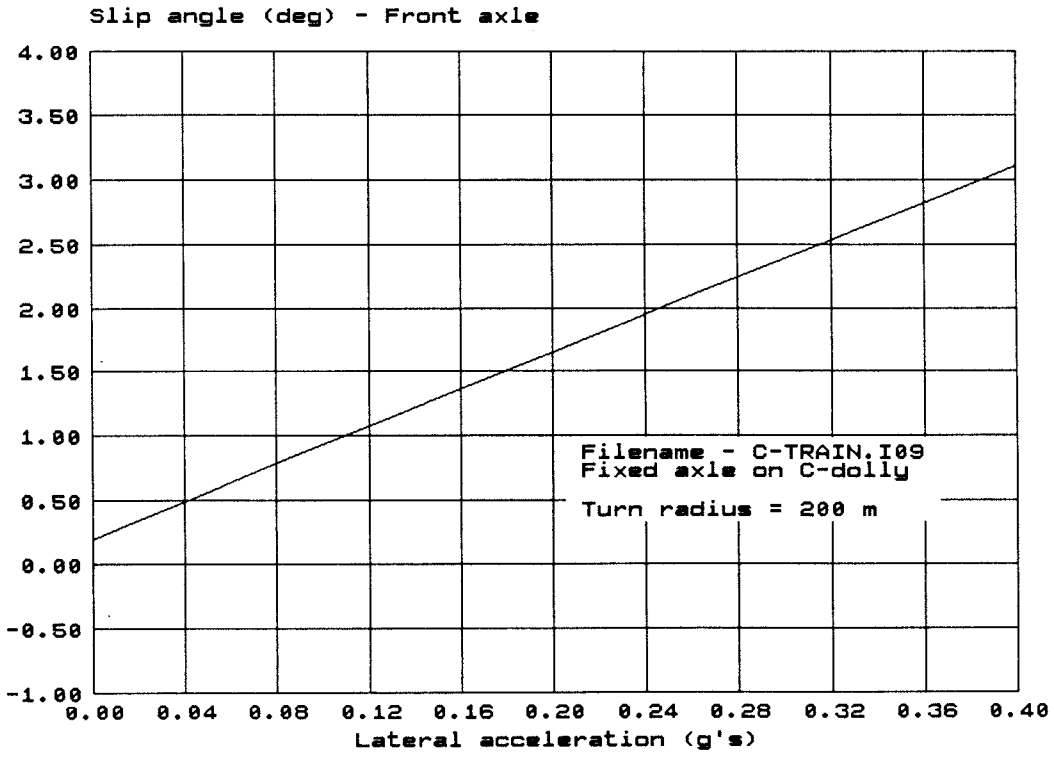
Slip angle (deg) - Front axle
4.00
3.50
3.00
2.50
2.00
1.50
1.00
0.50
0.00
-0.50
-1.00
0.00 0.04 0.08 0.12 0.16 0.20 0.24 0.28 0.32 0.36 0.40
Lateral acceleration (g's)
Filename - C-TRAIN.I09
Fixed axle on C-dolly
Turn radius = 200 m

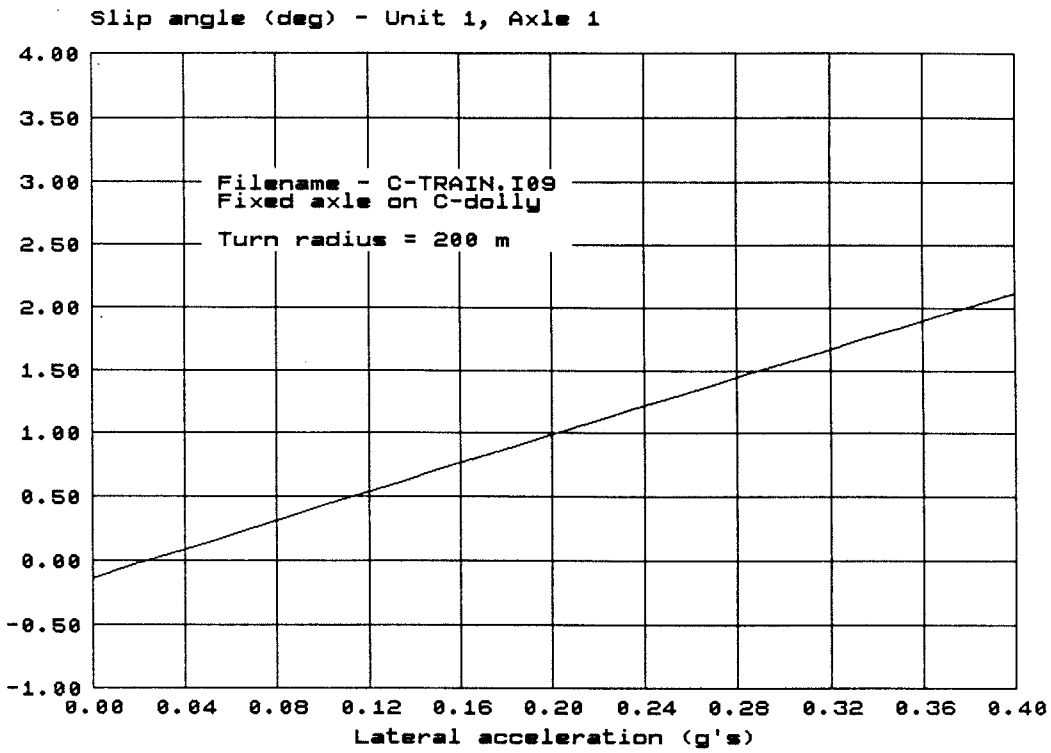
Slip angle (deg) - Unit 1, Axle 1
4.00
3.50
3.00
2.50
2.00
1.50
1.00
0.50
0.00
-0.50
-1.00
Filename - C-TRAIN.I09
Fixed axle on C-dolly
Turn radius = 200 m
0.00 0.04 0.08 0.12 0.16 0.20 0.24 0.28 0.32 0.36 0.40
Lateral acceleration (g's)

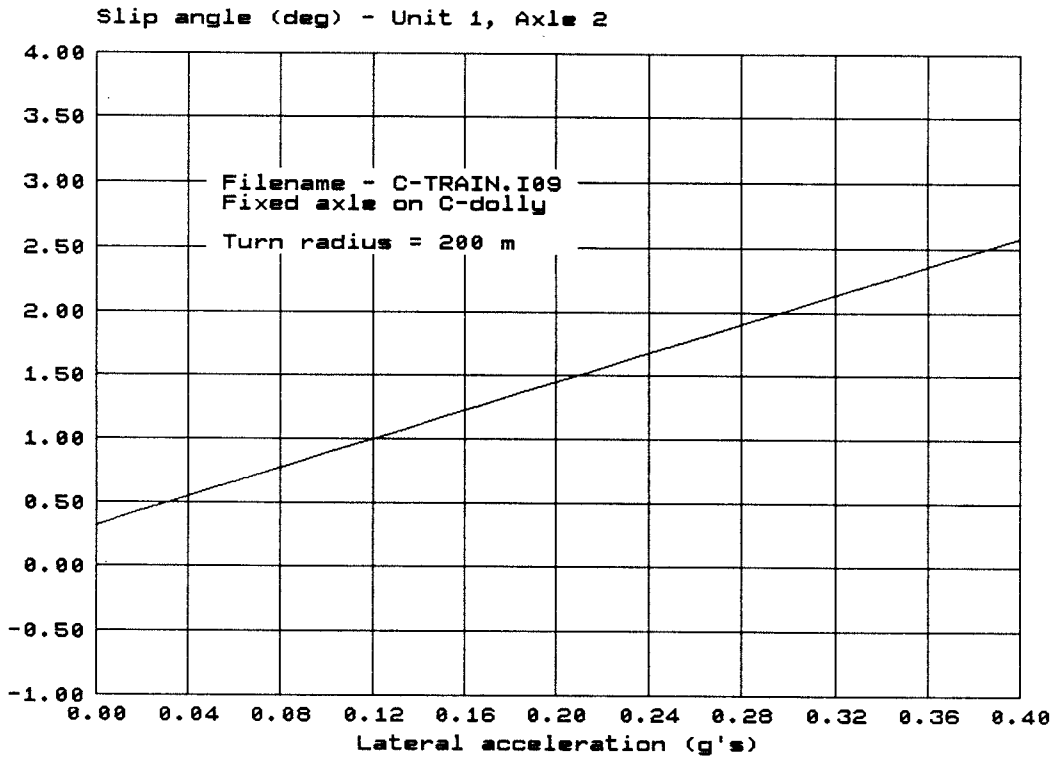
Slip angle (deg) - Unit 1, Axle 2
4.00
3.50
3.00
2.50
2.00
1.50
1.00
0.50
0.00
-0.50
-1.00
Filename - C-TRAIN.I09
Fixed axle on C-dolly
Turn radius = 200 m
0.00 0.04 0.08 0.12 0.16 0.20 0.24 0.28 0.32 0.36 0.40
Lateral acceleration (g's)

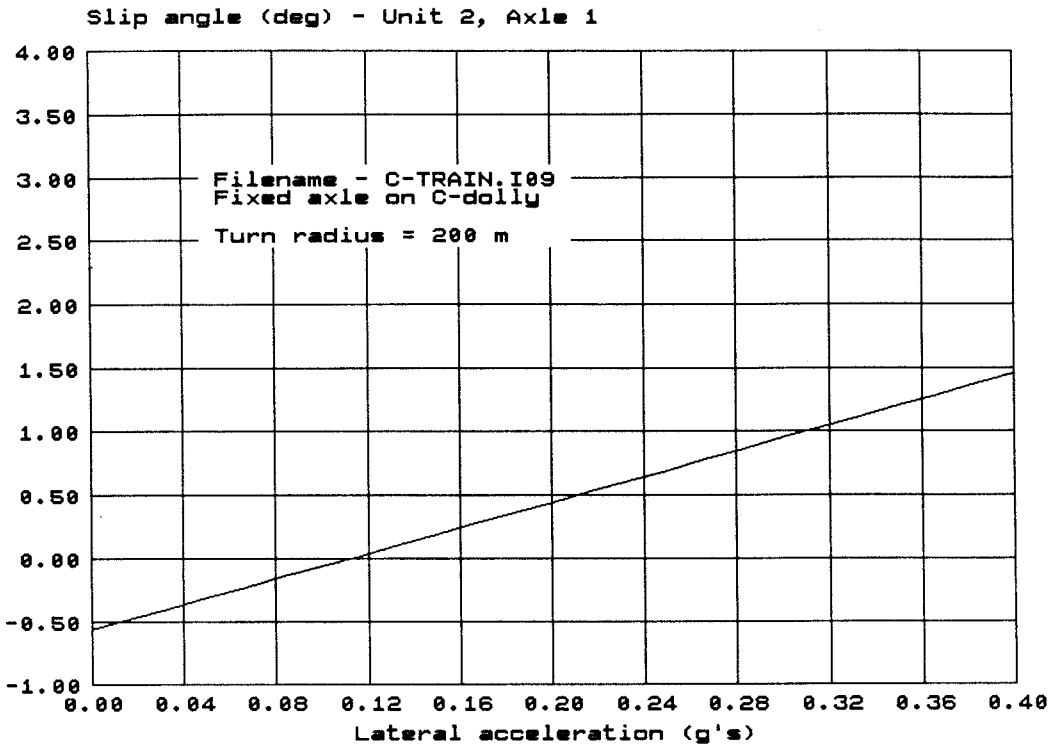
Slip angle (deg) - Unit 2, Axle 1
4.00
3.50
3.00
2.50
2.00
1.50
1.00
0.50
0.00
-0.50
-1.00
Filename - C-TRAIN.I09
Fixed axle on C-dolly
Turn radius = 200 m
0.00 0.04 0.08 0.12 0.16 0.20 0.24 0.28 0.32 0.36 0.40
Lateral acceleration (g's)

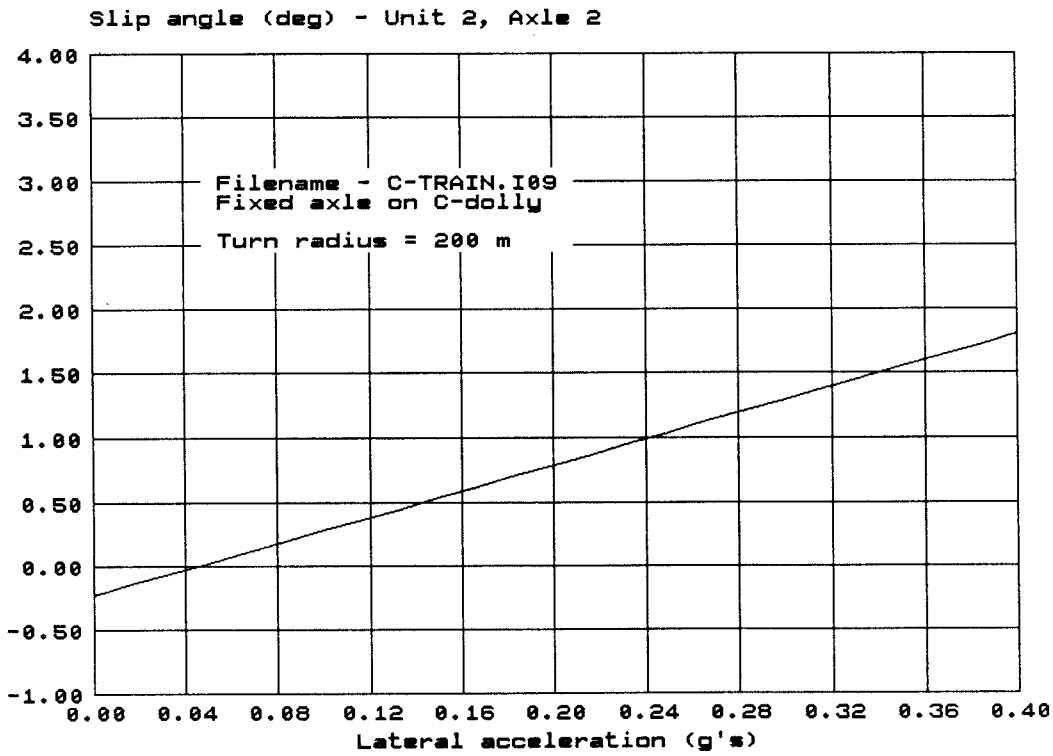
Slip angle (deg) - Unit 2, Axle 2
4.00
3.50
3.00
2.50
2.00
1.50
1.00
0.50
0.00
-0.50
-1.00
Filename - C-TRAIN.I09
Fixed axle on C-dolly
Turn radius = 200 m
0.00 0.04 0.08 0.12 0.16 0.20 0.24 0.28 0.32 0.36 0.40
Lateral acceleration (g's)

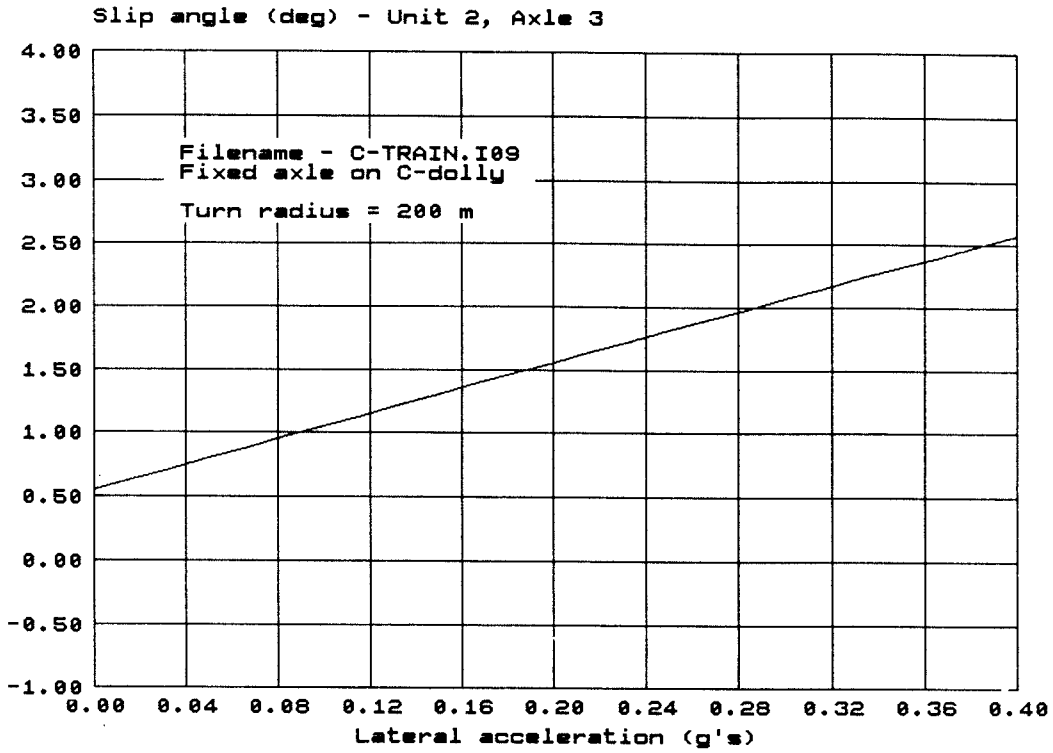
Slip angle (deg) - Unit 2, Axle 3
Filename - C-TRAIN.I09
Fixed axle on C-dolly
Turn radius = 200 m
4.00
3.50
3.00
2.50
2.00
1.50
1.00
0.50
0.00
-0.50
-1.00
0.00 0.04 0.08 0.12 0.16 0.20 0.24 0.28 0.32 0.36 0.40
Lateral acceleration (g's)

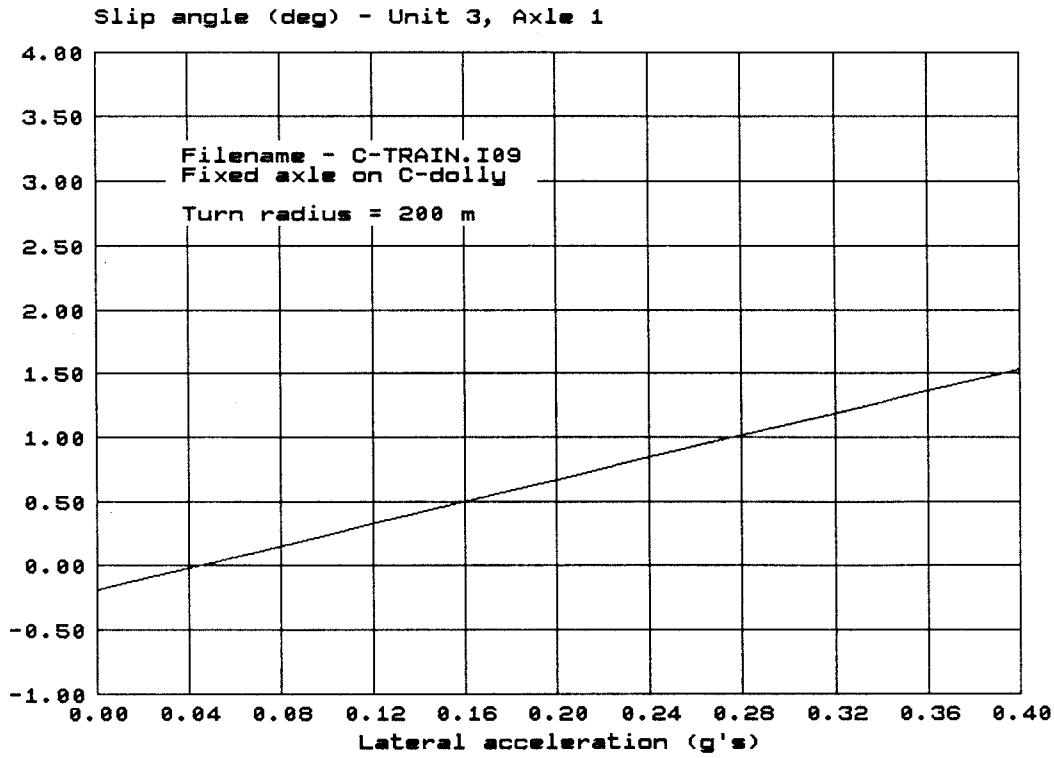
Slip angle (deg) - Unit 3, Axle 1
Filename - C-TRAIN.I09
Fixed axle on C-dolly
Turn radius = 200 m
4.00
3.50
3.00
2.50
2.00
1.50
1.00
0.50
0.00
-0.50
-1.00
0.00 0.04 0.08 0.12 0.16 0.20 0.24 0.28 0.32 0.36 0.40
Lateral acceleration (g's)

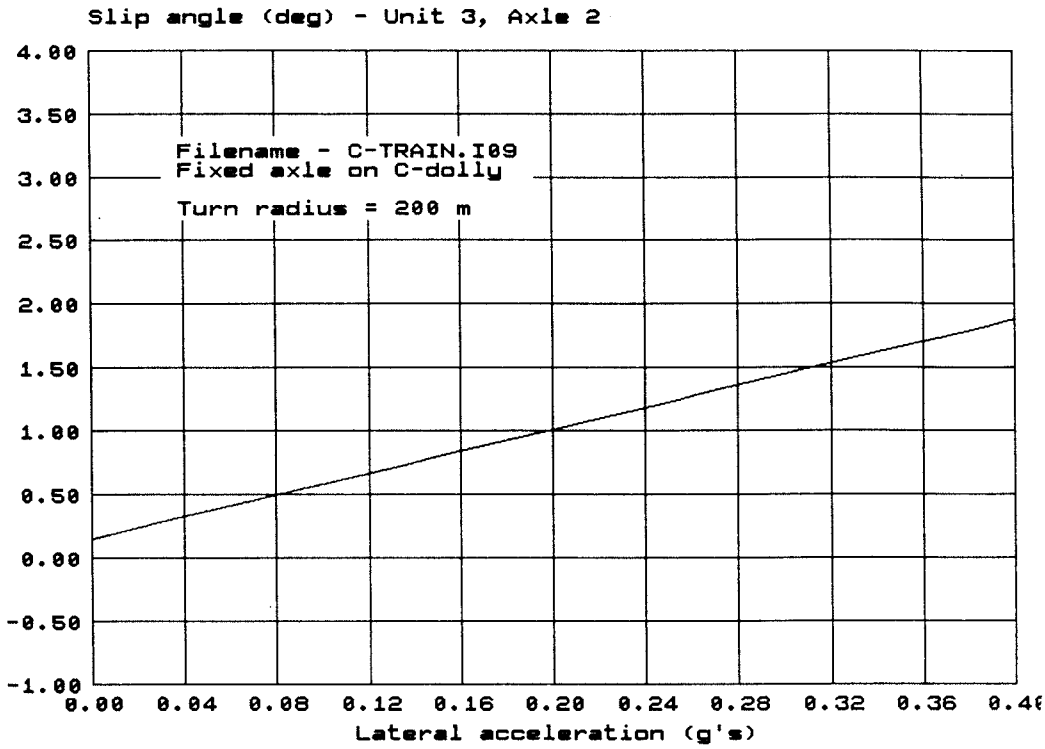
Slip angle (deg) - Unit 3, Axle 2
4.00
3.50
3.00
2.50
2.00
1.50
1.00
0.50
0.00
-0.50
-1.00
Filename - C-TRAIN.I09
Fixed axle on C-dolly
Turn radius = 200 m
0.00
0.04
0.08
0.12
0.16
0.20
0.24
0.28
0.32
0.36
Lateral acceleration (g's)

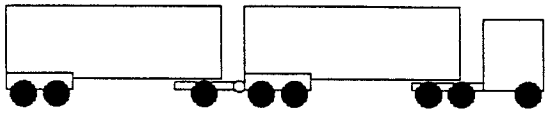

C-TRAIN WITH FIXED AXLE ON C-DOLLY

Filename: C-TRAIN.I08

UNIT 1 - TRACTOR

	1	2	3	4	5	6	7	8	9
AXLE	LOAD kg	Cα norm.	DUAL -	e m	k1 g/deg	t m	Ms kg	Fco g	k2 g/deg
1 1st DRIVE	8500.	1.000	Y	-	∞	∞	0.0	∞	∞
2 2nd DRIVE	8500.	1.000	Y	-	∞	∞	0.0	∞	∞
	L m	q m	x m	del t m	del d m	W5 kg			
3 UNIT DATA	4.40	0.00	0.20	1.60	0.00	5500.			

UNIT 2 - 1st SEMITRAILER

	1	2	3	4	5	6	7	8	9
AXLE	LOAD kg	Cα norm.	DUAL -	e m	k1 g/deg	t m	Ms kg	Fco g	k2 g/deg
1 1st TRAILER	7750.	1.000	Y	-	∞	∞	0.0	∞	∞
2 2nd TRAILER	7750.	1.000	Y	-	∞	∞	0.0	∞	∞
3 1st DOLLY	7500.	1.000	Y	-	∞	∞	0.0	∞	∞
	L m	q m	x m	del t m	del d m	W5 kg			
4 UNIT DATA	6.80	3.30	0.00	1.20	0.00	15000.			

UNIT 3 - 2nd SEMITRAILER

	1	2	3	4	5	6	7	8	9
AXLE	LOAD kg	Cα norm.	DUAL -	e m	k1 g/deg	t m	Ms kg	Fco g	k2 g/deg
1 1st TRAILER	6500.	1.000	Y	-	∞	∞	0.0	∞	∞
2 2nd TRAILER	6500.	1.000	Y	-	∞	∞	0.0	∞	∞
	L m	q m	x m	del t m	del d m	W5 kg			
3 UNIT DATA	5.80	0.00	0.00	1.20	0.00	6000.			

GENERAL DATA

1	2	3	4
DUAL WHEEL m	Cαs normalized	RADIUS m	ACCELERATION g
0.33	1.000	100.	0.0

Independent Variable - LATERAL ACCELERATION
- Range: 0.00 to 0.40

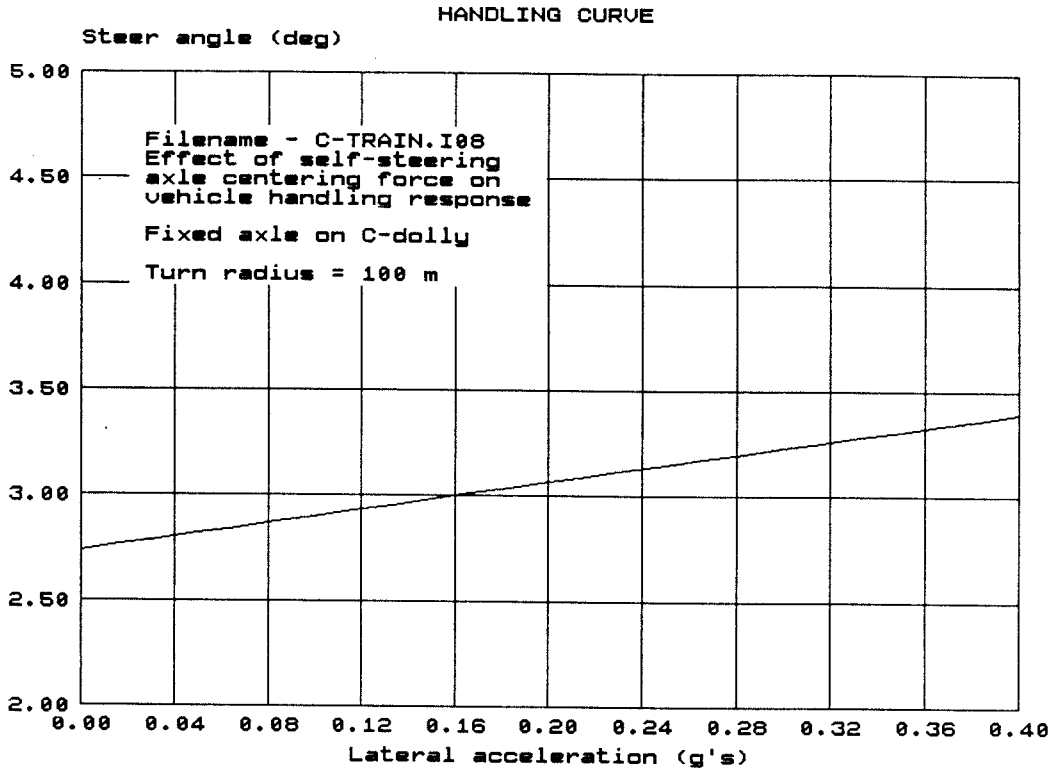
HANDLING CURVE
Steer angle (deg)
5.00
4.50
4.00
3.50
3.00
2.50
2.00
Filename - C-TRAIN.I08
Effect of self-steering
axle centering force on
vehicle handling response
Fixed axle on C-dolly
Turn radius = 100 m
0.00 0.04 0.08 0.12 0.16 0.20 0.24 0.28 0.32 0.36 0.40
Lateral acceleration (g's)

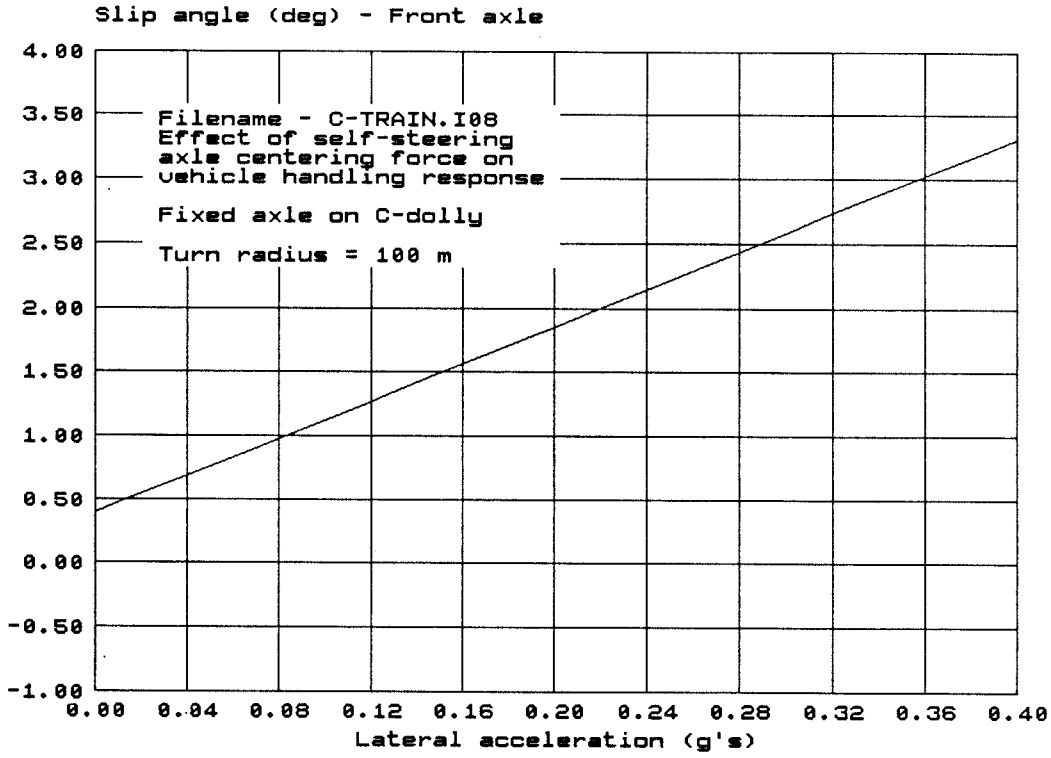
Slip angle (deg) - Front axle
4.00
3.50
3.00
2.50
2.00
1.50
1.00
0.50
0.00
-0.50
-1.00
Filename - C-TRAIN.I08
Effect of self-steering
axle centering force on
vehicle handling response
Fixed axle on C-dolly
Turn radius = 100 m
0.00 0.04 0.08 0.12 0.16 0.20 0.24 0.28 0.32 0.36 0.40
Lateral acceleration (g's)

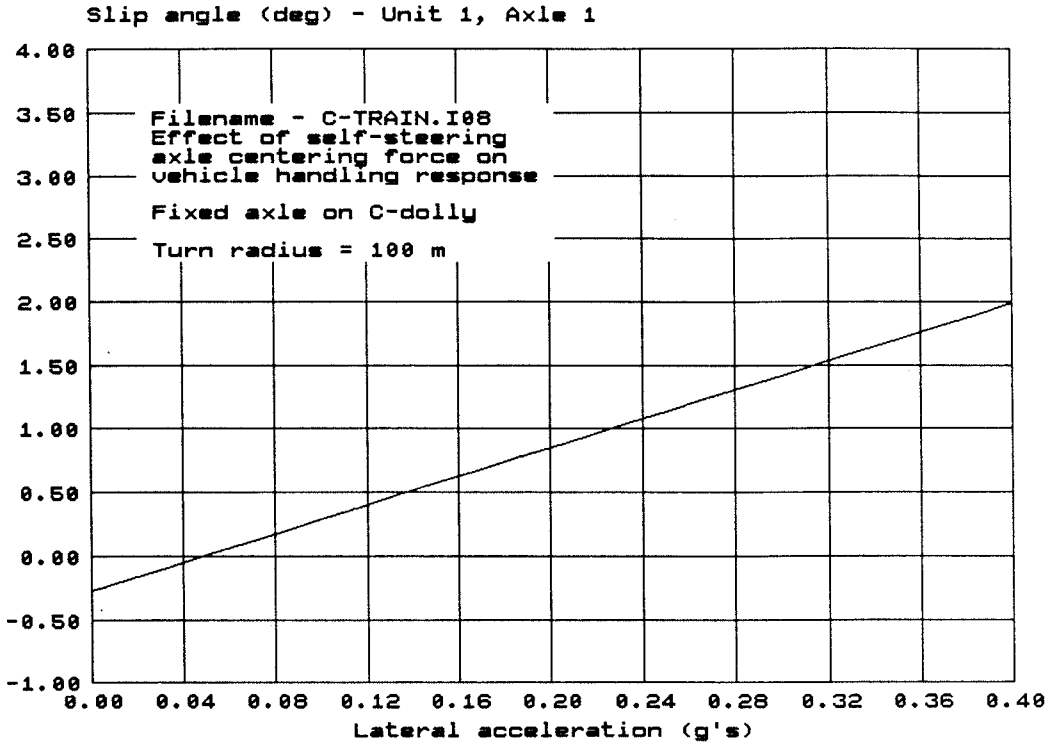
Slip angle (deg) - Unit 1, Axle 1
4.00
3.50
3.00
2.50
2.00
1.50
1.00
0.50
0.00
-0.50
-1.00
Filename - C-TRAIN.I08
Effect of self-steering
axle centering force on
vehicle handling response
Fixed axle on C-dolly
Turn radius = 100 m
0.00 0.04 0.08 0.12 0.16 0.20 0.24 0.28 0.32 0.36 0.40
Lateral acceleration (g's)

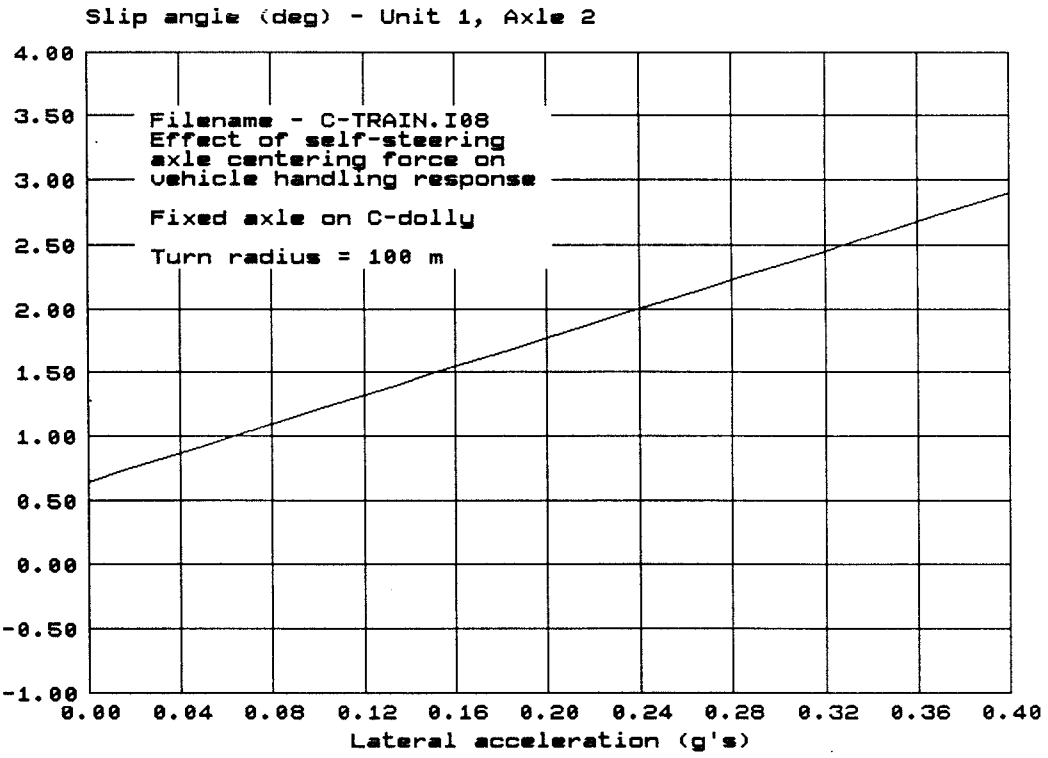
Slip angle (deg) - Unit 1, Axle 2
4.00
3.50
3.00
2.50
2.00
1.50
1.00
0.50
0.00
-0.50
-1.00
Filename - C-TRAIN.I08
Effect of self-steering
axle centering force on
vehicle handling response
Fixed axle on C-dolly
Turn radius = 100 m
0.00 0.04 0.08 0.12 0.16 0.20 0.24 0.28 0.32 0.36 0.40
Lateral acceleration (g's)

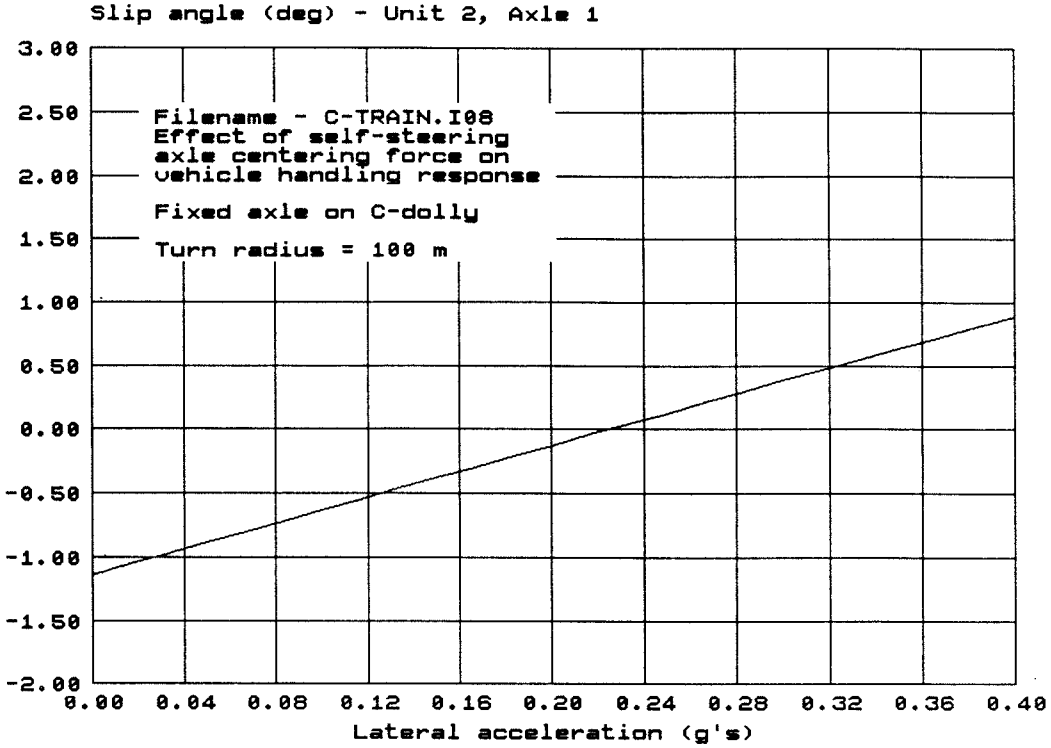
Slip angle (deg) - Unit 2, Axle 1
3.00
2.50
2.00
1.50
1.00
0.50
0.00
-0.50
-1.00
-1.50
-2.00
Filename - C-TRAIN.I08
Effect of self-steering
axle centering force on
vehicle handling response
Fixed axle on C-dolly
Turn radius = 100 m
0.00 0.04 0.08 0.12 0.16 0.20 0.24 0.28 0.32 0.36 0.40
Lateral acceleration (g's)

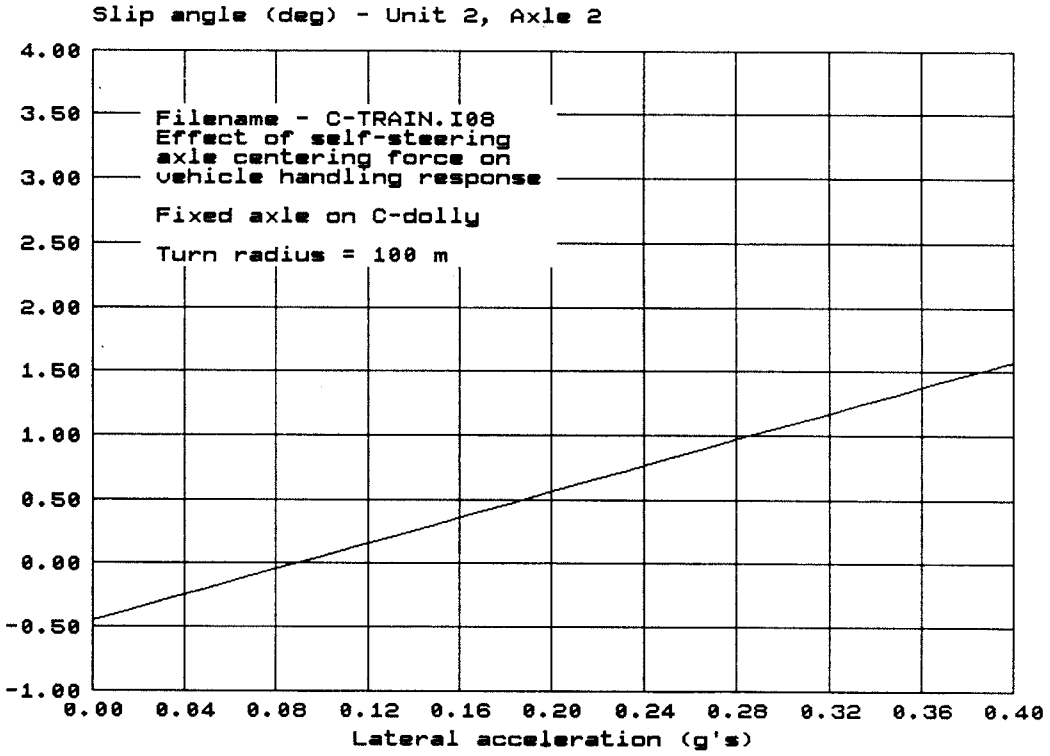
Slip angle (deg) - Unit 2, Axle 2
4.00
3.50
3.00
2.50
2.00
1.50
1.00
0.50
0.00
-0.50
-1.00
Filename - C-TRAIN.I08
Effect of self-steering
axle centering force on
vehicle handling response
Fixed axle on C-dolly
Turn radius = 100 m
0.00 0.04 0.08 0.12 0.16 0.20 0.24 0.28 0.32 0.36 0.40
Lateral acceleration (g's)

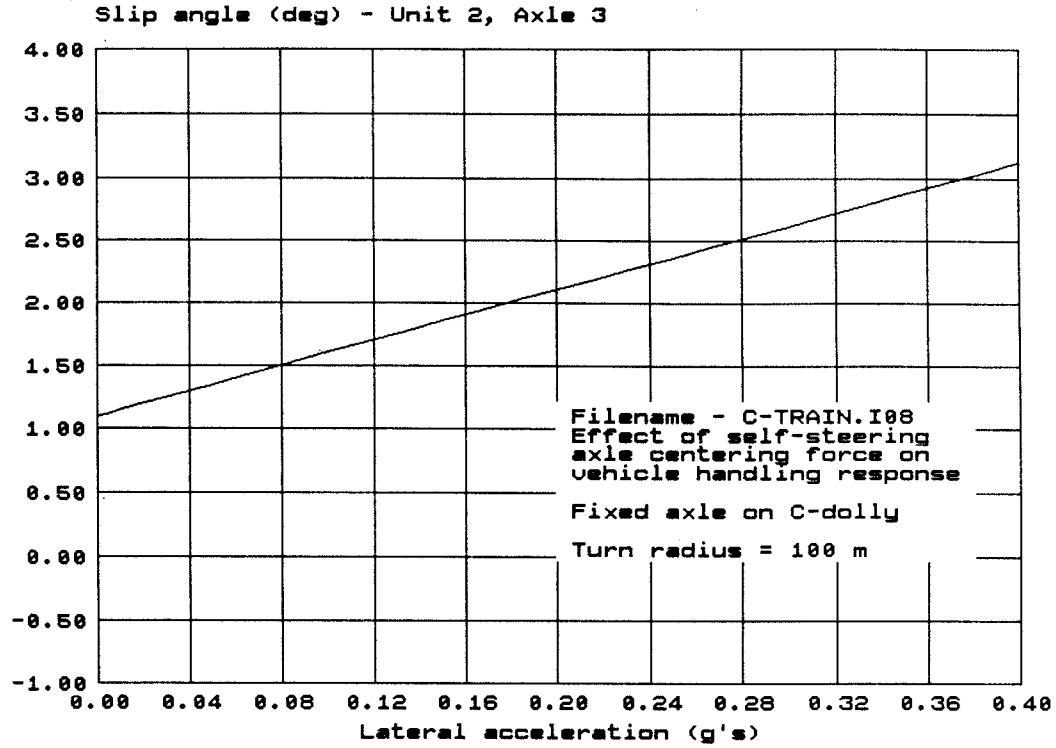
Slip angle (deg) - Unit 2, Axle 3
4.00
3.50
3.00
2.50
2.00
1.50
1.00
0.50
0.00
-0.50
-1.00
0.00 0.04 0.08 0.12 0.16 0.20 0.24 0.28 0.32 0.36 0.40
Lateral acceleration (g's)
Filename - C-TRAIN.I08
Effect of self-steering
axle centering force on
vehicle handling response
Fixed axle on C-dolly
Turn radius = 100 m

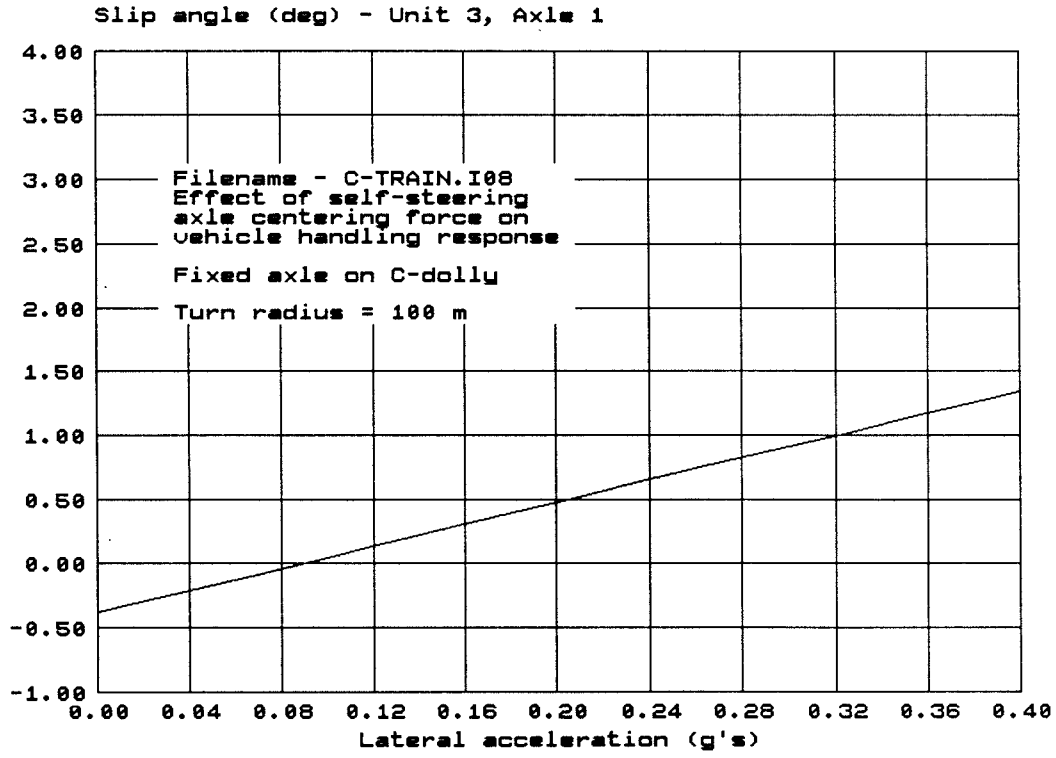
Slip angle (deg) - Unit 3, Axle 1
4.00
3.50
3.00
2.50
2.00
1.50
1.00
0.50
0.00
-0.50
-1.00
0.00 0.04 0.08 0.12 0.16 0.20 0.24 0.28 0.32 0.36 0.40
Lateral acceleration (g's)
Filename - C-TRAIN.I08
Effect of self-steering
axle centering force on
vehicle handling response
Fixed axle on C-dolly
Turn radius = 100 m

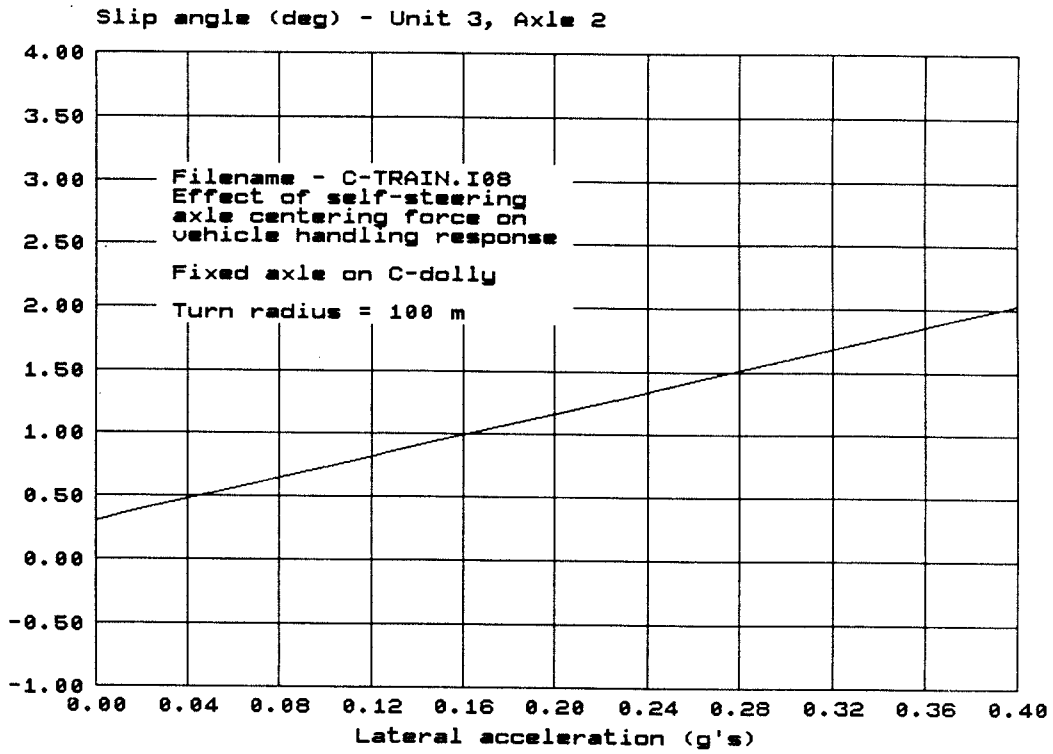
Slip angle (deg) - Unit 3, Axle 2
4.00
3.50
3.00
2.50
2.00
1.50
1.00
0.50
0.00
-0.50
-1.00
Filename - C-TRAIN.I08
Effect of self-steering
axle centering force on
vehicle handling response
Fixed axle on C-dolly
Turn radius = 100 m
0.00 0.04 0.08 0.12 0.16 0.20 0.24 0.28 0.32 0.36 0.40
Lateral acceleration (g's)

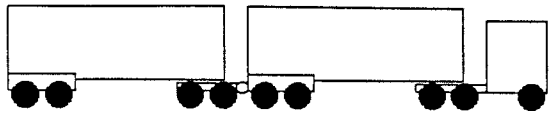

ROAD TRAIN WITH DOLLY EQUIPPED WITH TWO SELF-STEERING AXLES

Filename: C-TRAIN2.I03

UNIT 1 - TRACTOR

	1	2	3	4	5	6	7	8	9
AXLE	LOAD kg	Cα norm.	DUAL -	e m	k1 g/deg	t m	Ms kg	Fco g	k2 g/deg
1 1st DRIVE	8500.	1.000	Y	-	∞	∞	0.0	∞	∞
2 2nd DRIVE	8500.	1.000	Y	-	∞	∞	0.0	∞	∞
	L m	q m	x m	del t m	del d m	W5 kg			
3 UNIT DATA	4.40	0.00	0.20	1.60	0.00	5500.			

UNIT 2 - 1st SEMITRAILER

	1	2	3	4	5	6	7	8	9
AXLE	LOAD kg	Cα norm.	DUAL -	e m	k1 g/deg	t m	Ms kg	Fco g	k2 g/deg
1 1st TRAILER	7750.	1.000	Y	-	∞	∞	0.0	∞	∞
2 2nd TRAILER	7750.	1.000	Y	-	∞	∞	0.0	∞	∞
3 1st DOLLY	7500.	1.000	Y	-	0.250	0.364	600.	0.200	0.004
4 2nd DOLLY	7500.	1.000	Y	-	0.250	0.364	600.	0.200	0.004
	L m	q m	x m	del t m	del d m	W5 kg			
5 UNIT DATA	6.80	3.90	0.00	1.20	1.20	15000.			

Arbitrarily Set Values - AXLE CENTRING FORCE (Fco)
- 1st DOLLY AXLE
- 2nd DOLLY AXLE
- Values: 0.20 0.25 0.30 ∞

UNIT 3 - 2nd SEMITRAILER

	1	2	3	4	5	6	7	8	9
AXLE	LOAD kg	Cα norm.	DUAL -	e m	k1 g/deg	t m	Ms kg	Fco g	k2 g/deg
1 1st TRAILER	6500.	1.000	Y	-	∞	∞	0.0	∞	∞
2 2nd TRAILER	6500.	1.000	Y	-	∞	∞	0.0	∞	∞
	L m	q m	x m	del t m	del d m	W5 kg			
3 UNIT DATA	5.80	0.00	0.00	1.20	0.00	13000.			

GENERAL DATA

1	2	3	4
DUAL WHEEL m	Cαs normalized	RADIUS m	ACCELERATION g
0.33	1.000	200.	0.0

Independent Variable - LATERAL ACCELERATION
- Range: 0.00 to 0.40

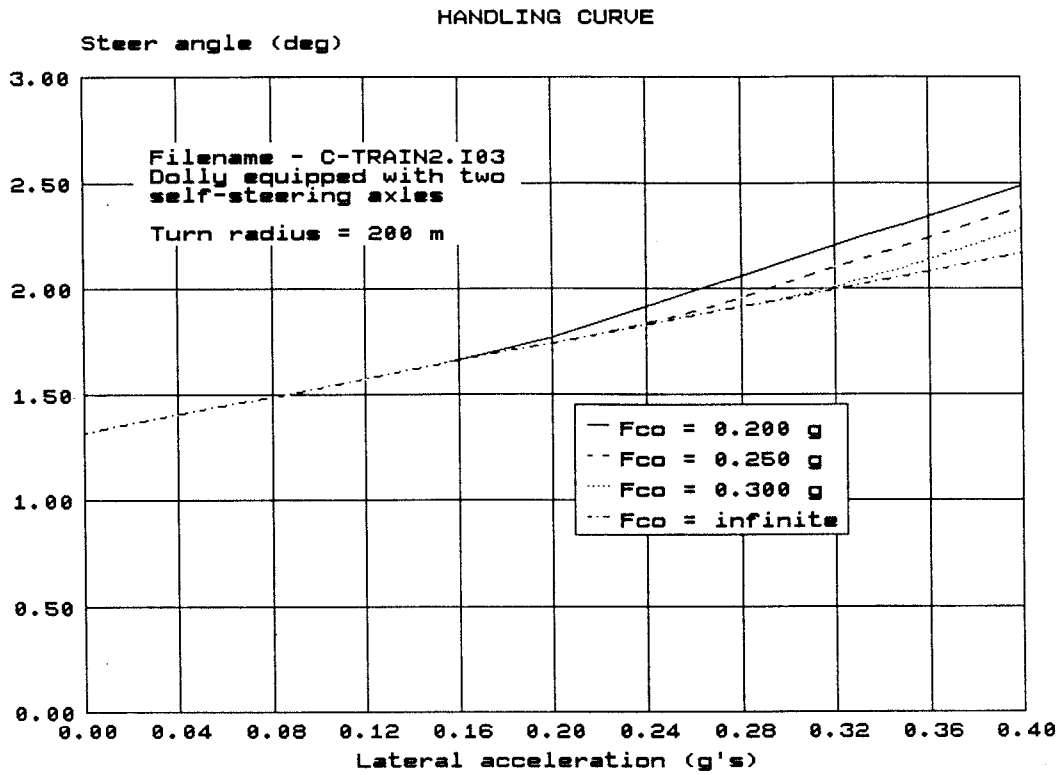
HANDLING CURVE
Steer angle (deg)
3.00
2.50
2.00
1.50
1.00
0.50
0.00
Filename - C-TRAIN2.I03
Dolly equipped with two
self-steering axles
Turn radius = 200 m
Fco = 0.200 g
Fco = 0.250 g
Fco = 0.300 g
Fco = infinite
0.00 0.04 0.08 0.12 0.16 0.20 0.24 0.28 0.32 0.36 0.40
Lateral acceleration (g's)

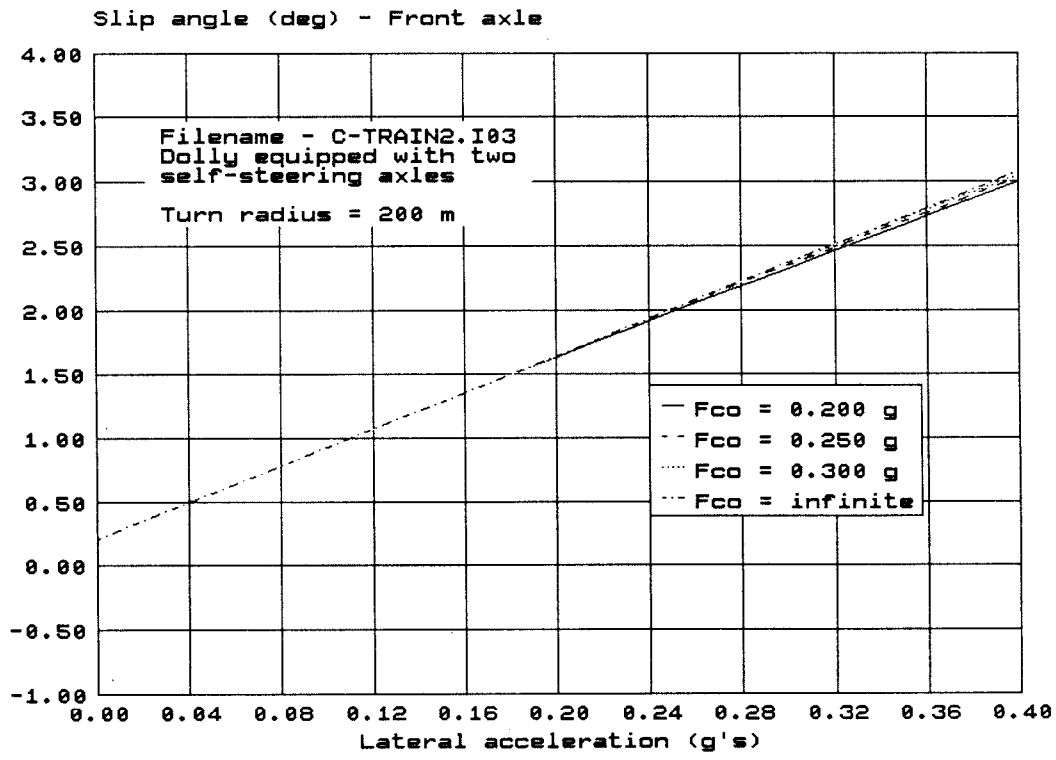
Slip angle (deg) - Front axle
4.00
3.50
3.00
2.50
2.00
1.50
1.00
0.50
0.00
-0.50
-1.00
Filename - C-TRAIN2.I03
Dolly equipped with two
self-steering axles
Turn radius = 200 m
Fco = 0.200 g
Fco = 0.250 g
Fco = 0.300 g
Fco = infinite
0.00 0.04 0.08 0.12 0.16 0.20 0.24 0.28 0.32 0.36 0.40
Lateral acceleration (g's)

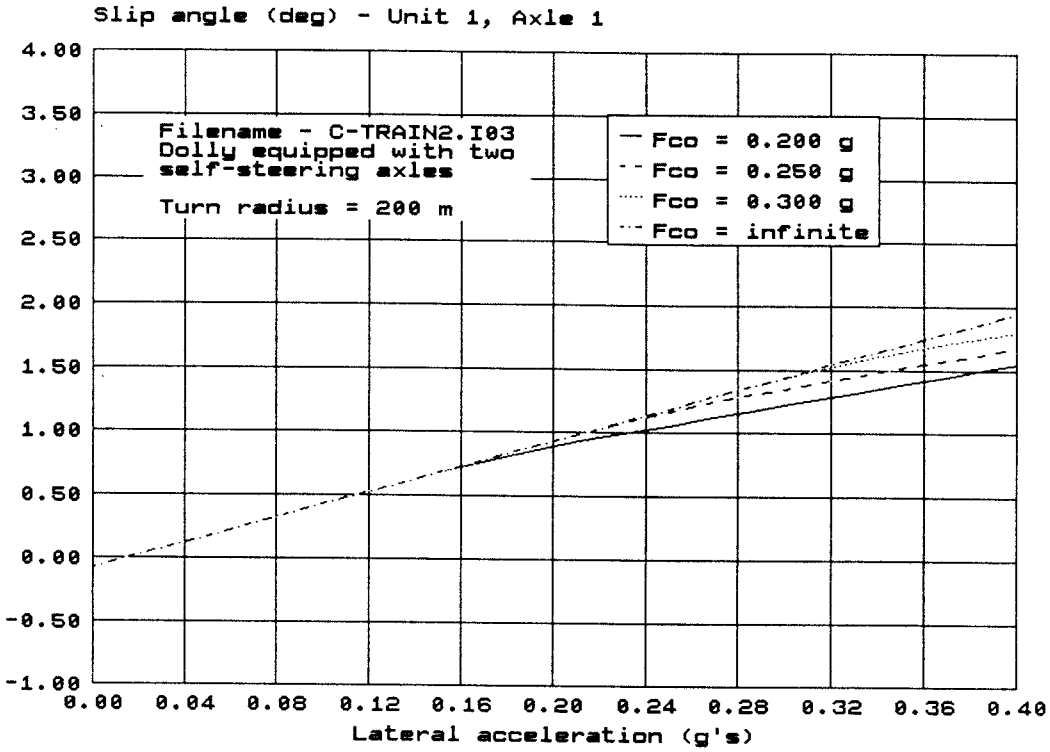
Slip angle (deg) - Unit 1, Axle 1
Filename - C-TRAIN2.I03
Dolly equipped with two
self-steering axles
Turn radius = 200 m
Fco = 0.200 g
Fco = 0.250 g
Fco = 0.300 g
Fco = infinite
4.00
3.50
3.00
2.50
2.00
1.50
1.00
0.50
0.00
-0.50
-1.00
0.00 0.04 0.08 0.12 0.16 0.20 0.24 0.28 0.32 0.36 0.40
Lateral acceleration (g's)

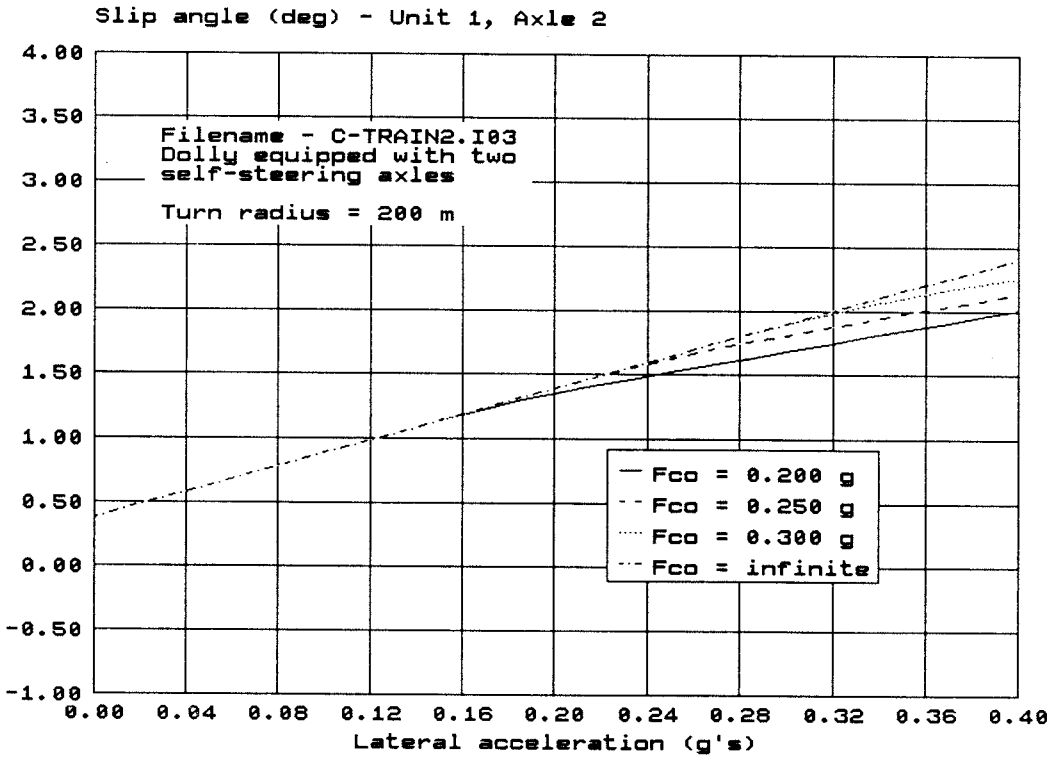
Slip angle (deg) - Unit 1, Axle 2
Filename - C-TRAIN2.I03
Dolly equipped with two
self-steering axles
Turn radius = 200 m
Fco = 0.200 g
Fco = 0.250 g
Fco = 0.300 g
Fco = infinite
4.00
3.50
3.00
2.50
2.00
1.50
1.00
0.50
0.00
-0.50
-1.00
0.00 0.04 0.08 0.12 0.16 0.20 0.24 0.28 0.32 0.36 0.40
Lateral acceleration (g's)

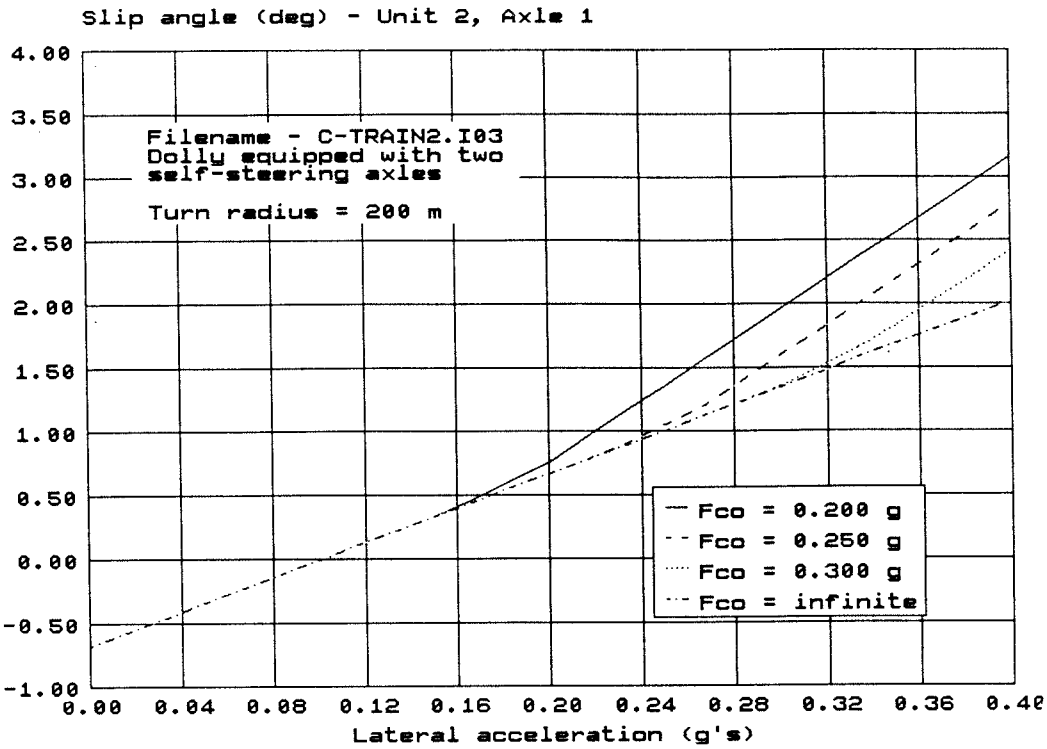
Slip angle (deg) - Unit 2, Axle 1
Filename - C-TRAIN2.I03
Dolly equipped with two
self-steering axles
Turn radius = 200 m
Fco = 0.200 g
Fco = 0.250 g
Fco = 0.300 g
Fco = infinite
4.00
3.50
3.00
2.50
2.00
1.50
1.00
0.50
0.00
-0.50
-1.00
0.00 0.04 0.08 0.12 0.16 0.20 0.24 0.28 0.32 0.36 0.40
Lateral acceleration (g's)

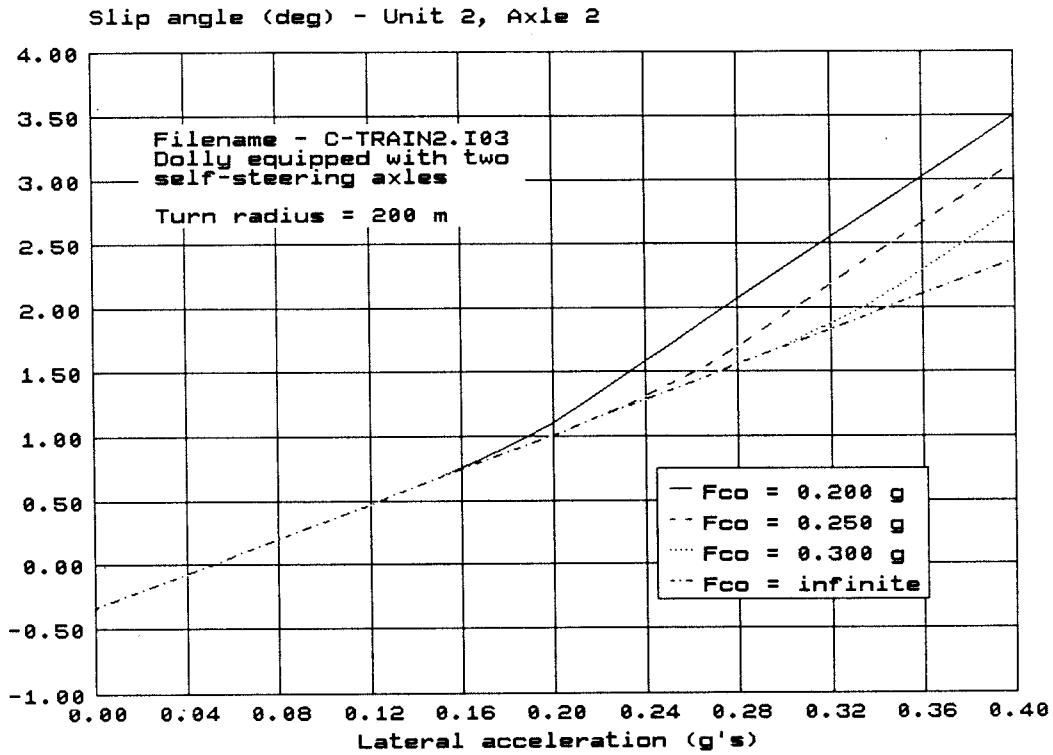
Slip angle (deg) - Unit 2, Axle 2
Filename - C-TRAIN2.I03
Dolly equipped with two
self-steering axles
Turn radius = 200 m
Fco = 0.200 g
Fco = 0.250 g
Fco = 0.300 g
Fco = infinite
4.00
3.50
3.00
2.50
2.00
1.50
1.00
0.50
0.00
-0.50
-1.00
0.00 0.04 0.08 0.12 0.16 0.20 0.24 0.28 0.32 0.36 0.40
Lateral acceleration (g's)

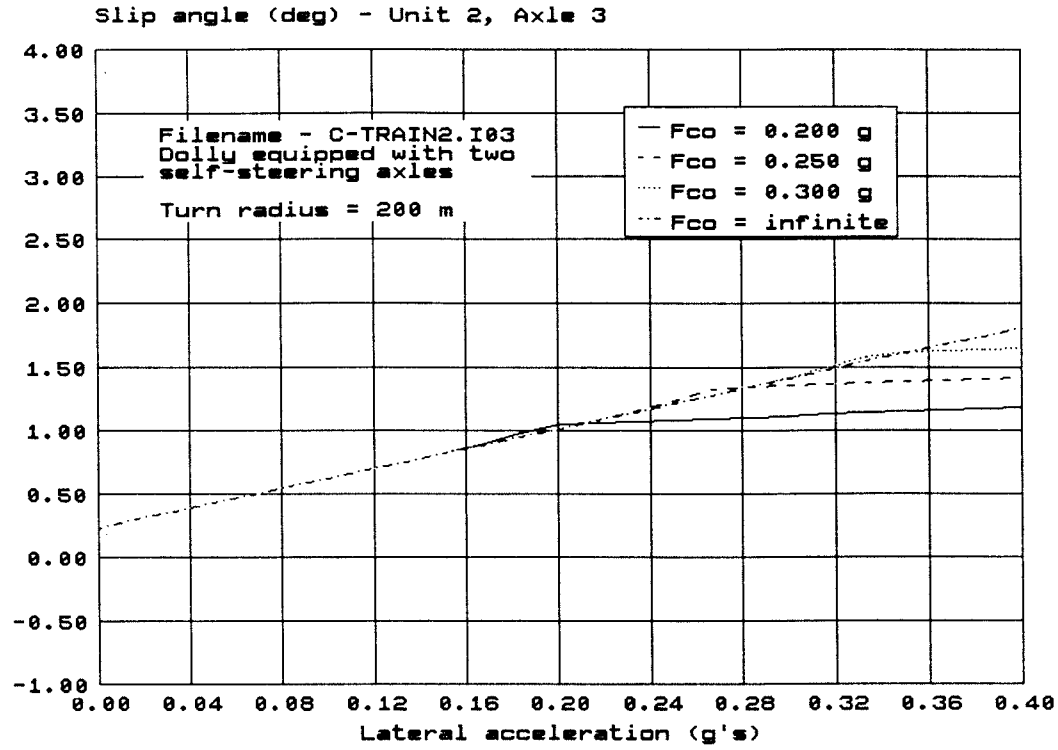
Slip angle (deg) - Unit 2, Axle 3
Filename - C-TRAIN2.I03
Dolly equipped with two
self-steering axles
Turn radius = 200 m
Fco = 0.200 g
Fco = 0.250 g
Fco = 0.300 g
Fco = infinite
4.00
3.50
3.00
2.50
2.00
1.50
1.00
0.50
0.00
-0.50
-1.00
0.00 0.04 0.08 0.12 0.16 0.20 0.24 0.28 0.32 0.36 0.40
Lateral acceleration (g's)

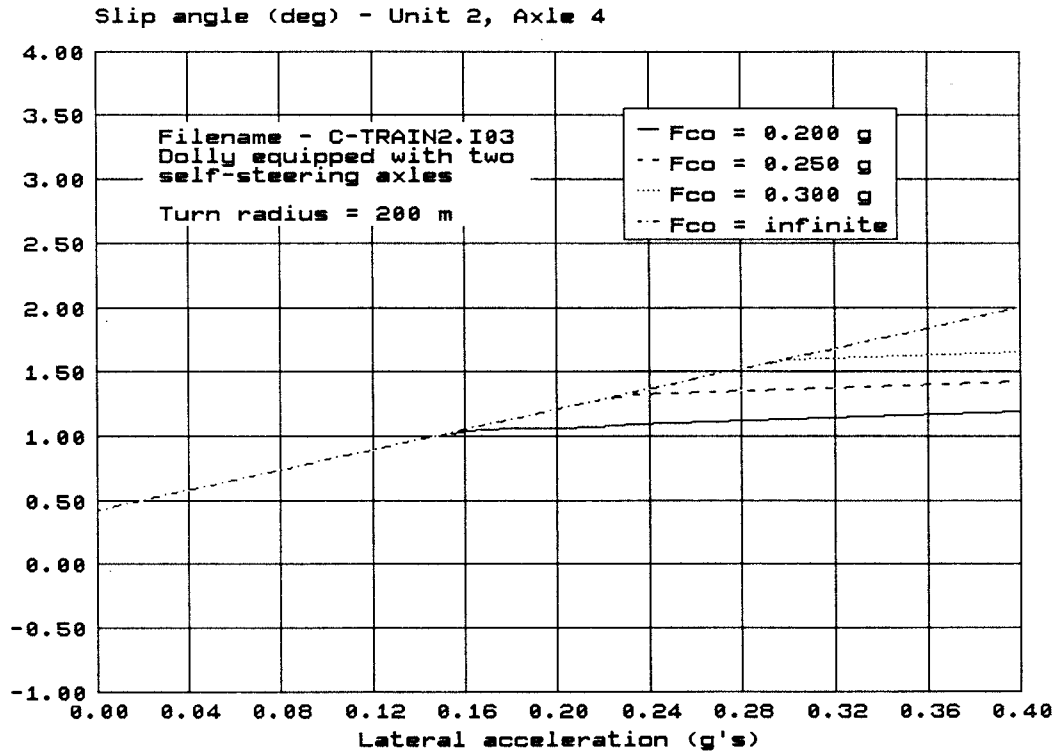
Slip angle (deg) - Unit 2, Axle 4
Filename - C-TRAIN2.I03
Dolly equipped with two
self-steering axles
Turn radius = 200 m
Fco = 0.200 g
Fco = 0.250 g
Fco = 0.300 g
Fco = infinite
4.00
3.50
3.00
2.50
2.00
1.50
1.00
0.50
0.00
-0.50
-1.00
0.00 0.04 0.08 0.12 0.16 0.20 0.24 0.28 0.32 0.36 0.40
Lateral acceleration (g's)

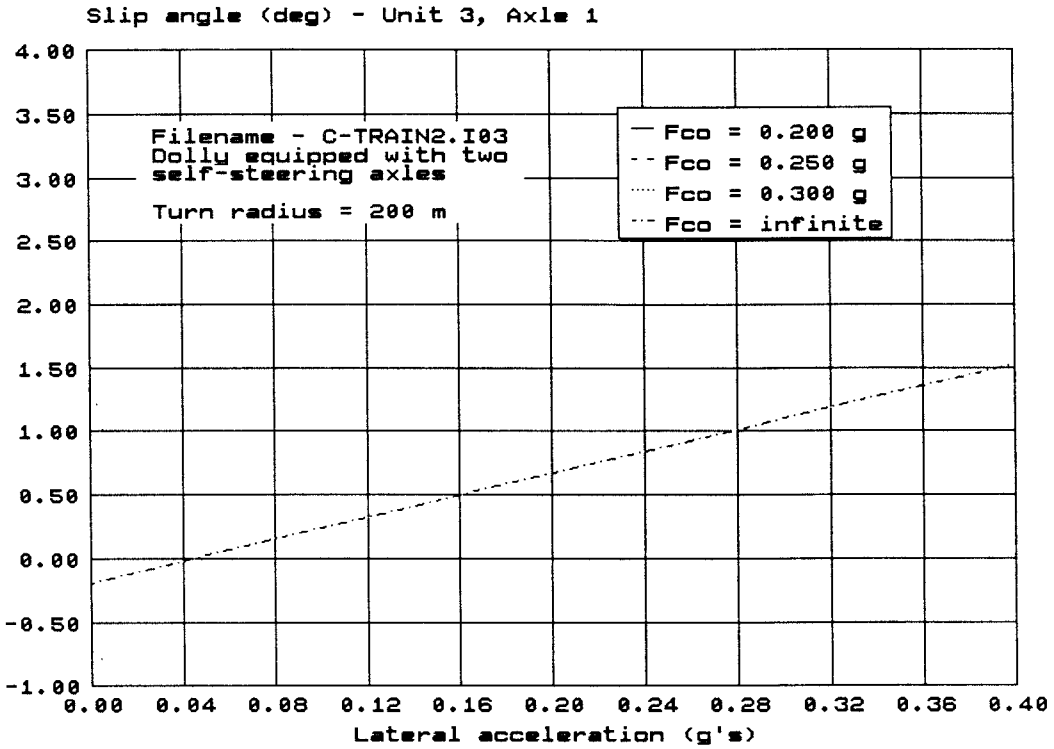
Slip angle (deg) - Unit 3, Axle 1
Filename - C-TRAIN2.I03
Dolly equipped with two
self-steering axles
Turn radius = 200 m
Fco = 0.200 g
Fco = 0.250 g
Fco = 0.300 g
Fco = infinite
4.00
3.50
3.00
2.50
2.00
1.50
1.00
0.50
0.00
-0.50
-1.00
0.00 0.04 0.08 0.12 0.16 0.20 0.24 0.28 0.32 0.36 0.40
Lateral acceleration (g's)

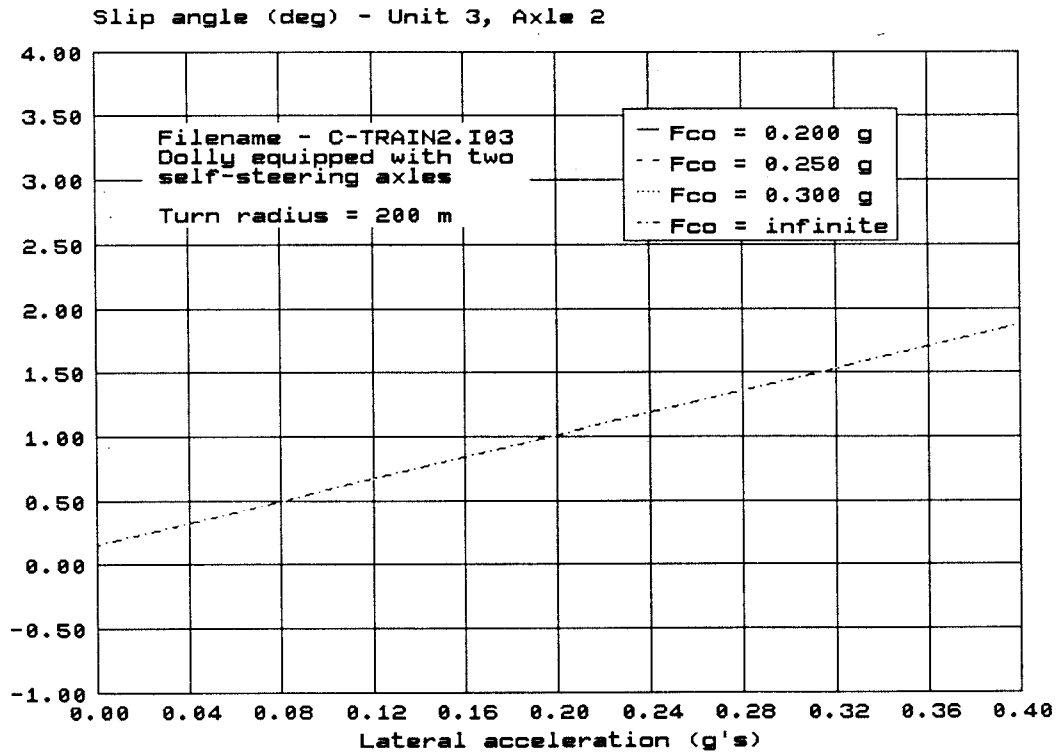
Slip angle (deg) - Unit 3, Axle 2
Filename - C-TRAIN2.I03
Dolly equipped with two
self-steering axles
Turn radius = 200 m
Fco = 0.200 g
Fco = 0.250 g
Fco = 0.300 g
Fco = infinite
4.00
3.50
3.00
2.50
2.00
1.50
1.00
0.50
0.00
-0.50
-1.00
0.00 0.04 0.08 0.12 0.16 0.20 0.24 0.28 0.32 0.36 0.40
Lateral acceleration (g's)

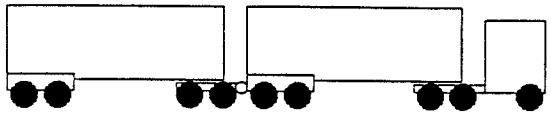

ROAD TRAIN WITH DOLLY EQUIPPED WITH TWO SELF-STEERING AXLES

Filename: C-TRAIN2.I02

UNIT 1 - TRACTOR

	1	2	3	4	5	6	7	8	9
AXLE	LOAD kg	Cα norm.	DUAL -	e m	k1 g/deg	t m	Ms kg	Fco g	k2 g/deg
1 1st DRIVE	8500.	1.000	Y	-	∞	∞	0.0	∞	∞
2 2nd DRIVE	8500.	1.000	Y	-	∞	∞	0.0	∞	∞
	L m	q m	x m	del t m	del d m	W5 kg			
3 UNIT DATA	4.40	0.00	0.20	1.60	0.00	5500.			

UNIT 2 - 1st SEMITRAILER

	1	2	3	4	5	6	7	8	9
AXLE	LOAD kg	Cα norm.	DUAL -	e m	k1 g/deg	t m	Ms kg	Fco g	k2 g/deg
1 1st TRAILER	7750.	1.000	Y	-	∞	∞	0.0	∞	∞
2 2nd TRAILER	7750.	1.000	Y	-	∞	∞	0.0	∞	∞
3 1st DOLLY	7500.	1.000	Y	-	0.250	0.364	600.	0.200	0.004
4 2nd DOLLY	7500.	1.000	Y	-	0.250	0.364	600.	0.200	0.004
	L m	q m	x m	del t m	del d m	W5 kg			
5 UNIT DATA	6.80	3.90	0.00	1.20	1.20	15000.			

Arbitrarily Set Values - AXLE CENTRING FORCE (Fco)
- 1st DOLLY AXLE
- 2nd DOLLY AXLE
- Values: 0.20 0.25 0.30 ∞

UNIT 3 - 2nd SEMITRAILER

	1	2	3	4	5	6	7	8	9
AXLE	LOAD kg	Cα norm.	DUAL -	e m	k1 g/deg	t m	Ms kg	Fco g	k2 g/deg
1 1st TRAILER	6500.	1.000	Y	-	∞	∞	0.0	∞	∞
2 2nd TRAILER	6500.	1.000	Y	-	∞	∞	0.0	∞	∞
	L m	q m	x m	del t m	del d m	W5 kg			
3 UNIT DATA	5.80	0.00	0.00	1.20	0.00	13000.			

GENERAL DATA

1	2	3	4
DUAL WHEEL m	Cαs normalized	RADIUS m	ACCELERATION g
0.33	1.000	100.	0.0

Independent Variable - LATERAL ACCELERATION
- Range: 0.00 to 0.40

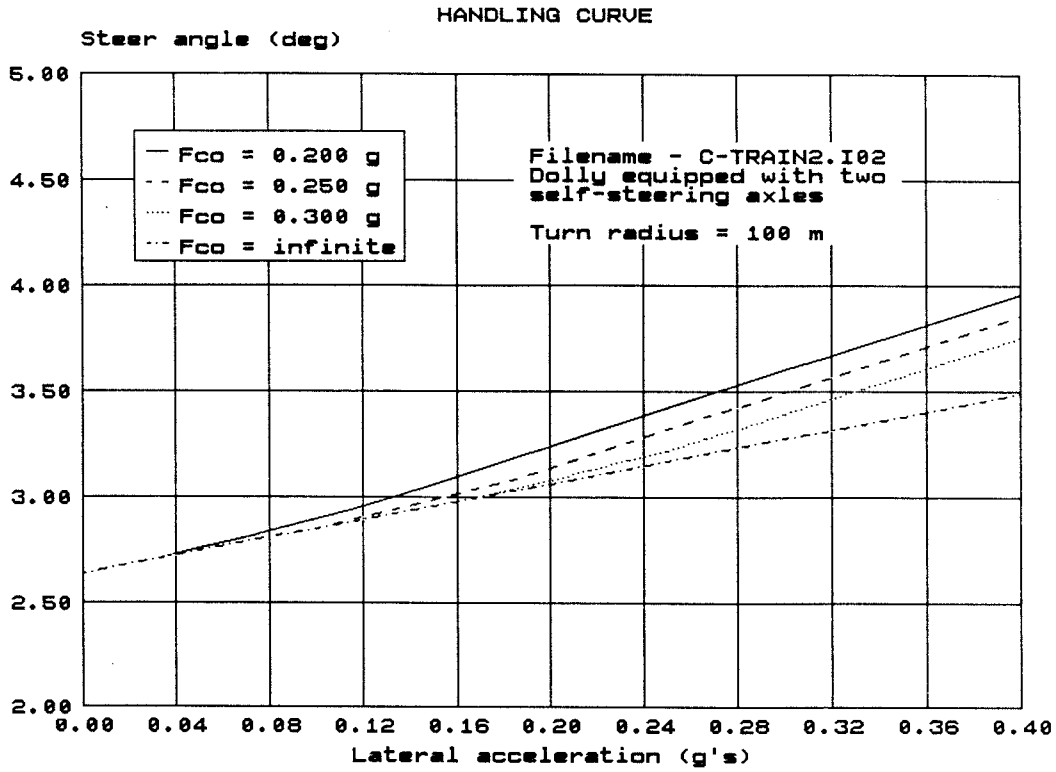
HANDLING CURVE
Steer angle (deg)
5.00
4.50
4.00
3.50
3.00
2.50
2.00
Fco = 0.200 g
Fco = 0.250 g
Fco = 0.300 g
Fco = infinite
Filename - C-TRAIN2.I02
Dolly equipped with two
self-steering axles
Turn radius = 100 m
0.00 0.04 0.08 0.12 0.16 0.20 0.24 0.28 0.32 0.36 0.40
Lateral acceleration (g's)

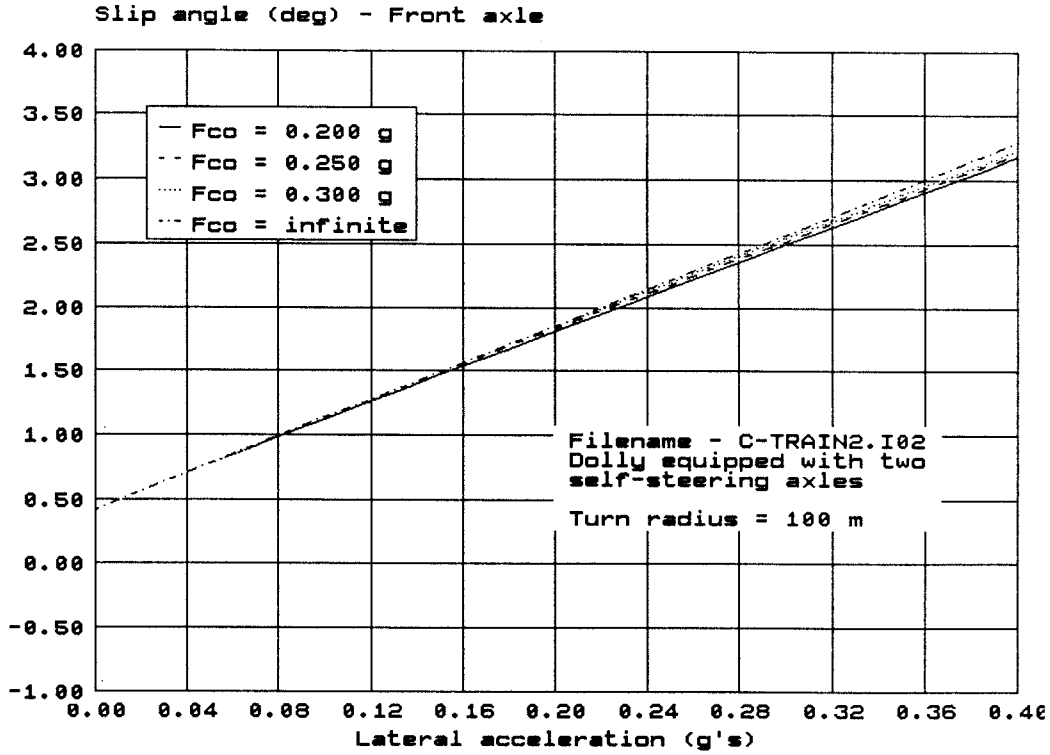
Slip angle (deg) - Front axle
4.00
3.50
3.00
2.50
2.00
1.50
1.00
0.50
0.00
-0.50
-1.00
Fco = 0.200 g
Fco = 0.250 g
Fco = 0.300 g
Fco = infinite
Filename - C-TRAIN2.I02
Dolly equipped with two
self-steering axles
Turn radius = 100 m
0.00 0.04 0.08 0.12 0.16 0.20 0.24 0.28 0.32 0.36
Lateral acceleration (g's)

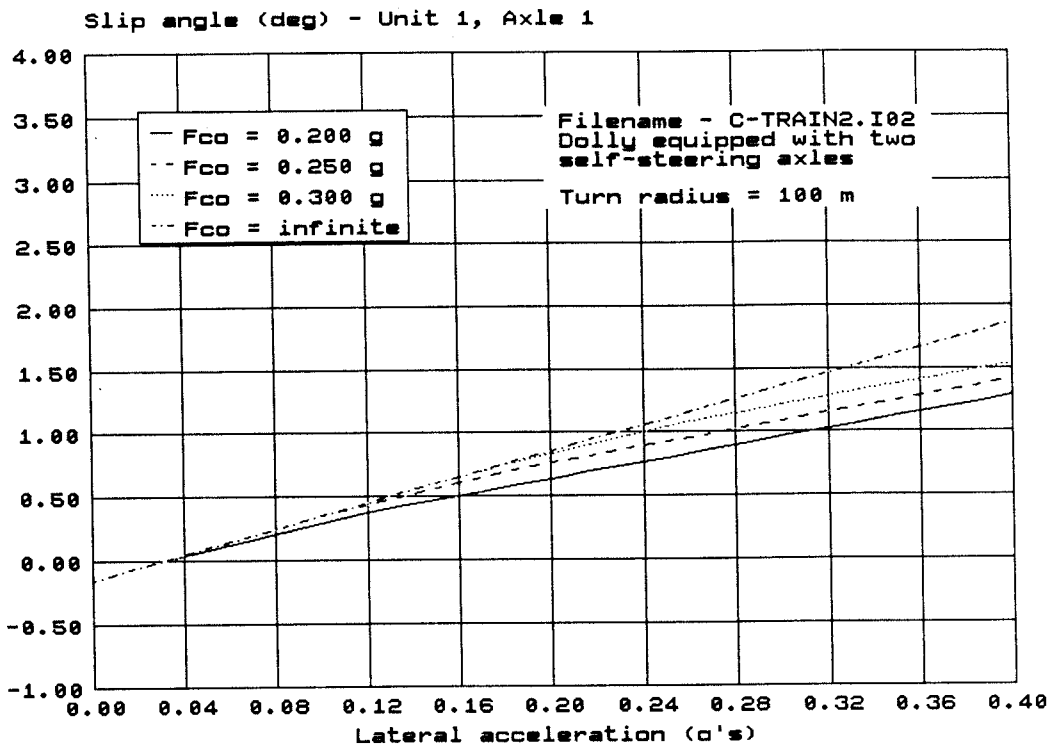
Slip angle (deg) - Unit 1, Axle 1
4.00
3.50
3.00
2.50
2.00
1.50
1.00
0.50
0.00
-0.50
-1.00
0.00 0.04 0.08 0.12 0.16 0.20 0.24 0.28 0.32 0.36 0.40
Lateral acceleration (g's)
Fco = 0.200 g
Fco = 0.250 g
Fco = 0.300 g
Fco = infinite
Filename - C-TRAIN2.I02
Dolly equipped with two
self-steering axles
Turn radius = 100 m

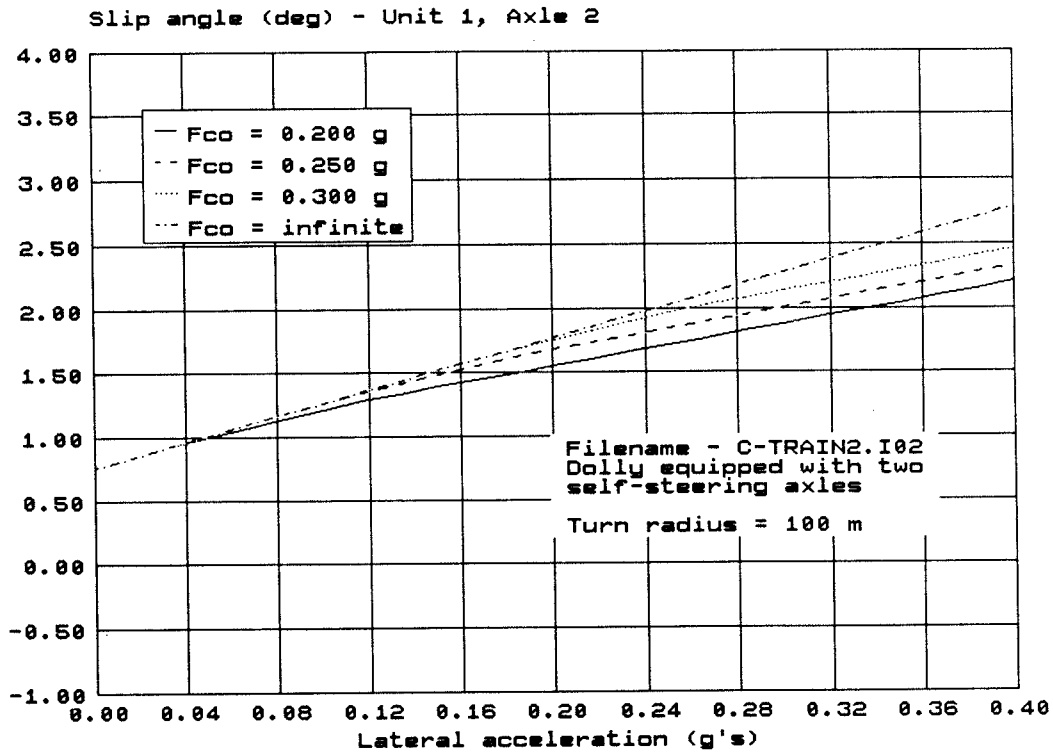
Slip angle (deg) - Unit 1, Axle 2
4.00
3.50
3.00
2.50
2.00
1.50
1.00
0.50
0.00
-0.50
-1.00
0.00 0.04 0.08 0.12 0.16 0.20 0.24 0.28 0.32 0.36 0.40
Lateral acceleration (g's)
Fco = 0.200 g
Fco = 0.250 g
Fco = 0.300 g
Fco = infinite
Filename - C-TRAIN2.I02
Dolly equipped with two
self-steering axles
Turn radius = 100 m

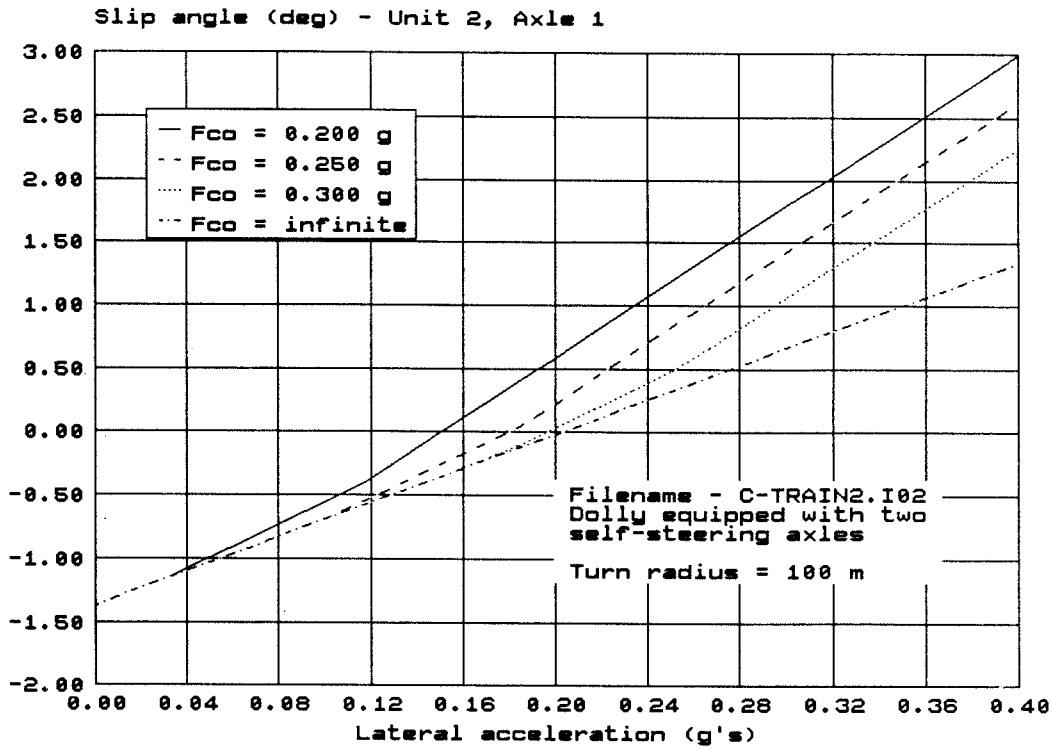
Slip angle (deg) - Unit 2, Axle 1
3.00
2.50
2.00
1.50
1.00
0.50
0.00
-0.50
-1.00
-1.50
-2.00
Fco = 0.200 g
Fco = 0.250 g
Fco = 0.300 g
Fco = infinite
Filename - C-TRAIN2.I02
Dolly equipped with two
self-steering axles
Turn radius = 100 m
0.00 0.04 0.08 0.12 0.16 0.20 0.24 0.28 0.32 0.36 0.40
Lateral acceleration (g's)

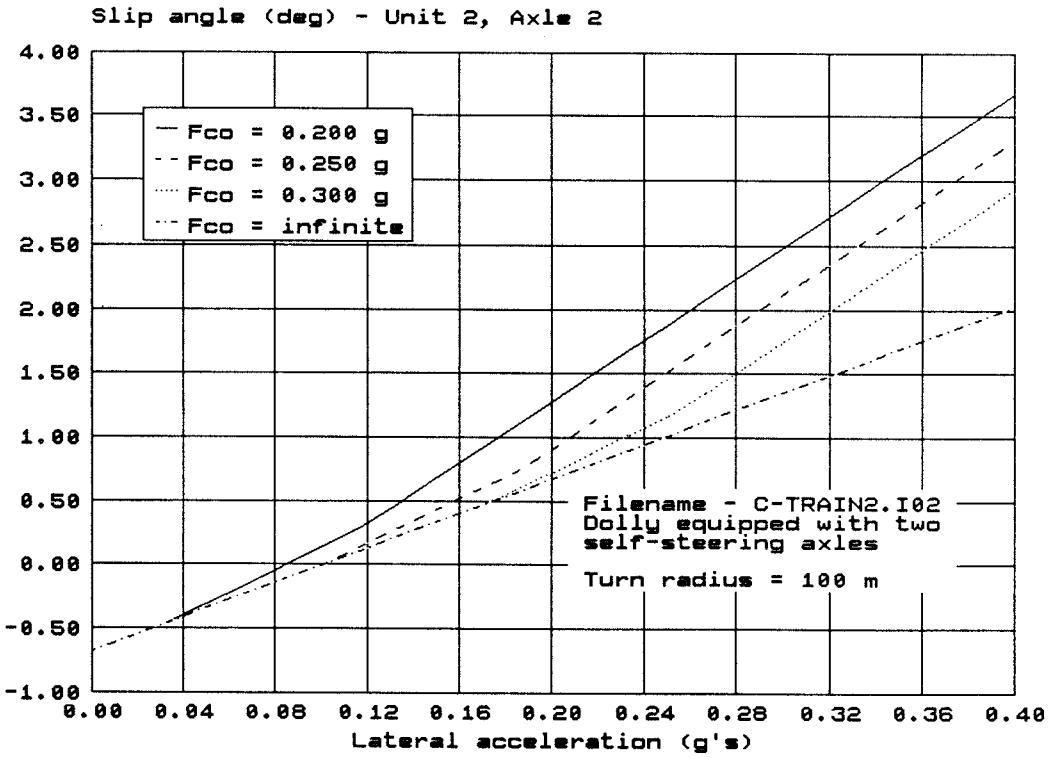
Slip angle (deg) - Unit 2, Axle 2
4.00
3.50
3.00
2.50
2.00
1.50
1.00
0.50
0.00
-0.50
-1.00
Fco = 0.200 g
Fco = 0.250 g
Fco = 0.300 g
Fco = infinite
Filename - C-TRAIN2.I02
Dolly equipped with two
self-steering axles
Turn radius = 100 m
0.00 0.04 0.08 0.12 0.16 0.20 0.24 0.28 0.32 0.36 0.40
Lateral acceleration (g's)

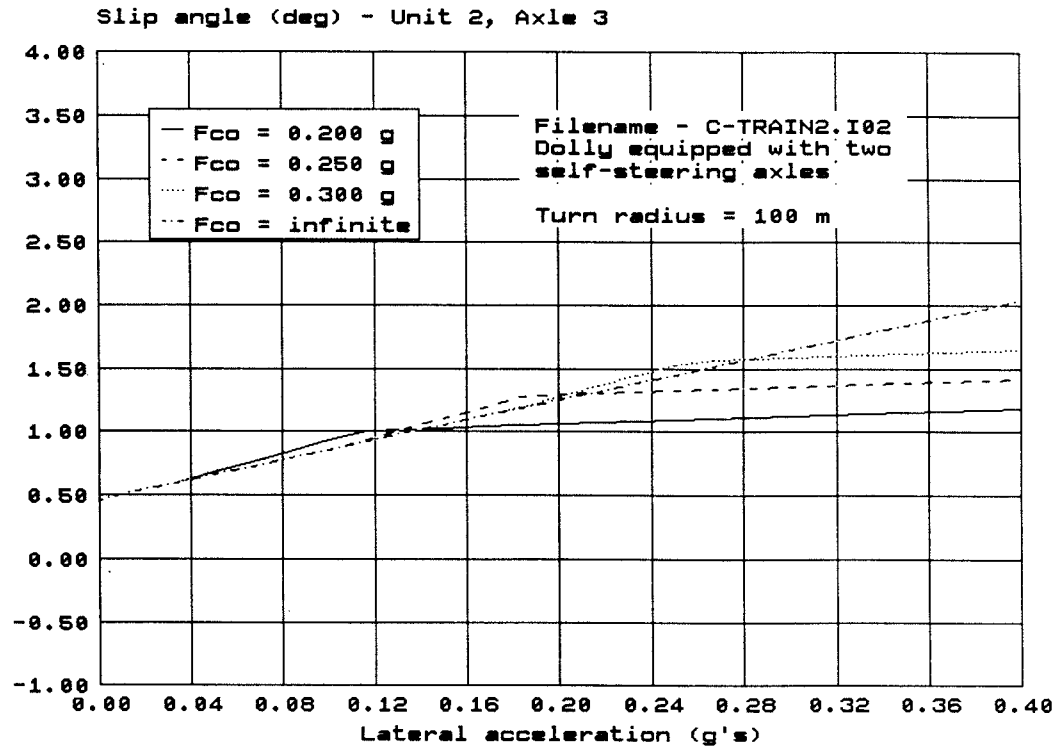
Slip angle (deg) - Unit 2, Axle 3
4.00
3.50
3.00
2.50
2.00
1.50
1.00
0.50
0.00
-0.50
-1.00
Fco = 0.200 g
Fco = 0.250 g
Fco = 0.300 g
Fco = infinite
Filename - C-TRAIN2.I02
Dolly equipped with two
self-steering axles
Turn radius = 100 m
0.00 0.04 0.08 0.12 0.16 0.20 0.24 0.28 0.32 0.36 0.40
Lateral acceleration (g's)

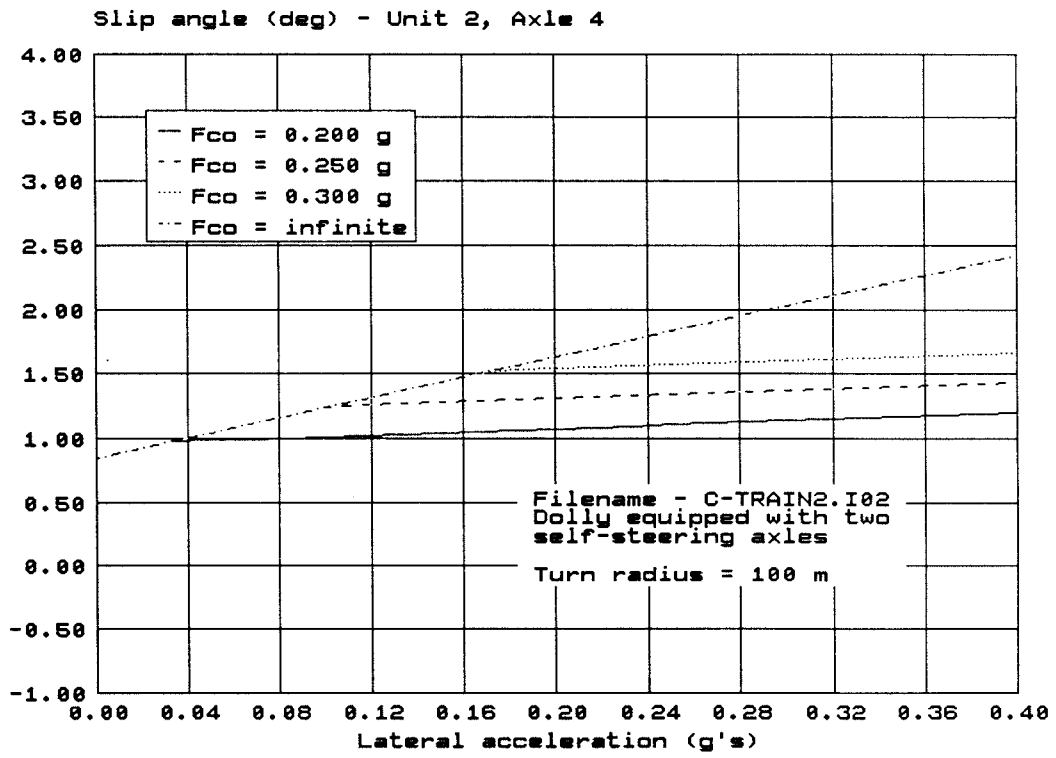
Slip angle (deg) - Unit 2, Axle 4
4.00
3.50
3.00
2.50
2.00
1.50
1.00
0.50
0.00
-0.50
-1.00
Fco = 0.200 g
Fco = 0.250 g
Fco = 0.300 g
Fco = infinite
Filename - C-TRAIN2.I02
Dolly equipped with two
self-steering axles
Turn radius = 100 m
0.00 0.04 0.08 0.12 0.16 0.20 0.24 0.28 0.32 0.36 0.40
Lateral acceleration (g's)

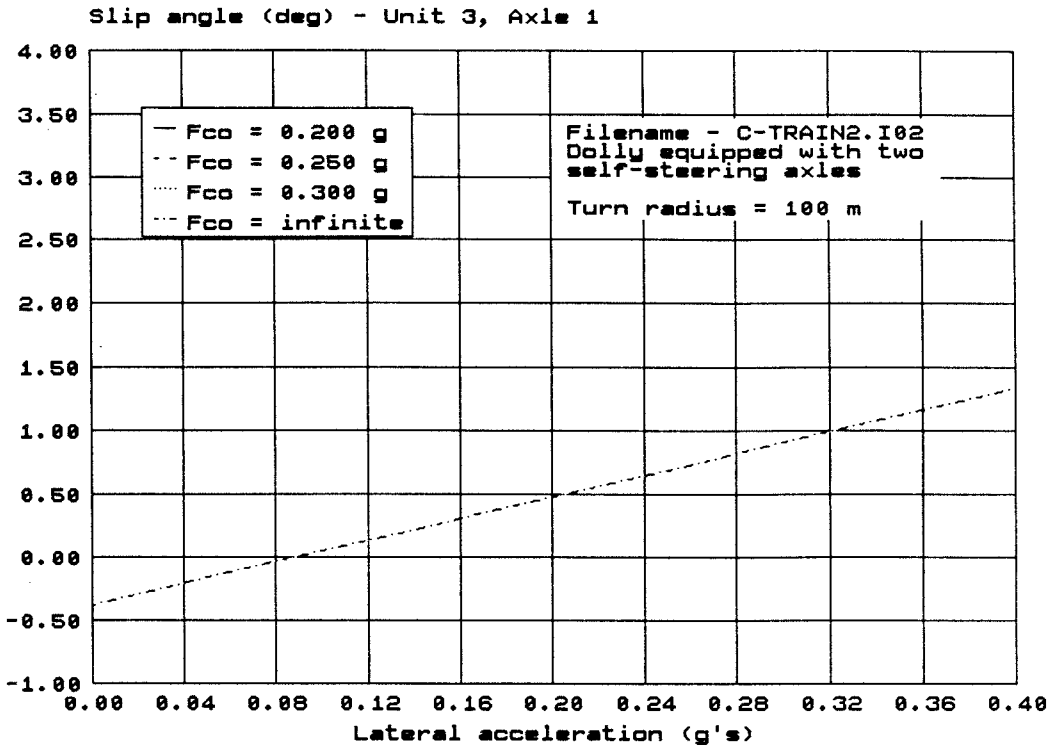
Slip angle (deg) - Unit 3, Axle 1
4.00
3.50
3.00
2.50
2.00
1.50
1.00
0.50
0.00
-0.50
-1.00
Fco = 0.200 g
Fco = 0.250 g
Fco = 0.300 g
Fco = infinite
Filename - C-TRAIN2.I02
Dolly equipped with two
self-steering axles
Turn radius = 100 m
0.00 0.04 0.08 0.12 0.16 0.20 0.24 0.28 0.32 0.36 0.40
Lateral acceleration (g's)

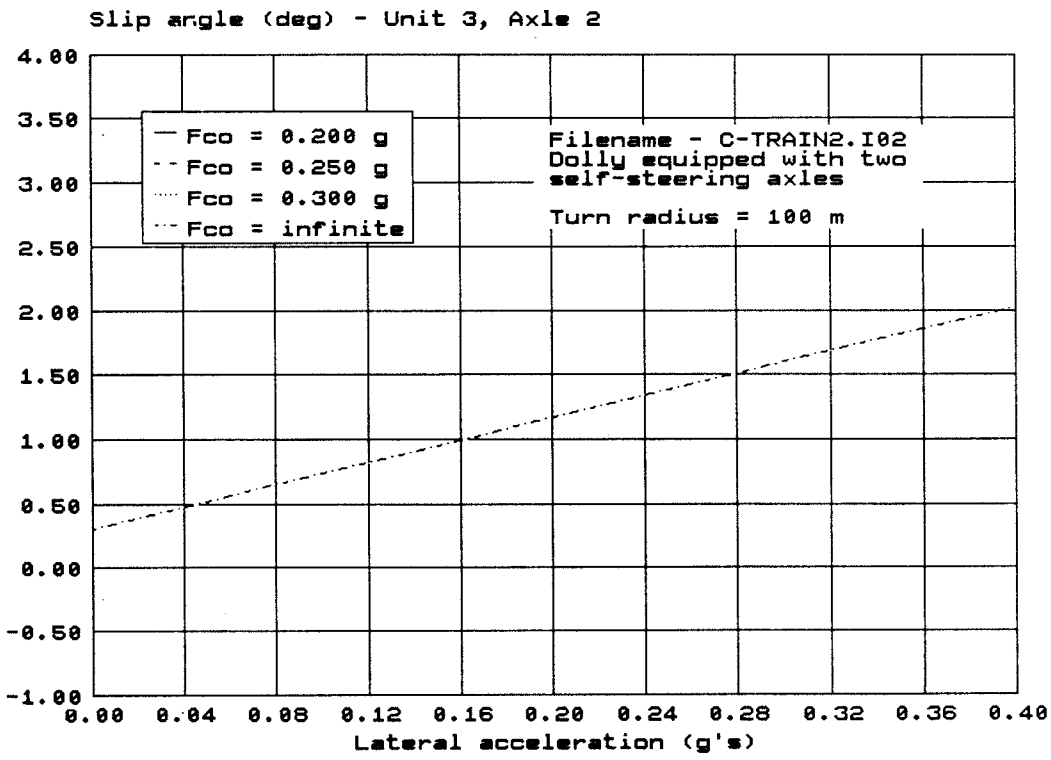
Slip angle (deg) - Unit 3, Axle 2
4.00
3.50
3.00
2.50
2.00
1.50
1.00
0.50
0.00
-0.50
-1.00
Fco = 0.200 g
Fco = 0.250 g
Fco = 0.300 g
Fco = infinite
Filename - C-TRAIN2.I02
Dolly equipped with two
self-steering axles
Turn radius = 100 m
0.00 0.04 0.08 0.12 0.16 0.20 0.24 0.28 0.32 0.36 0.40
Lateral acceleration (g's)

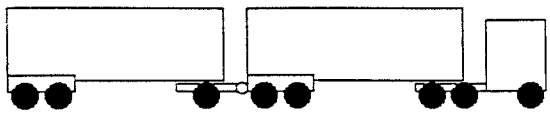

BASELINE C-TRAIN - 58,500 KG

Filename: C-TRAIN.I05

UNIT 1 - TRACTOR

	1	2	3	4	5	6	7	8	9
AXLE	LOAD kg	Cα norm.	DUAL -	e m	k1 g/deg	t m	Ms kg	Fco g	k2 g/deg
1 1st DRIVE	8500.	1.000	Y	-	∞	∞	0.0	∞	∞
2 2nd DRIVE	8500.	1.000	Y	-	∞	∞	0.0	∞	∞
	L m	q m	x m	del t m	del d m	W5 kg			
3 UNIT DATA	4.40	0.00	0.20	1.60	0.00	5500.			

UNIT 2 - 1st SEMITRAILER

	1	2	3	4	5	6	7	8	9
AXLE	LOAD kg	Cα norm.	DUAL -	e m	k1 g/deg	t m	Ms kg	Fco g	k2 g/deg
1 1st TRAILER	7750.	1.000	Y	-	∞	∞	0.0	∞	∞
2 2nd TRAILER	7750.	1.000	Y	-	∞	∞	0.0	∞	∞
3 1st DOLLY	7500.	1.000	Y	-	0.250	0.364	600.	0.200	0.004
	L m	q m	x m	del t m	del d m	W5 kg			
4 UNIT DATA	6.80	3.30	0.00	1.20	0.00	15000.			

Arbitrarily Set Values - AXLE CENTRING FORCE (Fco)
- 1st DOLLY AXLE
- Values: 0.20 0.25 0.30 ∞

UNIT 3 - 2nd SEMITRAILER

	1	2	3	4	5	6	7	8	9
AXLE	LOAD kg	Cα norm.	DUAL -	e m	k1 g/deg	t m	Ms kg	Fco g	k2 g/deg
1 1st TRAILER	6500.	1.000	Y	-	∞	∞	0.0	∞	∞
2 2nd TRAILER	6500.	1.000	Y	-	∞	∞	0.0	∞	∞
	L m	q m	x m	del t m	del d m	W5 kg			
3 UNIT DATA	5.80	0.00	0.00	1.20	0.00	6000.			

GENERAL DATA

1	2	3	4
DUAL WHEEL m	Cαs normalized	RADIUS m	ACCELERATION g
0.33	1.000	200.	0.0

Independent Variable - LATERAL ACCELERATION
- Range: 0.00 to 0.40

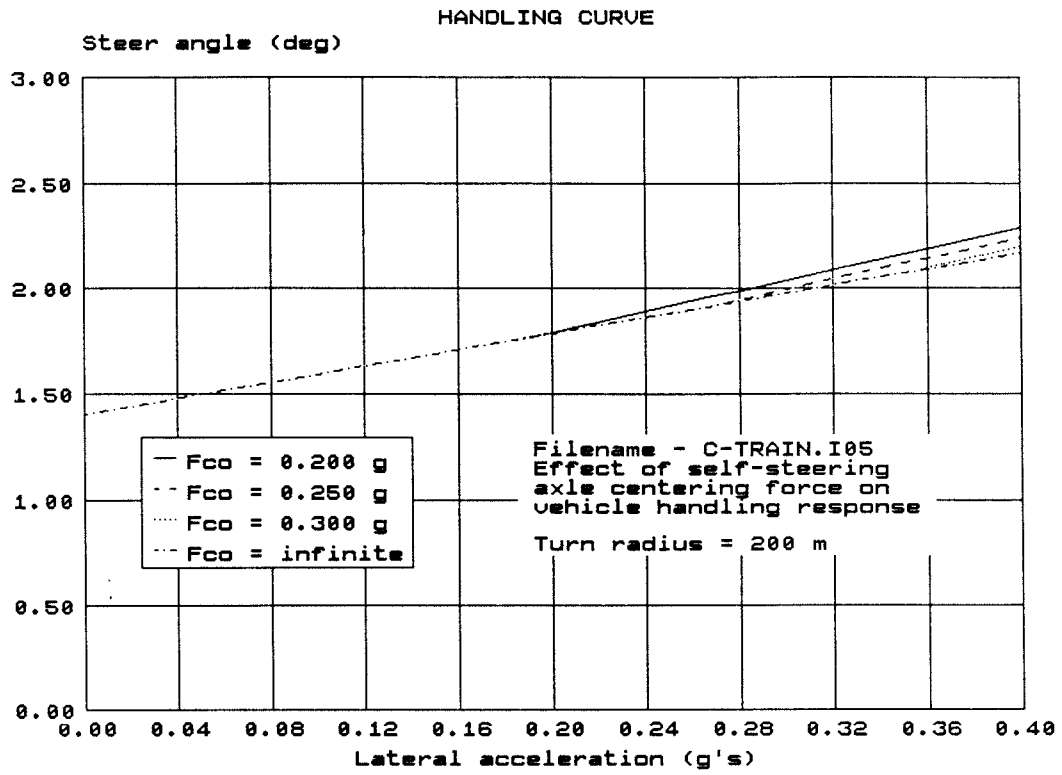
HANDLING CURVE
Steer angle (deg)
3.00
2.50
2.00
1.50
1.00
0.50
0.00
0.00 0.04 0.08 0.12 0.16 0.20 0.24 0.28 0.32 0.36 0.40
Lateral acceleration (g's)
Fco = 0.200 g
Fco = 0.250 g
Fco = 0.300 g
Fco = infinite
Filename - C-TRAIN.I05
Effect of self-steering
axle centering force on
vehicle handling response
Turn radius = 200 m

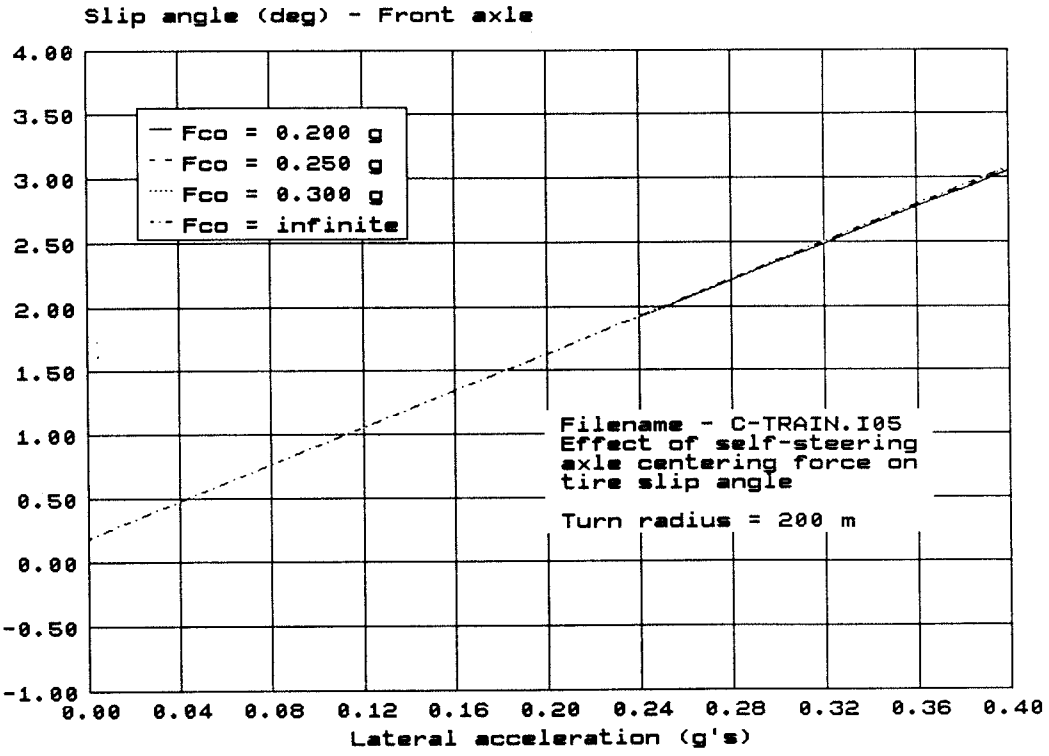
Slip angle (deg) - Front axle
4.00
3.50
3.00
2.50
2.00
1.50
1.00
0.50
0.00
-0.50
-1.00
0.00 0.04 0.08 0.12 0.16 0.20 0.24 0.28 0.32 0.36 0.40
Lateral acceleration (g's)
Fco = 0.200 g
Fco = 0.250 g
Fco = 0.300 g
Fco = infinite
Filename - C-TRAIN.I05
Effect of self-steering
axle centering force on
tire slip angle
Turn radius = 200 m

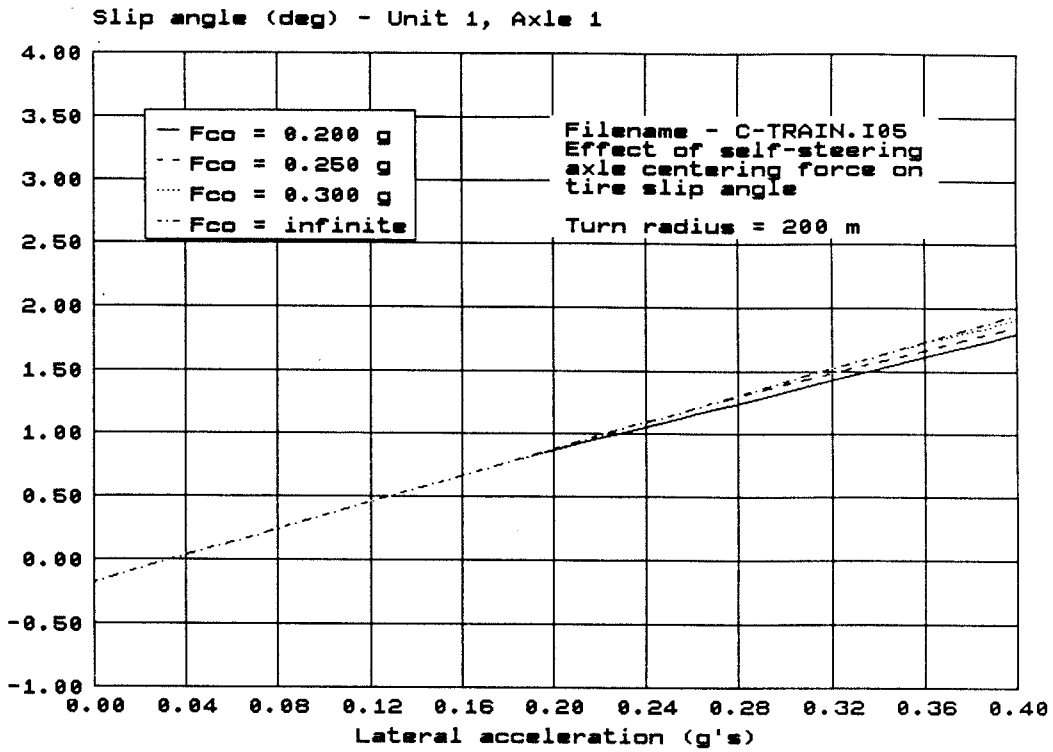
Slip angle (deg) - Unit 1, Axle 1
4.00
3.50
3.00
2.50
2.00
1.50
1.00
0.50
0.00
-0.50
-1.00
Fco = 0.200 g
Fco = 0.250 g
Fco = 0.300 g
Fco = infinite
Filename - C-TRAIN.I05
Effect of self-steering axle centering force on tire slip angle
Turn radius = 200 m
0.00 0.04 0.08 0.12 0.16 0.20 0.24 0.28 0.32 0.36 0.40
Lateral acceleration (g's)

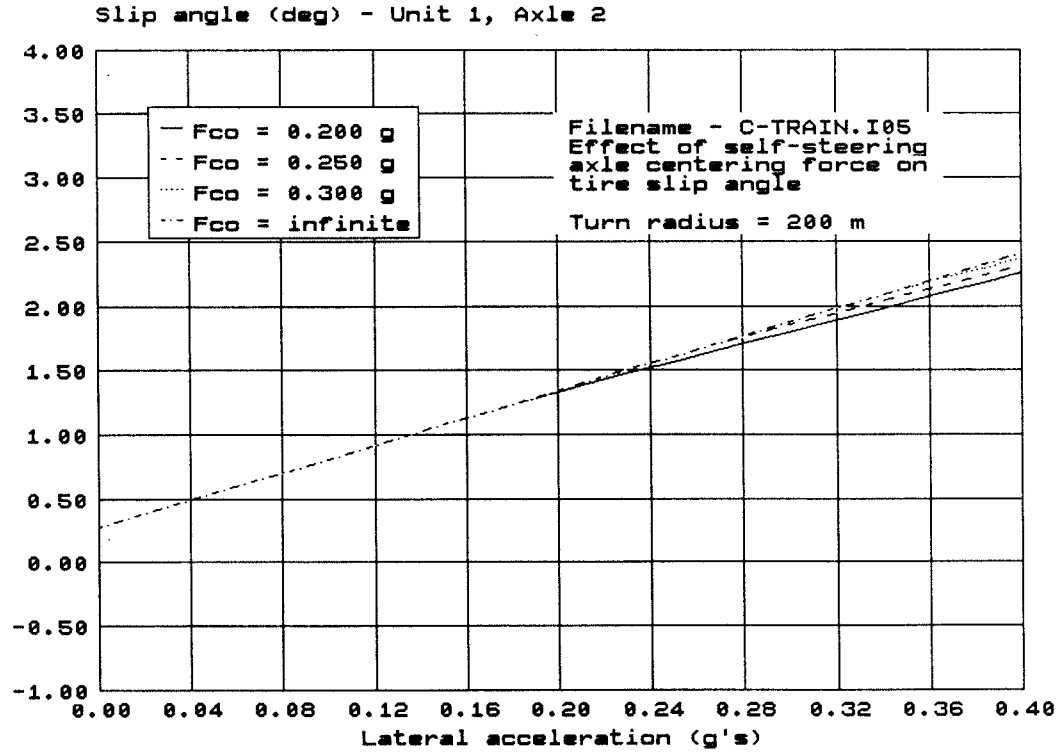
Slip angle (deg) - Unit 1, Axle 2
4.00
3.50
3.00
2.50
2.00
1.50
1.00
0.50
0.00
-0.50
-1.00
Fco = 0.200 g
Fco = 0.250 g
Fco = 0.300 g
Fco = infinite
Filename - C-TRAIN.I05
Effect of self-steering axle centering force on tire slip angle
Turn radius = 200 m
0.00 0.04 0.08 0.12 0.16 0.20 0.24 0.28 0.32 0.36 0.40
Lateral acceleration (g's)

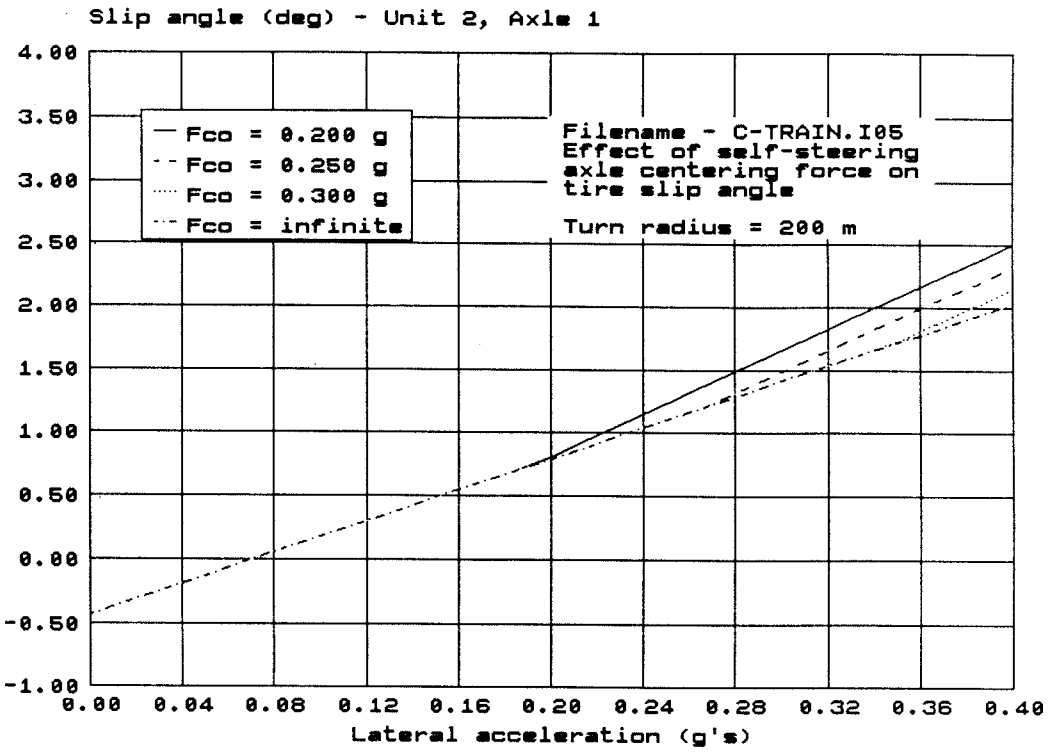
Slip angle (deg) - Unit 2, Axle 1
4.00
3.50
3.00
2.50
2.00
1.50
1.00
0.50
0.00
-0.50
-1.00
Fco = 0.200 g
Fco = 0.250 g
Fco = 0.300 g
Fco = infinite
Filename - C-TRAIN.I05
Effect of self-steering axle centering force on tire slip angle
Turn radius = 200 m
0.00 0.04 0.08 0.12 0.16 0.20 0.24 0.28 0.32 0.36 0.40
Lateral acceleration (g's)

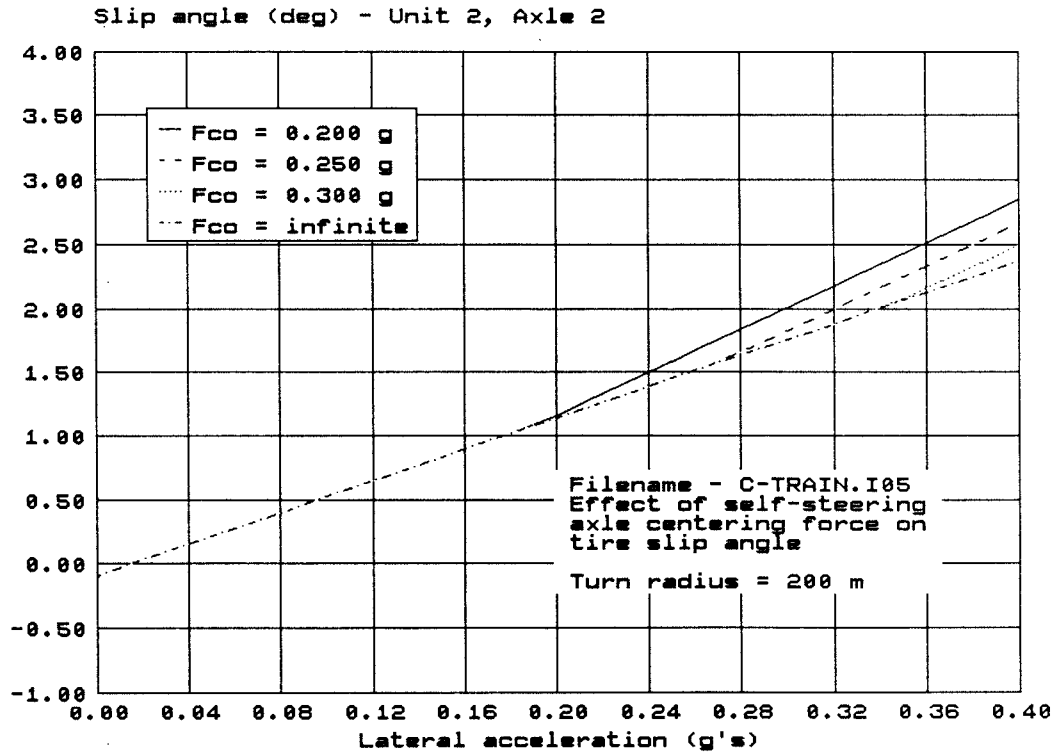
Slip angle (deg) - Unit 2, Axle 2
4.00
3.50
3.00
2.50
2.00
1.50
1.00
0.50
0.00
-0.50
-1.00
Fco = 0.200 g
Fco = 0.250 g
Fco = 0.300 g
Fco = infinite
Filename - C-TRAIN.I05
Effect of self-steering axle centering force on tire slip angle
Turn radius = 200 m
0.00 0.04 0.08 0.12 0.16 0.20 0.24 0.28 0.32 0.36 0.40
Lateral acceleration (g's)

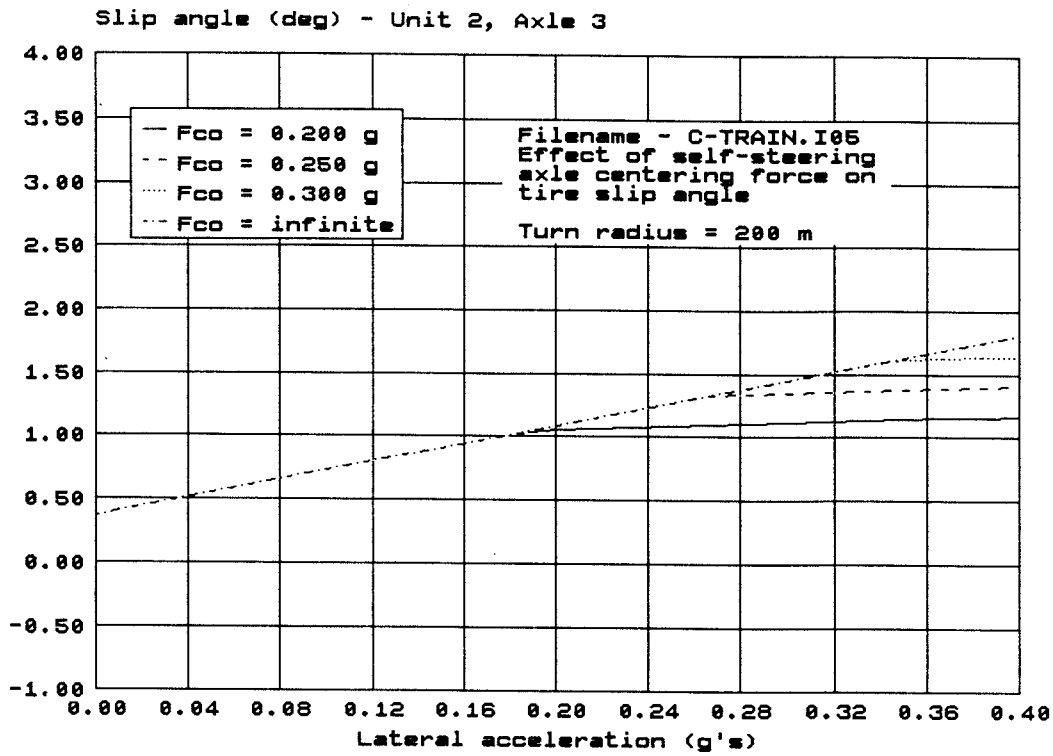
Slip angle (deg) - Unit 2, Axle 3
Fco = 0.200 g
Fco = 0.250 g
Fco = 0.300 g
Fco = infinite
Filename - C-TRAIN.I05
Effect of self-steering axle centering force on tire slip angle
Turn radius = 200 m
4.00
3.50
3.00
2.50
2.00
1.50
1.00
0.50
0.00
-0.50
-1.00
0.00 0.04 0.08 0.12 0.16 0.20 0.24 0.28 0.32 0.36 0.40
Lateral acceleration (g's)

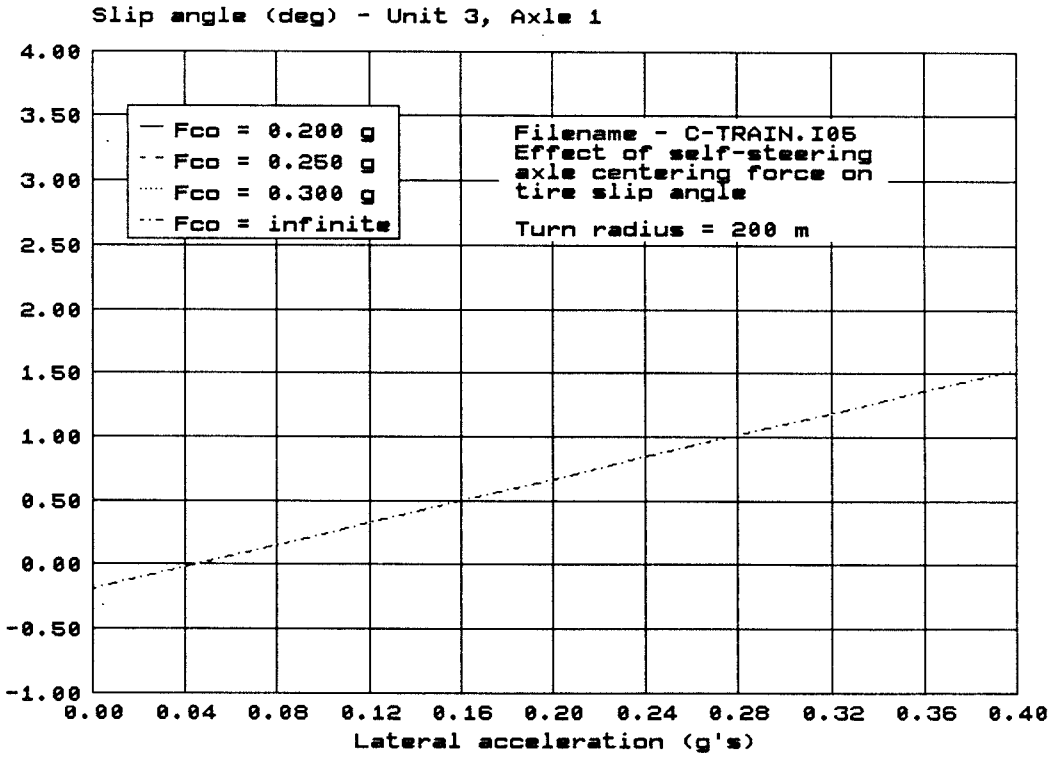
Slip angle (deg) - Unit 3, Axle 1
Fco = 0.200 g
Fco = 0.250 g
Fco = 0.300 g
Fco = infinite
Filename - C-TRAIN.I05
Effect of self-steering axle centering force on tire slip angle
Turn radius = 200 m
4.00
3.50
3.00
2.50
2.00
1.50
1.00
0.50
0.00
-0.50
-1.00
0.00 0.04 0.08 0.12 0.16 0.20 0.24 0.28 0.32 0.36 0.40
Lateral acceleration (g's)

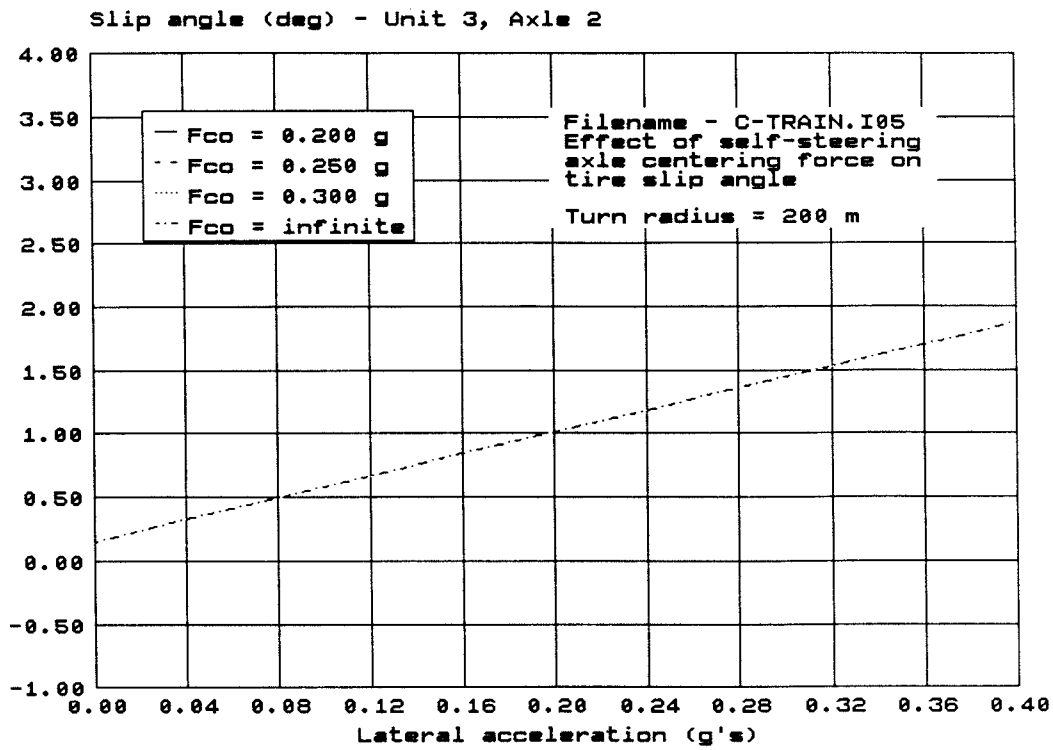
Slip angle (deg) - Unit 3, Axle 2
4.00
3.50
3.00
2.50
2.00
1.50
1.00
0.50
0.00
-0.50
-1.00
Fco = 0.200 g
Fco = 0.250 g
Fco = 0.300 g
Fco = infinite
Filename - C-TRAIN.I05
Effect of self-steering axle centering force on tire slip angle
Turn radius = 200 m
0.00 0.04 0.08 0.12 0.16 0.20 0.24 0.28 0.32 0.36 0.40
Lateral acceleration (g's)

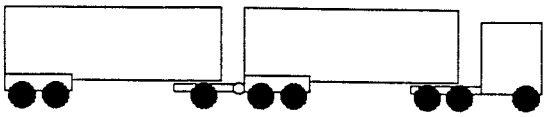

BASELINE C-TRAIN - 58,500 KG

Filename: C-TRAIN.I06

UNIT 1 - TRACTOR

	1	2	3	4	5	6	7	8	9
AXLE	LOAD kg	Cα norm.	DUAL -	e m	k1 g/deg	t m	Ms kg	Fco g	k2 g/deg
1 1st DRIVE	8500.	1.000	Y	-	∞	∞	0.0	∞	∞
2 2nd DRIVE	8500.	1.000	Y	-	∞	∞	0.0	∞	∞
	L m	q m	x m	del t m	del d m	W5 kg			
3 UNIT DATA	4.40	0.00	0.20	1.60	0.00	5500.			

UNIT 2 - 1st SEMITRAILER

	1	2	3	4	5	6	7	8	9
AXLE	LOAD kg	Cα norm.	DUAL -	e m	k1 g/deg	t m	Ms kg	Fco g	k2 g/deg
1 1st TRAILER	7750.	1.000	Y	-	∞	∞	0.0	∞	∞
2 2nd TRAILER	7750.	1.000	Y	-	∞	∞	0.0	∞	∞
3 1st DOLLY	7500.	1.000	Y	-	0.250	0.364	600.	0.200	0.004
	L m	q m	x m	del t m	del d m	W5 kg			
4 UNIT DATA	6.80	3.30	0.00	1.20	0.00	15000.			

Arbitrarily Set Values - AXLE CENTRING FORCE (Fco)
- 1st DOLLY AXLE
- Values: 0.20 0.25 0.30 ∞

UNIT 3 - 2nd SEMITRAILER

	1	2	3	4	5	6	7	8	9
AXLE	LOAD kg	Cα norm.	DUAL -	e m	k1 g/deg	t m	Ms kg	Fco g	k2 g/deg
1 1st TRAILER	6500.	1.000	Y	-	∞	∞	0.0	∞	∞
2 2nd TRAILER	6500.	1.000	Y	-	∞	∞	0.0	∞	∞
	L m	q m	x m	del t m	del d m	W5 kg			
3 UNIT DATA	5.80	0.00	0.00	1.20	0.00	6000.			

GENERAL DATA

1	2	3	4
DUAL WHEEL m	Cαs normalized	RADIUS m	ACCELERATION g
0.33	1.000	100.	0.0

Independent Variable - LATERAL ACCELERATION
- Range: 0.00 to 0.40

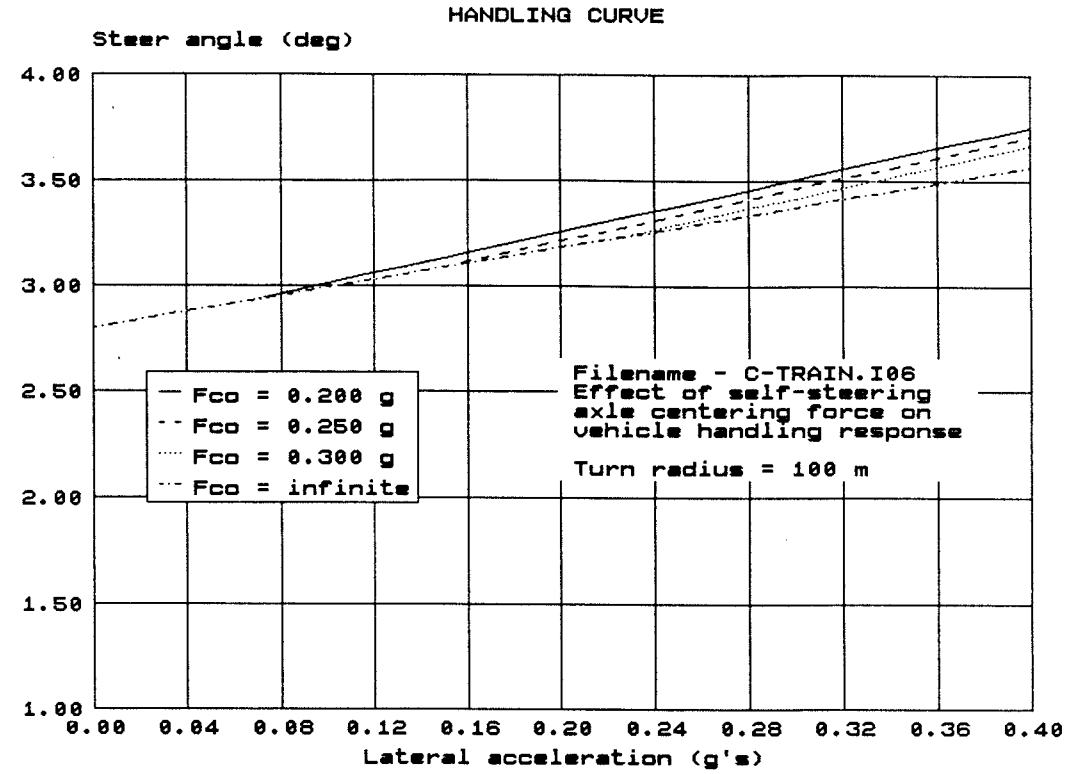
HANDLING CURVE
Steer angle (deg)
4.00
3.50
3.00
2.50
2.00
1.50
1.00
0.00 0.04 0.08 0.12 0.16 0.20 0.24 0.28 0.32 0.36 0.40
Lateral acceleration (g's)
Fco = 0.200 g
Fco = 0.250 g
Fco = 0.300 g
Fco = infinite
Filename - C-TRAIN.I06
Effect of self-steering axle centering force on vehicle handling response
Turn radius = 100 m

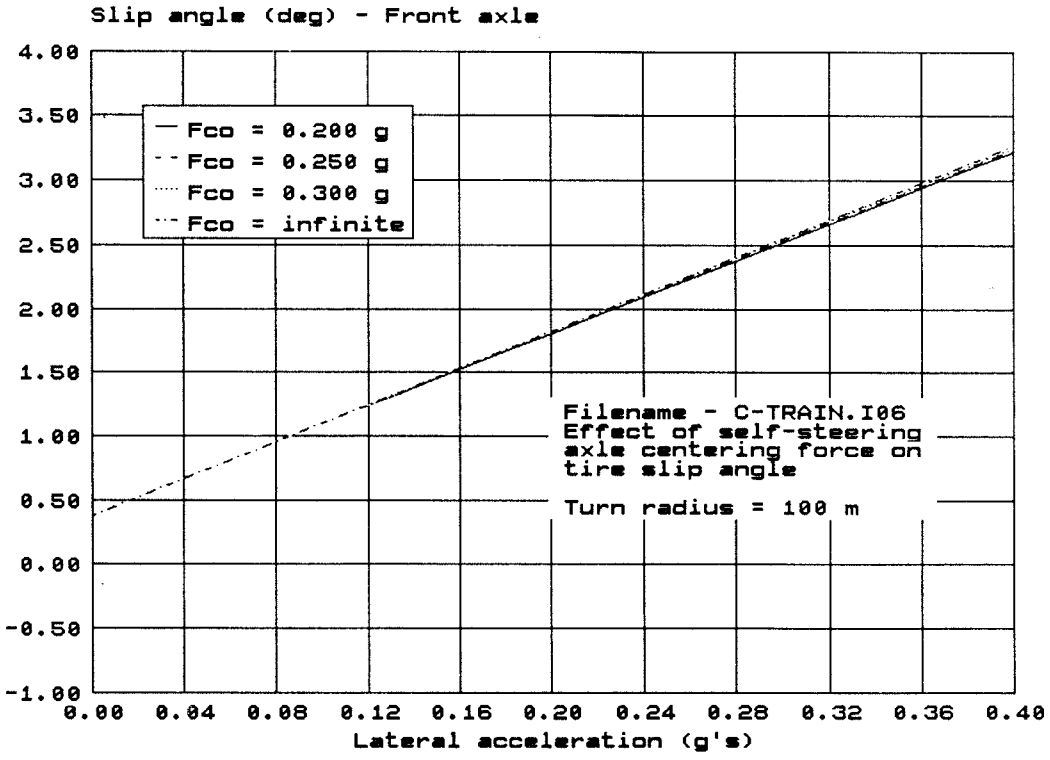
Slip angle (deg) - Front axle
4.00
3.50
3.00
2.50
2.00
1.50
1.00
0.50
0.00
-0.50
-1.00
0.00 0.04 0.08 0.12 0.16 0.20 0.24 0.28 0.32 0.36 0.40
Lateral acceleration (g's)
Fco = 0.200 g
Fco = 0.250 g
Fco = 0.300 g
Fco = infinite
Filename - C-TRAIN.I06
Effect of self-steering axle centering force on tire slip angle
Turn radius = 100 m

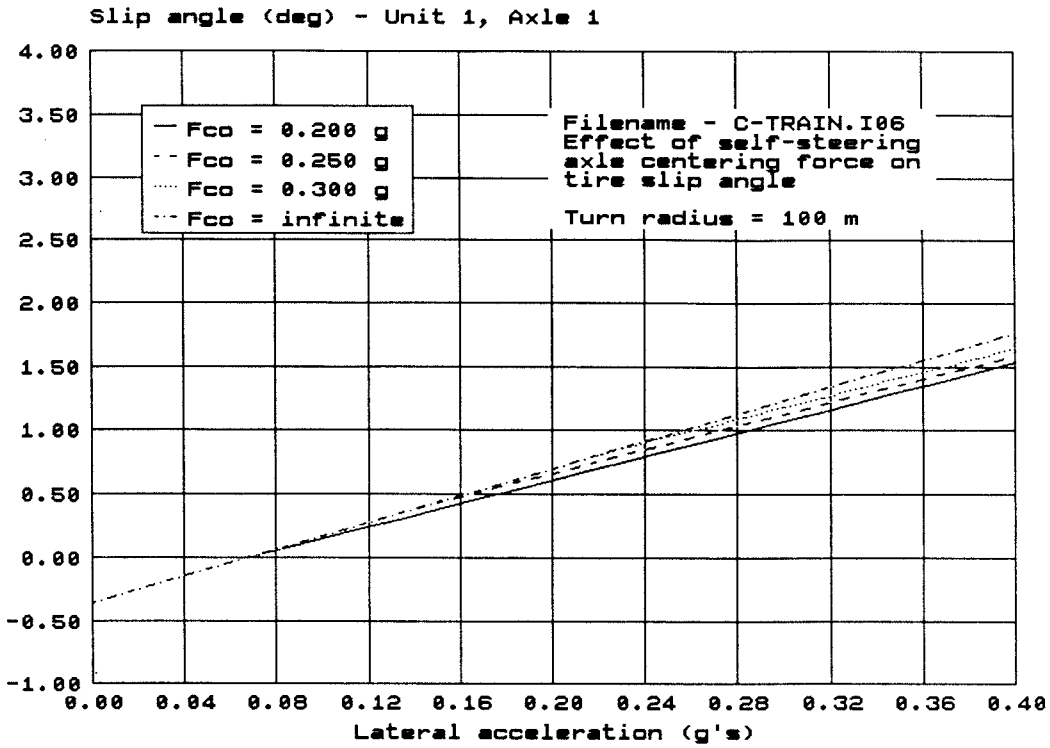
Slip angle (deg) - Unit 1, Axle 1
4.00
3.50
3.00
2.50
2.00
1.50
1.00
0.50
0.00
-0.50
-1.00
Fco = 0.200 g
Fco = 0.250 g
Fco = 0.300 g
Fco = infinite
Filename - C-TRAIN.I06
Effect of self-steering axle centering force on tire slip angle
Turn radius = 100 m
0.00 0.04 0.08 0.12 0.16 0.20 0.24 0.28 0.32 0.36 0.40
Lateral acceleration (g's)

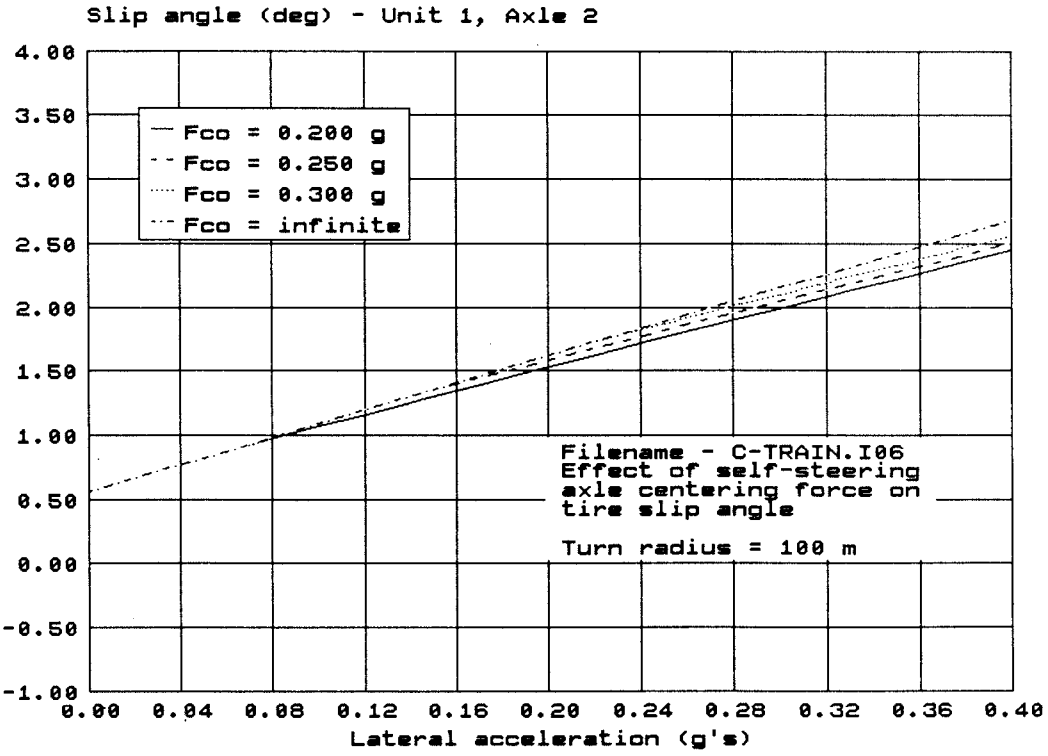
Slip angle (deg) - Unit 1, Axle 2
4.00
3.50
3.00
2.50
2.00
1.50
1.00
0.50
0.00
-0.50
-1.00
Fco = 0.200 g
Fco = 0.250 g
Fco = 0.300 g
Fco = infinite
Filename - C-TRAIN.I06
Effect of self-steering axle centering force on tire slip angle
Turn radius = 100 m
0.00 0.04 0.08 0.12 0.16 0.20 0.24 0.28 0.32 0.36 0.40
Lateral acceleration (g's)

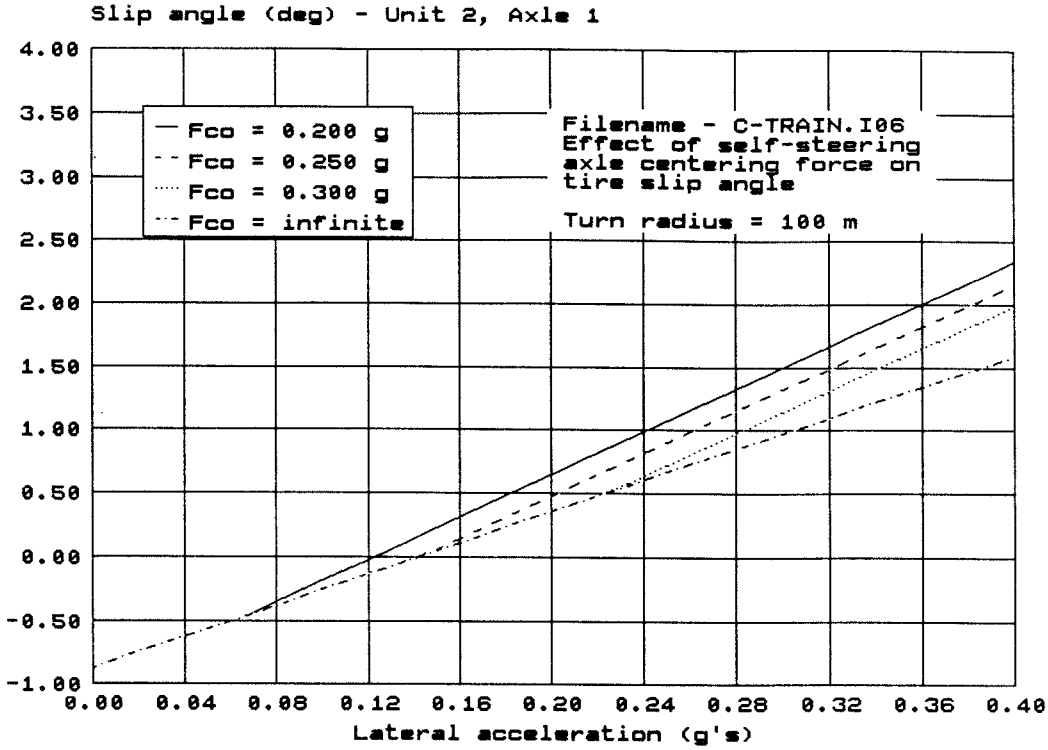
Slip angle (deg) - Unit 2, Axle 1
4.00
3.50
3.00
2.50
2.00
1.50
1.00
0.50
0.00
-0.50
-1.00
Fco = 0.200 g
Fco = 0.250 g
Fco = 0.300 g
Fco = infinite
Filename - C-TRAIN.I06
Effect of self-steering axle centering force on tire slip angle
Turn radius = 100 m
0.00 0.04 0.08 0.12 0.16 0.20 0.24 0.28 0.32 0.36 0.40
Lateral acceleration (g's)

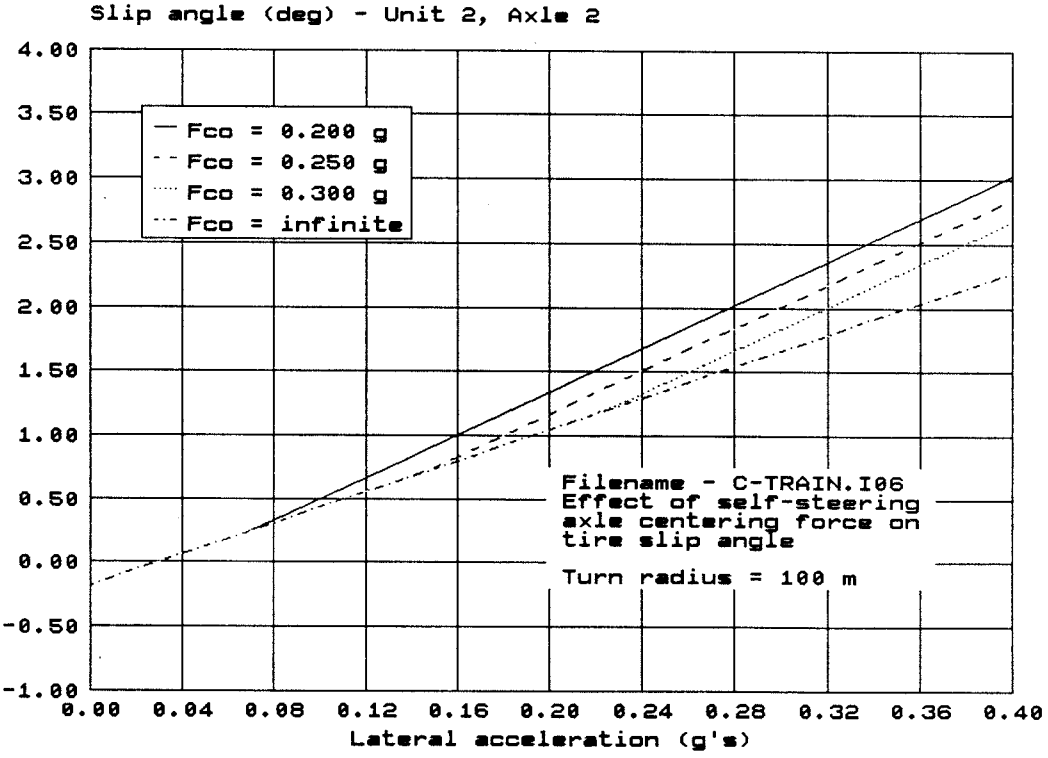
Slip angle (deg) - Unit 2, Axle 2
4.00
3.50
3.00
2.50
2.00
1.50
1.00
0.50
0.00
-0.50
-1.00
Fco = 0.200 g
Fco = 0.250 g
Fco = 0.300 g
Fco = infinite
Filename - C-TRAIN.I06
Effect of self-steering axle centering force on tire slip angle
Turn radius = 100 m
0.00 0.04 0.08 0.12 0.16 0.20 0.24 0.28 0.32 0.36 0.40
Lateral acceleration (g's)

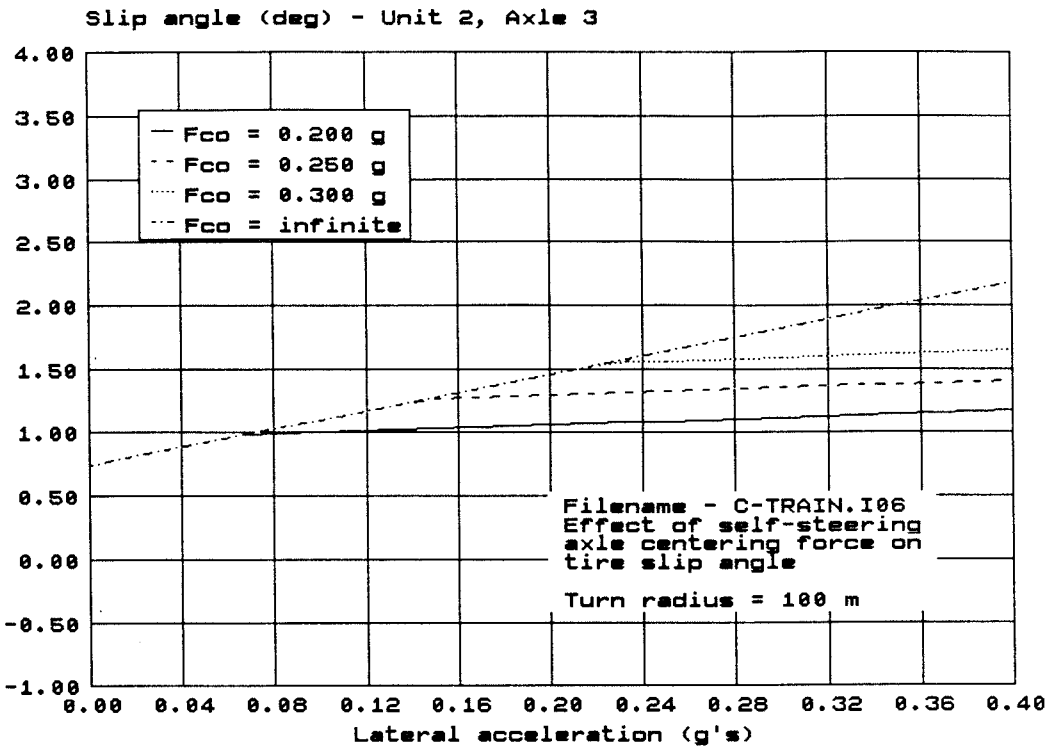
Slip angle (deg) - Unit 2, Axle 3
4.00
3.50
3.00
2.50
2.00
1.50
1.00
0.50
0.00
-0.50
-1.00
Fco = 0.200 g
Fco = 0.250 g
Fco = 0.300 g
Fco = infinite
Filename - C-TRAIN.I06
Effect of self-steering axle centering force on tire slip angle
Turn radius = 100 m
0.00 0.04 0.08 0.12 0.16 0.20 0.24 0.28 0.32 0.36 0.40
Lateral acceleration (g's)

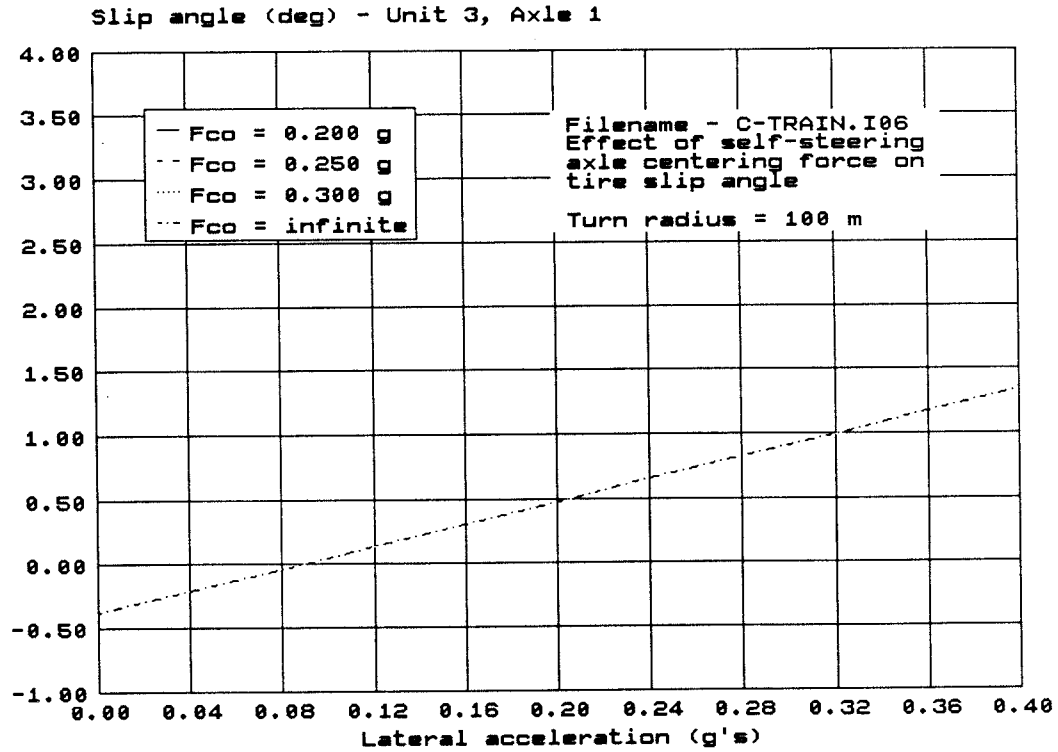
Slip angle (deg) - Unit 3, Axle 1
4.00
3.50
3.00
2.50
2.00
1.50
1.00
0.50
0.00
-0.50
-1.00
Fco = 0.200 g
Fco = 0.250 g
Fco = 0.300 g
Fco = infinite
Filename - C-TRAIN.I06
Effect of self-steering axle centering force on tire slip angle
Turn radius = 100 m
0.00 0.04 0.08 0.12 0.16 0.20 0.24 0.28 0.32 0.36 0.40
Lateral acceleration (g's)

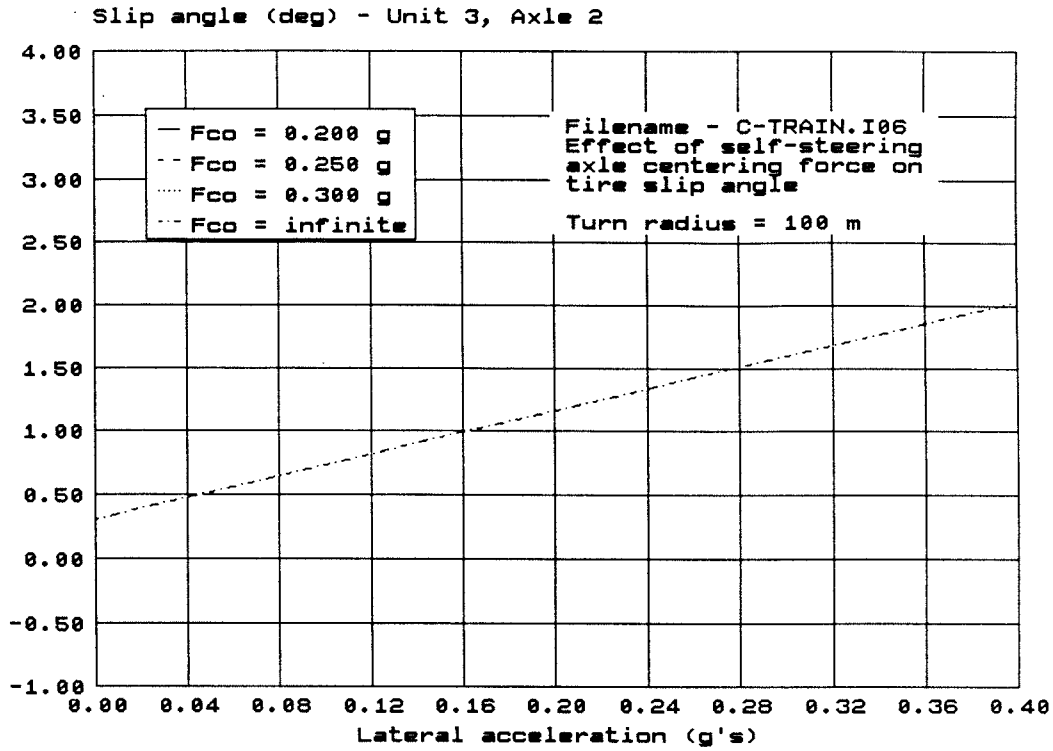
Slip angle (deg) - Unit 3, Axle 2
4.00
3.50
3.00
2.50
2.00
1.50
1.00
0.50
0.00
-0.50
-1.00
Fco = 0.200 g
Fco = 0.250 g
Fco = 0.300 g
Fco = infinite
Filename - C-TRAIN.I06
Effect of self-steering axle centering force on tire slip angle
Turn radius = 100 m
0.00 0.04 0.08 0.12 0.16 0.20 0.24 0.28 0.32 0.36 0.40
Lateral acceleration (g's)

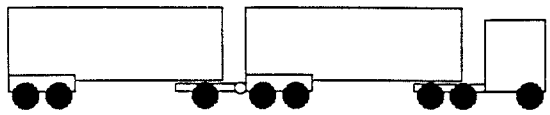

BASELINE C-TRAIN - 58,500 KG

Filename: c-train.I07

UNIT 1 - TRACTOR

	1	2	3	4	5	6	7	8	9
AXLE	LOAD kg	Cα norm.	DUAL -	e m	k1 g/deg	t m	Ms kg	Fco g	k2 g/deg
1 1st DRIVE	8500.	1.000	Y	-	∞	∞	0.0	∞	∞
2 2nd DRIVE	8500.	1.000	Y	-	∞	∞	0.0	∞	∞
	L m	q m	x m	del t m	del d m	W5 kg			
3 UNIT DATA	4.40	0.00	0.20	1.60	0.00	5500.			

UNIT 2 - 1st SEMITRAILER

	1	2	3	4	5	6	7	8	9
AXLE	LOAD kg	Cα norm.	DUAL -	e m	k1 g/deg	t m	Ms kg	Fco g	k2 g/deg
1 1st TRAILER	7750.	1.000	Y	-	∞	∞	0.0	∞	∞
2 2nd TRAILER	7750.	1.000	Y	-	∞	∞	0.0	∞	∞
3 1st DOLLY	7500.	1.000	Y	-	0.250	0.364	600.	0.200	0.004
	L m	q m	x m	del t m	del d m	W5 kg			
4 UNIT DATA	6.80	3.30	0.00	1.20	0.00	15000.			

Arbitrarily Set Values - AXLE CENTRING FORCE (Fco)
- 1st DOLLY AXLE
- Values: 0.20 0.25 0.30 ∞

UNIT 3 - 2nd SEMITRAILER

	1	2	3	4	5	6	7	8	9
AXLE	LOAD kg	Cα norm.	DUAL -	e m	k1 g/deg	t m	Ms kg	Fco g	k2 g/deg
1 1st TRAILER	6500.	1.000	Y	-	∞	∞	0.0	∞	∞
2 2nd TRAILER	6500.	1.000	Y	-	∞	∞	0.0	∞	∞
	L m	q m	x m	del t m	del d m	W5 kg			
3 UNIT DATA	5.80	0.00	0.00	1.20	0.00	6000.			

GENERAL DATA

1	2	3	4
DUAL WHEEL m	Cαs normalized	RADIUS m	ACCELERATION g
0.33	1.000	50.	0.0

Independent Variable - LATERAL ACCELERATION
- Range: 0.00 to 0.40

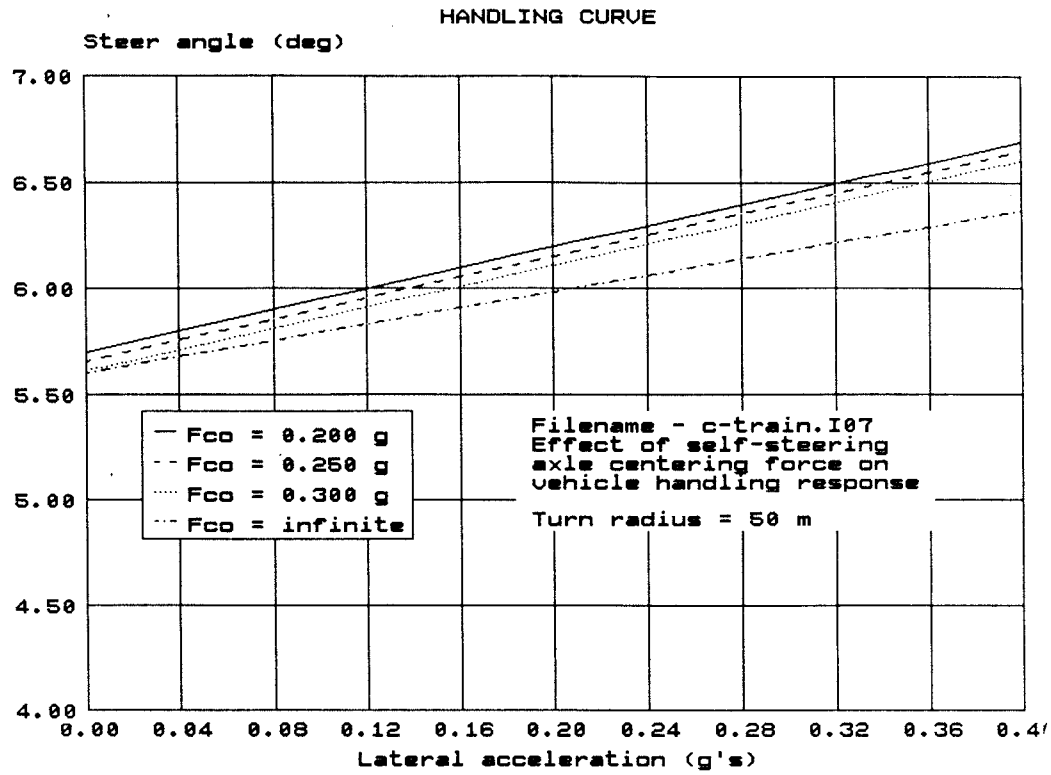
HANDLING CURVE
Steer angle (deg)
7.00
6.50
6.00
5.50
5.00
4.50
4.00
0.00 0.04 0.08 0.12 0.16 0.20 0.24 0.28 0.32 0.36
Lateral acceleration (g's)
Fco = 0.200 g
Fco = 0.250 g
Fco = 0.300 g
Fco = infinite
Filename - c-train.I07
Effect of self-steering
axle centering force on
vehicle handling response
Turn radius = 50 m

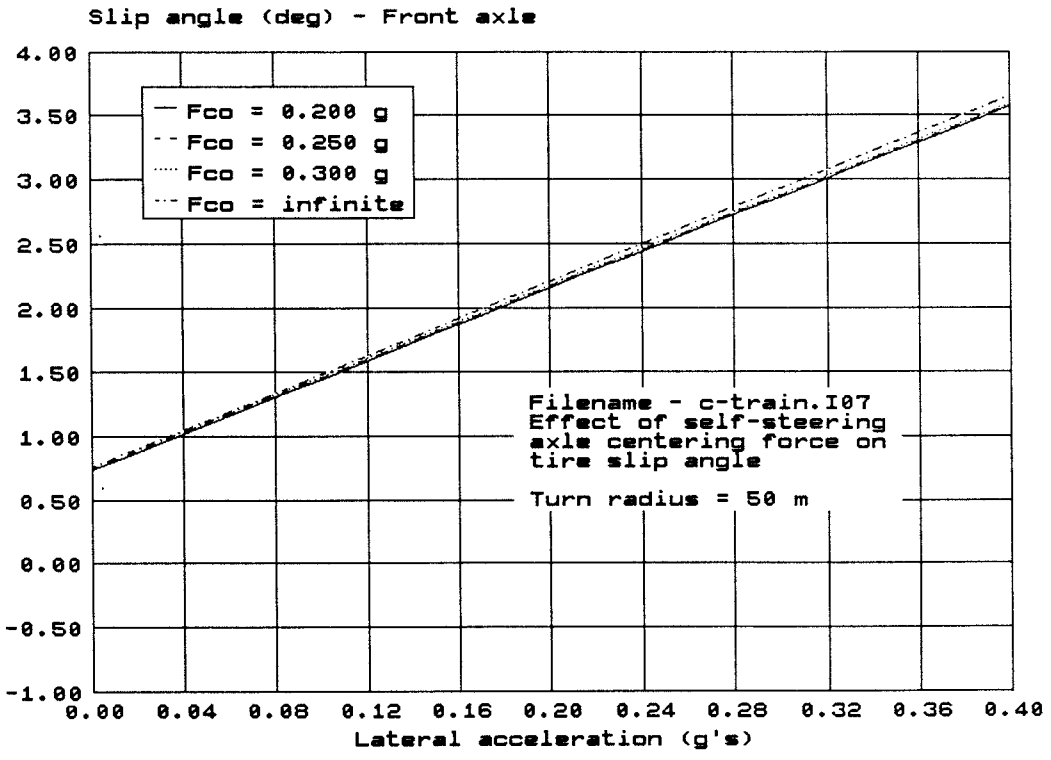
Slip angle (deg) - Front axle
4.00
3.50
3.00
2.50
2.00
1.50
1.00
0.50
0.00
-0.50
-1.00
0.00 0.04 0.08 0.12 0.16 0.20 0.24 0.28 0.32 0.36 0.40
Lateral acceleration (g's)
Fco = 0.200 g
Fco = 0.250 g
Fco = 0.300 g
Fco = infinite
Filename - c-train.I07
Effect of self-steering
axle centering force on
tire slip angle
Turn radius = 50 m

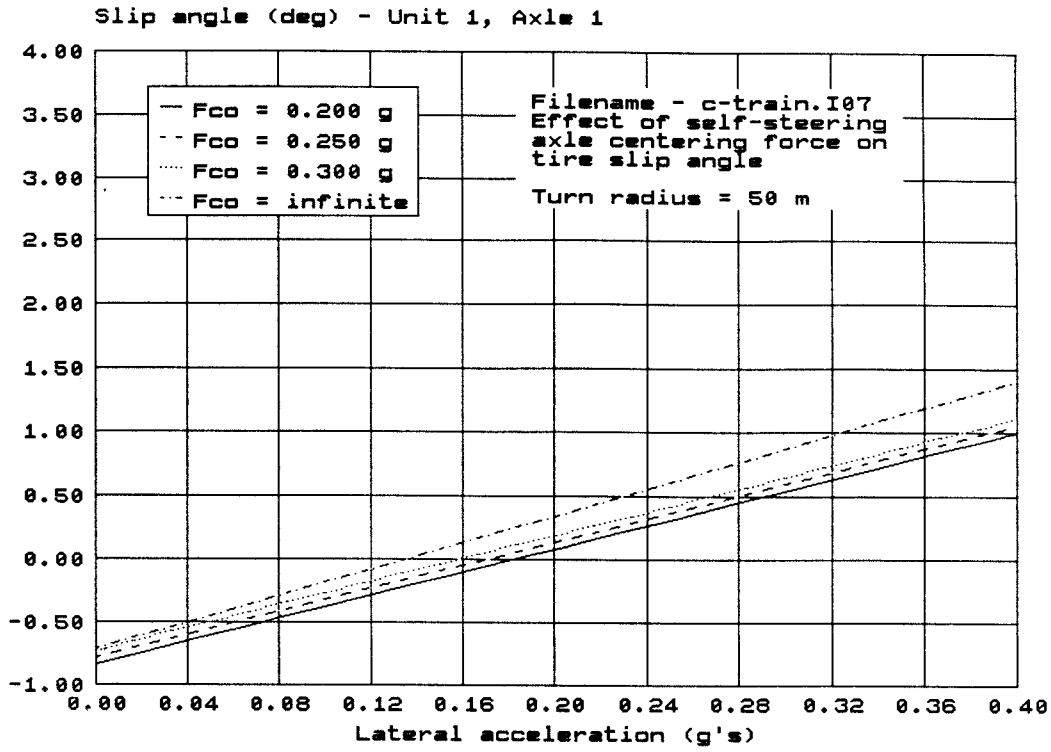
Slip angle (deg) - Unit 1, Axle 1
4.00
3.50
3.00
2.50
2.00
1.50
1.00
0.50
0.00
-0.50
-1.00
Fco = 0.200 g
Fco = 0.250 g
Fco = 0.300 g
Fco = infinite
Filename - c-train.I07
Effect of self-steering
axle centering force on
tire slip angle
Turn radius = 50 m
0.00 0.04 0.08 0.12 0.16 0.20 0.24 0.28 0.32 0.36 0.40
Lateral acceleration (g's)

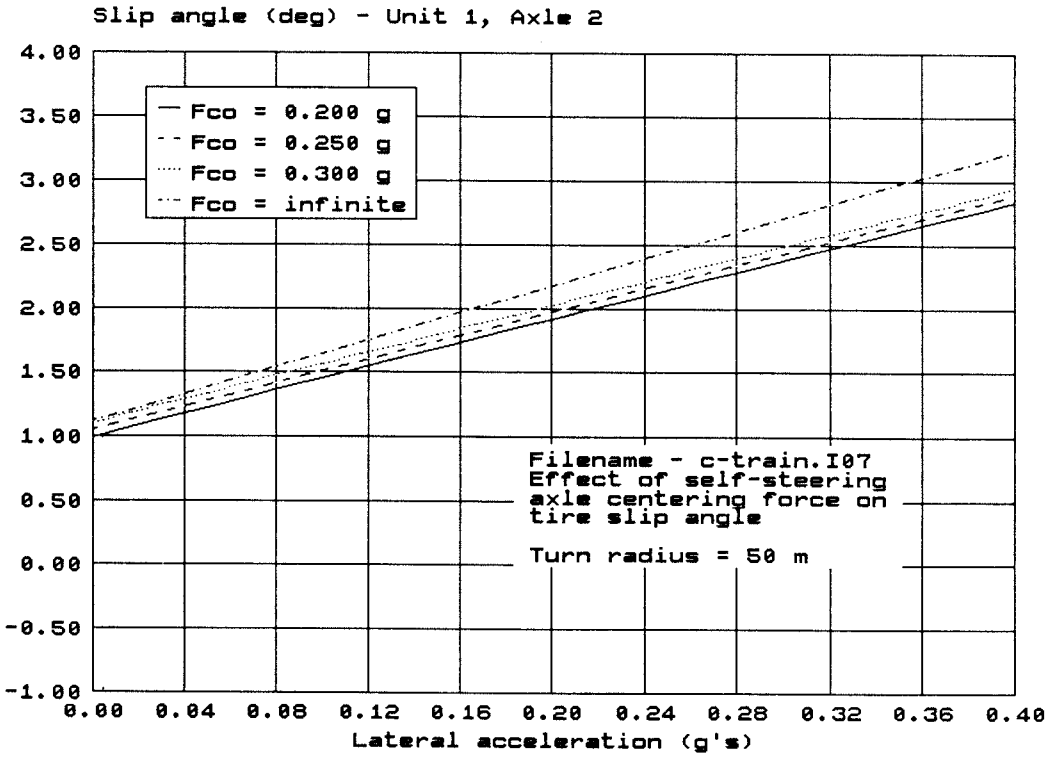
Slip angle (deg) - Unit 1, Axle 2
4.00
3.50
3.00
2.50
2.00
1.50
1.00
0.50
0.00
-0.50
-1.00
Fco = 0.200 g
Fco = 0.250 g
Fco = 0.300 g
Fco = infinite
Filename - c-train.I07
Effect of self-steering
axle centering force on
tire slip angle
Turn radius = 50 m
0.00 0.04 0.08 0.12 0.16 0.20 0.24 0.28 0.32 0.36 0.40
Lateral acceleration (g's)

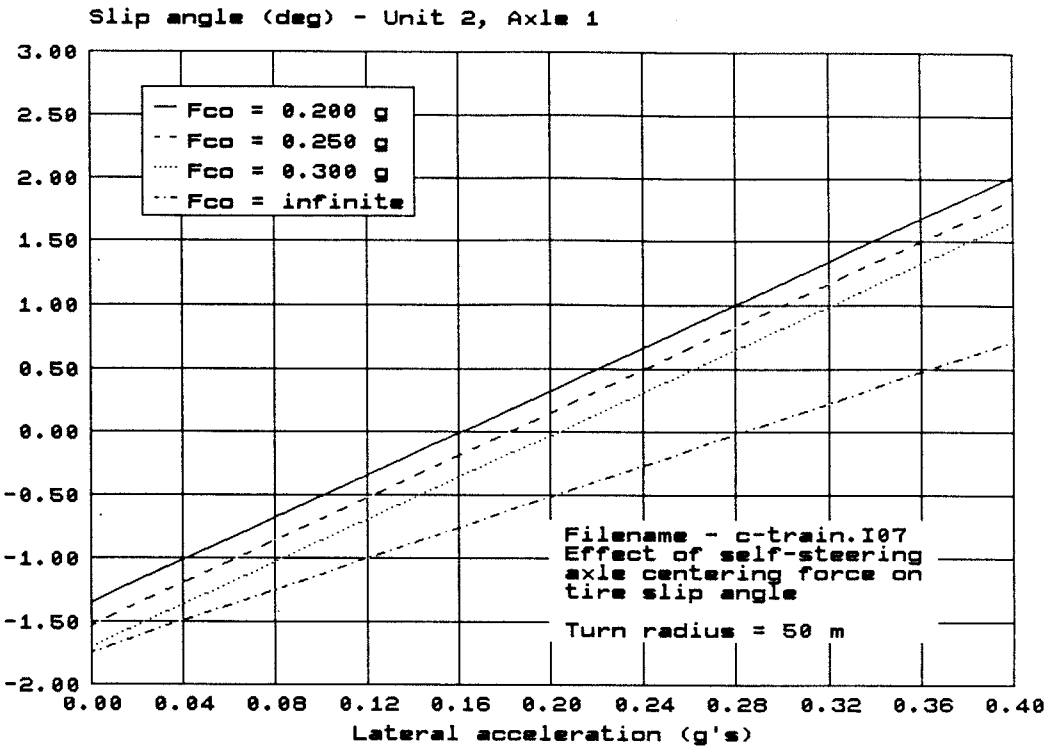
Slip angle (deg) - Unit 2, Axle 1
3.00
2.50
2.00
1.50
1.00
0.50
0.00
-0.50
-1.00
-1.50
-2.00
Fco = 0.200 g
Fco = 0.250 g
Fco = 0.300 g
Fco = infinite
Filename - c-train.I07
Effect of self-steering axle centering force on tire slip angle
Turn radius = 50 m
0.00 0.04 0.08 0.12 0.16 0.20 0.24 0.28 0.32 0.36 0.40
Lateral acceleration (g's)

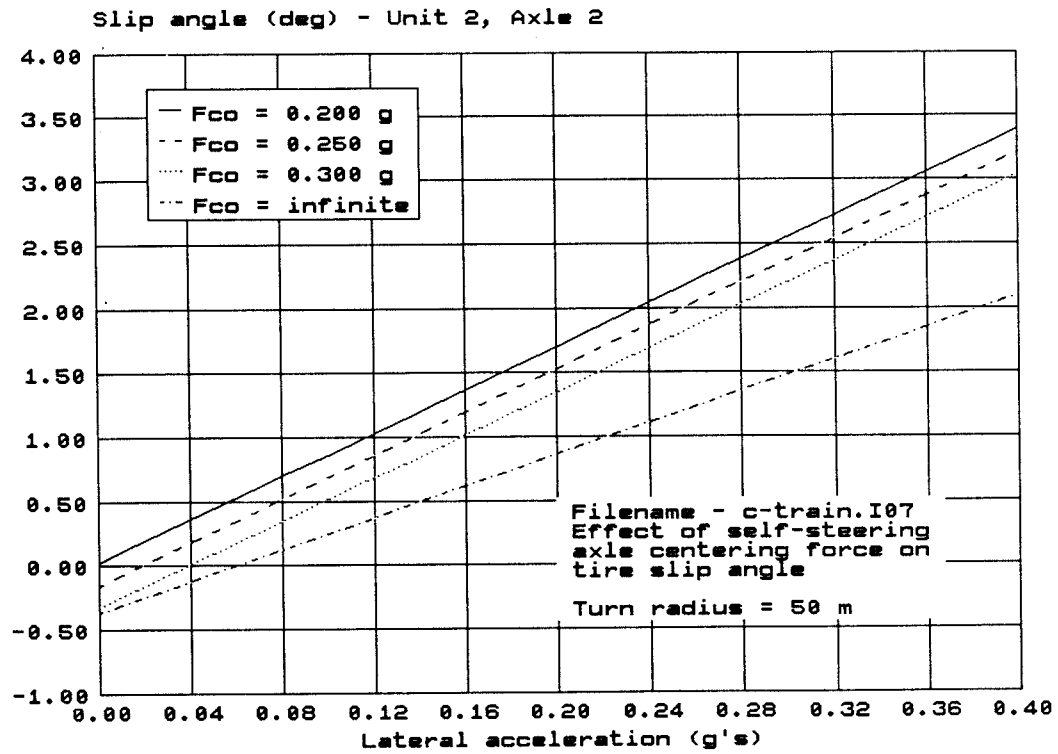
Slip angle (deg) - Unit 2, Axle 2
4.00
3.50
3.00
2.50
2.00
1.50
1.00
0.50
0.00
-0.50
-1.00
Fco = 0.200 g
Fco = 0.250 g
Fco = 0.300 g
Fco = infinite
Filename - c-train.I07
Effect of self-steering axle centering force on tire slip angle
Turn radius = 50 m
0.00 0.04 0.08 0.12 0.16 0.20 0.24 0.28 0.32 0.36 0.40
Lateral acceleration (g's)

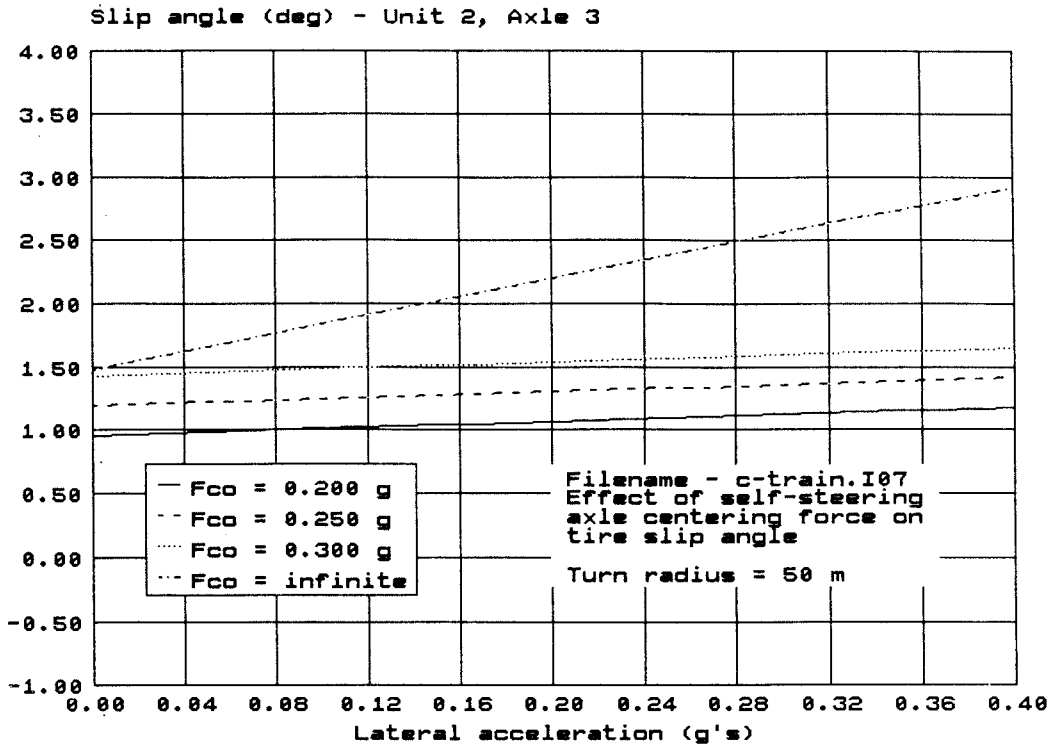
Slip angle (deg) - Unit 2, Axle 3
4.00
3.50
3.00
2.50
2.00
1.50
1.00
0.50
0.00
-0.50
-1.00
0.00 0.04 0.08 0.12 0.16 0.20 0.24 0.28 0.32 0.36 0.40
Lateral acceleration (g's)
Fco = 0.200 g
Fco = 0.250 g
Fco = 0.300 g
Fco = infinite
Filename - c-train.I07
Effect of self-steering axle centering force on tire slip angle
Turn radius = 50 m

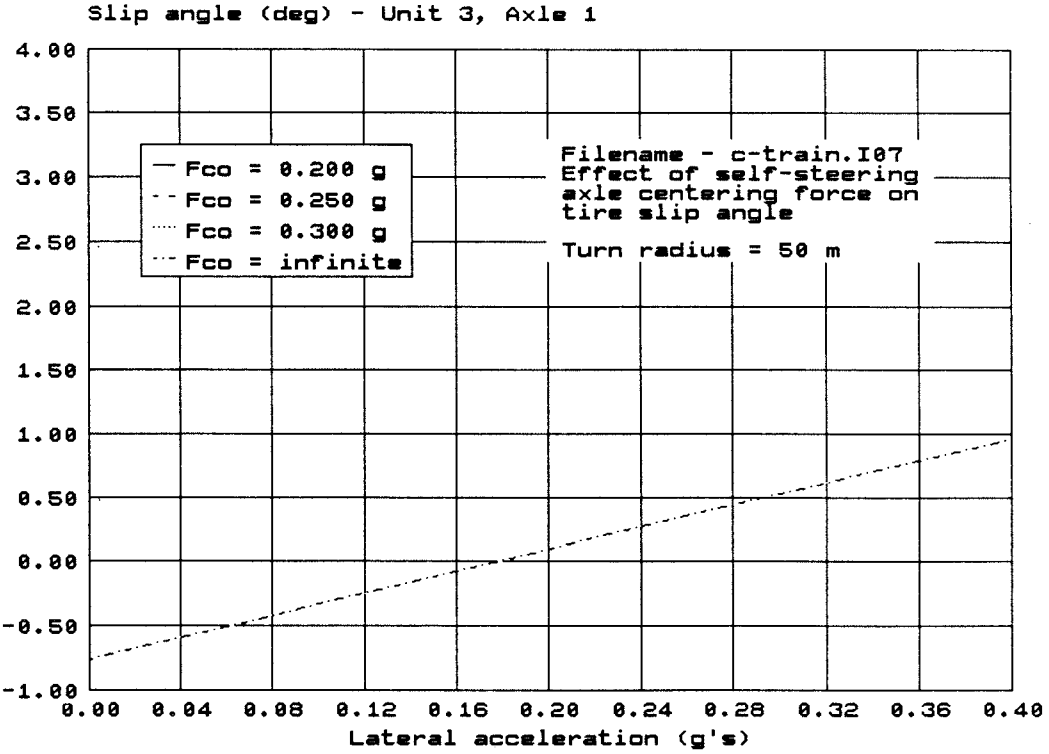
Slip angle (deg) - Unit 3, Axle 1
4.00
3.50
3.00
2.50
2.00
1.50
1.00
0.50
0.00
-0.50
-1.00
0.00 0.04 0.08 0.12 0.16 0.20 0.24 0.28 0.32 0.36 0.40
Lateral acceleration (g's)
Fco = 0.200 g
Fco = 0.250 g
Fco = 0.300 g
Fco = infinite
Filename - c-train.I07
Effect of self-steering axle centering force on tire slip angle
Turn radius = 50 m

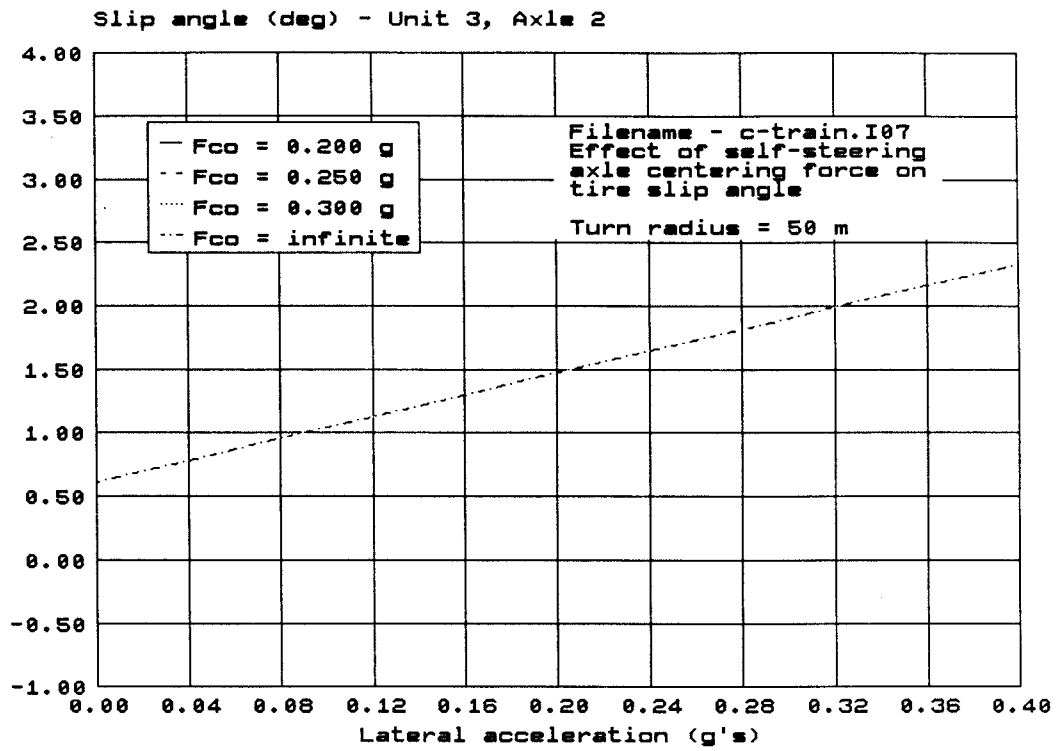
Slip angle (deg) - Unit 3, Axle 2
4.00
3.50
3.00
2.50
2.00
1.50
1.00
0.50
0.00
-0.50
-1.00
0.00
0.04
0.08
0.12
0.16
0.20
0.24
0.28
0.32
0.36
0.40
Lateral acceleration (g's)
Fco = 0.200 g
Fco = 0.250 g
Fco = 0.300 g
Fco = infinite
Filename - c-train.I07
Effect of self-steering axle centering force on tire slip angle
Turn radius = 50 m

APPENDIX E

CHARACTERISTICS OF SELF-STEERING AXLES AS MEASURED ON NRC'S C-DOLLY TEST FACILITY

The axle cornering characteristics and the axle brake-steer characteristics shown in this Appendix are for both the automotive and turntable-type dollies. For each of these steering concepts, typical axles having satisfactory and unsatisfactory characteristics are shown. The satisfactory criteria are an axle cornering force equal to or greater than 0.25 g and an axle brake-steer force equal to or greater than 0.1 g.

The manufacturers of these axles have not been identified in this Appendix.

C-DOLLY DIMENSIONS

TOP VIEW

FRONT

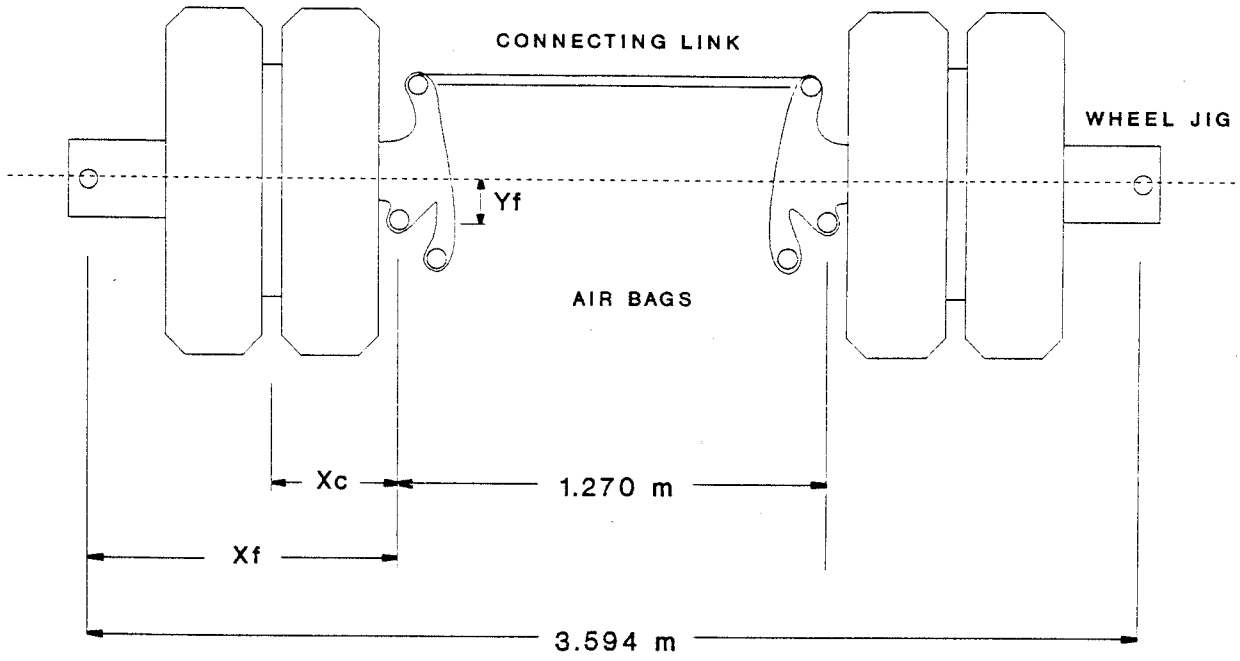

Xc = 0.356 m
Xf = 1.162 m
Yc = 0.187 m
Yf = 0.137 m

AXLE CORNERING CHARACTERISTICS

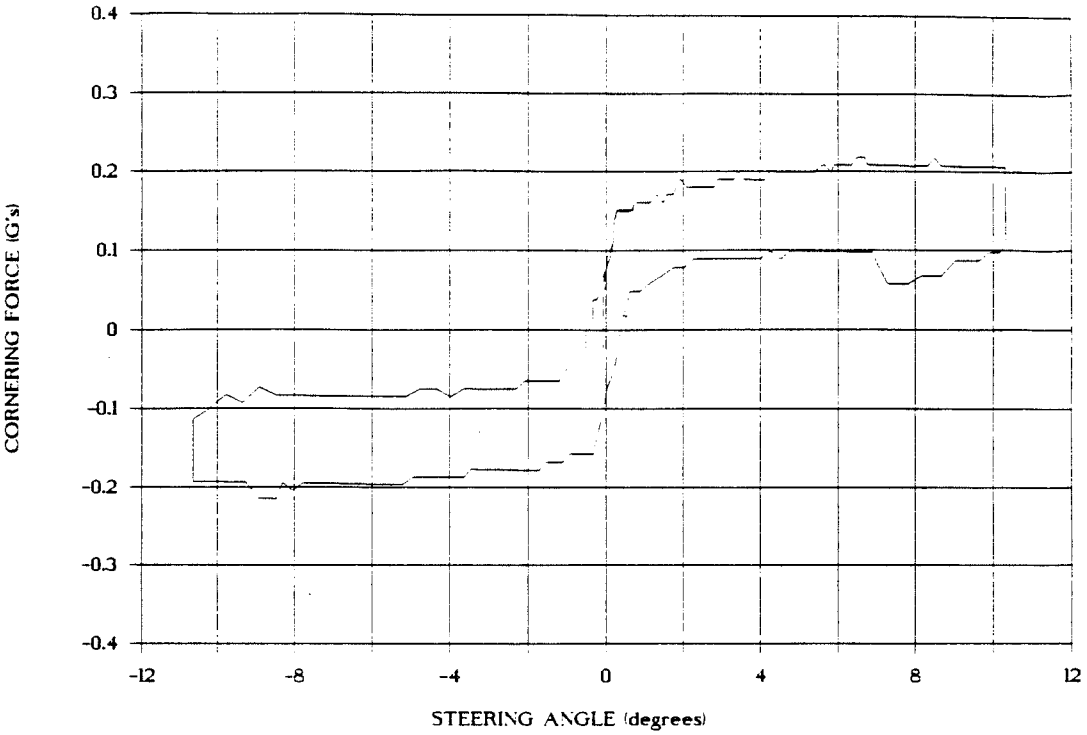

AXLE BRAKE-STEER CHARACTERISTICS

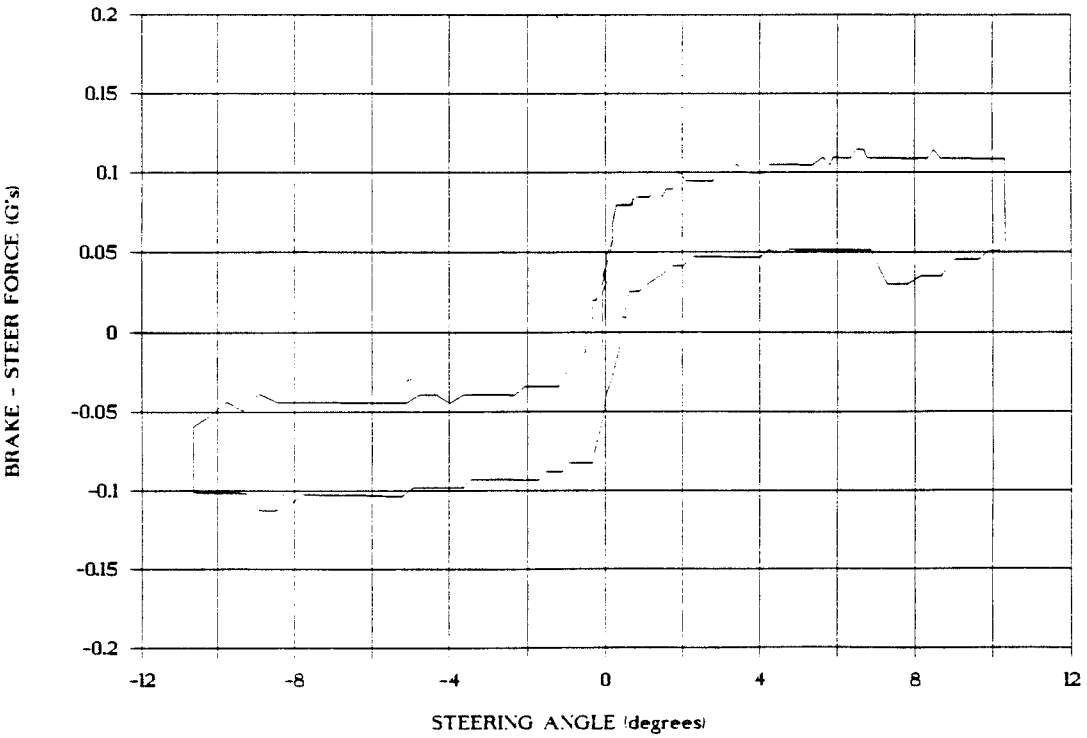

C-DOLLY DIMENSIONS

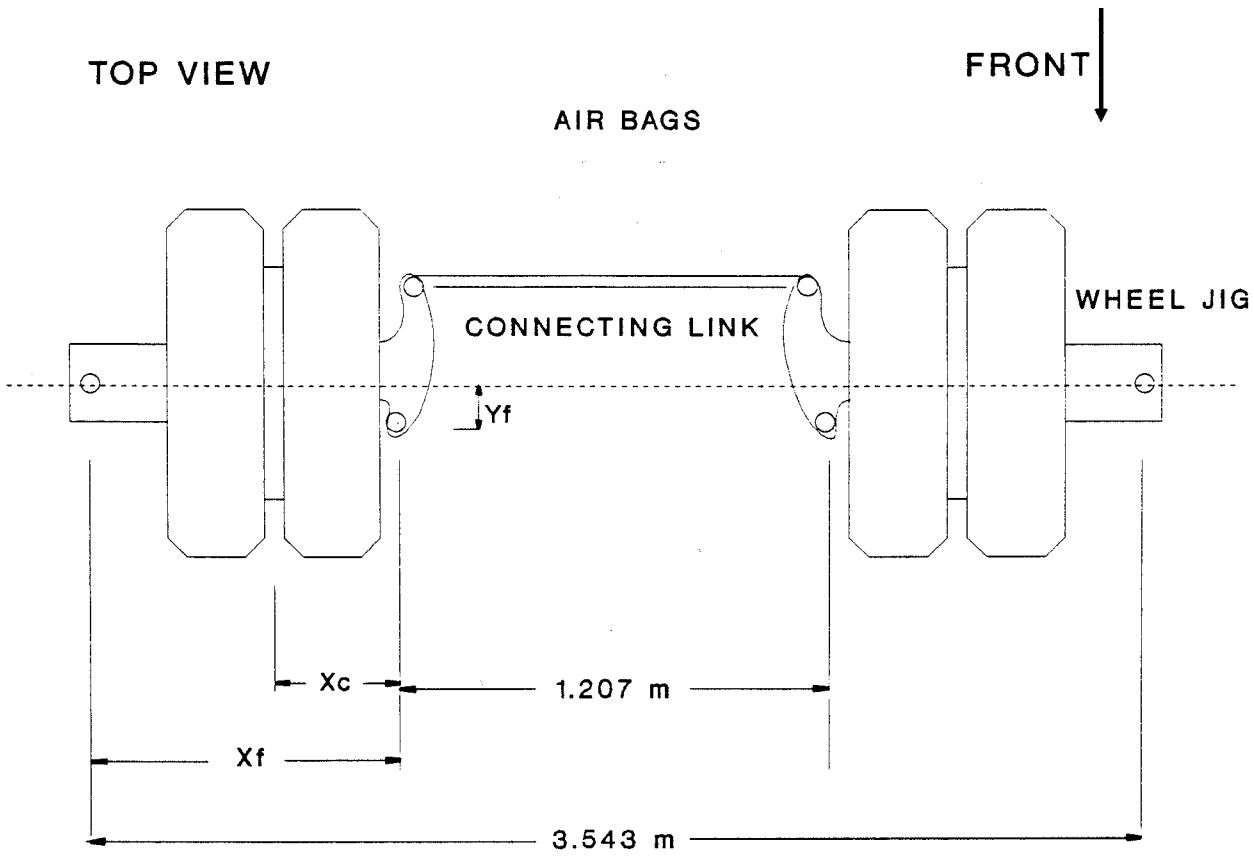

Xc = 0.357 m
Xf = 1.168 m
Yc = 0.193 m
Yf = 0.143 m

AXLE CORNERING CHARACTERISTICS

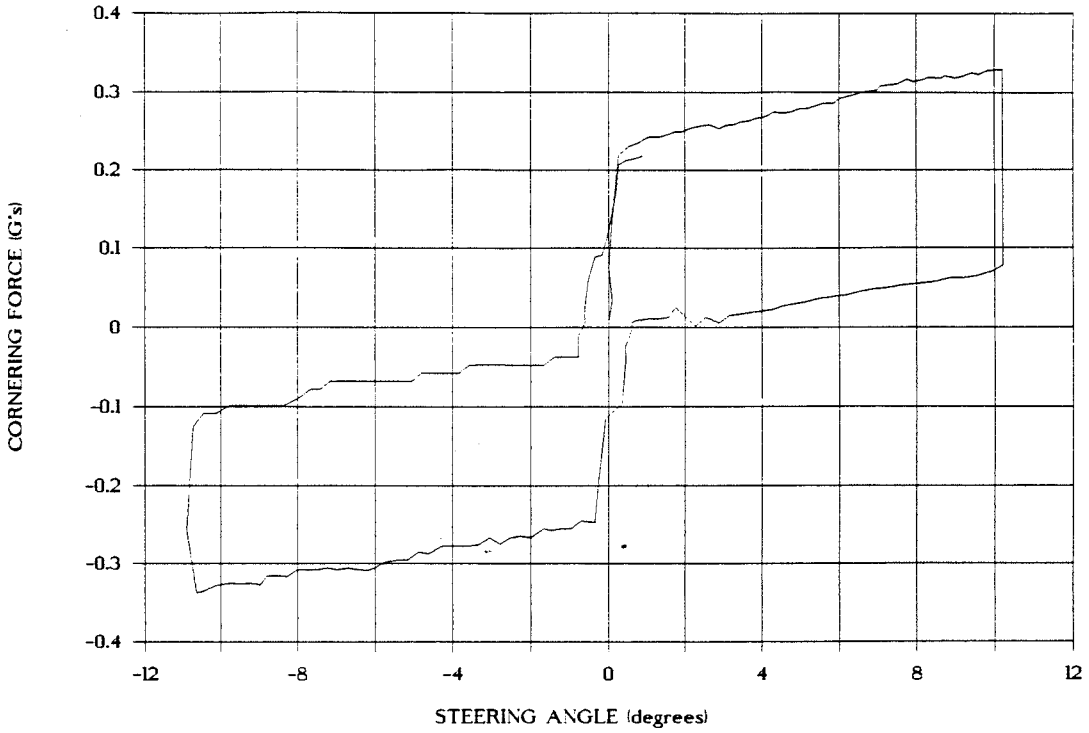

AXLE BRAKE-STEER CHARACTERISTICS

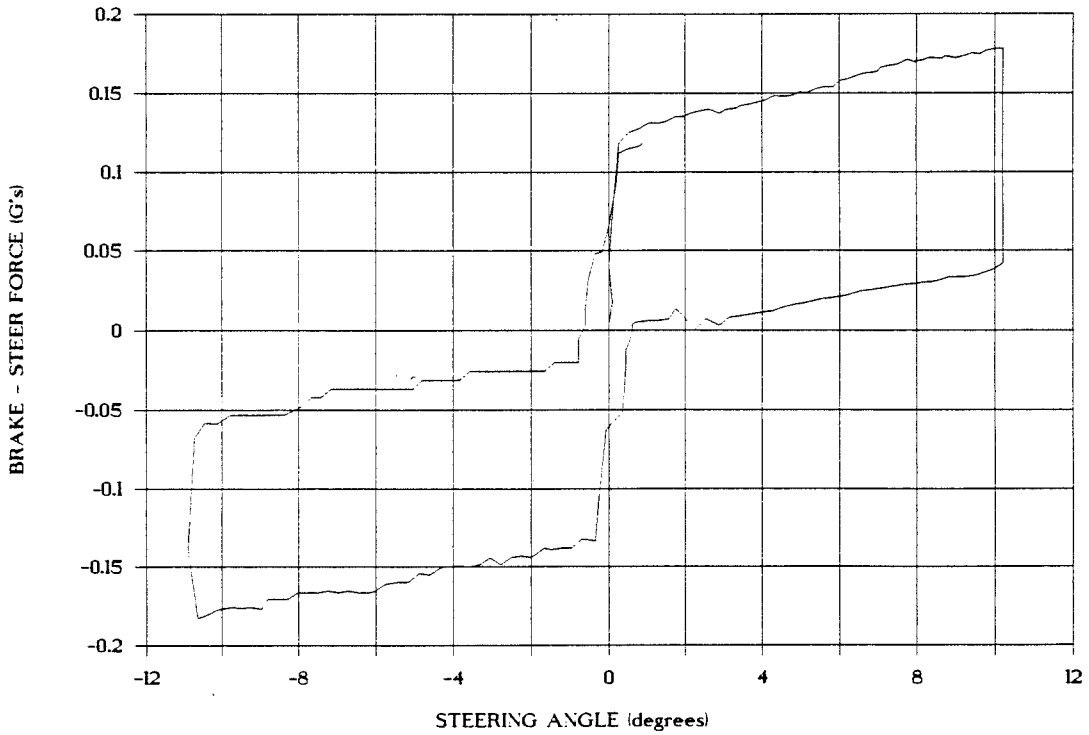

C-DOLLY DIMENSIONS

TOP VIEW

FRONT

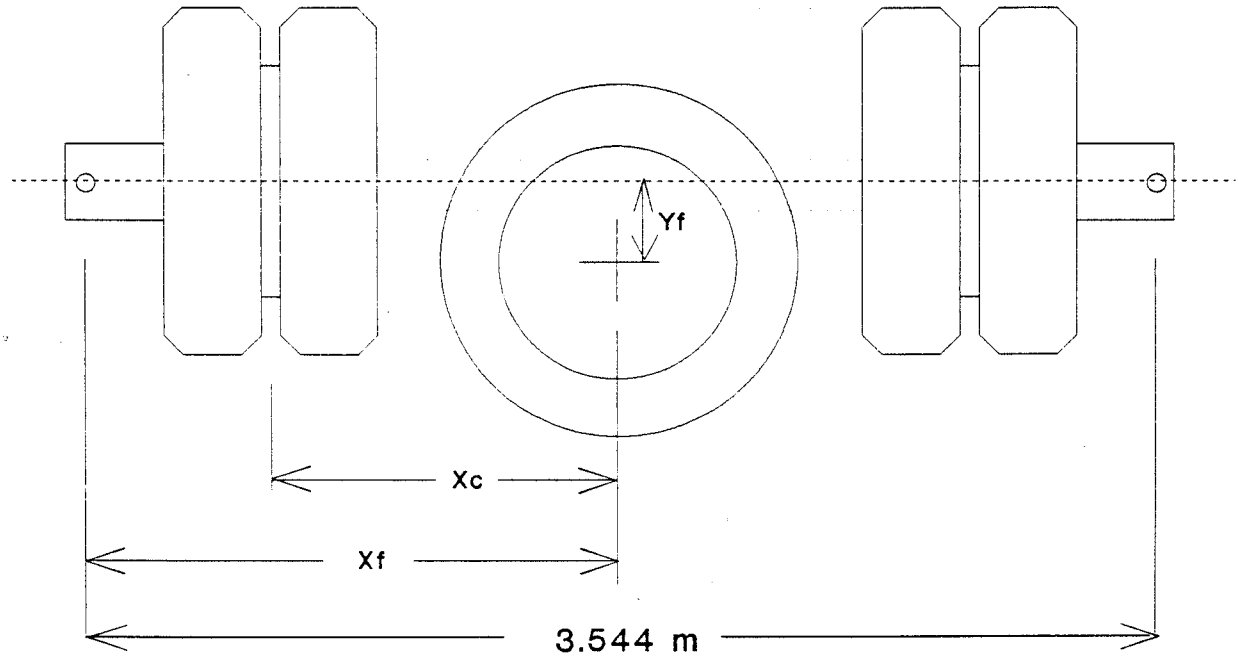

Xc = 0.978 m
Xf = 1.772 m
Yc = 0.356 m
Yf = 0.305 m

AXLE CORNERING CHARACTERISTICS

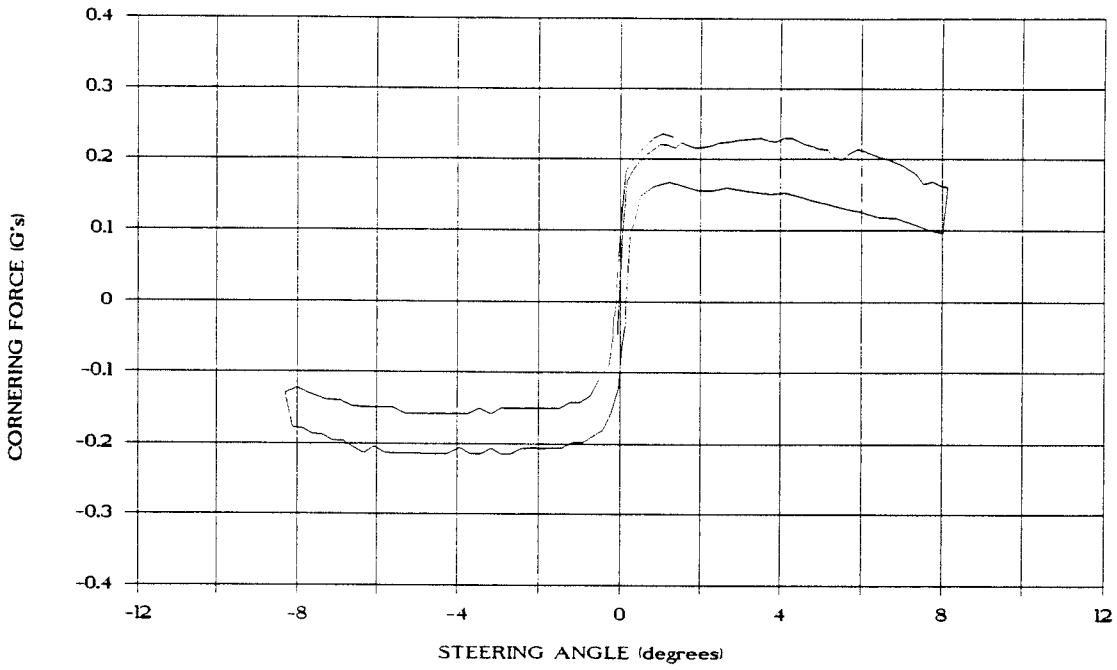

AXLE BRAKE-STEER CHARACTERISTICS

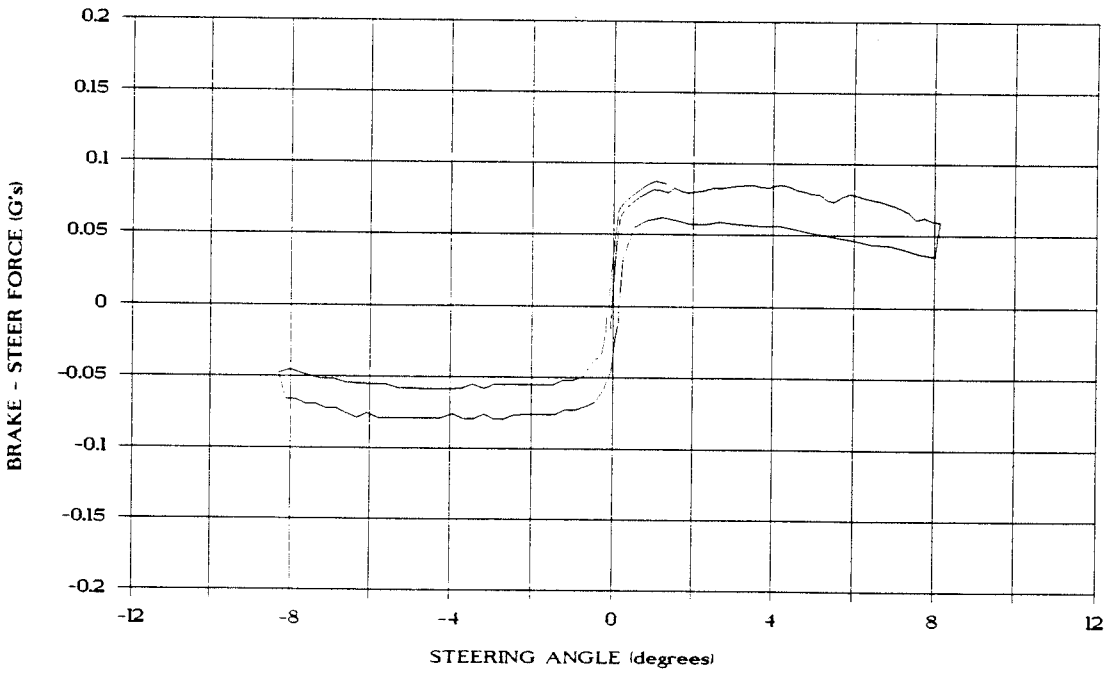

AXLE CORNERING CHARACTERISTICS

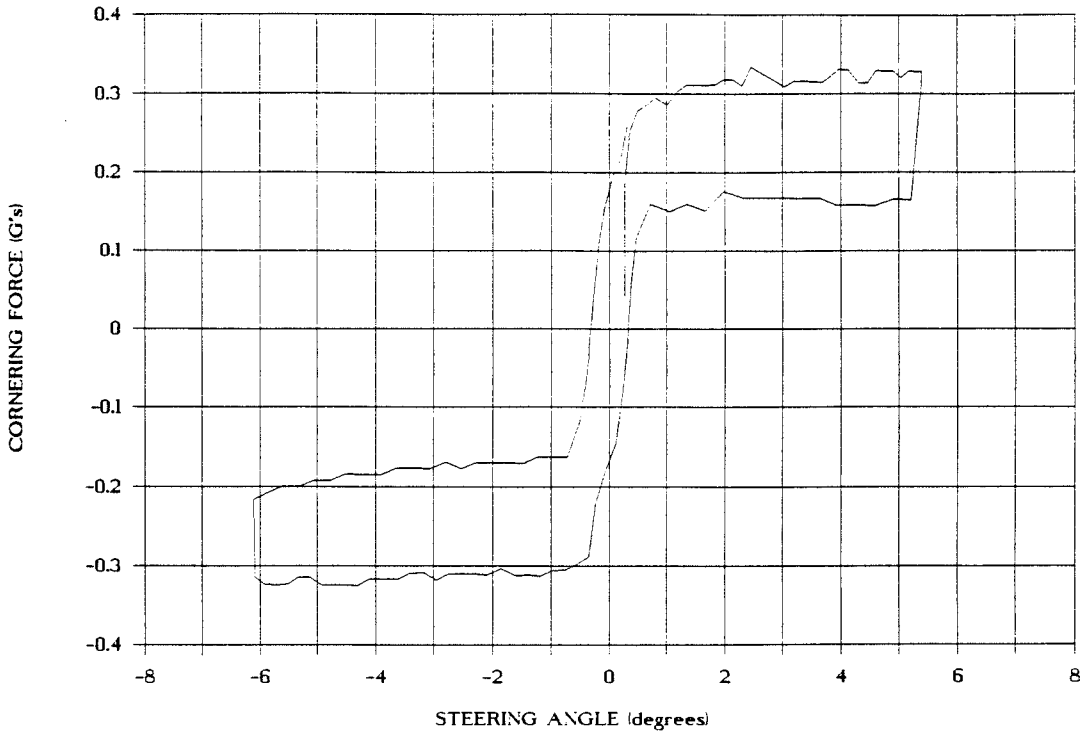

AXLE BRAKE-STEER CHARACTERISTICS